

Vibrational Spectra of Some Organotrisulphides and Homologues



Brian Michael Catchpaugh

A thesis submitted to the Faculty of Graduate
Studies and Research of McGill University
in partial fulfillment of the requirements for
the degree of Doctor of Philosophy.

From the Inorganic Chemistry Laboratory
under the supervision of
Dr. I.S. Butler

McGill University
Montreal, Quebec

March 1980

Vibrational Spectra of Some Organotrisulphides and Homologues

Acknowledgements

The author is grateful to Dr. Ian S. Butler for his patience and encouragement during the course of this work.

Dr. David N. Harpp is thanked for helpful discussions regarding organotrisulphides and for providing many of the samples used in this study.

Very special thanks is extended to the author's wife for her un-daunting perserverance and attention to detail in the typing of this thesis and for her constant moral support.

*Vibrational Spectra of Some Organotrisulphides and Homologues**Abstract*

The infrared and laser-Raman spectra of the organosulphur compounds R_2S_3 ($R = \text{Me}, \text{Me-}d_6, \text{Et}, n\text{-Pr}, i\text{-Pr}, t\text{-Bu}$), Et_2S_4 , Bz_2S_n ($n = 1-4$), $(4\text{-R-Ph})_2S_3$ ($R = \text{Br}, \text{Me}, \text{OMe}, t\text{-Bu}$) and $(4\text{-R-Ph})_2S_2$ ($R = \text{Br}, \text{Me}, \text{OMe}$) have been recorded in the accessible regions for fundamental vibrations and complete assignments have been proposed. Apart from coupling of skeletal and phenyl group vibrations in the diphenyl derivatives, the vibrations are highly localized in the substituents and in the CS_nC skeletons of the molecules. Normal coordinate analysis of Me_2S_3 and $\text{Me}_2S_3\text{-}d_6$ has confirmed the assignments for the skeletal vibrations and has indicated the *trans* rotamer to predominate in the liquid trisulphides. Only for Me_2S_3 has any evidence for some *cis* rotamer in the liquids been observed. The two solid-state variations (Solids I and II) obtained for Me_2S_3 have been deduced to correspond to the *cis* and *trans* rotamers, respectively. Evidence of rotational isomerism about the C-S bonds has been found in the spectra of Et_2S_3 , $n\text{-Pr}_2S_3$, $i\text{-Pr}_2S_3$ and Et_2S_4 . Detailed studies of the temperature-dependence for the Raman spectra of Et_2S_3 and $i\text{-Pr}_2S_3$ in light of the available evidence concerning the C-S isomerism in organodisulphides has led to a complete assessment of this isomerism. Enthalpy differences between the rotamers of Et_2S_3 and $i\text{-Pr}_2S_3$ have been calculated to be 1.10 ± 0.29 and $0.39 \pm 0.13 \text{ kJ mol}^{-1}$, respectively. The spectra of $n\text{-Pr}_2S_3$ and Et_2S_4 also show isomerism about the C-C and S-S bonds, respectively.

*Vibrational Spectra of Some Organotrisulphides and Homologues**Résumé*

Les spectres infrarouge et laser-Raman des composés de soufre R_2S_3 ($R = \text{Me}, \text{Me-d}_6, \text{Et}, n\text{-Pr}, i\text{-Pr}, t\text{-Bu}$), Et_2S_4 , Bz_2S_n ($n = 1-4$), $(4\text{-R-Ph})_2S_3$ ($R = \text{Br}, \text{Me}, \text{OMe}, t\text{-Bu}$) et $(4\text{-R-Ph})_2S_2$ ($R = \text{Br}, \text{Me}, \text{OMe}$) ont été enregistrés dans les régions des vibrations fondamentales et les attributions complètes ont été proposées. Sauf que les vibrations du squelette et du cycle benzène sont couplées dans les dérivés de benzène, les vibrations sont très localisées dans les substituants et dans les chaînes CS_nC . L'analyse en coordonnées normales de Me_2S_3 et $\text{Me}_2S_3\text{-d}_6$ a vérifié les attributions des vibrations des chaînes et aussi a indiqué que la conformation *trans* est la plus favorisée pour les trisulfures dans l'état liquide. De l'évidence pour la conformation *cis* dans l'état liquide a été trouvée seulement pour Me_2S_3 . Les deux structures observées pour Me_2S_3 dans l'état solide (Solid I et Solid II) ont été attribuées aux conformations *cis* et *trans*, respectivement. La présence des isomères rotationnels pour les liaisons C-S a été mise en évidence dans les spectres de Et_2S_3 , $n\text{-Pr}_2S_3$, $i\text{-Pr}_2S_3$ et Et_2S_4 . Des études détaillées de la dépendance de la température des spectres Raman de Et_2S_3 et $i\text{-Pr}_2S_3$, en vue de l'évidence disponible pour les disulfures, ont permis une compréhension totale de cet isomérisme. Les différences entre les énergies des isomères de Et_2S_3 et de $i\text{-Pr}_2S_3$ ont été calculées comme 1.10 ± 0.029 et $0.39 \pm 0.13 \text{ kJ mol}^{-1}$, respectivement. Les spectres de $n\text{-Pr}_2S_3$ et Et_2S_4 ont montré aussi l'existence de l'isomérisme rotationnel pour les liaisons C-C et C-S, respectivement.

Abbreviations

Bz	benzyl
Et	ethyl
<i>i</i> -Bu	isobutyl
<i>i</i> -Pr	isopropyl
OMe	methoxy
Me	methyl
<i>n</i> -Bu	normal butyl
<i>n</i> -Pr	normal propyl
Ph	phenyl
Δ -Bu	secondary butyl
<i>t</i> -Bu	tertiary butyl

Table of Contents:

<u>Chapter</u>		<u>Page</u>
Chapter I	Introduction.....	1
Chapter II	Natural Occurrence of Organopolysulphides.....	4
Chapter III	Structure of Organopolysulphides.....	7
Chapter IV	Vibrational Spectra of Sulphur-Chain Compounds.....	23
Chapter V	Experimental.....	29
V.A	Preparation and Purification of Compounds.....	29
V.A.1	Dialkyl Compounds.....	29
V.A.2	Dibenzyl Compounds.....	30
V.A.3	Diphenyl Compounds.....	31
V.B	Instrumentation.....	32
Chapter VI	Results and Discussion.....	37
VI.A	Dialkyl Polysulphides.....	37
VI.A.1	Rotational Isomerism.....	50
VI.A.1.i	C-S Isomerism.....	56
VI.A.1.ii	S-S Isomerism.....	99
VI.A.2	Vibrational Assignments.....	108
VI.A.2.i	Dimethyl Trisulphide and Dimethyl Trisulphide-d ₆	114
VI.A.2.i.a	Normal Coordinate Calculations.....	128
VI.A.2.ii	Diethyl Trisulphide and Diethyl Tetrasulphide...	137
VI.A.2.iii	Di-n-propyl Trisulphide.....	148

Table of Contents (continued)

<u>Chapter</u>		<u>Page</u>
VI.A.2.iv	Di- <i>i</i> -propyl Trisulphide.....	151
VI.A.2.v	Di- <i>t</i> -butyl Trisulphide.....	156
VI.B	Dibenzyl Derivatives.....	161
VI.C	Diphenyl Di- and Trisulphides.....	177
VI.C.1	Di-4-Bromophenyl Di- and Trisulphide.....	180
VI.C.2	Di-4-Methylphenyl Di- and Trisulphide.....	186
VI.C.3	Di-4-Methoxyphenyl Di- and Trisulphide.....	190
VI.C.4	Di- <i>t</i> -Butylphenyl Trisulphide.....	195
VII.	Summary and Contributions to Knowledge.....	200
VIII.	Appendix.....	204
IX.	References.....	217

Index of Tables

<u>Table No.</u>		<u>Page</u>
1.	Intensity Ratios for the $\nu(\text{C-S})$ Vibrations of Et_2S_3 , $i\text{-Pr}_2\text{S}_3$ and Et_2S_2 as a Function of Temperature, and Enthalpy Differences Between the Rotamers	46
2.	Raman $\nu(\text{S-S})$ Vibrations for Liquid Dialkyl Disulphides	58
3.	Proposed $\nu(\text{S-S})$ - Structure Correlation for Dialkyl Disulphides	59
4.	Vibrational and Structural Data for Class II Primary Organodisulphides	63
5.	Relative Energies (kJ mol^{-1}) for Rotamers of EtSSMe from Various Calculations.....	72
6.	Nonbonded Contact Distances (\AA) for Et_2S_2	80
7.	Nonbonded Contact Distances (\AA) for Et_2S_3	81
8.	Vibrational Wavenumbers (cm^{-1}) and Assignments for Me_2S_3	115
9.	Vibrational Wavenumbers (cm^{-1}) and Assignments for Liquid $\text{Me}_2\text{S}_3\text{-}d_6$	118
10.	Fundamental Vibrations and Potential Energy Distributions for <i>trans</i> - Me_2S_3	120
11.	Fundamental Vibrations and Potential Energy Distributions for <i>trans</i> - $\text{Me}_2\text{S}_3\text{-}d_6$	122
12.	Skeletal Vibrations of Me_2S_3 and $\text{Me}_2\text{S}_3\text{-}d_6$	127

Index of Tables (continued):

<u>Table No.</u>	<u>Page</u>
13.	Modified Urey-Bradley Force Fields for Me_2S_3 and $\text{Me}_2\text{-S}_3\text{-d}_6$ 134
14.	Internal Coordinate Force Fields for the CSSSC Skeleton of Me_2S_3 and $\text{Me}_2\text{S}_3\text{-d}_6$ 135
15.	Vibrational Wavenumbers (cm^{-1}) and Assignments for Et_2S_3 139
16.	Vibrational Wavenumbers (cm^{-1}) and Assign- ments for Liquid Et_2S_4 145
17.	Vibrational Wavenumbers (cm^{-1}) and Assign- ments for Liquid $n\text{-Pr}_2\text{S}_3$ 149
18.	Vibrational Wavenumbers (cm^{-1}) and Assign- ments for $i\text{-Pr}_2\text{S}_3$ 152
19.	Vibrational Wavenumbers (cm^{-1}) and Assign- ments for $t\text{-Bu}_2\text{S}_3$ 157
20.	Vibrational Wavenumbers (cm^{-1}) and Assign- ments for crystalline Bz_2S_n ($n = 1-4$)..... 162
21.	Raman Spectra ($750-400 \text{ cm}^{-1}$) for Bz_2S_n ($n = 1-3$) in Various States..... 173
22.	Vibrational Wavenumbers (cm^{-1}) and Assign- ments for Crystalline $(4\text{-Br-Ph})_2\text{S}_n$ ($n = 2,3$)..... 181
23.	Vibrational Wavenumbers (cm^{-1}) and Assign- ments for Crystalline $(4\text{-Me-Ph})_2\text{S}_n$ ($n = 2,3$)..... 187
24.	Vibrational Wavenumbers (cm^{-1}) and Assign- for Crystalline $(4\text{-MeO-Ph})_2\text{S}_n$ ($n = 2,3$)..... 191
25.	Vibrational Wavenumbers (cm^{-1}) and Assign- ments for Crystalline $(4\text{-}t\text{-Bu-Ph})_2\text{S}_3$ 196

Index of Figures:

<u>Figure No.</u>		<u>Page</u>
1a	Infrared Spectrum of Me_2S_3 : Liquid, Ambient Temperature.....	49
1b	Laser-Raman Spectrum of Me_2S_3 : Liquid, Ambient Temperature.....	49
1c	Laser-Raman Spectrum of Me_2S_3 : Solid I, $\sim 15\text{K}$	49
1d	Laser-Raman Spectrum of Me_2S_3 : Solid II, $\sim 15\text{K}$	49
2a	Infrared Spectrum of $\text{Me}_2\text{S}_3-d_6$: Liquid, Ambient Temperature.....	49
2b	Laser-Raman Spectrum of $\text{Me}_2\text{S}_3-d_6$: Liquid, Ambient Temperature.....	49
3a	Infrared Spectrum of Et_2S_3 : Liquid, Ambient Temperature.....	49
3b	Laser-Raman Spectrum of Et_2S_3 : Liquid, Ambient Temperature.....	49
3c	Laser-Raman Spectrum of Et_2S_3 : Metastable Phase $\sim 15\text{K}$	49
3d	Laser-Raman Spectrum of Et_2S_3 : Solid, $\sim 15\text{K}$	49
4a	Infrared Spectrum of $n\text{-Pr}_2\text{S}_3$: Liquid, Ambient Temperature.....	49
4b	Laser-Raman Spectrum of $n\text{-Pr}_2\text{S}_3$: Liquid, Ambient Temperature.....	49
5a	Infrared Spectrum of $i\text{-Pr}_2\text{S}_3$: Liquid, Ambient Temperature.....	49
5b	Laser-Raman Spectrum of $i\text{-Pr}_2\text{S}_3$: Liquid, Ambient Temperature.....	49

Index of Figures (continued)

<u>Figure No.</u>		<u>Page</u>
5c	Laser-Raman Spectrum of $i\text{-Pr}_2\text{S}_3$: Metastable Phase, $\sim 15\text{K}$	49
5d	Laser-Raman Spectrum of $i\text{-Pr}_2\text{S}_3$: Solid, $\sim 15\text{K}$	49
6a	Infrared Spectrum of $t\text{-Bu}_2\text{S}_3$: Liquid, Ambient Temperature.....	49
6b	Laser-Raman Spectrum of $t\text{-Bu}_2\text{S}_3$: Liquid, Ambient Temperature.....	49
6c	Laser-Raman Spectrum of $t\text{-Bu}_2\text{S}_3$: Solid, $\sim 15\text{K}$	49
7a	Infrared Spectrum of Et_2S_4 : Liquid, Ambient Temperature.....	49
7b	Laser-Raman Spectrum of Et_2S_4 : Liquid, Ambient Temperature.....	49
8	Plots of the Variation with Temperature for the $\nu(\text{C-S})$ Band Intensity Ratios of Et_2S_3 , Et_2S_2 and $i\text{-Pr}_2\text{S}_3$ from the Data of Table 1.....	47
9	Stable Configurations for the Central Core of Organodi-, Tri- and Tetrasulphides.....	51
10	Newman Projections for Various Conformations About the C-S Bonds of the Primary Disulphide Et_2S_2 ($\text{Y} = \text{CH}_2$) and the Primary Trisulphide Et_2S_3 ($\text{Y} = \text{S}$). 52	
11	Newman Projections for Various Conformations About the C-S Bonds of the Secondary Disulphide $i\text{-Pr}_2\text{S}_2$ ($\text{Y} = \text{CH}$) and the Secondary Trisulphide $i\text{-Pr}_2\text{S}_3$ ($\text{Y} = \text{S}$).....	53

Index of Figures (continued)

<u>Figure No.</u>		<u>Page</u>
12	Alkyl Group Vibrations for R_2S_3 (R = Me, Et, <i>n</i> -Pr, <i>i</i> -Pr, <i>t</i> -Bu).....	109
13	Internal and Symmetry Coordinates for <i>trans</i> - and <i>cis</i> - Me_2S_3	130
14a	Infrared Spectrum of Crystalline Bz_2S	175
14b	Laser-Raman Spectrum of Crystalline Bz_2S	175
15a	Infrared Spectrum of Crystalline Bz_2S_2	175
15b	Laser-Raman Spectrum of Crystalline Bz_2S_2	175
16a	Infrared Spectrum of Crystalline Bz_2S_3	175
16b	Laser-Raman Spectrum of Crystalline Bz_2S_3	175
17a	Infrared Spectrum of Crystalline Bz_2S_4	175
17b	Laser-Raman Spectrum of Crystalline Bz_2S_4	175
18	Laser-Raman Spectra of Dibenzyl Derivatives in the Liquid State.....	176
19a	Infrared Spectrum of Crystalline $(4-Br-Ph)_2S_3$	199
19b	Laser-Raman Spectrum of Crystalline $(4-Br-Ph)_2S_3$	199
20a	Infrared Spectrum of Crystalline $(4-Br-Ph)_2S_2$	199
20b	Laser-Raman Spectrum of Crystalline $(4-Br-Ph)_2S_2$	199
21a	Infrared Spectrum of Crystalline $(4-Me-Ph)_2S_3$	199
21b	Laser-Raman Spectrum of Crystalline $(4-Me-Ph)_2S_3$	199
22a	Infrared Spectrum of Crystalline $(4-Me-Ph)_2S_2$	199
22b	Laser-Raman Spectrum of Crystalline $(4-Me-Ph)_2S_2$	199

Index of Figures (continued)

<u>Figure No.</u>		<u>Page</u>
23a	Infrared Spectrum of Crystalline $(4\text{-MeO-Ph})_2\text{S}_3$	199
23b	Laser-Raman Spectrum of Crystalline $(4\text{-MeO-Ph})_2\text{S}_3$	199
24a	Infrared Spectrum of Crystalline $(4\text{-MeO-Ph})_2\text{S}_2$	199
24b	Laser-Raman Spectrum of Crystalline $(4\text{-MeO-Ph})_2\text{S}_2$	199
25a	Infrared Spectrum of Crystalline $(4\text{-}t\text{-Bu-Ph})_2\text{S}_3$	199
25b	Laser-Raman Spectrum of Crystalline $(4\text{-}t\text{-Bu-Ph})_2\text{S}_3$...	199

CHAPTER 1

INTRODUCTION

Sulphur, unlike its congeners in Group VIA, demonstrates a strong tendency towards catenation as is illustrated by the various allotropes formed by the free element itself.¹ Thus the well-known orthorhombic and rhombohedral crystalline modifications of sulphur are composed of S₈ and S₆ rings, respectively,^{2,3} while the species present in the liquid state include the S₇, S₁₂, S₁₈, and S₂₀ rings as well, all of which can be isolated as pure substances.^{4,5} The last three of these molecules have been noted to be remarkably stable.^{4,5} In recent years, the rather unstable rings S₉ and S₁₀ have also been synthesized.⁵ The most highly catenated allotropes of sulphur, open-chain polymers that may exceed a hundred thousand atoms in length, are found in the fibrous state.¹

The propensity of sulphur to form chains is further evidenced by the interesting class of organosulphur compounds known as organopolysulphides wherein the terminal sulphurs in an unbranched chain are bonded to organic substituents at carbon:



These polysulphides may be symmetric with identical R groups, or unsymmetric with different R groups. Then again, the sulphur chain may bridge between two carbon atoms in a single organic moiety to give a cyclic organopolysulphide. Since the organodisulphides (n=2) constitute an extensive and important collection of compounds by themselves, they are generally treated as a distinct class of organosulphur compounds.

The organotrisulphides (n=3) account for the majority of organopolysulphides, although many longer-chain homologues are known. For instance, the

preparation and characterization of the complete series of symmetric polysulphides up to the octasulphide ($n=8$) have been reported for R the benzyl⁶ or triphenylmethyl⁷ substituent. Studies by nuclear magnetic resonance spectroscopy have afforded evidence for derivatives up to the decasulphide ($n=10$) for R the methyl or *t*-butyl group.⁸ However, the decreased stability of organopolysulphides with increased sulphur chain length seems to impose a practical limit on the size of the chain for any substituents.

This thesis concerns an investigation of the infrared and laser-Raman spectra of symmetric organotrisulphides whose spectra, hitherto, have received little attention (Chapter IV). For purposes of comparison, the spectra of a number of homologues have also been studied. The compounds examined divide conveniently into three categories: (1) dialkyltrisulphides R_2S_3 ($R=Me, Et, n-Pr, i-Pr, t-Bu$) and diethyltetrasulphide Et_2S_4 , (2) mono- through tetrasulphide dibenzyl derivatives Bz_2S_n ($n=1-4$), and (3) *para*-substituted diphenyl tri- and disulphides $(4-R-Ph)_2S_3$ ($R=Me, OMe, Br, t-Bu$) and $(4-R-Ph)_2S_2$ ($R=Me, OMe, Br$). In all cases, the primary focus of this work has been on the fundamental vibrations of the CSSSC backbone of the trisulphides, especially the S-S and C-S stretching vibrations. A normal coordinate analysis of Me_2S_3 and $Me_2S_3-d_6$ has been undertaken to gain further insight into the nature of these vibrations. Of primary interest in the study of the dialkyl and dibenzyl compounds has been the effects of rotational isomerism about the C-S and S-S bonds.

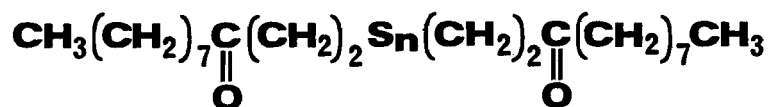
The remainder of this treatise is partitioned as follows. Chapters II, III, and IV provide background information on the natural occurrence and

structure of organopolysulphides, and on the vibrational assignments to date for sulphur-chain molecules. The experimental details of the present work are given in Chapter V, while the results and discussion are reported in Chapter VI. A brief summary of the findings and contributions to knowledge is then presented in Chapter VIII. Finally, an Appendix on normal coordinate calculations and the list of references appear at the end of the thesis.

CHAPTER 11

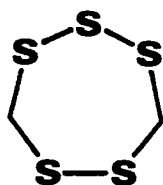
NATURAL OCCURRENCE OF ORGANOPOLYSULPHIDES

Organopolysulphides of varying degrees of complexity have been discovered in rather diverse sources in nature. Both symmetric and unsymmetric trisulphides with methyl, propyl, propenyl and allyl substituents are identifiable as constituents of the flavours and essential oils of onions, garlic, leeks, shallots and related substances,⁹ while tetrasulphides are detectable in some cases.^{9b,g} Methyl propyl trisulphide is also a component of cocoa aroma,¹⁰ and dimethyl trisulphide is an ingredient of the secretion from the mandibular glands of the *Paltothyreus tarsatus* species of ant.¹¹ Somewhat more complex examples of natural polysulphides are di-(3-oxoundecyl) tri- and tetrasulphide found in the Hawaiian algae *Dictyopteris plagiogramma* and *australis*.¹² The alga *Chondria californica* contains

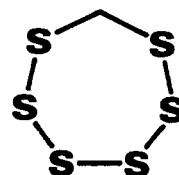


- (1) di-(3-oxoundecyl) trisulphide (n=3) and
(2) tetrasulphide (n=4)

the seven-membered ring lenthionine¹³ which also imparts the distinctive odour to the mushroom *Lentinus edodes* and further shows fairly strong antibiotic activity against some fungi and bacteria.¹⁴ Present as well in this mushroom is hexathiepane.¹⁴

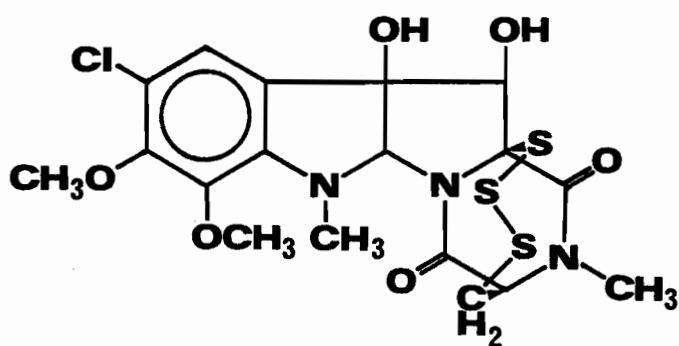


(3) lenthionine
(1,2,3,5,6-pentathiepane)

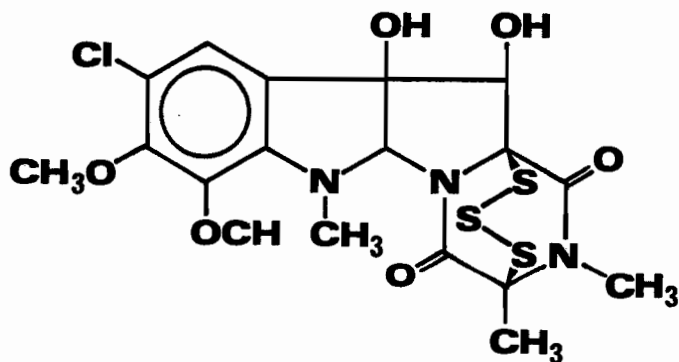


(4) hexathiepane

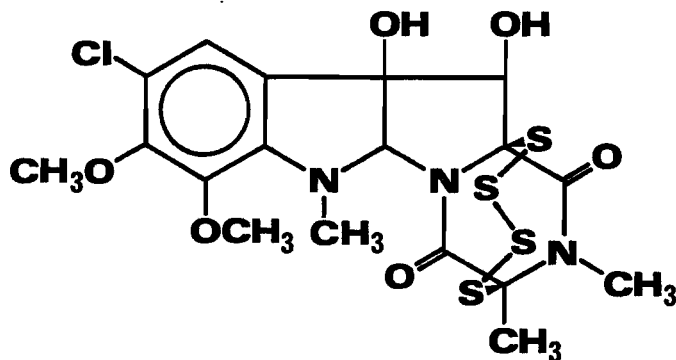
The compounds sporidesmin C, E and G are highly complex polysulphides forming part of a mixture of metabolites produced by the fungus *Pithomyces chartarum* that are capable of causing fatal liver damage in sheep.¹⁵ Sporidesmin E, in particular, is a highly toxic mould metabolite.^{15b} In view of the vastly different types of organopolysulphides now known to exist naturally



(5) sporidesmin C



(6) sporidesmin E



(7) sporidesmin G

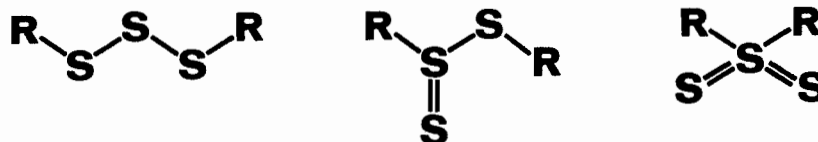
but usually in minor concentrations, their actual distribution in nature may be considerably greater than has been realized thus far.

It is noteworthy as well that polyalkyl polysulphide polymers are important as synthetic rubbers possessing outstanding resistance to weathering and to attack by oxygen and most solvents, but with low tensile strength and resistance to abrasion.¹⁶ Poly(ethylene) tetrasulphide, $(-SSCH_2CH_2SS-)_n$, known commercially as Thiokol A, is especially inert towards solvents because of its high sulphur content.

CHAPTER III

STRUCTURE OF ORGANOPOLYSULPHIDES

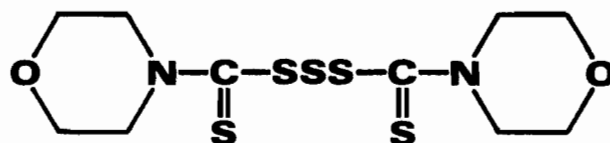
The sulphur fragments of organopolysulphides can theoretically be either branched or unbranched in structure owing to the ability of sulphur to assume a valency of two, four or six in its compounds. For example, there are three possible structures for a trisulphide:¹⁷



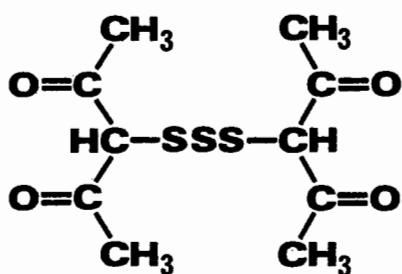
However, investigations by a variety of physical techniques have now established the straight-chain arrangement for organopolysulphides in general. Evidence for unbranched sulphur chains has emerged from ultraviolet,^{6,7,18} infrared^{6,18c,d} and Raman¹⁹ spectroscopic studies and from dipole moment,²⁰ molar refraction^{6,18e,19,21} and diamagnetic susceptibility²² measurements, as well as from structure elucidations by X-ray²³ and electron diffraction methods.^{17a,24} The sulphur rings S_6 , S_7 , S_8 , S_{10} , S_{18} , and S_{20} ^{2,3,5e,25} and the polysulphide anions S_3^{2-} , S_4^{2-} , S_5^{2-} and S_6^{2-} ²⁶ have also been shown to be unbranched by X-ray diffraction. Although branching may happen under special circumstances, e.g., in some reaction mechanisms,²⁷ the available data overwhelmingly favour the straight-chain formulation for organopolysulphides as a class.

Over the past thirty years or so, a great deal of structural information on organodisulphides, and to a lesser extent on organopolysulphides, has been accumulating in the literature.²⁸⁻³¹ Among the polysulphides whose structures have been elucidated are the simple trisulphides Me_2S_3 ,²⁴ $(\text{CCl}_3)_2\text{S}_3$,^{23c,d} $(\text{CF}_3)_2\text{S}_3$ ^{17a} and $(\text{I}-\text{CH}_2\text{CH}_2)_2\text{S}_3$ ^{23a,b} and also a variety of more complex linear and cyclic compounds including lenthionine³² (compd. 3),

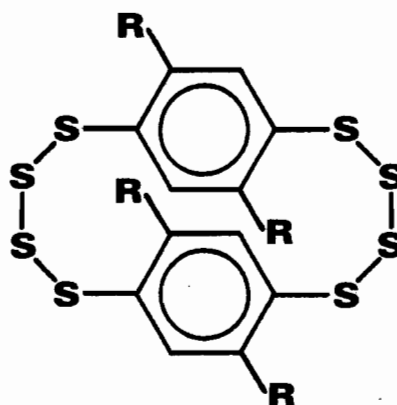
hexathiepane³³ (compd. 4), sporidesmin G (compd. 7) and several related species³⁴ as well as the following compounds^{33,35-39}



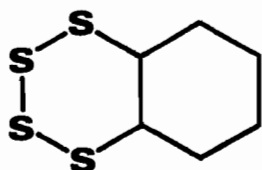
(8) bis-(4-morpholine thiocarbonyl) trisulphide



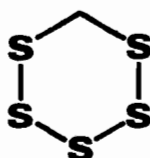
(9) 2,2'-trithiobis-(1,3-butanedione)



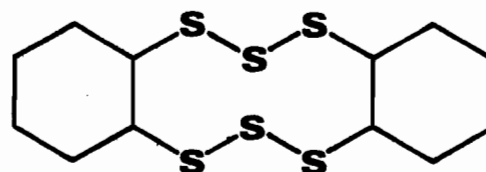
(10)* R=OCH₂CH₃



(11) 1,2,3,4-tetra-thiadekalin



(12) pentathiane



(13) perhydrodibenzo-1,2,3,6,7,8-hexathiecin

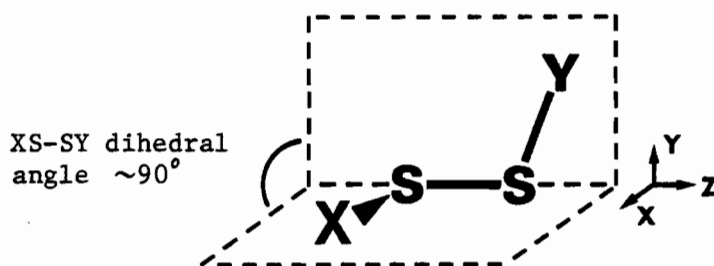
*7,15,17,19-tetraethoxy-2,3,4,5,10,11,12,13-octathiatricyclo (12,2,2,2^{6,9}) eicosa-6,8,14,16,17,19-hexaene

The available data indicate the S-S bond length in both di- and polysulphides to be usually in the range 2.02-2.08Å. Of note is the fact that cyclic tetra- and higher polysulphides tend to exhibit regular variations in S-S bond length around the ring. Thus, a tetrasulphide bridge across a diketopiperazine ring, as in sporidesmin G (compd. 7),³⁴ has a long central S-S bond and short end S-S bonds with values at the extremes of the above range. A very similar situation is found in compound 10.³⁷ On the other hand, compound 11 appears to have only a slightly longer S-S bond in the middle than at the ends of the chain.³⁸ The cyclic hexasulphide hexathiepane (compd. 4) shows a distinct pattern of alternating short-long S-S bonds around the ring,³³ whereas for the cyclic pentasulphide pentathiane (compd. 12), the pattern of S-S bonds is short-long-long-short.³³ The polysulphide anions S_3^{2-} , S_4^{2-} , S_5^{2-} and S_6^{2-} have S-S bond lengths over a significantly wider range than for organopolysulphides with some indication of regular variations across the chains.²⁶ Then again, the bond lengths reported for the sulphur rings S_6 , S_8 , S_{12} , S_{18} and S_{20} all fall within the narrow range 2.04-2.06Å.^{2,3,5e,25} A somewhat broader range (2.03-2.07Å) has been found for the S_{10} ring,^{25c} while a large range (2.00-2.18Å) occurs within the S_7 ring owing to its irregular structure^{25a} (*vide infra*). The C-S bond lengths in di- and polysulphides usually lie in the range 1.80-1.86Å for sp^3 -hybridized carbon and 1.74-1.80Å for sp^2 -hybridized carbon, irrespective of whether the compounds are linear or cyclic. The CSS valency angle is generally 102-106° for both sp^3 and sp^2 carbon, while the SSS valency angle is normally close to 105°*. Ring closure, however,

* Note the anomolous SSS and CSS angles of 114° and 98°, respectively, reported for $(I-CH_2CH_2)_2S_3$ in an early X-ray diffraction structure determination,^{23b} implying the need for a re-investigation of this molecule.

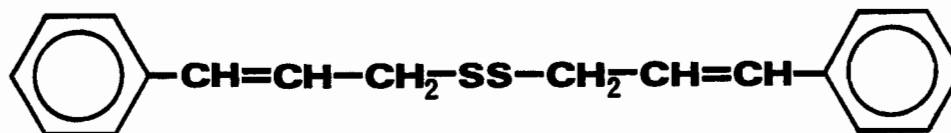
can constrain these angles to smaller values, e.g., the SSS angles in compound 11 are only 99.5° .³⁸ The SSS angles in polysulphide anions²⁶ and sulphur rings^{2,3,5e,25} are much like those of the polysulphides, although an unusually large angle has been observed for the S_3^{2-} moiety in BaS_3 (115°),^{26a,b} but not in SrS_3 (108°).^{26a}

A distinguishing characteristic of the bonding between divalent sulphur atoms is the marked tendency for the dihedral angle, the angle of intersection between the XSS and SSY planes in the XSSY fragment, to be near 90° , as depicted below. Since the mirror images are non-superimposable, the

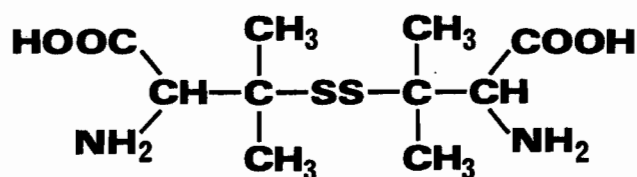


isolated entity is chiral and would exist as *dl* pairs. Among the array of acyclic di- and polysulphides whose structures have been solved, departures from 90° in the dihedral angles about the S-S bonds are usually less than 10° . Substantial deviations, in excess of 20° , have been reported, however.⁴⁰⁻⁴³ In the case of compound 14, the CS-SC dihedral angle of 66° has been suggested⁴² to relate to intramolecular hydrogen-bonding involving sulphur. On the other hand, the CS-SC dihedral angle of 115° found⁴³ for compound 15 may arise from steric interaction across the S-S bond (Sect. VI.A.1.i).

The geometric constraints from ring closure in di- and polysulphides can preclude 90° dihedral angles for the S-S bonds, resulting in strained

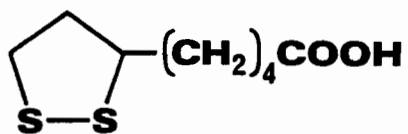


(14) dicinnamyl disulphide

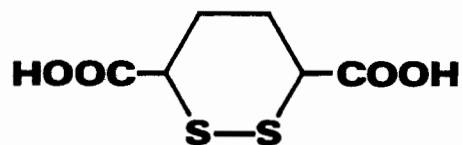


(15) D-pencillamine disulphide

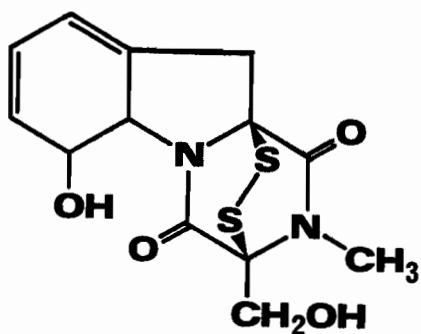
compounds. Particularly good examples of this circumstance occur among the disulphides. Thus, the 1,2-dithiolane ring (e.g., in compound 16) and the 1,2-dithiane ring (e.g., in compound 17) are restricted to CS-SC dihedral angles of $\sim 30^\circ$ and $\sim 60^\circ$, respectively.^{44,45} The CSSC unit in species such as compound 18 with a disulphide-bridged diketopiperazine ring is compelled to be close to planar with a dihedral angle of $\sim 10^\circ$.^{31,46} An even more extreme situation is that of compound 19 for which the CS-SC dihedral angles are essentially 0° .⁴⁷ An unexpected condition arises in the case of compound 20 in that it exists in the solid state in a pseudo-chair conformation with a CS-SC dihedral angle of 56° , despite the possibility of a tub-like conformation with a dihedral angle near 90° .⁴⁸ Molecular mechanics calculations⁴⁹ have indicated the former geometry to be the more stable primarily because of torsional strain about the C-S bonds in the latter.



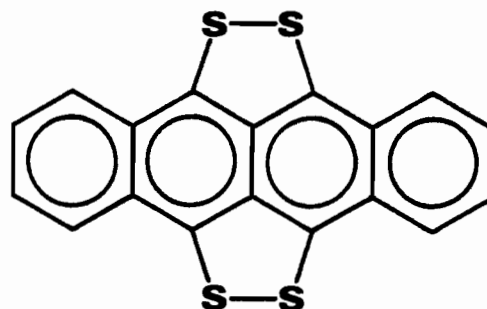
(16) D,L-thioctic acid



(17) *trans*-1,2-dithiane-3,6-dicarboxylic acid

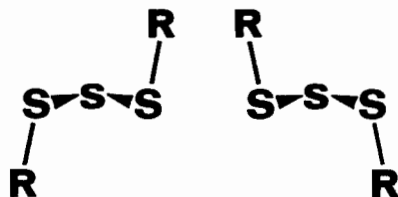


(18) gliotoxin



dihedral angles ($\sim 70^\circ$) and large SS-SS dihedral angle ($\sim 105^\circ$) found for the tetrasulphide bridge across a diketopiperazine ring,³⁴ as in sporidesmin G (compd. 7), appear to arise from intramolecular nonbonded interactions between the sulphurs and the ring.⁵⁰ The preference for a 90° dihedral angle about the S-S bond is evident in the structures of compounds 10³⁷ and 13,³⁹ and also of the sulphur rings S_8 , S_{12} , S_{18} and S_{20} ,^{2,5e,25} insofar as these large-ring molecules all adopt configurations affording dihedral angles near this value. The S_{10} ring has dihedral angles of $75-79^\circ$ with respect to six of its S-S bonds, and $122-124^\circ$ about the other four bonds.^{25c} An interesting comparison of structures are those of the seven-membered rings hexathiepane³³ (compd. 4) and S_7 ,^{25a} neither of which can accommodate $\sim 90^\circ$ dihedral angles throughout owing to the odd number of atoms. The latter molecule has a very distorted geometry with one planar SSSS fragment (SS-SS dihedral angle $\sim 0^\circ$) in the δ crystalline modification, the only one of at least four known forms yet to be structurally elucidated.^{25a} By way of contrast, the former molecule is twisted so as to have SC-SS dihedral angles of $\sim 45^\circ$ which permits fairly normal CS-SS and SS-SS dihedral angles in the vicinity of 90° .³³

An important ramification of the $\sim 90^\circ$ dihedral angles for the S-S bonds of unstrained organotrisulphides is the possible existence of two rotational isomeric forms. These are the *trans* and *cis* rotamers differing in the rotation of the substituents to opposite sides and to the same side of the sulphur plane, respectively. Only the *trans* rotamer is chiral. Electron diffraction data for gaseous Me_2S_3 have been interpreted in terms of the *trans* geometry,²⁴ while X-ray diffraction studies of $(CCl_3)_2S_3$ ^{23c,d}



trans rotamer (*dl* pairs)



cis rotamer

(I-CH₂CH₂)₂S₃^{23a,b} and compounds 8³⁵ and 9³⁶ have shown the *trans* configuration in the solid state. On the other hand, the inorganic trisulphide S₃(CN)₂⁵¹ and compound 21⁵² are *cis* in the solid state. Among the higher



(21) sulphur di(methylxanthate)

polysulphides, the number of different configurations consistent with 90° dihedral angles about the S-S bonds increases rapidly with sulphur chain length.

The incorporation of a sulphur chain into a cyclic system greatly limits its structural freedom. Lenthionine³² (compd. 3), hexathiepane³³ (compd. 4), sporidesmin G³⁴ (compd. 7) and compounds 11-13^{33,38,39} with six- to eight-membered polysulphide rings hence have exclusively *cis* CSSSC and SSSSS fragments, as does compound 10.³⁷ Similarly, the SSSSS moieties of the S₆ and S₈ sulphur rings are all *cis*.^{2,3,25b} On the other hand, the larger

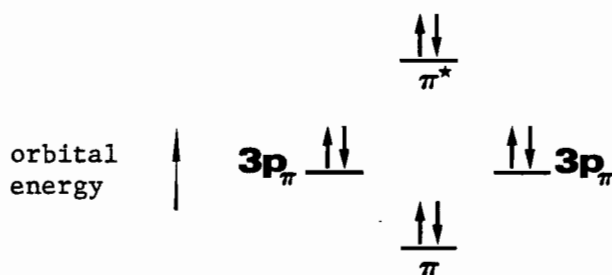
S_{12} ring has alternating *cis-trans* arrangements,^{25d} while S_{10} , S_{18} and S_{20} have complicated geometries with both *cis* and *trans* fragments.^{5e,25c,e}

It is worth noting that the CS-SC dihedral angle in organodisulphides influences appreciably other properties of the S-S bond. Thus there is an approximately linear correlation between bond length and dihedral angle wherein the bond extends on closing of the angle^{31,53} with an attendant weakening in the bonding; witness the greater susceptibility to S-S bond cleavage for 1,2-dithiolane derivatives with $\sim 30^\circ$ dihedral angles vs. unstrained disulphides with $\sim 90^\circ$ dihedral angles.⁵⁴ Also linearly dependent on dihedral angle is the splitting between the first two bands in the photoelectron spectra of disulphides, small angles giving large splittings.⁵⁵ In the case of the vibrational spectra, the $\nu(\text{S-S})$ band shifts to lower wavenumbers as the dihedral angle is reduced, again in a roughly linear relationship.³¹ The first absorption maximum in the ultraviolet-visible spectra of organodisulphides undergoes a red shift (to lower energy) as the CS-SC dihedral angle diminishes,⁵⁶ e.g., 1,2-dithiolane compounds (CS-SC dihedral angle $\sim 30^\circ$ ⁴⁴) are yellow, whereas unstrained disulphides are colorless.

The characteristic dihedral angle of $\sim 90^\circ$ with respect to the S-S bond is dictated by the nature of the bonding at sulphur. In a valence bond description of this bonding, Pauling⁵⁷ depicted the two σ bonds formed by each sulphur as involving mainly 3p atomic orbitals with the unshared valence electrons filling the remaining 3p orbital and an s orbital. Repulsion between the lone-pair electron clouds of the two sulphurs is then minimized when the lone-pair 3p orbitals lie in mutually perpendicular planes,

i.e., when these orbitals are the $3p_x$ of one sulphur and the $3p_y$ of the other sulphur with z being the S-S bond axis. This condition is concomitant with a 90° dihedral angle which, accordingly, gives the most stable geometry about the bond.

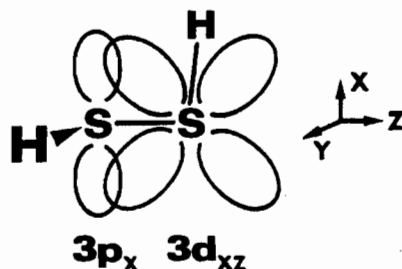
In the simple molecular orbital counterpart of this description, first discussed by Bergson,⁵⁸ π molecular orbitals are constructed as linear combinations of the overlapping lone-pair $3p$ atomic orbitals on sulphur. As illustrated below, the energies of the π bonding and π^* antibonding orbitals so generated are nonsymmetrically disposed with respect to the original $3p$ orbitals. Consequently, the lone-pair electron configuration $(\pi)^2(\pi^*)^2$ with doubly-occupied molecular orbitals is less stable than the config-



uration $(3p)^2(3p)^2$ with doubly-occupied atomic orbitals. The π interaction therefore destabilizes the S-S bond at all dihedral angles other than 90° , since only at this angle do the $3p$ orbitals of π symmetry become orthogonal with no net overlap. Extending this concept to sulphur chains, Bergson⁵⁸ showed 90° dihedral angles to again provide the least destabilization from

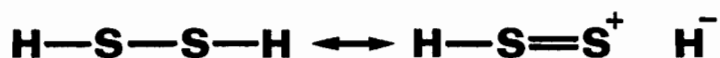
π bonding. Thus, overlap between 3p atomic orbitals of π symmetry on two or more neighboring sulphur atoms favours 90° dihedral angles. In noting that the bond angles observed for sulphur chains imply approximately sp^3 hybridization for the atoms, Bergson⁵⁸ also demonstrated on the basis of simple molecular orbital calculations that 90° dihedral angles minimize the destabilizing interaction between sp^3 lone-pair orbitals on adjacent sulphurs. This situation comes about because two of the molecular orbitals built-up from linear combinations of sp^3 lone-pair orbitals are really combinations of 3p orbitals alone owing to the cancellation of 3s orbital contributions.⁵⁹

From a consideration of experimental S-S bond lengths, Hordvik⁵³ has suggested that the prevalence of the 90° dihedral angle is at least partly due to maximization in this configuration of π electron donation from filled 3p orbitals into vacant 3d orbitals on sulphur. For S-S bonding along the z axis, these π overlaps are $3p_x-3d'_{xz}$ and $3p'_y-3d_{yz}$ where the prime distinguishes the orbitals of one sulphur from those of the other. The former interaction in the 90° geometry is illustrated below for H_2S_2 .



Since distortion from 90° diminishes these overlaps, the attendant lengthening of the S-S bond was thought by Hordvik⁵³ to reflect loss of double-bond

character from 3p-3d π bonding as well as destabilization from increased 3p-3p π interaction. Calculations on H_2S_2 by Saethre⁶⁰ have confirmed that the 3p-3d π bonding of the type pictured above is weakened as the dihedral angle is altered from 90° and these calculations also predicted a corresponding extension in the S-S bond. It should be noted, however, that the orientation of the 3p and 3d orbitals is also suitable for π bonding at a dihedral angle of 0° , although now this bonding occurs all in one plane, i.e., both overlaps would be $3p_x-3d_{xz}$ or $3p_y-3d_{yz}$ depending on the definition of the axes. Accordingly, it remains questionable whether 3p-3d π bonding favours significantly the 90° over the 0° dihedral angle. On the other hand, such bonding should favour either of these over intermediate angles, and may well shorten the S-S bond in the preferred 90° configuration. Another way in which the S-S bond of H_2S_2 has been suggested to be stabilized by π bonding is *via* a hyperconjugative delocalization of electron density, as expressed by the resonance⁶¹



The 90° dihedral angle is favoured because such transfer of electron density between the hydrogens through the 3p lone-pair orbitals is most feasible when the 3p orbital of one sulphur and the S-H bond of the other are in the same plane.

Subsequent to the rudimentary theoretical treatments of S-S bonding by Bergson,⁵⁸ there have been numerous semi-empirical^{55b,d,56,62-68} and

*ab initio*⁶⁹⁻⁷⁵ molecular orbital calculations on the bonding, particularly for the model disulphides H_2S_2 and Me_2S_2 . These studies have been concerned with understanding such aspects of disulphides as their ultraviolet, circular dichroism and photoelectron spectra, and the barriers to rotation about the S-S bond. Sulphur 3d atomic orbitals in addition to the 3s and 3p orbitals have been included in only some of the calculations. Nevertheless, the results are by and large in good agreement as regards the fundamental representations of the molecular orbitals and their relative energies throughout the dihedral angle range $0-180^\circ$. This is especially true of the orbitals occupied in the ground state because the 3d orbitals participate predominantly in molecular orbitals populated only in the excited states.^{56,62,65,68,70} The very similar descriptions obtained for the higher-energy occupied orbitals of H_2S_2 and Me_2S_2 in their ground states imply that these orbitals are characteristic of the S-S bond *per se*.

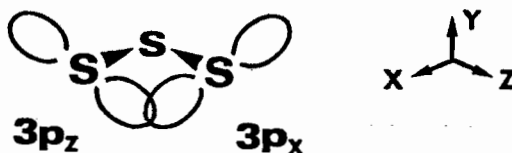
In accordance with the experimental dihedral angles for gaseous H_2S_2 (90.6°)⁶¹ and Me_2S_2 (85°)⁷⁶, the calculations have all yielded the minimum total energy for the molecules at dihedral angles near 90° . Since the S-S overlap population is greatest for this angle,^{56,69-71,73} the most stable geometry also has the strongest S-S bonding. Decomposing this overlap population for H_2S_2 into σ and π components, Boyd⁵⁶ found the former to increase monotonically as the dihedral angle is opened from 0° to 180° , and the latter to peak at approximately 90° because the smallest negative, i.e., antibonding, contribution from 3p-3p π overlap obtains at this angle. The net π component was determined to be positive at all dihedral angles, however, owing to

appreciable 3p-3d π bonding. Hence, the atomic orbitals of π symmetry were concluded⁵⁶ to be responsible for the 90° dihedral angle and for the strength of the S-S bond in this configuration. Furthermore, the charge density on sulphur in both H₂S₂ and Me₂S₂ has been computed to be least for this geometry,^{56,64,73} pointing to additional stabilization through delocalization of electron density away from the sulphur atoms towards the substituents.

The descriptions of the lone-pair orbitals on sulphur differ somewhat between various theoretical approaches. Whereas the extended-Huckel (EH)⁵⁶ and zero-differential-overlap (ZDO)⁶⁴ methods have shown essentially p-type and sp²-type lone-pairs, the complete-neglect-of-differential-overlap (CNDO)⁵⁶ method has indicated more sp³-type lone-pairs. Electron density maps plotted for H₂S₂ from EH data reveal the lone-pair zones to be roughly "C" shaped and most widely separated at the 90° dihedral angle.⁵⁶ Despite the uncertainties about the exact shapes of the lone-pair regions, the molecular orbital treatments to date of H₂S₂ and Me₂S₂ have generally depicted the two highest filled orbitals in the ground state as lone-pair orbitals formed primarily from the sulphur 3p atomic orbitals of π symmetry. In addition, repulsive interaction between these lone-pairs has been deduced by most authors to be chiefly responsible for the 90° dihedral angle. The stability of this geometry is apparently augmented, though, by 3p-3d π bonding and by redistribution of electron density away from the sulphur atoms. Despite these latter facets of S-S bonding, the outcome of the detailed calculations demonstrate that the original Bergson model of destabilizing 3p-3p π bonding at dihedral angles other than 90°⁵⁸ does essentially explain the preference for this angle about

the S-S bond. Consistent with this simple model are the planar configurations predicted for the first excited state of $\text{H}_2\text{S}_2^{63}$ and for the ions H_2S_2^+ and Me_2S_2^+ ,⁷⁷ in that the 3p-3p π bonding, maximized at dihedral angles of 0° and 180° , is expected to become stabilizing for the S-S bond once a lone-pair electron has been removed.

In the case of compounds such as organopolysulphides with three or more sulphur atoms bonded in sequence, the dihedral angles have been suggested⁷⁸ to be intrinsically distorted somewhat from 90° by repulsion between $3p_\pi$ lone-pair orbitals separated by two S-S bonds, since this interaction is most pronounced at 90° , as illustrated below. However, the simple



molecular orbital calculations on sulphur chains by Bergson⁵⁸ revealed no effects from long-range lone-pair interactions. More recent treatments of Me_2S_n ($n=3,4$),⁶² H_2S_n ($n=2-8$)⁷⁹ and polysulphide anions⁷⁹ have not addressed the issue of preferred structure, the last two studies in fact assuming planar sulphur chains. The available structural data on organopolysulphides (*vide supra*) show dihedral angles in the same range as that for organodisulphides. Furthermore, cyclic polysulphides, and also sulphur rings, generally adopt geometries with dihedral angles about the S-S bonds as close to 90° as ring closure will permit. At this juncture, therefore, and until evidence is presented to the contrary, the interaction between lone-pair orbitals on

next-but-one sulphur atoms in a chain may be presumed to influence the molecular geometry but minimally. Repulsion between nearest neighbour lone-pairs leads to a 90° preference for the dihedral angles with respect to the S-S bonds.

CHAPTER IV

VIBRATIONAL SPECTRA OF SULPHUR-CHAIN COMPOUNDS

Early reports⁸⁰ on the vibrational spectra of organopolysulphides, dating back some forty years in the literature, concerned the Raman spectra of Me_2S_3 , Et_2S_3 , and Et_2S_4 for which prominent $\nu(\text{S-S})$ vibrations were observed in the $500\text{--}435\text{ cm}^{-1}$ region. The $\nu(\text{S-S})$ wavenumbers in the series H_2S_n , Me_2S_n and Et_2S_n ($n=2\text{--}5$) were later noted by Féher *et al.*^{19b} to correlate with sulphur chain length as summarized below

Raman $\nu(\text{S-S})$ Vibrations (cm^{-1}) ^{19b}				
R	R_2S_2	R_2S_3	R_2S_4	R_2S_5
H	509	483	450, 483	439, 464, 485
Me	509	486	441, 487	-
Et	509, 523	486, 499	438, 486	435, 456, 488

However, fewer than the theoretical number of bands, equal to the number of S-S bonds, were generally discerned. Moreover, the ability to distinguish among the hydrogen polysulphides H_2S_n ($n=3\text{--}8$) in the Raman spectra was found to extend only to the pentasulphide owing to the virtually identical spectra for the higher members of the series.⁸¹ In an early investigation of the infrared spectra of Et_2S_3 and Et_2S_4 , Schotte^{18d} accredited absorptions at about 495 and 480 cm^{-1} for the two compounds to $\nu(\text{S-S})$ vibrations.

On the basis of force field calculations for H_2S_3 and H_2S_4 , Wieser and associates⁸² have confirmed the vibrations in the $500\text{--}450\text{ cm}^{-1}$ region to be highly S-S stretching in character. In the case of H_2S_3 in CS_2 solution, the antisymmetric $\nu(\text{S-S})$ vibration (out-of-phase stretching of the two S-S bonds) was detected as a weak shoulder at 470 cm^{-1} on the strong Raman band

at 488 cm^{-1} due to the symmetric (in-phase) $\nu(\text{S-S})$ vibration; the relative intensities are reversed in the infrared spectrum. On the other hand, because of the near degeneracy of the symmetric and antisymmetric $\nu(\text{S-S})$ vibrations for the terminal S-S bonds of H_2S_4 , the two give rise to a single feature at 484 cm^{-1} in both the Raman and infrared spectra along with a $\nu(\text{S-S})$ band near 450 cm^{-1} for the central S-S bond. The SSS angle deformation vibrations were observed in the Raman spectrum at 211 cm^{-1} for H_2S_3 and at 225 and 184 cm^{-1} for H_2S_4 . Although concluding that each compound exists as a single rotamer in solution, the authors⁸² noted their calculations to predict very similar spectra for various molecular geometries.

In a recent account of his own as yet unpublished Raman studies ($700\text{--}450\text{ cm}^{-1}$) of Me_2S_3 , Et_2S_3 and $n\text{-Pr}_2\text{S}_3$ in a book by Freeman,⁸³ the author assigned the intense band at $487\text{--}485\text{ cm}^{-1}$ for each molecule to the symmetric $\nu(\text{S-S})$ vibration. A second band at 482 cm^{-1} for Me_2S_3 , exposed by rotating a polarizing analyzer in the beam of scattered radiation, was tentatively ascribed to the antisymmetric $\nu(\text{S-S})$ vibration, whereas the high-frequency shoulder on the main $\nu(\text{S-S})$ feature of both Et_2S_3 and $n\text{-Pr}_2\text{S}_3$ was attributed to rotational isomerism with respect to the S-S bonds. Isomerism about the C-S bonds of these latter compounds, and about the C-C bonds for $n\text{-Pr}_2\text{S}_3$, was deduced on the basis of the multiple $\nu(\text{C-S})$ bands ($750\text{--}630\text{ cm}^{-1}$) compared to the single band (697 cm^{-1}) for Me_2S_3 . Freeman⁸³ assigned $\nu(\text{S-S})$ vibrations for the tri- and disulphide bridges of lenthionine (compd. 3) at 482 and 502 cm^{-1} , respectively, and a $\nu(\text{C-S})$ vibration at 647 cm^{-1} .

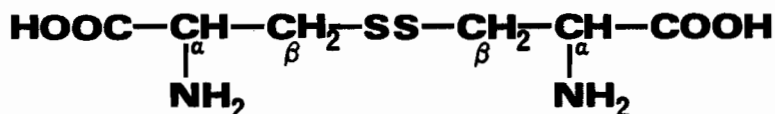
Other reports on the vibrational spectra of organopolysulphides include assignments by Schotte^{18d} of a band at $486\text{--}482\text{ cm}^{-1}$ in the infrared

spectra of 1,2,3,-trithianes and bands at 494 and 480 cm^{-1} in the spectrum of $(\text{HOOCCH}_2)_2\text{S}_4$ to $\nu(\text{S-S})$ vibrations. Minoura and Moriyoshi⁶ attributed infrared absorptions at 488-470 cm^{-1} and 655-647 cm^{-1} for Bz_2S_n ($n=3-8$) to $\nu(\text{S-S})$ and $\nu(\text{C-S})$ vibrations, respectively. For $(\text{Ph}_2\text{CH})_2\text{S}_n$ ($n=3-5$), Tsurugi and Nakabayashi⁸⁴ ascribed an infrared band at 491-486 cm^{-1} to a $\nu(\text{S-S})$ vibration and two bands, at 726-714 cm^{-1} and 512-501 cm^{-1} , to $\nu(\text{C-S})$ vibrations. The infrared and Raman spectra of $(\text{Me}_2\text{NC(S)})_2\text{S}_4$ have been assigned by Coleman and co-workers⁸⁵ with the aid of normal coordinate calculations which indicated the collection of bands at 515,461 and 432 cm^{-1} , prominent in the Raman spectrum, to be predominantly $\nu(\text{S-S})$ modes. The $\nu(\text{C-S})$ modes were concluded to contribute substantially to quite a few vibrations over the wide range 860-270 cm^{-1} . These results are suspect, however, owing to the planar SSSS geometry assumed, as opposed to the normal twisted geometry with 90° dihedral angles (Chapter III).

Finally, the vibrational spectra of some perhalo organopolysulphides have also received attention in the literature. Feher and Berthold^{19a} have attributed Raman bands at 510 and 474 cm^{-1} for $(\text{CCl}_3)_2\text{S}_3$ and at 503 and 430 cm^{-1} for $(\text{CCl}_3)_2\text{S}_4$ to $\nu(\text{S-S})$ vibrations, and a band at 444-442 cm^{-1} to a $\nu(\text{C-Cl})$ vibration. Desjardin and Passmore⁸⁶ have recently assigned $\nu(\text{S-S})$ vibrations at 516 and 490 cm^{-1} for $(\text{C}_2\text{F}_5)_2\text{S}_3$ and at 514,504 and 446 cm^{-1} for $(\text{C}_2\text{F}_5)_2\text{S}_4$. The $\nu(\text{C-S})$ vibrations were attributed to bands at 459-455 cm^{-1} and 435-433 cm^{-1} . However, because of the proximity of substituent vibrations, these assignments for the CCl_3 and C_2F_5 compounds are more tenuous than those for the methyl and ethyl analogues.^{19b} In an early discussion of the

infrared spectra of $(\text{CF}_3)_2\text{S}_n$ ($n=3,4$), Hazeldine and Kidd^{18c} suggested partial assignments only for the CF_3 groups. For $(\text{C}_6\text{F}_5)_2\text{S}_n$ ($n=3,4$), Peach⁸⁷ has proposed a single $\nu(\text{S-S})$ assignment at $484\text{--}475\text{ cm}^{-1}$ in the Raman spectra, and a single $\nu(\text{C-S})$ assignment at $512\text{--}510\text{ cm}^{-1}$.

In contrast to the paucity of vibrational information to date on organopolysulphides, there exists a wealth of such data for organodisulphides from both Raman and infrared spectra.^{31,83,88-94} Of late, there has been a resurgence of interest in the Raman spectra of disulphides^{31,66,91-94} stemming largely from the biological importance of the S-S functional group, notably in proteins incorporating the amino acid cystine. A primary goal of these recent studies has been to establish systematic correlations of $\nu(\text{S-S})$



(22) Cystine

with the conformational properties of the CCSSCC moiety. Since the $\nu(\text{S-S})$ vibrations are usually distinct features in the spectra of proteins, such correlations could render the Raman technique a powerful probe of cystine residues in proteins. Assignments hitherto for the $\nu(\text{S-S})$ vibration of disulphides span the range $550\text{--}465\text{ cm}^{-1}$ with the band position depending in part on the conformations about both the S-S and C-S bonds. Similarly, the $\nu(\text{C-S})$ vibrations fall in the range $750\text{--}570\text{ cm}^{-1}$ with the variation in wave-number relating significantly to conformational differences with respect to the C-S bonds and the C-C bonds of the substituents. As noted above, the

spectra of the trisulphides Et_2S_3 and $n\text{-Pr}_2\text{S}_3$ also manifest rotational isomerism.⁸³

Comparisons between the spectra of organopolysulphides and the symmetrical sulphur rings S_6 (D_{3d} symmetry), S_8 (D_{4d} symmetry) and S_{12} (D_{3d} symmetry), for which complete assignments have been proposed on the basis of normal coordinate calculations,⁹⁵ reveal considerable similarity. Because of degeneracies and mutual exclusion of vibrations between the infrared and Raman spectra, the rings yield simple $\nu(\text{S-S})$ patterns in the $480\text{--}420\text{ cm}^{-1}$ region. Both S_6 and S_8 display only two prominent Raman bands and one strong infrared absorption, while S_{12} differs only in an additional, very weak feature in each spectrum. The wavenumber patterns for the three allotropes resemble those for organotetra- and pentasulphides.^{19b} On the other hand, the low symmetry ring S_7 (C_s symmetry) exhibits seven separate $\nu(\text{S-S})$ vibrations (one per bond) over the wide range $530\text{--}350\text{ cm}^{-1}$ with considerable correspondence between the Raman and infrared spectra.⁹⁶ The S_{18} ring (C_{2h} symmetry) yields six $\nu(\text{S-S})$ vibrations ($480\text{--}420\text{ cm}^{-1}$) in the Raman spectrum and three in the infrared, while S_{20} (C_{2v} symmetry) gives eight $\nu(\text{S-S})$ bands ($470\text{--}410\text{ cm}^{-1}$) in the Raman and two in the infrared.^{4c} The SSS deformation vibrations of sulphur rings occur for the most part in the region $300\text{--}150\text{ cm}^{-1}$.

Recent reports by Janz *et al.*⁹⁷ on the spectra of K_2S_n ($n=3\text{--}6$), Na_2S_n ($n=3\text{--}5$) and Ba_2S_3 indicate $\nu(\text{S-S})$ vibrations over the range $505\text{--}355\text{ cm}^{-1}$ and SSS deformation vibrations over the range $340\text{--}205\text{ cm}^{-1}$ for the polysulphide anions. Depolarization data for K_2S_4 and Na_2S_4 as glasses permitted specific assignments for the symmetric and antisymmetric $\nu(\text{S-S})$ vibrations

of the terminal S-S bonds at 485 and 478 cm^{-1} , respectively, for the former species, and at 482 and 468 cm^{-1} , respectively, for the latter. The central $\nu(\text{S-S})$ vibration in the glasses occurs at 454 cm^{-1} for K_2S_4 and at 445 cm^{-1} for Na_2S_4 . These patterns are comparable to that for H_2S_4 .⁸² Quite different $\nu(\text{S-S})$ wavenumbers have been observed for the S_4^{2-} ion in aqueous solution (approximately 495, 450 and 415 cm^{-1}) and in solution in various amines (approximately 500, 435 and 400 cm^{-1}).⁹⁸ For the trisulphide anion in K_2S_3 , the symmetric and antisymmetric $\nu(\text{S-S})$ vibrations are apparently degenerate at 466 cm^{-1} , while three $\nu(\text{S-S})$ bands at 476, ~472 and 458 cm^{-1} have been noted for Ba_2S_3 at room temperature, the middle band increasing in relative intensity at higher temperatures.⁹⁷ The $\nu(\text{S-S})$ bands are found at 476 and 458 cm^{-1} in the case of the unstable species Na_2S_3 . Thus, the S_3^{2-} ion yields $\nu(\text{S-S})$ vibrations at somewhat lower wavenumbers than do organotrisulphides.^{19b,83} On the other hand, the $\nu(\text{S-S})$ bands for the S_3^- ion in solution in hexamethylphosphoramide or in various amines appear near 535 and 580 cm^{-1} in the Raman and infrared spectra, respectively,¹⁰⁰ the higher wavenumbers relating to the presence of one less antibonding electron in the S-S bonding.

The available Raman and infrared data on organopolysulphides point to the region 510-430 cm^{-1} for the $\nu(\text{S-S})$ vibrations, while generalizations for the $\nu(\text{C-S})$ and deformation vibrations do not seem warranted at this juncture. Moreover, the studies reported to date have been limited in scope. In particular, the effects of rotational isomerism on the spectra have received minimal attention. The present work has been aimed at ameliorating this deficiency in the literature through detailed investigation of a variety of organotrisulphides and some homologues as outlined in the Introduction.

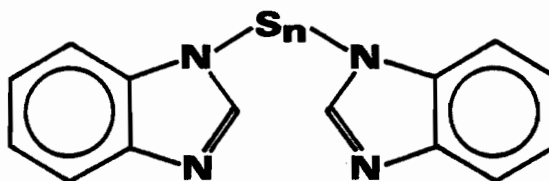
CHAPTER V

EXPERIMENTAL

V.A Preparation and Purification of Compounds

V.A.1 Dialkyl Compounds

The Me_2S_3 used in this work was a commercial sample (Eastman Organic Chem. Co.) that was purified by fractional distillation *in vacuo* twice (bp $46^\circ\text{C}/6$ torr). The $\text{Me}_2\text{S}_3\text{-}d_6$, a 99% pure sample prepared by Harpp and Back,¹⁰¹ was kindly provided by Dr. Harpp (McGill University) who also supplied samples of Et_2S_3 , $n\text{-Pr}_2\text{S}_3$, $i\text{-Pr}_2\text{S}_3$ and $t\text{-Bu}_2\text{S}_3$. These latter trisulphides were obtained by the reaction of the appropriate thiols with SCl_2 .¹⁰² Additional quantities of Et_2S_3 , $i\text{-Pr}_2\text{S}_3$ and $t\text{-Bu}_2\text{S}_3$ and also a sample of Et_2S_4 were synthesized by the present author according to the method recently developed by Harpp *et al.*¹⁰³ which involves reacting the thiol precursors with the sulphur-transfer reagents



1,1'-thio- and -dithiobisbenzimidazole
($n=1$ and 2 , respectively)

These reagents were generously made available by the authors.¹⁰³ In a typical preparation, 0.040 mole of freshly distilled thiol (Aldrich Chem. Co.) dissolved in 50 ml benzene was added dropwise over a half-hour period to a stirred slurry of 0.015 mole of transfer reagent in 75 ml benzene.*

* Although Harpp *et al.*¹⁰³ recommended a $2:1$ molar ratio of thiol to reagent with a $0\text{--}10\%$ excess of reagent depending on its purity, the present reactions proceeded smoothly when a significant excess of thiol was employed.

After stirring overnight, the solid benzimidazole by-product was filtered off and the solvent and excess thiol were removed on a rotary evaporator. Redissolving the residue in CCl_4 and refiltering served to eliminate any remaining benzimidazole and/or unreacted transfer reagent, following which removal of the solvent by rotary evaporation yielded a yellow liquid. The Raman spectrum of this product in the $\nu(\text{S-S})$ region revealed appreciable contamination from other sulphur compounds, necessitating further purification by fractional distillation *in vacuo*: Et_2S_3 , pale yellow liquid, bp $57^\circ\text{C}/2$ torr; *i*- Pr_2S_3 , clear liquid, bp $39^\circ\text{C}/1$ torr; *t*- Bu_2S_3 , clear liquid, bp $45^\circ\text{C}/1$ torr; Et_2S_4 , canary yellow liquid, bp $67\text{--}68^\circ\text{C}/1$ torr. The Raman spectra of the purified samples showed that the impurities had been reduced to very low levels.

The commercial sample (Eastman Organic Chem. Co.) of Et_2S_2 used in this study was purified by fractional distillation under atmospheric pressure, bp $152\text{--}153^\circ\text{C}$.

V.A.2 Dibenzyl Compounds

The Bz_2S and Bz_2S_2 samples were obtained commercially (Eastman Organic and Aldrich Chem. Co., respectively) and were recrystallized as white needles from absolute ethanol: Bz_2S , mp $48.5\text{--}49.5^\circ\text{C}$ (lit.^{6,104} 48.5°C , $49\text{--}50^\circ\text{C}$); Bz_2S_2 , mp $70.5\text{--}71.5^\circ\text{C}$ (lit.^{6,105} 71°C , $71\text{--}72^\circ\text{C}$). Recrystallized samples of Bz_2S_3 and Bz_2S_4 were generously provided by the research group of Dr. Harpp. The trisulphide derivative was also prepared by the present author following the procedure outlined above (Sect. V.A.1), except that

an excess of transfer reagent (~10%) was employed to minimize the presence of residual, nonvolatile benzenethiol in the product. With some difficulty, the yellow oil isolated from the reaction was induced to crystallize from absolute ethanol/hexanes as pale yellow flakes of Bz_2S_3 , mp 48-49.5°C (lit.^{6,105} 49°C). The purity of the Bz_2S_3 was confirmed by the appearance of a singlet CH_2 resonance at 4.0 ppm (lit.¹⁰⁶ 3.88 ppm, CS_2 solution) in the ^1H nmr spectrum (CCl_4 solution) compared to the singlet at 3.5 ppm (lit.¹⁰⁶ 3.49 ppm, CS_2 solution) for Bz_2S_2 . The Raman spectra of all the benzyl compounds exhibited no evidence of significant contamination from other homologues.

V.A.3 Diphenyl Compounds

The trisulphides $(4\text{-R-Ph})_2\text{S}_3$ ($\text{R}=\text{Me}$, OMe , Br , $t\text{-Bu}$) were again kindly supplied as recrystallized solids by Dr. Harpp's group. Further purification of these compounds was not attempted. The disulphide $(4\text{-Me-Ph})_2\text{S}_2$ was a commercial sample (Eastman Kodak Co.) that was purified by recrystallization from acetone, mp 45-46°C (lit.^{104,105,107} 47-48°C, 47°C, 46°C), while the disulphides $(4\text{-R-Ph})_2\text{S}_2$ ($\text{R}=\text{OMe}$, Br) were produced from the action of iodine on the appropriate thiols (Aldrich Chem. Co.) in alkali solution as reported by Wallace.¹⁰⁸ Thus, 1.1g of iodine was added in small portions over an hour period to a vigorously stirred solution of 0.010 mole of thiol in 8 ml of 15% aqueous NaOH under an N_2 atmosphere. Stirring overnight resulted in a whitish precipitate that was filtered off and recrystallized from acetone as very pale yellow flakes: $(4\text{-MeO-Ph})_2\text{S}_2$, mp 42.5-43.5°C (lit.^{109,110} 44-45°C); $(4\text{-Br-Ph})_2\text{S}_2$, mp 93.5-95°C (lit.^{109,111} 93-94°C).

V.B Instrumentation

Infrared spectra were recorded on a dual-beam Perkin-Elmer model 521 grating infrared spectrophotometer using a normal slit program setting of 1000. Accordingly, the spectral resolution is about 2.2 cm^{-1} in the region $3000\text{--}2700\text{ cm}^{-1}$ and decreases from about 0.8 to 2.1 cm^{-1} across the region $1600\text{--}400\text{ cm}^{-1}$. The liquids were run neat in a KBr cell of 0.025 mm pathlength, while the solids were studied as Nujol mulls between KBr plates. The reproducibility of all the spectra was verified in at least duplicate scans using fresh samples. The spectra were calibrated against standard polystyrene absorptions and the known air peaks at 1653.3 and 667.3 cm^{-1} . Band positions are considered accurate to $\pm 2\text{ cm}^{-1}$ in the lower of the abovementioned regions, and $\pm 5\text{ cm}^{-1}$ in the upper region.

Raman spectra were recorded on a Jarrell-Ash model 25-300 Raman spectrometer equipped with an FW 130 photomultiplier tube (Electron Tube Division, I.T.T.) and operated with an argon ion laser (Coherent Radiation, model 52K). The liquids and solids were run in sealed 1-mm capillary tubes, while solutions were run in a thin-walled 5-mm nmr tube cut to about 50 mm in length and bent at roughly 45° in the middle to obviate the build-up of air bubbles at the point of laser irradiation. In all cases, the scattered radiation was measured at right angles to the direction of incident radiation. A narrow bandpass filter situated in the laser beam before the sample served to exclude plasma emission lines of the laser from the spectra. In view of the yellow tinge to most of the samples, the 515.5 nm green exciting line was used to help minimize any photochemical

decomposition. Apart from Et_2S_4 , however, the compounds proved to be remarkably stable under laser irradiation as intense as 300 mW, with only slow break-down as evidenced by the growth of new bands in the $\nu(\text{S-S})$ region of the Raman spectra. The laser power at the sample was usually kept below 200 mW. Still, it was found desirable to cool the solids to approximately -40°C in a stream of cold nitrogen gas to prevent drifting intensities while obtaining the spectra. Depending on the sample, the monochromator slits were adjusted to give a spectral resolution of $2\text{--}3\text{ cm}^{-1}$. However, due to the fixed slit widths during a scan, the resolution improves somewhat with increasing vibrational wavenumber across the spectrum, e.g., a mechanical slit setting of 76 microns corresponds to a resolution of 2.0 cm^{-1} at 500 cm^{-1} , but 1.8 cm^{-1} at 1500 cm^{-1} . At the same time, there is an inherent 'falling-off' in band intensity on scanning to higher wavenumbers both because of the direct dependence of intensity on the difference $(\nu_0 - \Delta\nu)^4$ between the Rayleigh line frequency ν_0 and the Raman shift $\Delta\nu$,¹¹² and because of the decreasing sensitivity of the photomultiplier tube. Despite these influences, good signal-to-noise ratios were generally achieved over the full spectral regions of interest owing to the strong Raman scattering of the samples. The reproducibility of the spectra was confirmed by performing several scans for each compound. Calibration of the spectra was afforded by standard neon emission lines with estimated uncertainties on the measured wavenumbers of $\pm 2\text{ cm}^{-1}$ except for broad or very weak features.

The depolarizing characteristics of the Raman vibrations in the liquid

and solution states were investigated by conventional techniques.¹¹³ Thus, the band intensities were separated into parallel and perpendicular components either by rotating a polaroid analyzer in the beam of scattered radiation while keeping the polarization plane of the incident beam parallel to the monochromator slit, or by rotating, by means of a half-wave plate, the plane of the incident radiation itself with the analyzer removed. In both arrangements, a quartz scrambler wedge was placed in front of the slit to depolarize the light entering the monochromator, the optics of which may otherwise affect the intensities. For the first method, a depolarization ratio of $\frac{3}{4}$ defines a depolarized vibration, i.e., one that totally destroys the polarization of the incident beam. The corresponding value for the second method is $6/7$. Smaller ratios signify polarized vibrations that at least partially preserve the original polarization. The liquid-state spectra below 700 cm^{-1} were generally studied by the first technique, while the higher regions and the solution spectra were studied by the second. Although less reliable, the latter approach has the advantage of considerably better signal-to-noise ratios in the absence of the analyzer. In any event, apart from some numerical estimates of depolarization ratios for Me_2S_3 and $\text{Me}_2\text{S}_3\text{-}d_6$ on the basis of band areas, only the qualitative character of the vibrations, polarized or depolarized, has been determined.

The low-temperature Raman spectra were obtained with a model 21 Cryodyne closed-cycle helium refrigerator (Cryogenics Technology Inc.) capable of regulating temperature in the range $350\text{--}15\text{K}$ within $\pm 0.5^\circ$, i.e., the temperature fluctuates between the value set on the temperature controller and 1° lower. Samples were sealed in 1-mm capillary tubes under vacuum.

The tubes were mounted horizontally in a slotted copper block using indium foil around the tubes to ensure good heat conduction away from the samples. A cut-away in the copper block permitted laser irradiation over approximately 5 mm of the samples.

The accuracy of the temperature read-out of the cryogenic unit was investigated on the basis of the observed melting points for CCl_4 (lit.¹⁰⁴ -22.99°C), CHCl_3 (lit.¹⁰⁴ -63.5°C) and CH_2Cl_2 (lit.¹⁰⁴ -95.1°C). These samples were freshly purified by drying over CaCl_2 followed by fractional distillation. In the case of CHCl_3 , the ethanol preservative was initially removed by sequential washings with concentrated H_2SO_4 , dilute NaOH solution and distilled water. Visual monitoring of the samples in the instrument showed gradual melting across the 5 mm exposed region over a range of about 3° , the middle of the range lying within 5° of the literature melting points. However, the estimated melting points varied from one experiment to another on a given sample depending on how firmly the tube was mounted in the copper block.* In order to assess the thermal effects of laser irradiation, the melting of the reference compounds was studied also on the basis of the variations with temperature in the depolarization ratios for the strongly polarized $\nu(\text{C-Cl})$ vibrations at 459, 668 and 700 cm^{-1} for CCl_4 , CHCl_3 and CH_2Cl_2 , respectively. The melting point was taken to be the temperature corresponding to a sharp decrease in the depolarization ratio, after which the value remained constant for the liquid-state vibration.

* It should be noted that the determinations of the melting points were complicated by the tendency of the samples to turn glassy upon approaching the melting temperature.

These changes for all three compounds occurred at temperatures within 3° of the literature melting points and were highly reproducible for a given sample once mounted in the cryogenic unit. On the other hand, the melting points measured in this fashion varied by a few degrees between different mountings of the sample. The conclusions drawn from the above observations are that laser irradiation produces minimal thermal effects, but that the temperature at the sample is governed significantly by the firmness of the contact between the capillary tube, indium foil and copper block. Nevertheless, the melting points determined for CCl_4 , CHCl_3 , and CH_2Cl_2 deviate from the literature values by generally no more than $\pm 5^{\circ}$ which is hence considered to be the uncertainty in the reported temperatures. A somewhat greater uncertainty may apply for temperatures below 175K, but in view of the imprecise nature of the phase changes observed for the dialkyl trisulphides (Sect. VI.A.1), this possibility was not explored in depth.*

Raman spectra of the benzyl compounds at approximately 60°C were obtained using a heated sample holder. The ^1H nmr spectra of Bz_2S_2 and Bz_2S_3 were recorded at ambient temperature on a Varian T-60 instrument.

* Attempts to study the melting of ethanethiol (lit.¹⁰⁹ -144.4°C) were abandoned when the sample could not be induced to solidify in the capillary tube.

CHAPTER VI

RESULTS AND DISCUSSION

VI.A Dialkyl Polysulphides

The infrared and laser-Raman spectra recorded for Me_2S_3 , $\text{Me}_2\text{S}_3\text{-d}_6$, Et_2S_3 , $n\text{-Pr}_2\text{S}_3$, $i\text{-Pr}_2\text{S}_3$, $t\text{-Bu}_2\text{S}_3$ and Et_2S_4 as liquids at ambient temperature are reproduced in Figs. 1-7, while the corresponding vibrational wavenumbers and proposed assignments are tabulated in Section VI.A.2 . Only the accessible regions expected to show fundamental vibrations of the molecules were examined. The present Raman data for Me_2S_3 , Et_2S_3 , $n\text{-Pr}_2\text{S}_3$ and Et_2S_4 are by and large in good agreement with prior accounts of the spectra,^{19b,80,83} apart from the superior band resolution in this work compared to the early studies^{19b,80} owing to the use of laser instead of mercury-lamp excitation. On the other hand, the present infrared data for Et_2S_3 and Et_2S_4 are in only fair agreement with the previous report^{18d} on the spectra in that several of the earlier-noted absorptions, presumably due to impurities, were not observed in this work. The vibrational spectra of $\text{Me}_2\text{S}_3\text{-d}_6$, $i\text{-Pr}_2\text{S}_3$ and $t\text{-Bu}_2\text{S}_3$ have yet to be described in the literature.

Prolonged exposure of the trisulphides to laser radiation tended to bring about the slow growth of two extra Raman features, one at $50\text{--}70\text{ cm}^{-1}$ to low energy of the primary $\nu(\text{S-S})$ vibration and the other $20\text{--}30\text{ cm}^{-1}$ to higher energy (see, e.g., Fig. 2b). These additional bands are attributable to the tetra- and disulphide, respectively,^{19b} and therefore point to thermally or photolytically induced disproportionation of the trisulphides. In the case of Et_2S_4 , even low-power irradiation (60–80 mW) for short periods caused the appearance of a new feature at 458 cm^{-1} along with enhancement of intensity of the 488 cm^{-1} band relative to the 438 cm^{-1} band of the tetrasulphide. These observations are consistent with disproportionation of the

tetrasulphide to the penta- and trisulphide.^{19b} In support of the disproportionation explanation for the gradual changes noted in the Raman spectra, studies by nmr spectroscopy of the thermal decomposition of Me_2S_3 and Me_2S_4 have revealed the initial stages in each instance to involve the formation of the next higher and lower homologues.¹¹⁴ Moreover, the tetrasulphide was discovered to break-down considerably more easily than the trisulphide, in line with the present findings for Et_2S_4 and Et_2S_3 . Free radical mechanisms have been proposed for these disproportionation reactions.^{114,115}

Selected low-temperature (approximately 15K) Raman spectra of Me_2S_3 , Et_2S_3 , $i\text{-Pr}_2\text{S}_3$ and $t\text{-Bu}_2\text{S}_3$ are displayed in Figs. 1,3,5 and 6. The $t\text{-Bu}_2\text{S}_3$ sample solidified quite readily when cooled below its freezing point (17°C)¹⁰⁹ after which it could not be induced to undergo further detectable change with variation in the temperature. In contrast, the other trisulphides (freezing points near -70°C)¹⁰⁹ showed pronounced hysteresis, i.e., the phases observed depended markedly on the thermal history of the samples. Thus the compounds failed to solidify upon initial cooling down to 15K, but rather persisted as transparent glasses* down to the vicinity of 100K where a sudden 'fracturing' of the glasses was visibly apparent. On reheating, however, the samples reverted to clear glasses at around 100K^\dagger , indicating

* The glassy state has previously been noted for example of thiols,¹¹⁶ sulphides¹¹⁷ and polysulphide anions,⁹⁷ and also for Me_2S_2 .^{90b}

[†] In one experiment with Me_2S_3 , the fracturing was sufficiently violent to snap off one end of the capillary tube. As the sample began to clear on reheating a significant portion flowed to this end under the influence of the vacuum in the cryogenic chamber, showing considerable mobility in the glassy phase.

the fracturing phenomenon to be merely a physical effect of shrinkage with decreasing temperature. Solidification of the trisulphides could be initiated by further reheating the glasses to a temperature above 120K and the process could be monitored visually. Although tending to accelerate rapidly with increasing temperature, this change of state still required generally in excess of an hour to complete at 140K for Me_2S_3 and Et_2S_3 , and at 160K for $i\text{-Pr}_2\text{S}_3$. In the case of this last compound, the conversion remained quite gradual even at 190K. Because of the marked temperature dependence of the phase transformation for each trisulphide, the process could be arrested in progress simply by recooling to 15K, and hence the spectra of metastable states in-between the glassy and solid states were obtained. These metastable phases were usually of highly non-uniform composition across the sample with rather dramatic differences occurring between spectra recorded at various points along it. The sequence of events leading to the solid state was found to be essentially reproducible for all three trisulphides, despite some variation in the time-dependence of the changes from one experiment to another on a given sample. It should be mentioned, though, that upon first cooling the samples from room temperature down to temperatures in the range 120-190K, no solidification was discerned over test periods as long as three hours, underscoring the importance of thermal history in the phase transformations. The possible influences of the physical and chemical characteristics of the capillary tubes containing the samples on the phase changes were not investigated.

As anticipated, the band resolution in the Raman spectra of any of

the liquid, glassy, metastable or solid phases observed for the trisulphides was seen to improve gradually with lowering of the temperature. The best resolution achieved at 15K came about from cooling in 5° steps every 5-10 minutes from the initial temperature down to about 80K below which the rate of cooling appeared to be inconsequential. Such cooling in the case of the metastable phases means that the states examined were actually formed over a fairly wide range of temperature. Repeated and varied attempts at enhancing the resolution in the solid-state spectra of *i*-Pr₂S₃ and *t*-Bu₂S₃ beyond that of Figs. 5d and 6c were unsuccessful. The broadness of some of the bands in these spectra suggests that the positions of the molecules (or at least of their methyl groups) in the crystal lattice are less well defined than for Me₂S₃ and Et₂S₃ whose spectra (Figs. 1d and 3d) exhibit superior resolution. Nonetheless, the solid states obtained for all four trisulphides are indicated to be polycrystalline by their complete scrambling of the polarization of the laser radiation,¹¹³ as evidenced by the invariance in the band intensities with rotation of the polarization plane of the incident laser beam (Sect. V.B). On the other hand, the vibrations of Me₂S₃, Et₂S₃ and *i*-Pr₂S₃ as glasses showed depolarizing characteristics virtually identical to those of the corresponding liquid-state vibrations, implying a random orientation of the molecules in the glass as well as in the liquid. This close similarity between the liquid and glassy states holds true only up to the point of fracturing of the latter, however, since afterwards the depolarization ratios increased sharply in most experiments. It seems, therefore, that the fragmented glasses interfere with the laser light in much the same way as do polycrystalline solids.

Although manifesting comparable low-temperature behavior as outlined above, the trisulphides Me_2S_3 , Et_2S_3 and $i\text{-Pr}_2\text{S}_3$ were each discovered to possess unique characteristics. The peculiar aspect for Me_2S_3 is the existence of two distinct polycrystalline variations termed Solid I and Solid II (Figs. 1c and 1d). Solid I was the first to form in the glass at 140K (*vide supra*), though it subsequently transformed into Solid II. This conversion proceeded extremely slowly at 140K, but accelerated dramatically with increased temperature. At 180K, Solid II was formed preferentially in the glass. Complete solidification at 160K, on the other hand, resulted in a mixture of the solids giving spectra comprised of well-resolved bands of both phases with considerable variation in the relative band intensities across the sample in most experiments, indicating variable composition. Much the same mixed-phase spectra were recorded during the transition from Solid I to Solid II. Similarly, the spectra of the large range of metastable phases 'frozen-out' during the glass-to-solid transformation consistently analyze as superpositions of the spectra of Solids I and II, despite the generally poor resolution of the bands and the appearance of a few additional weak bands in some cases. These extraneous features probably reflect local structural distortions within the metastable states. Once attained, the Solid II could not be made to convert to Solid I by altering the temperature, demonstrating the transformation from the latter to the former to be irreversible. Discussion of the implications of these observations for Me_2S_3 is deferred to Section VI.A.1.ii.

The outstanding aspect of the low-temperature behavior of Et_2S_3 , is the disappearance of Raman bands between the liquid and solid states in

two essentially separate steps. Several of the room-temperature bands gradually diminished in relative intensity with cooling of the liquid and glassy states and were nearly eliminated from the spectrum of the fractured glass at 15K. These features, which clearly originate in one or more comparatively unstable rotamers present in the liquid and glass, are entirely missing from the spectra (Figs. 3c and 3d) of the metastable and solid states observed for the trisulphide. Apart from these absences, however, the only significant difference between the spectra of the fractured glass and metastable states is the superior resolution in the latter that reveals the majority of the bands below 800 cm^{-1} to actually consist of at least two components, the minor of which is discernible as a shoulder on the other (Fig. 3c). These shoulders were seen to vary in relative intensity between different metastable phases and to vanish with progressive solidification of the sample, showing the metastable states to consist of at least a pair of rotamers with quite similar stability. Of particular note is the disappearance of the $\nu(\text{S-S})$ band lying in-between the two $\nu(\text{S-S})$ vibrations that persist in the spectrum (Fig. 3d) of the final crystalline phase obtained for the trisulphide. These latter $\nu(\text{S-S})$ bands are consistent with the presence of a single rotamer in the eventual solid state.

The above findings for Et_2S_3 strongly imply the co-existence in the liquid of a minimum of three rotamers: two of approximately equal stability and a third, less favoured rotamer. Analogous rotational isomerism has previously been proposed for the disulphides EtSSMe and Et_2S_2 in light of the multiplicity of vibrations in the $400\text{-}150\text{ cm}^{-1}$ region of the Raman

spectra for the unannealed solids.^{94b} Similar 'band counts' in this reaction for Et_2S_3 also attest to the presence of no fewer than three rotamers in the liquid. Thus the exclusion of species between the liquid and metastable states leaves 11 detectable vibrations compared to the 7 theoretically predicted for a single rotamer (Sect. VI.A.2). Accordingly, at least two rotamers remain at this stage, as is confirmed by the disappearance of an additional 5 bands between the metastable and solid states, leaving 6 observable vibrations for the one rotamer in the crystalline solid. The number of vibrations attributable to each group of Et_2S_3 rotamers is within theoretical expectations.

Unlike the situation for Et_2S_3 the elimination of Raman bands between the liquid and solid states of $i\text{-Pr}_2\text{S}_3$ seems to take place in only one step. Despite the gradual demise in relative intensity for several of the room-temperature bands upon cooling, these features remain with a large proportion of their original intensities in the spectrum of the fractured glass at 15K. Consequently, only the spectra (Fig. 5c) of the metastable states clearly show the disappearance of bands during the formation of the solid; exclusion of these bands occurs in the early stages of solidification to which Fig. 5c corresponds. A single crystalline form was obtained for the trisulphide (Fig. 5d). Since all the vibrations absent for the solid vanish at apparently equal rates, only two rotamers, or groups of rotamers of comparable stability, can be deduced to co-exist in the initial liquid. However, since only one of the $\nu(\text{S-S})$ vibrations for a trisulphide rotamer is intense in the Raman spectrum (Sect. VI.A.2), the occurrence for the metastable states of two $\nu(\text{S-S})$ bands in-between those for the dominant rotamer suggests the

presence of a pair of less stable species in both the metastable and liquid states. In the case of the disulphide $i\text{-Pr}_2\text{S}_2$, for which the temperature-dependence of the vibrational spectra has not yet been reported in the literature, the room-temperature spectra of the liquid have been interpreted in terms of two rotamers.^{31,92} It is interesting that the higher-energy group of rotamers for $i\text{-Pr}_2\text{S}_3$ disappears less readily during solidification than does the highest-energy group of rotamers for Et_2S_3 . This implies a greater relative stability for this group in the former case, consistent with the outcome of the enthalpy difference calculations discussed below.

The relative enthalpies for the rotamer of Et_2S_3 and $i\text{-Pr}_2\text{S}_3$ were estimated on the basis of the van't Hoff equation adapted for vibrational studies:¹¹⁸

$$\ln \left[\frac{(I/I')_1}{(I/I')_2} \right] = \frac{-\Delta H}{R} \left[\frac{1}{T_1} - \frac{1}{T_2} \right]$$

where $(I/I')_i$ is the intensity ratio at temperature T_i for two vibrations belonging to different rotamers, R is the universal gas constant and ΔH is the enthalpy difference. The equation implicitly assumes that ΔH and the entropy difference (ΔS) between the rotamers are independent of temperature over the range investigated. According to this relationship, a plot of $\ln (I/I')$ against $1/T$ yields a straight line of slope $-\Delta H/R$ and thence ΔH . The bands chosen for the variable-temperature measurements were the pair of corresponding $\nu(\text{C-S})$ vibrations for the rotamers at 670 and 644 cm^{-1} for Et_2S_3 , and at 626 and 595 cm^{-1} for $i\text{-Pr}_2\text{S}_3$. In view of the smallness of

the enthalpy differences for both trisulphides, the ratios of peak heights were used as approximations for the intensity ratios in the graphical analysis. The determination of accurate band area ratios required for a rigorous treatment would be complicated for these trisulphides by the fact that at least one component of each $\nu(\text{C-S})$ band pair is a composite of vibrations for two or more rotamers, as well as by overlap within the pairs. This overlap is not sufficient to significantly affect the peak height measurements, however. To help place in perspective the findings of this study, identical calculations were performed for Et_2S_2 , using the $\nu(\text{C-S})$ band pair at 669 and 642 cm^{-1} , for comparison with previous ΔH estimates for this disulphide and the related species EtSMe .

The temperature dependence over the range 313-193K for the $\nu(\text{C-S})$ vibrations of the three compounds are summarized in Table 1. Figure 8 shows the linear least-squares plots from which the enthalpy differences, also reported in Table 1, were evaluated. The data points for Et_2S_3 seem to depict a curve more closely than a straight line, suggesting the van't Hoff equation to be not strictly applicable in this case. This is likely due to a slight change in ΔS with temperature, especially on passing through the freezing point (201K)¹⁰⁹ into the glassy phase. Accordingly, the intensity ratio at 192.5K was excluded from the least-squares fit for Et_2S_3 . The very similar ΔH results for Et_2S_3 and Et_2S_2 point to analogous rotational isomerism for the two compounds. The value obtained for the disulphide is considerably lower than that determined by Allinger *et al.*¹¹⁹ using molecular mechanics (2.5 kJ mol^{-1}) or by Sugeta *et al.*⁹² on the basis of the temperature dependence (293-205K) for the Raman $\nu(\text{S-S})$ band pair at 523

Table 1. Intensity Ratios for the $\nu(\text{C-S})$ Vibrations of Et_2S_3 , $i\text{-Pr}_2\text{S}_3$ and Et_2S_2 as a Function of Temperature, and Enthalpy Differences Between the Rotamers.

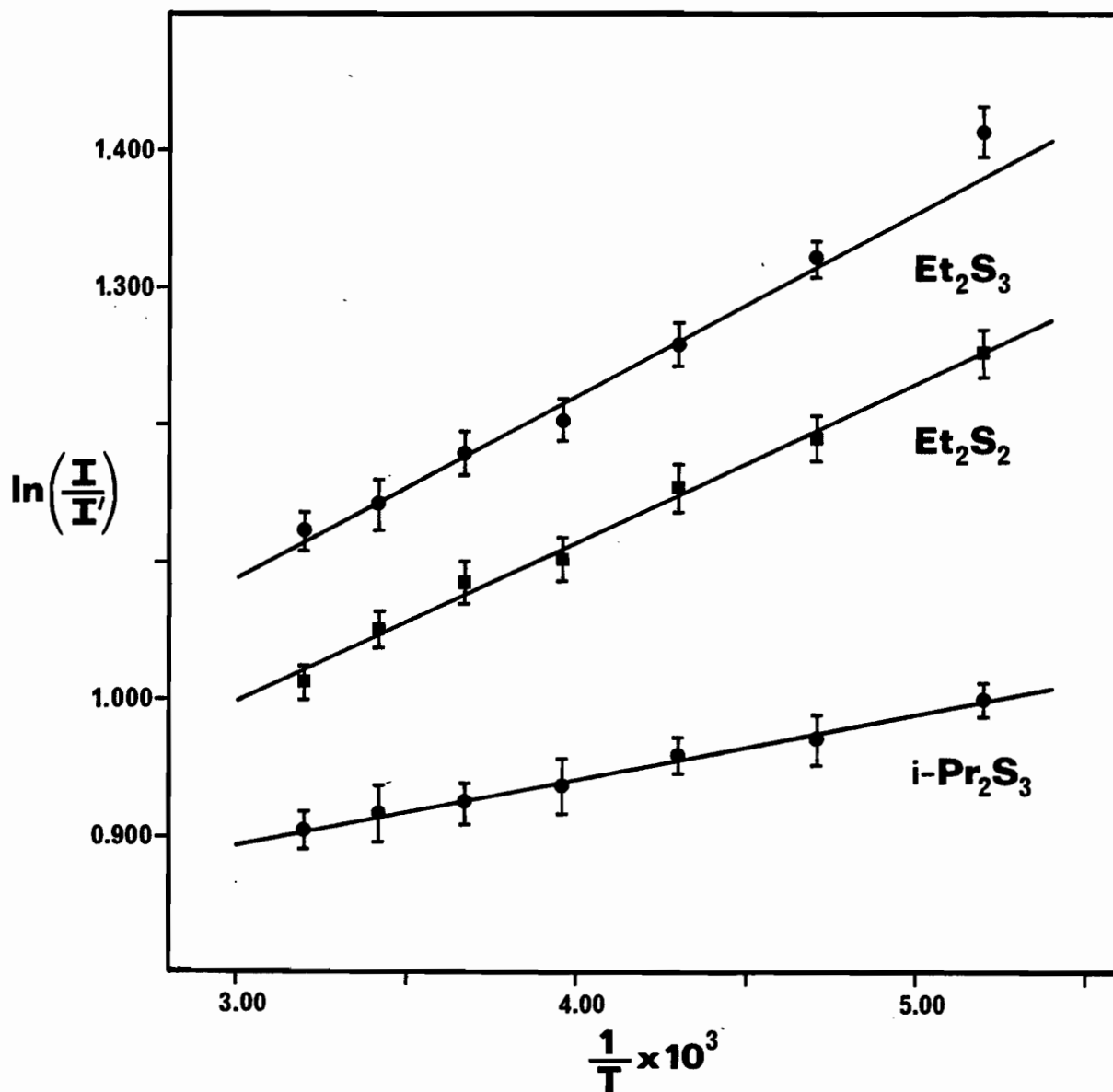
$\nu(\text{C-S})$ Intensity Ratio $(I/I')^a$			
Temperature (K) ^b	Et_2S_3	$i\text{-Pr}_2\text{S}_3$	Et_2S_2
312.5	3.07 ± 0.043	2.47 ± 0.033	2.75 ± 0.034
292.5	3.13 ± 0.061	2.50 ± 0.054	2.86 ± 0.040
272.5	3.25 ± 0.055	2.52 ± 0.038	2.96 ± 0.048
252.5	3.33 ± 0.051	2.55 ± 0.053	3.01 ± 0.051
232.5	3.52 ± 0.058	2.61 ± 0.036	3.17 ± 0.056
212.5	3.75 ± 0.052	2.64 ± 0.050	3.29 ± 0.059
192.5	4.11 ± 0.078	2.72 ± 0.036	3.50 ± 0.063
$\Delta H \text{ (kJ mol}^{-1}\text{)}^c$	1.10 ± 0.29	0.39 ± 0.13	0.97 ± 0.15

^a These are the peak height ratios for the Raman band pairs 644 and 670 cm^{-1} (Et_2S_3), 626 and 595 cm^{-1} ($i\text{-Pr}_2\text{S}_3$) and 642 and 669 cm^{-1} (Et_2S_2). Uncertainties are the standard deviations for a minimum of 16 measurements.

^b Temperature uncertainties were discussed in Section V.B.

^c Uncertainties are estimated from the maximum and minimum slopes in Fig. 8.

Figure 8. Plots of the Variation with Temperature for the $\nu(\text{C-S})$ Band Intensity Ratios of Et_2S_3 , Et_2S_2 and $i\text{-Pr}_2\text{S}_3$ from the Data of Table 1.^a



^a The least-squares fits were obtained using a Texas Instrument TL58 calculator.

and 508 cm^{-1} ($2.5 \pm 0.8\text{ kJ mol}^{-1}$). On the other hand, the value compares favourably with the average ΔH ($1.4 \pm 0.4\text{ kJ mol}^{-1}$) calculated for EtSSMe by Van Wart *et al.*^{94b} from the variation with temperature (room temperature - $\sim 200\text{K}$) for the 524 and 508 cm^{-1} and the 669 and 642 cm^{-1} Raman band pairs. Taking into account the 327 and 363 cm^{-1} Raman band pairs as well as the above two pairs, Sugeta *et al.*⁹² found a larger ΔH ($3.8 \pm 0.8\text{ kJ mol}^{-1}$) for EtSSMe, while molecular mechanics¹¹⁹ has yielded a value (2.86 kJ mol^{-1}) comparable to that for Et_2S_2 . A close correspondence between these two disulphides is expected on the grounds that their isomerism about the C-S bonds is the same (Sect. VI.A.1.i) To date, there are no data available, e.g., for $i\text{-Pr}_2\text{S}_2$ or $i\text{-PrSSMe}$, for comparison with the present results for $i\text{-Pr}_2\text{S}_3$. As a final note on the enthalpy differences between the rotamers of Et_2S_3 , $i\text{-Pr}_2\text{S}_3$ and Et_2S_2 , it should be reiterated that the calculated values appear to be differences between groups of rotamers of similar stability, and not between individual species. The nature of these rotamers is explored in the following section.

Figure 1-7. Infrared and Laser-Raman Spectra of Dialkyl Polysulphides.*

Figure 1.	Me_2S_3
Figure 2.	$\text{Me}_2\text{S}_3-d_6$
Figure 3.	Et_2S_3
Figure 4.	$n\text{-Pr}_2\text{S}_3$
Figure 5.	$i\text{-Pr}_2\text{S}_3$
Figure 6.	$t\text{-Bu}_2\text{S}_3$
Figure 7.	Et_2S_4

* In the Raman spectra of the liquids, the uppertrace gives the intensity in the same plane as the polarization of the incident laser beam (parallel intensity) and the lower trace gives the intensity in the plane at right angles (perpendicular intensity). Single traces show the parallel intensities.

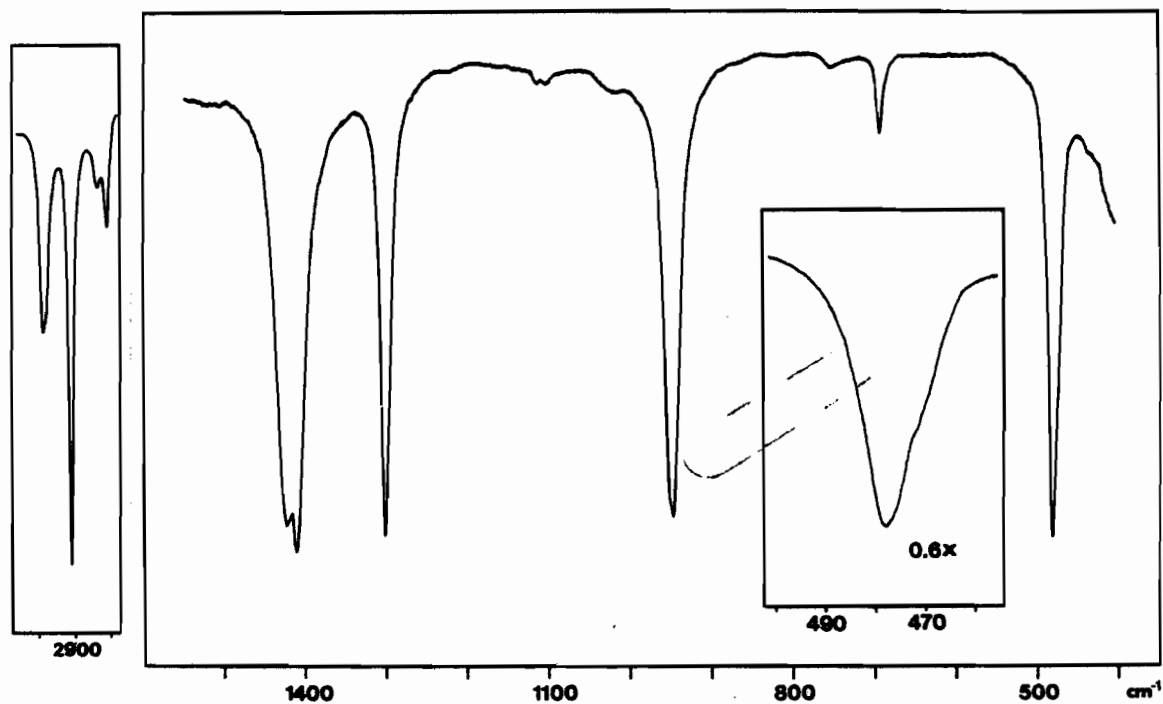


Figure 1a. Infrared Spectrum of Me_2S_3 : Liquid, Ambient Temperature.

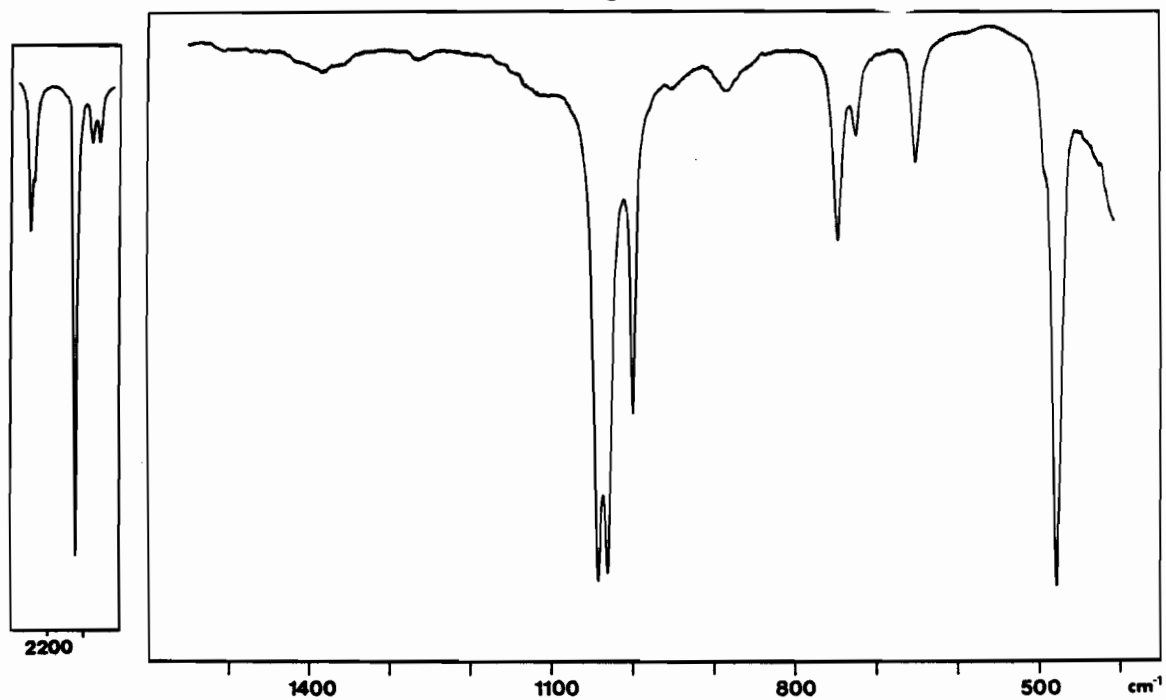


Figure 2a. Infrared Spectrum of $\text{Me}_2\text{S}_3\text{-}d_6$: Liquid, Ambient Temperature.

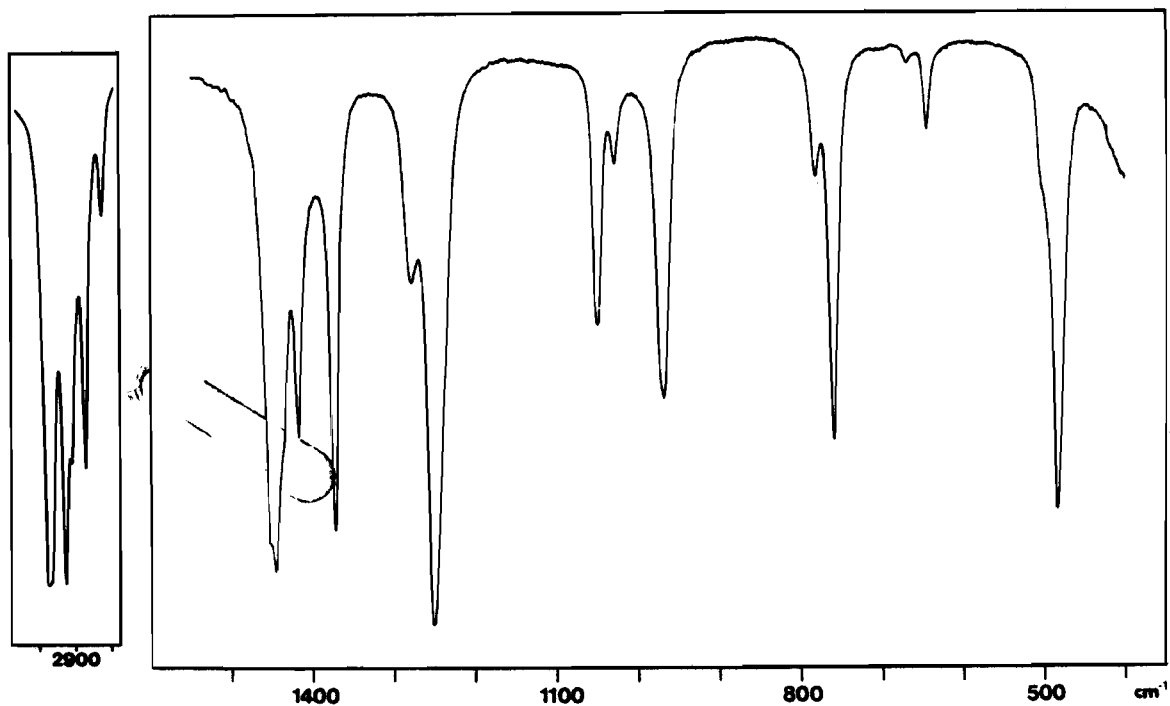


Figure 3a. Infrared Spectrum of Et_2S_3 : Liquid, Ambient Temperature.

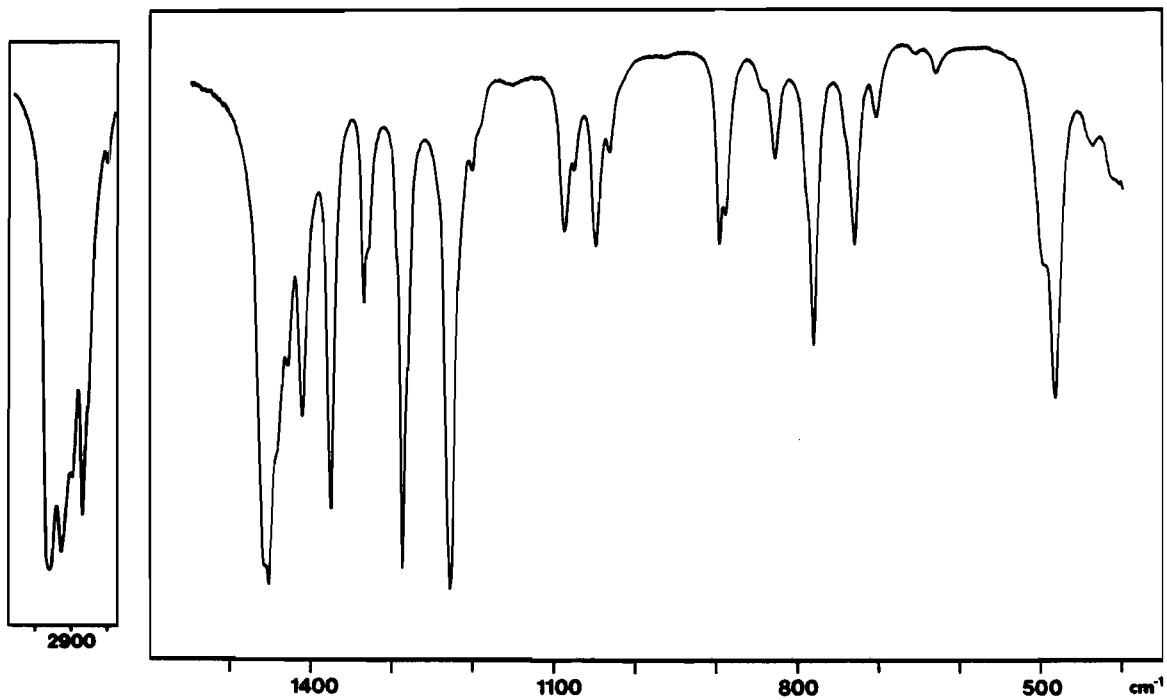


Figure 4a. Infrared Spectrum of $n\text{-Pr}_2\text{S}_3$: Liquid, Ambient Temperature.

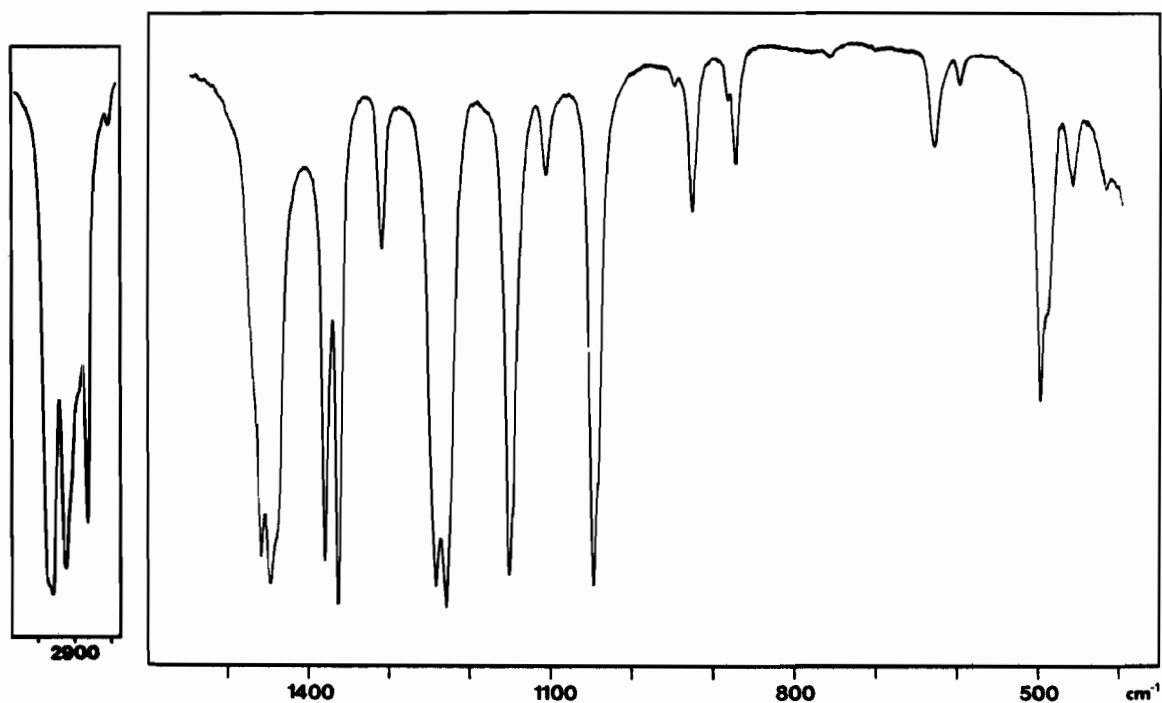


Figure 5a. Infrared Spectrum of *i*-Pr₂S₃: Liquid, Ambient Temperature.

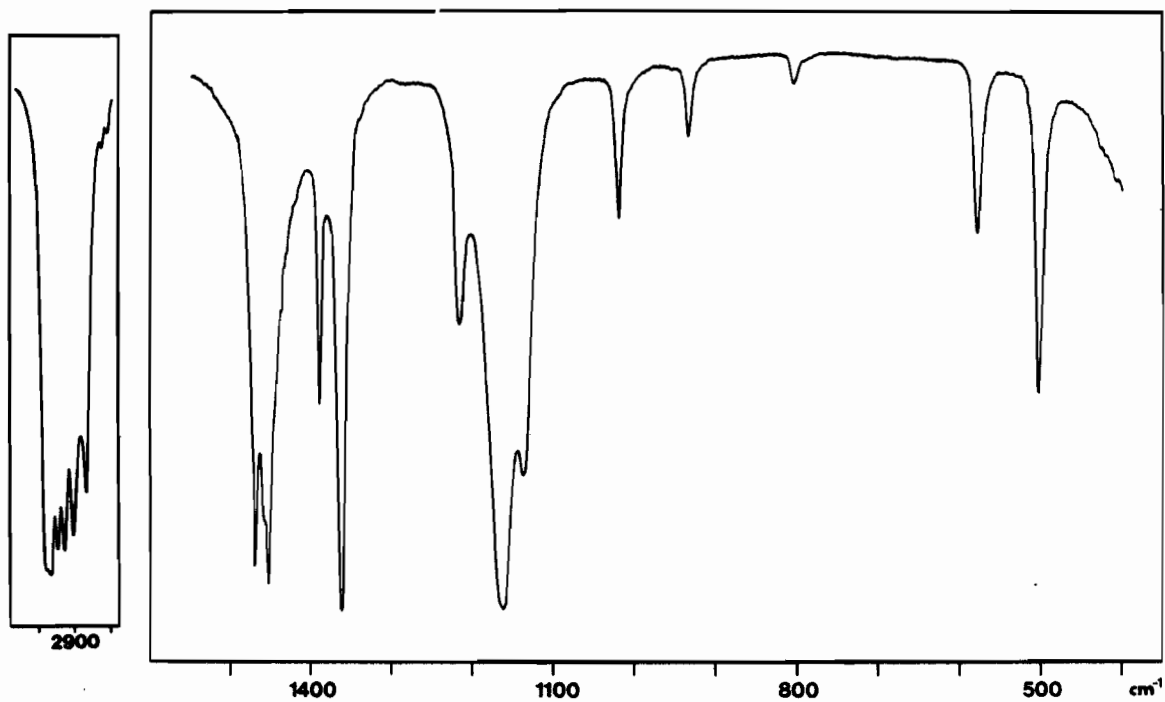


Figure 6a. Infrared Spectrum of *t*-Bu₂S₃: Liquid, Ambient Temperature.

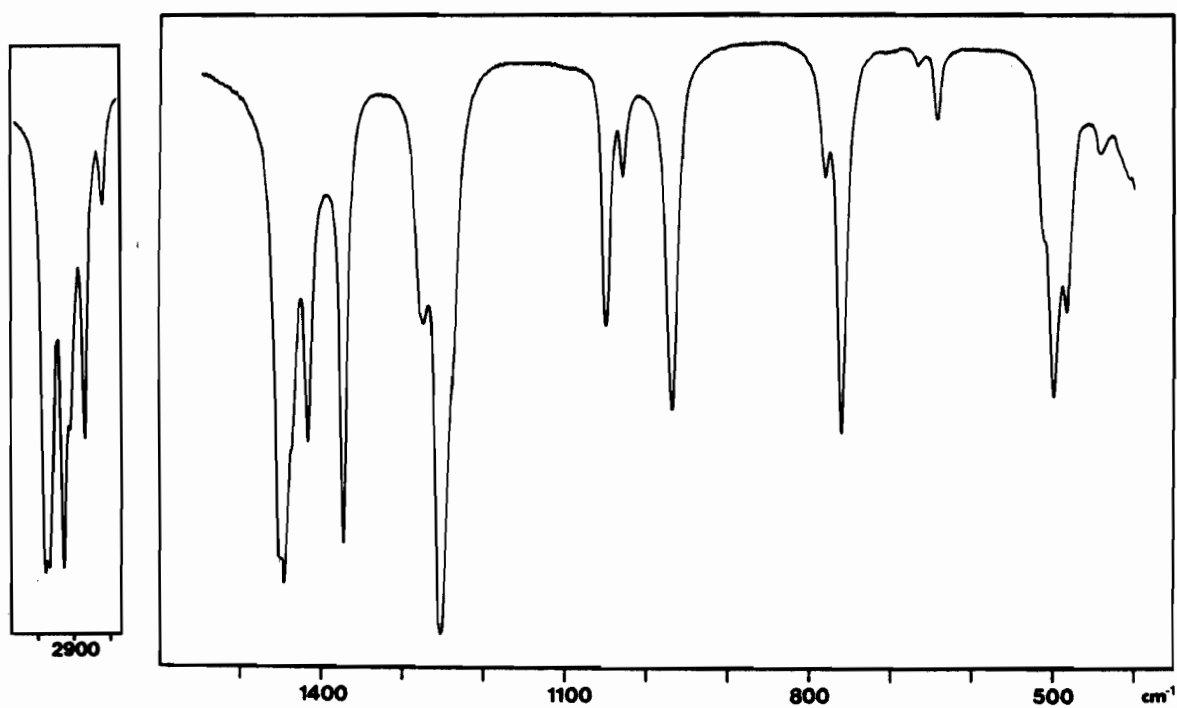


Figure 7a. Infrared Spectrum of Et_2S_4 : Liquid, Ambient Temperature.

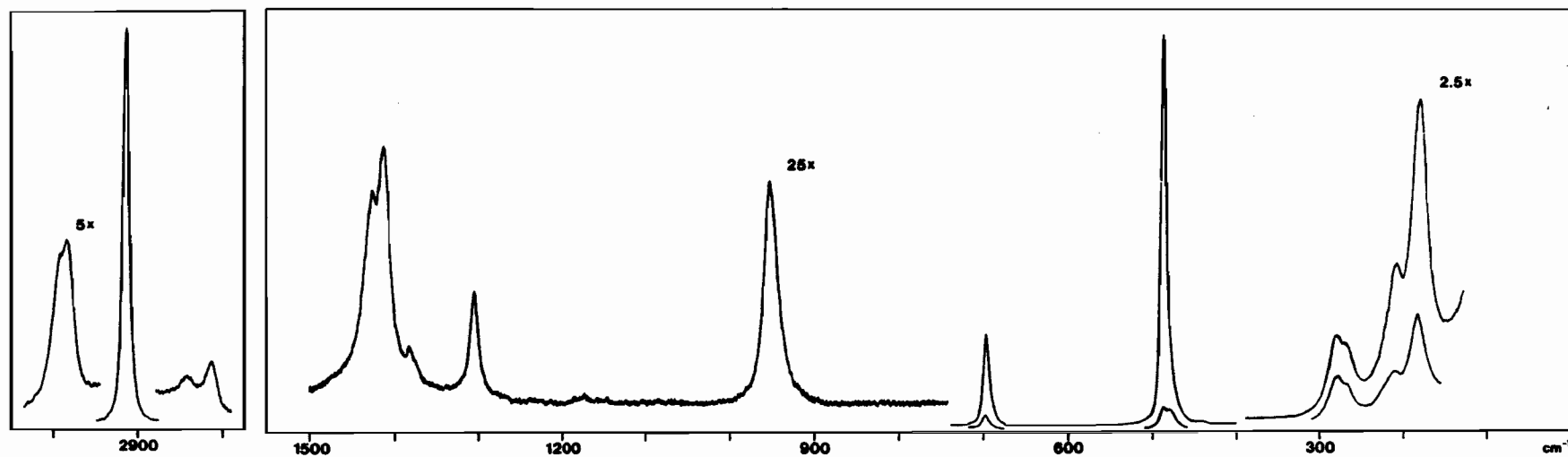


Figure 1b. Laser-Raman Spectrum of Me_2S_3 : Liquid, Ambient Temperature.

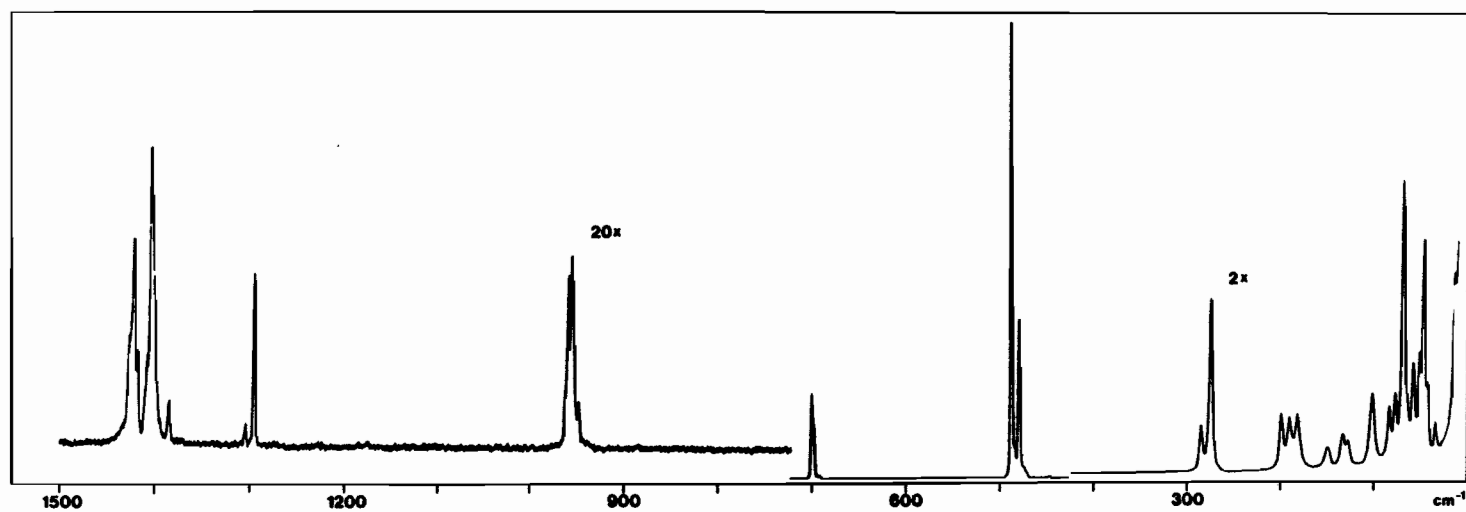


Figure 1c. Laser-Raman Spectrum of Me_2S_3 : Solid I, ~15K.

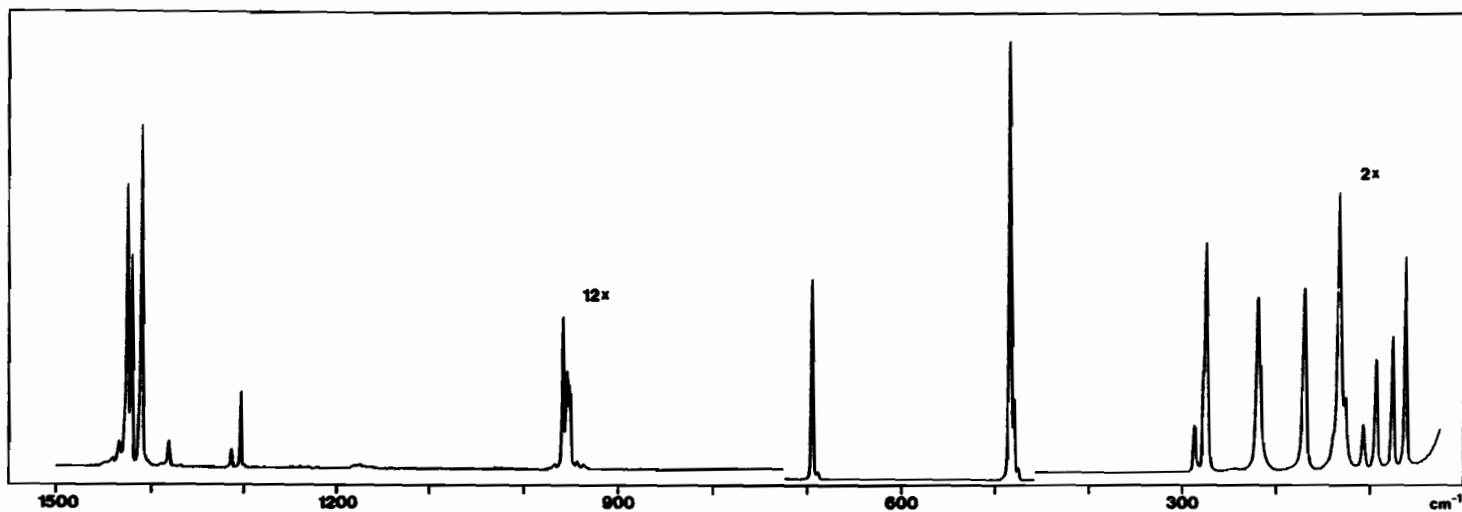


Figure 1d. Laser-Raman Spectrum of Me_2S_3 : Solid II, ~15K

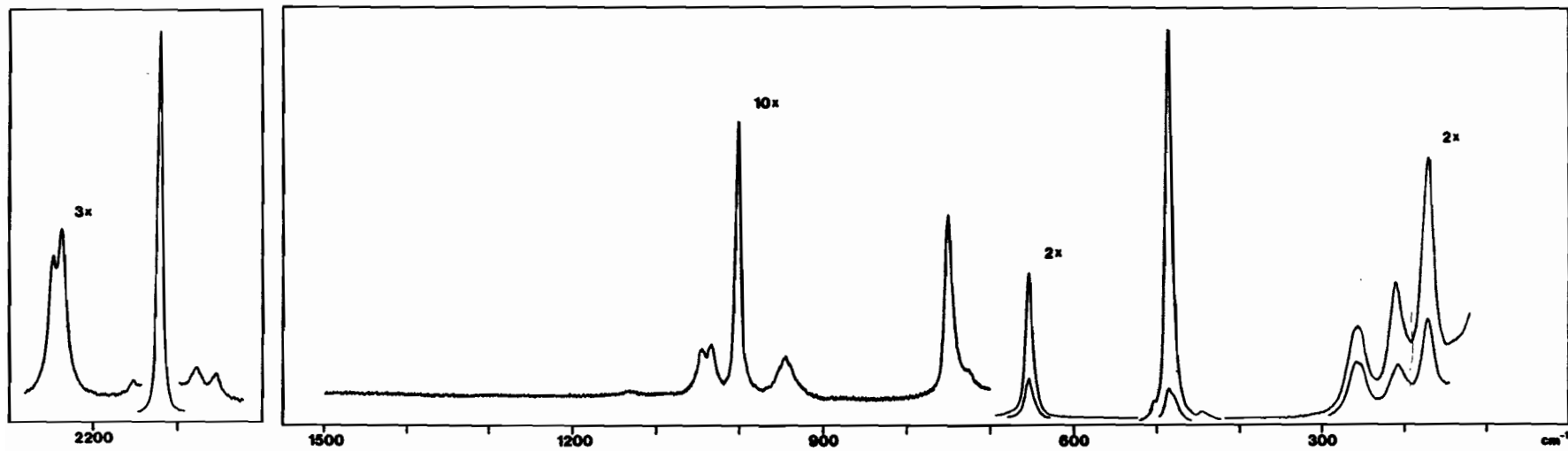


Figure 2b. Laser-Raman Spectrum of $\text{Me}_2\text{S}_3\text{-}d_6$: Liquid, Ambient Temperature.

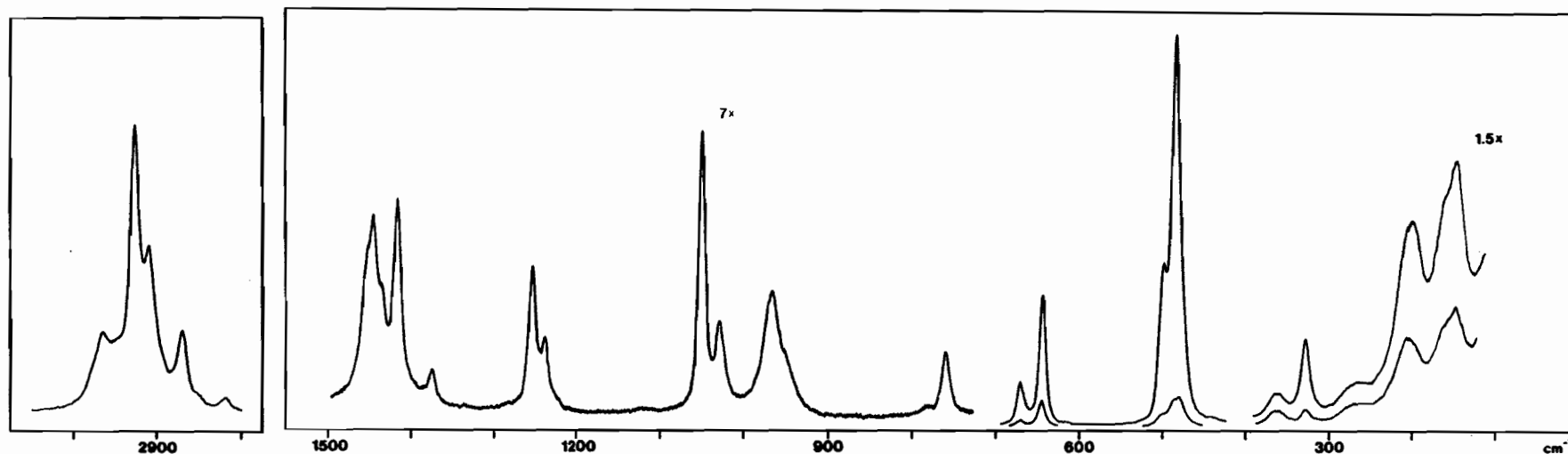


Figure 3b. Laser-Raman Spectrum of Et_2S_3 : Liquid, Ambient Temperature.

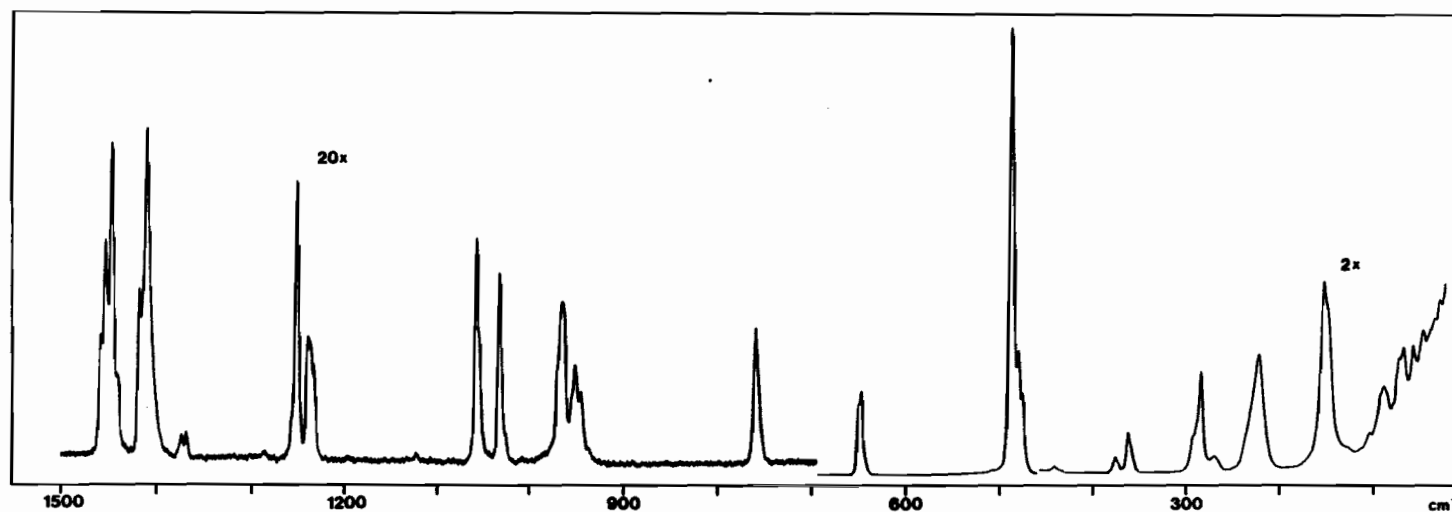


Figure 3c. Laser-Raman Spectrum of Et_2S_3 : Metastable Phase, $\sim 15\text{K}$.

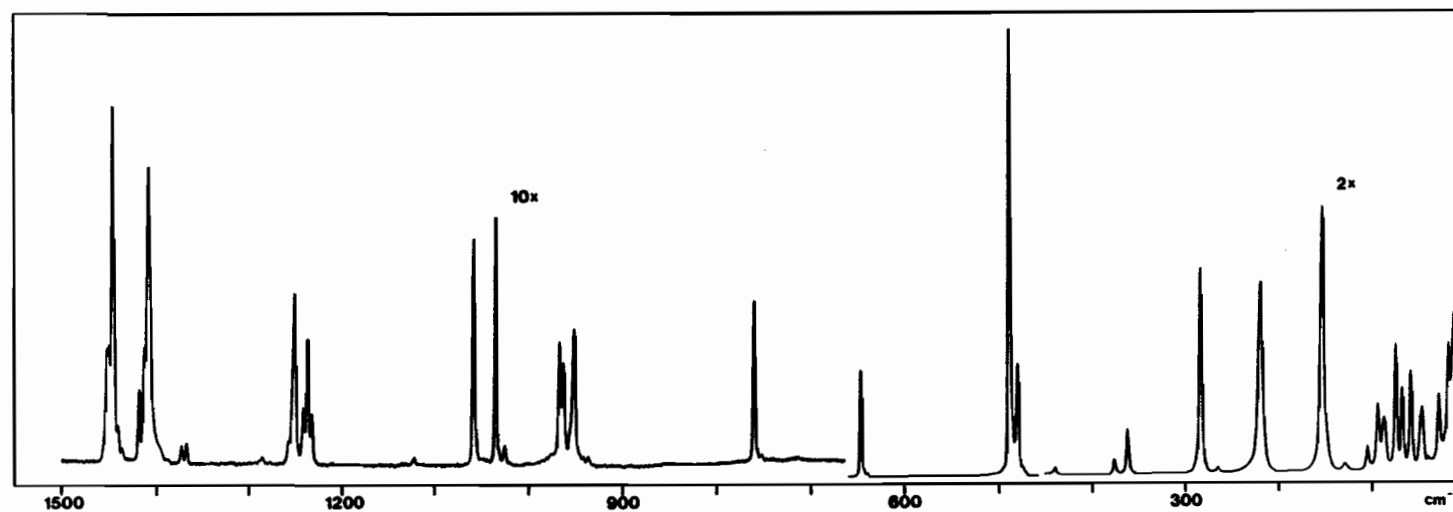


Figure 3d. Laser-Raman Spectrum of Et_2S_3 : Solid, $\sim 15\text{K}$.

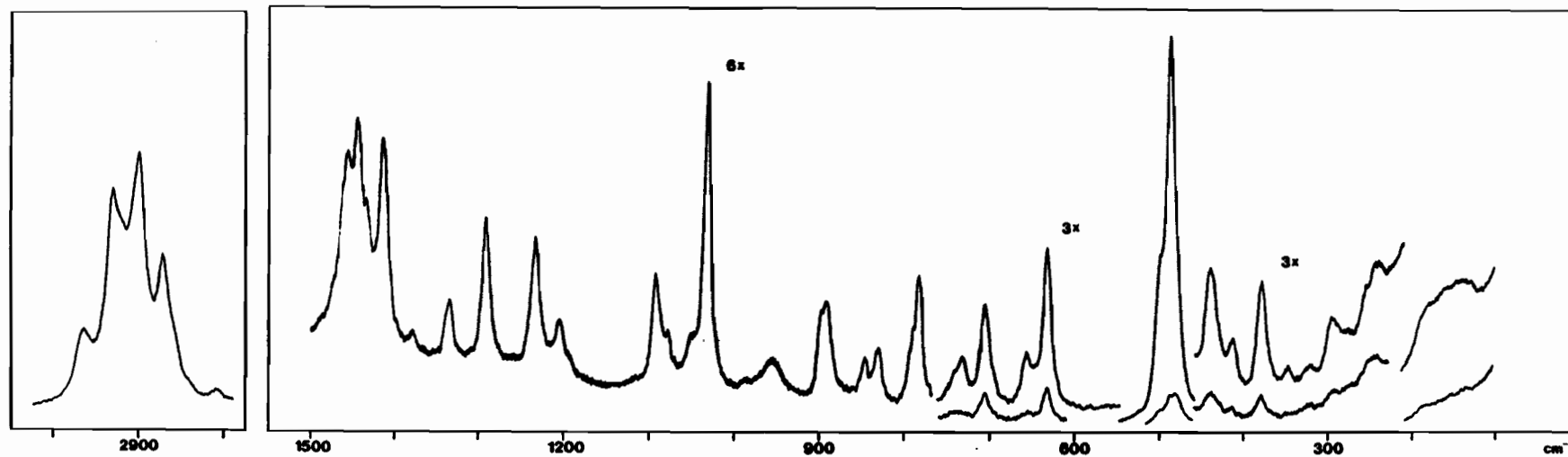


Figure 4b. Laser-Raman Spectrum of $n\text{-Pr}_2\text{S}_3$: Liquid, Ambient Temperature.

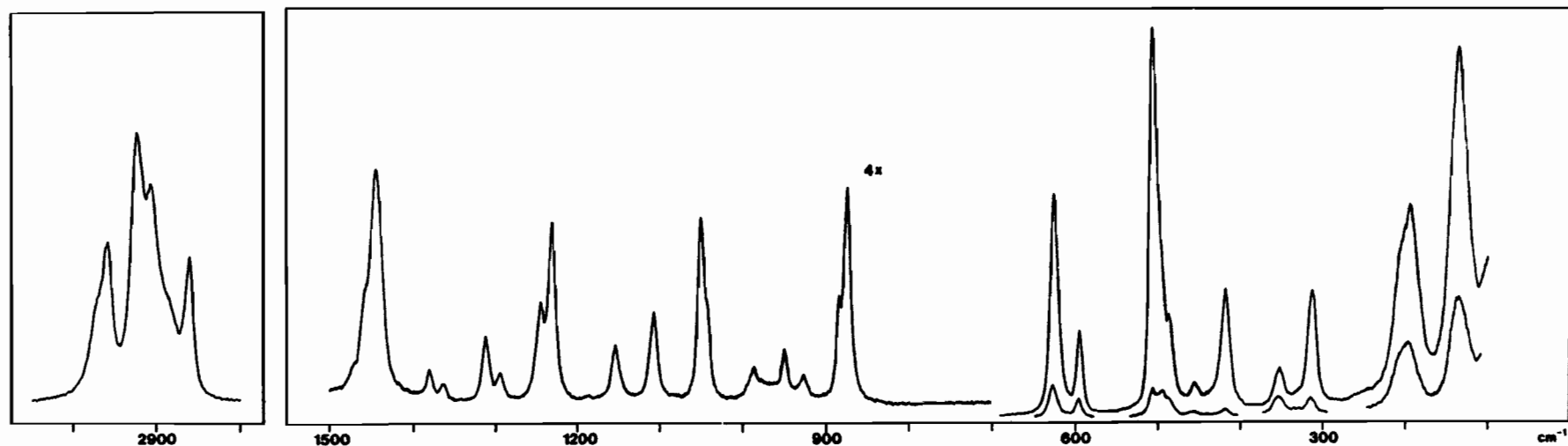


Figure 5b. Laser-Raman Spectrum of l -Pr₂S₃: Liquid, Ambient Temperature.

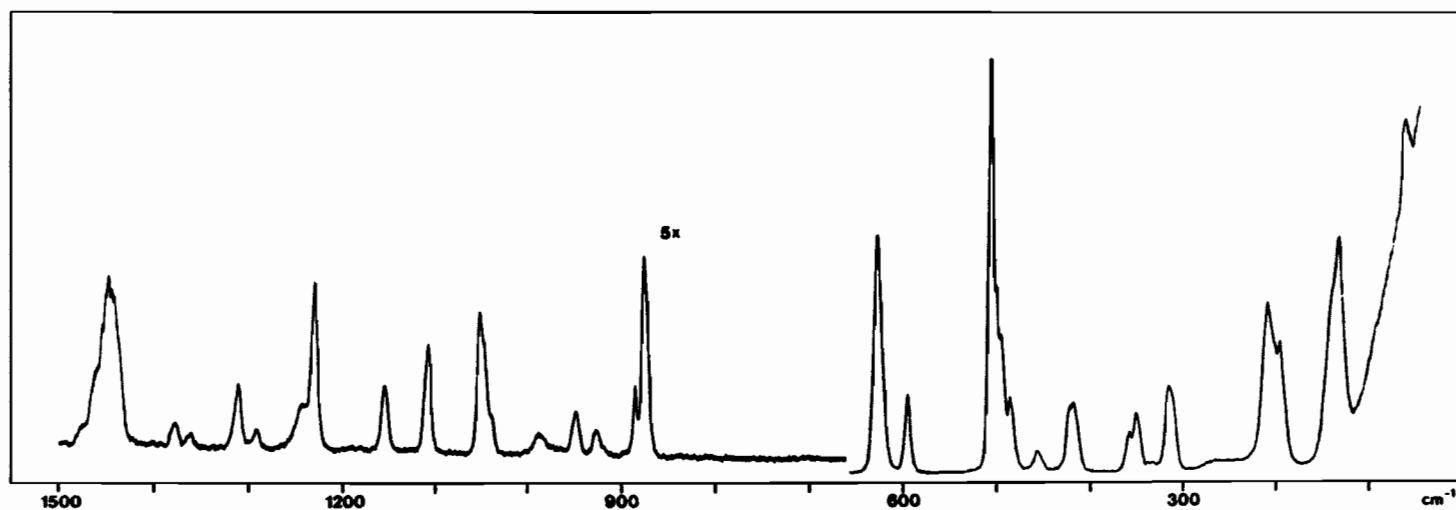


Figure 5c. Laser-Raman Spectrum of l -Pr₂S₃: Metastable Phase, ~ 15 K.

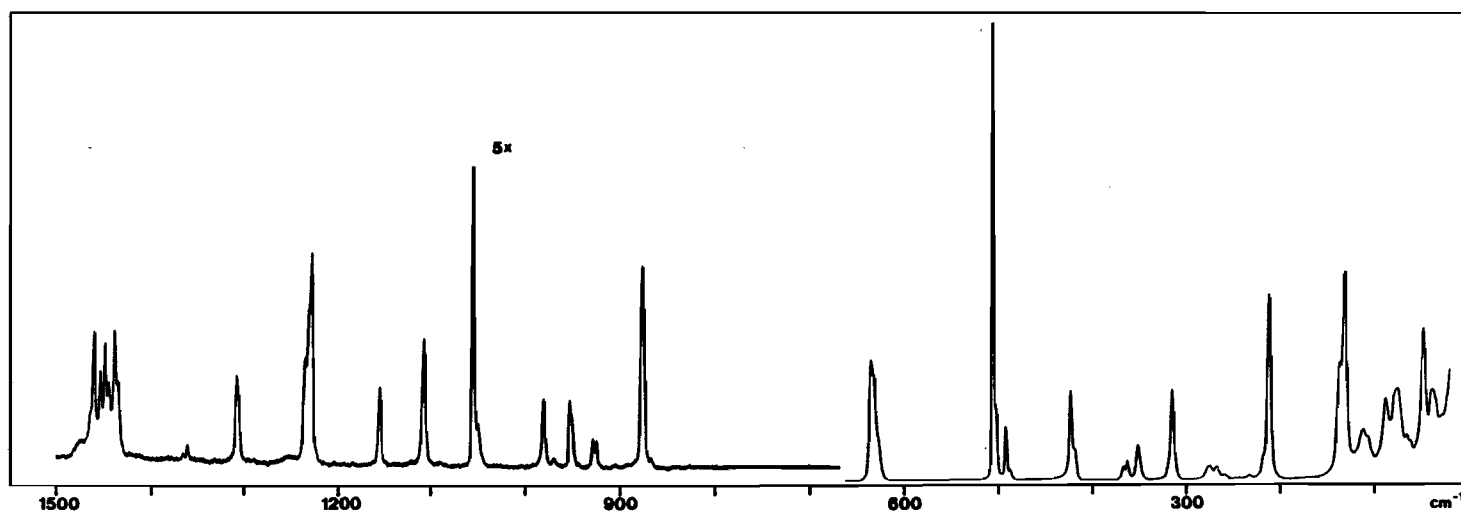


Figure 5d. Laser-Raman Spectrum of $i\text{-Pr}_2\text{S}_3$: Solid, $\sim 15\text{K}$.

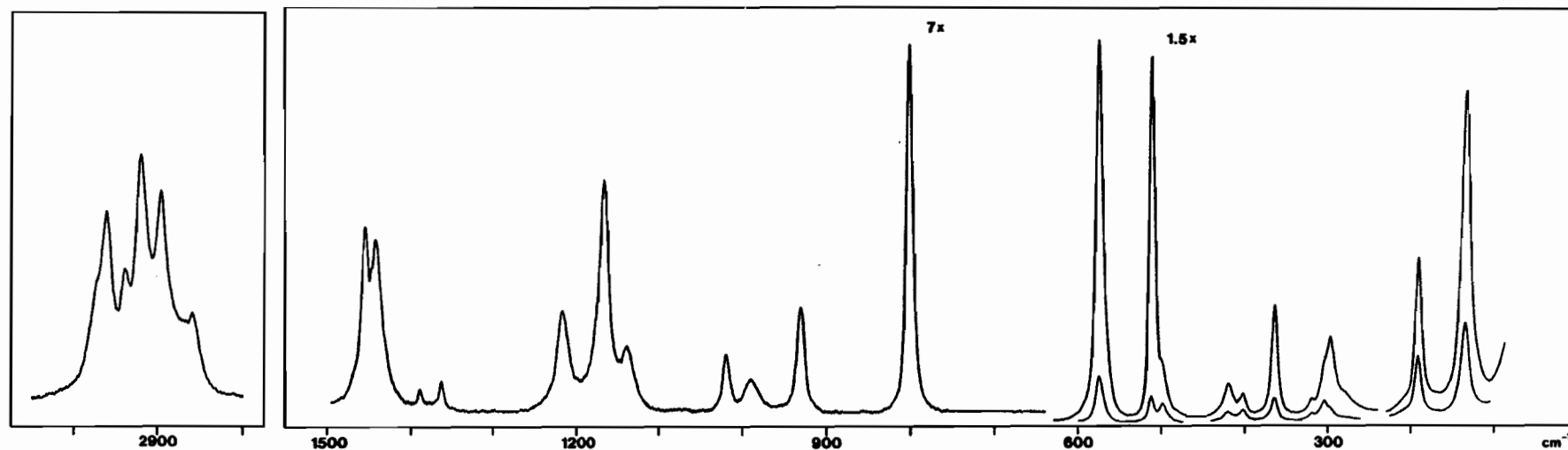


Figure 6b. Laser-Raman Spectrum of $t\text{-Bu}_2\text{S}_3$: Liquid, Ambient Temperature.

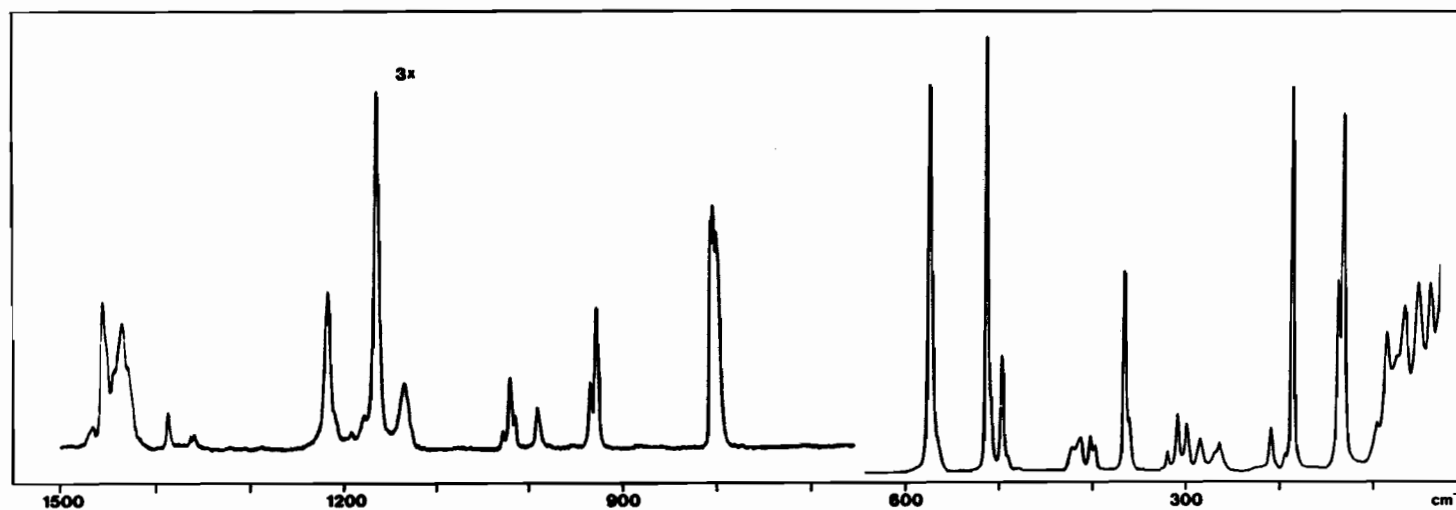


Figure 6c. Laser-Raman Spectrum of $t\text{-Bu}_2\text{S}_3$: Solid, $\sim 15\text{K}$.

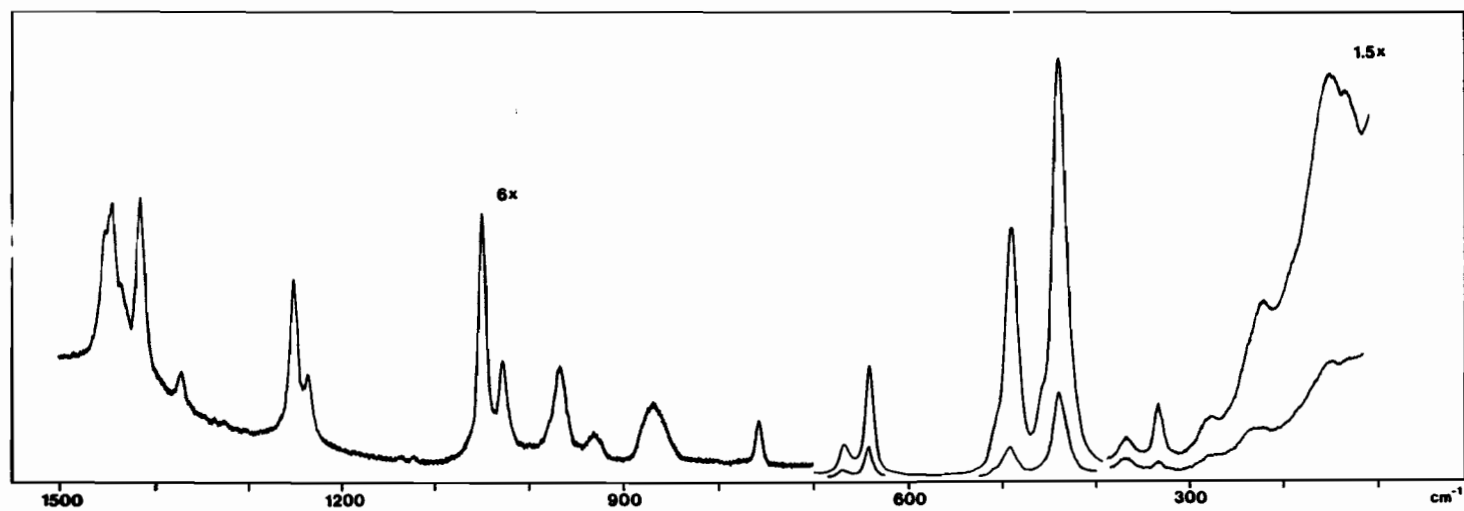


Figure 7b. Laser-Raman Spectrum of Et_2S_4 : Liquid, Ambient Temperature.

VI.A.1 Rotational Isomerism

As discussed earlier (Chapter III), the only stable conformation* for the S-S bonds of organodi- and polysulphides is characterized by a dihedral angle close to 90° , provided the molecules are not structurally constrained, by ring closure for instance. Accordingly, the CSSC skeleton of an unstrained disulphide exists in a single, *gauche* (G) configuration (Fig. 9). Since the mirror images are non-superimposable, the molecule is inherently chiral independent of the geometry about the substituents. The CSSSC backbone of an unstrained trisulphide can adopt either the *gauche-gauche* (GG) or *gauche-gauche'* (GG') configuration[†], giving the *trans* and *cis* rotamers, respectively (Fig. 9). Only the former configuration is chiral. In the case of a tetrasulphide, three distinct configurations with 90° dihedral angles are possible, all of which are chiral (Fig. 9).

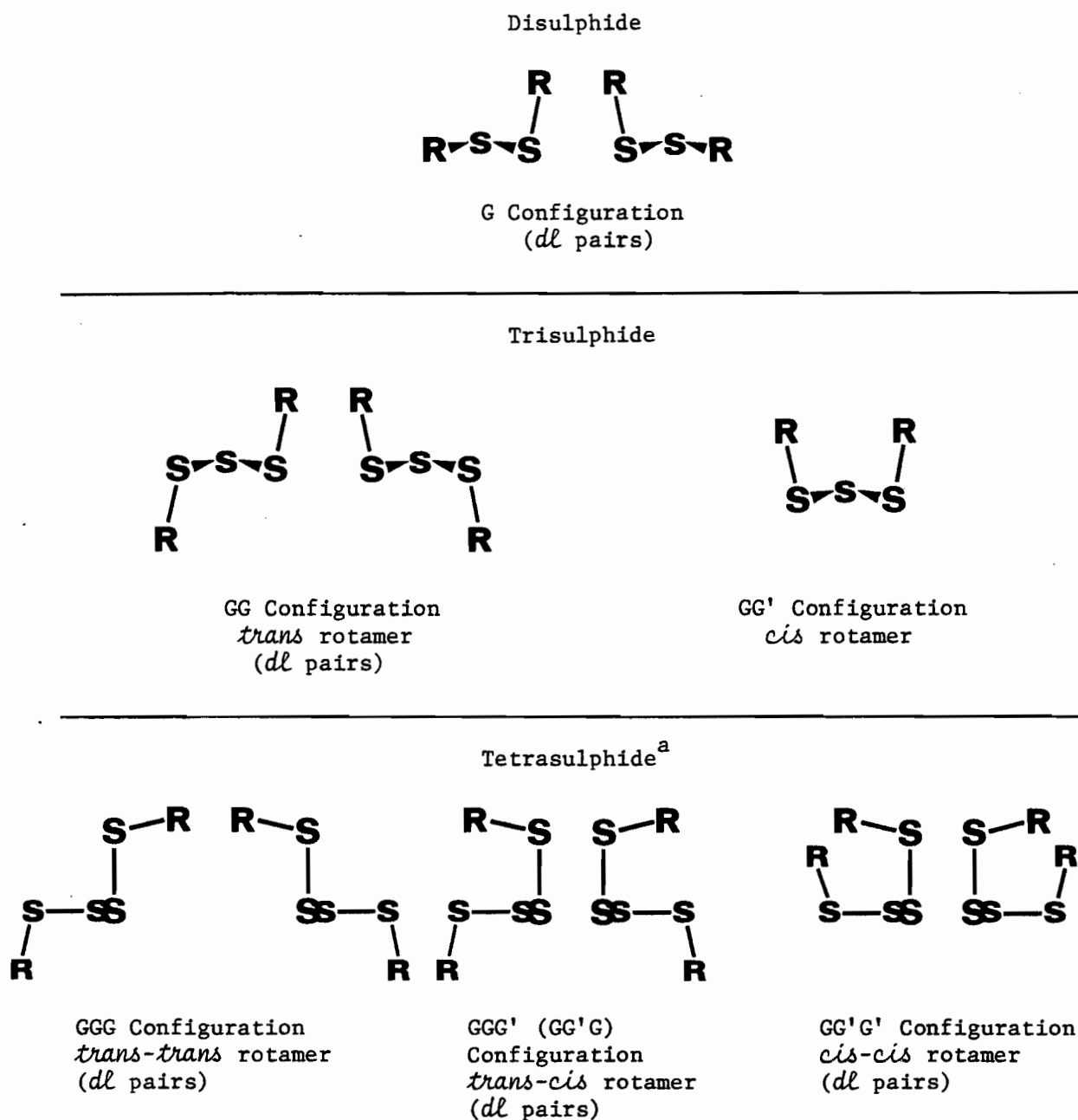
In considering internal rotation about the C-S bonds of organopolysulphides, it is convenient to categorize the molecules according to the nature of the β carbons** as primary ($-\text{CH}_2-$), secondary (>CH-) or tertiary (>C-), as for organodisulphides.³¹ Primary and secondary di- and polysulphides are capable of isomerism with respect to the C-S bonds owing to the possibility of *trans* (T), *gauche* (G) and *gauche'* (G') staggered conformations (Figs. 10 and 11). These would intuitively be expected to be the only

* The stable conformations about a bond are the geometries corresponding to minima in the rotational potential energy curve.

† The prime designates the higher energy of the non-equivalent *gauche* conformations.

** By analogy with cystine (compd. 22), the β carbons are the ones directly bonded to sulphur.

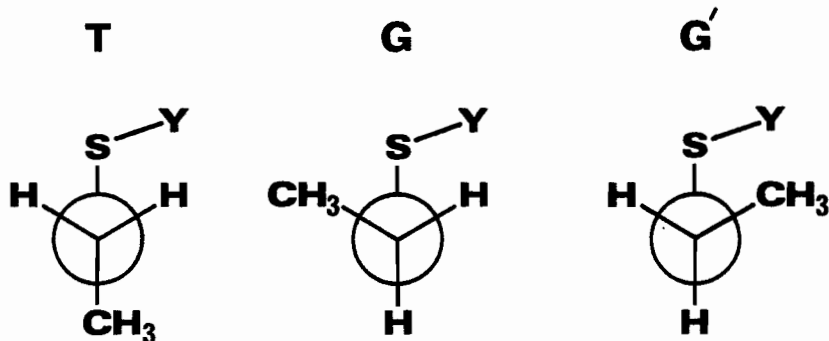
Figure 9. Stable Configurations for the Central Core of Organodi-, Tri- and Tetrasulphides.



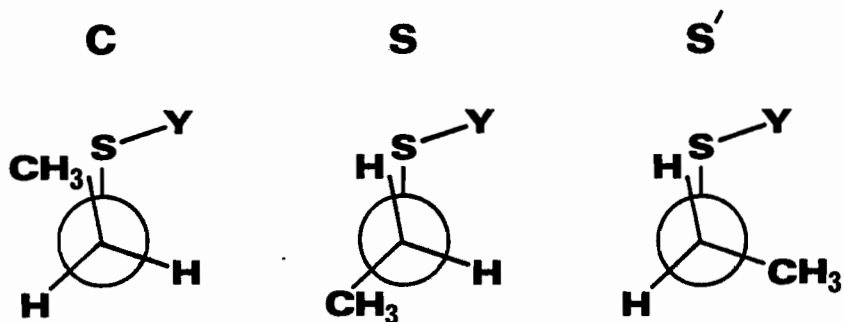
^a These configurations are viewed down the central S-S bond.

Figure 10. Newman Projections for Various Conformations About the C-S Bonds of the Primary Disulphide Et_2S_2 ($\text{Y}=\text{CH}_2$) and the Primary Trisulphide Et_2S_3 ($\text{Y}=\text{S}$).

Staggered Conformations^a



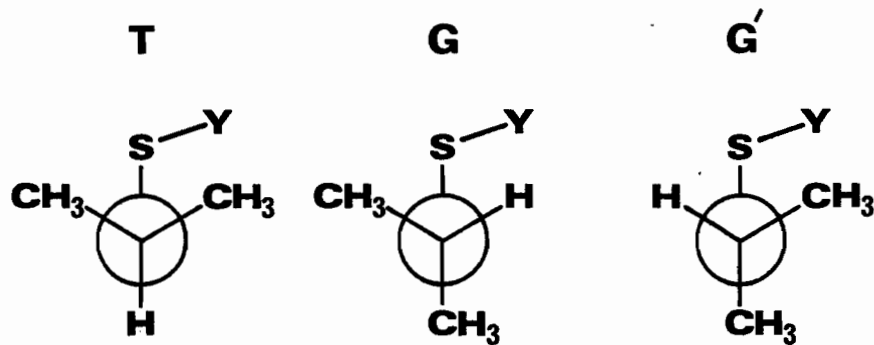
Eclipsed Conformations^a



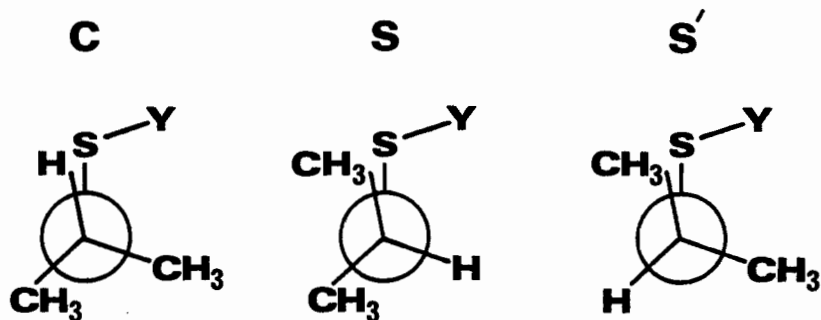
^a The idealized CC-SS dihedral angles are: *trans* (T), 180° ; *gauche* (G) and *gauche'* (G'), 60° ; *cis* (C), 0° ; *skew* (S) and *skew'* (S'), 120° .

Figure 11. Newman Projections for Various Conformations About the C-S Bonds of the Secondary Disulphide $i\text{-Pr}_2\text{S}_2$ ($\text{Y}=\text{CH}$) and the Secondary Trisulphide $i\text{-Pr}_2\text{S}_3$ ($\text{Y}=\text{S}$).

Staggered Conformations^a

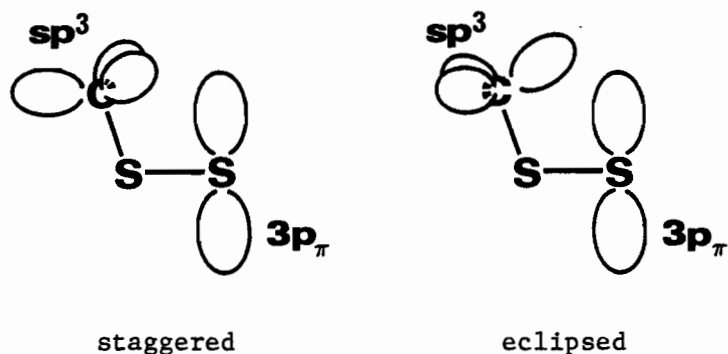


Eclipsed Conformations^a

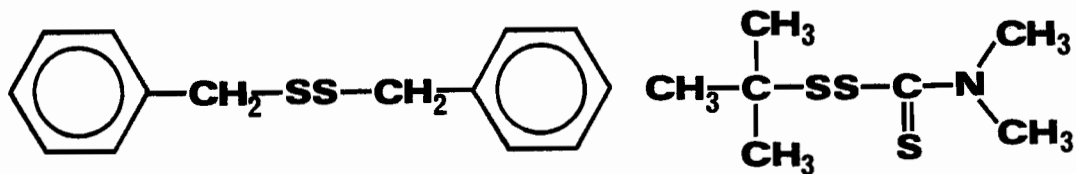


^a The idealized HC-SS dihedral angles are: *trans* (T), 180° ; *gauche* (G) and *gauche'* (G'), 60° ; *cis* (C), 0° ; *skew* (S) and *skew'* (S'), 120° .

stable conformations because they clearly entail the furthest nonbonded separations between the C-R (R=C,H) bonds and the *vicinal* S-S bond, whereas the *cis* (C), *skew* (S) and *skew'* (S') eclipsed conformations (Figs. 10 and 11) give the minimum separations. Furthermore, the staggered geometries minimize any repulsion between the $3p_{\pi}$ lone-pair orbital on sulphur (Chapter III) and the carbon sp^3 orbitals, as illustrated below. The lone-pair points between two sp^3 lobes in these arrangements, while directly at an sp^3 lobe in the eclipsed conformations.

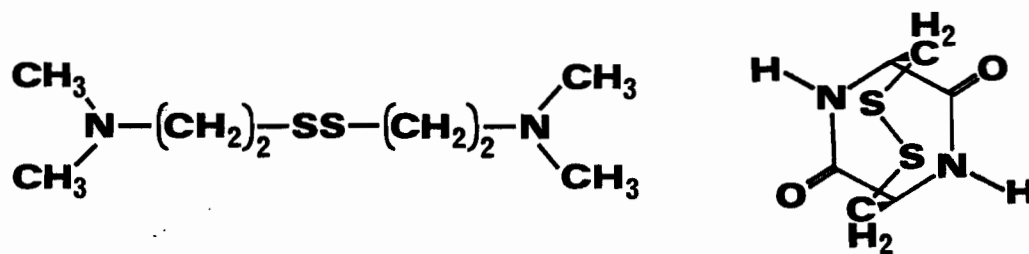


Electron diffraction data for gaseous Me_2S_2 and EtSSMe indicate staggered methyl and ethyl groups in these disulphides.⁷⁶ Similarly, X-ray diffraction studies have revealed staggered conformations (CC-SS dihedral angles within $\sim 10^\circ$ of the idealized values) for the solid-state structures of a number of disulphides including dicinnamyl disulphide⁴² (compd. 14), D-penicillamine disulphide⁴³ (compd. 15) and the following species^{31,120-123}



(23) dibenzyl disulphide

(24) *t*-butyl-N,N'-dimethyltrithio-percarbamate



(25) bis [2-(N,N'-dimethylamino)ethyl] disulphide

(26) cyclo-L-cystine



(27) dithiodiglycolic acid

Then again, the solid-state structures of most cystine derivatives and cystine residues in proteins involve substantial departures from staggered C-S conformations.³¹ As regards the crystalline organotrisulphides $(\text{CCl}_3)_2\text{S}_3$ and $(\text{I-CH}_2\text{CH}_2)_2\text{S}_3$, X-ray diffraction results²³ have indicated almost perfectly staggered CCl_3 groups for the former, but significant distortion from the formal G conformation about the C-S bonds in the latter (CC-SS dihedral angles $85 \pm 10^\circ$). The structure reported for the second compound is suspect, however (see footnote, page 9). Incidentally, staggered C-S conformations have also been found for compounds 11³⁸ and 13,³⁹ although this may be a consequence of the ring systems.

The rotational isomerism about the C-S bonds of organodisulphides in the liquid and solution phases has been at issue of late. In view of the ongoing controversy^{94,119} and the striking resemblances found in this work between di- and trisulphides, both in their vibrational spectra (Sect. VI.A.2) and in the enthalpy differences calculated for the rotamers of Et_2S_2 and Et_2S_3 (Sect. VI.A), it was felt that the evidence pertaining to the disulphides warranted careful scrutiny in the present study of the trisulphides. Section VI.A.1.i therefore deals in depth with isomerism about the C-S bonds of di- and trisulphides, while isomerism about the S-S bonds of the trisulphides is examined in Section VI.A.1.ii.

VI.A.1.i C-S Isomerism

The co-existence of different rotamers for an organodisulphide is manifest in its infrared and Raman spectra in the form of multiple bands (with temperature-sensitive relative intensities) for several of the

fundamental vibrations. These effects are particularly apparent in the $\nu(\text{S-S})$ and $\nu(\text{C-S})$ vibrations. Thus the $\nu(\text{S-S})$ vibrations of dialkyl disulphides occur characteristically as prominent Raman bands near 510, 525 and 540 cm^{-1} with doublet features only in the case of primary or secondary substituents (Table 2). The way in which the frequencies correlate with structure has been the focus of considerable attention in the recent literature.

Noting the positions of the lone $\nu(\text{S-S})$ vibration for Me_2S_2 , $t\text{-BuSSMe}$ and $t\text{-Bu}_2\text{S}_2$ (Tables 2 and 3), Sugeta and co-workers^{92a} proposed a simple correlation between $\nu(\text{S-S})$ and C-S conformation based on the identities (carbon or hydrogen) of the atoms situated *trans* to the distal sulphur across the two C-S bonds. Since the above three molecules exemplify the possible arrangements for dialkyl disulphides (two *trans* hydrogens, a *trans* hydrogen and a *trans* carbon, or two *trans* carbons), it was suggested that these geometries are responsible for the distinctive $\nu(\text{S-S})$ bands for disulphides at approximately 510, 525 and 540 cm^{-1} , respectively. The bands were hence designated $\nu(\text{H,H})$, $\nu(\text{C,H})$ and $\nu(\text{C,C})$ vibrations, as indicated in Table 3. For EtSSMe and Et_2S_2 , the simplest disulphides capable of C-S isomerism, the rotamers deduced to co-exist in the liquid state are, in the order of decreasing stability, GG and TG for the former and GGG and GGT for the latter.* The lower stability for the structures with a T C-S conformation was inferred from the disappearance

* The symbols specify, in sequence, the conformations about the C-S and S-S bonds for EtSSMe and the C-S, S-S and C-S bonds for Et_2S_2 .

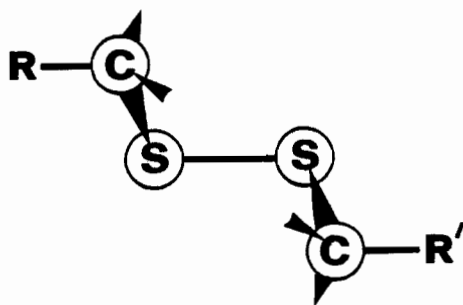
Table 2. Raman $\nu(\text{S-S})$ Vibrations for Liquid Dialkyl Disulphides.^{83,92}

Disulphide	$\nu(\text{S-S})$ Vibrations (cm^{-1})		
Me_2S_2	508		
EtSSMe	508	524	
$n\text{-PrSSMe}$	511	526	
Et_2S_2	508	523	
$n\text{-PrSSEt}$	504	518	
$n\text{-BuSSEt}$	508	522	
$i\text{-BuSSEt}$	508	522	
$n\text{-Pr}_2\text{S}_2$	510	524	
$n\text{-BuSS}(n\text{-Pr})$	512	525	
$n\text{-Bu}_2\text{S}_2$	510	524	
$i\text{-Bu}_2\text{S}_2$	512	525	
$(n\text{-pentyl})_2\text{S}_2$	510	524	
$(i\text{-pentyl})_2\text{S}_2$	511	522	
$(n\text{-hexyl})_2\text{S}_2$	510	522	
$i\text{-PrSSMe}$	510	526	
$i\text{-Pr}_2\text{S}_2$		527	543
$\delta\text{-Bu}_2\text{S}_2$	~ 510	527	543
$t\text{-BuSSMe}$		528	
$t\text{-BuSSEt}$		525	~ 540
$t\text{-Bu}_2\text{S}_2$			543
$(t\text{-pentyl})_2\text{S}_2$			541

Table 3. Proposed $\nu(\text{S-S})$ - Structure Correlation for Dialkyl Disulphides.⁹²

Disulphide	$\nu(\text{S-S})$ Vibrations ^a (cm^{-1})		
	$\nu(\text{H,H})$	$\nu(\text{C,H})$	$\nu(\text{C,C})$
Me_2S_2	508	b	b
EtSSMe	509	524	b
Et_2S_2	510	523	
$n\text{-Pr}_2\text{S}_2$	512	523	
$i\text{-Bu}_2\text{S}_2$		525	
$i\text{-Pr}_2\text{S}_2$		527	542
$\Delta\text{-Bu}_2\text{S}_2$		527	542
$t\text{-BuSSMe}$	b	528	b
$t\text{-Bu}_2\text{S}_2$	b	b	543
$(t\text{-pentyl})_2\text{S}_2$	b	b	543

^a Characteristic vibrations:



$\nu(\text{H,H})$: $\text{R} = \text{R}' = \text{H}$

$\nu(\text{C,H})$: $\text{R} = \text{C}, \text{R}' = \text{H}$

$\nu(\text{C,C})$: $\text{R} = \text{R}' = \text{C}$

^b No band expected on the basis of the correlation.

of the $\nu(\text{C,H})$ vibration for the annealed solids. In an earlier vibrational study, Scott and El-Sabban^{89e} arrived at the same conclusion regarding the rotamers present for these liquids.

The origins of the alleged structural dependence of the $\nu(\text{S-S})$ vibration were pursued by Sugeta^{92b} through normal coordinate calculations. For the molecules Me_2S_2 , $t\text{-BuSSMe}$ and $t\text{-Bu}_2\text{S}_2$, each of which exists as a single rotamer, the increase in $\nu(\text{S-S})$ across the series was found to be accompanied by a reduction in S-S stretching character in the vibration — evidenced by a diminished contribution from the S-S stretching force constant in the potential energy distribution (101% for Me_2S_2 , 85% for $t\text{-BuSSMe}$ and 77% for $t\text{-Bu}_2\text{S}_2$). Within the context of the calculations, these differences are due largely to substantial CC_3 rocking motion in the vibration for both $t\text{-BuSSMe}$ and $t\text{-Bu}_2\text{S}_2$, with a somewhat greater contribution in the latter (14% vs. 10% in the potential energy distribution). Accordingly, the trend in $\nu(\text{S-S})$ was concluded to relate to coupling with the t -butyl substituents.

In the case of Et_2S_2 , the normal coordinate treatment yielded the $\nu(\text{S-S})$ vibration at 508 cm^{-1} for the rotamers (GGG, GGG' and G'GG') with hydrogens occupying the sites *trans* to sulphur across the C-S bonds, at $527\text{--}528\text{ cm}^{-1}$ for the rotamers (GGT and TGG') with a carbon in one of the *trans* sites, and finally, at 544 cm^{-1} for the rotamer (TGT) with carbons in both *trans* sites, in agreement with the proposed correlation. Similarly for EtSSMe , the $\nu(\text{S-S})$ band was computed to lie at 507 cm^{-1} for the GG and G'G species, and at 527 cm^{-1} for the TG species. For both disulphides, the participation of the S-S stretching motion in the vibration was indicated to decrease between the rotamers with G and T C-S conformations

(98% vs. 91% for the GG and TG rotamers of EtSSMe and 94% vs. 88% for the GGG and GGT rotamers of Et₂S₂ in the potential energy distributions). According to the calculations, the shifts in $\nu(\text{S-S})$ between rotamers arise from significant involvement of the CCS deformation motion [$\delta(\text{CCS})$] in the $\nu(\text{S-S})$ vibration only for the T C-S conformation. Consequently, Sugeta^{92b} assumed that more effective mixing of these modes for a *trans* compared to a *gauche* carbon is the reason for the variation in $\nu(\text{S-S})$ among the rotamers.

Although the correlation of $\nu(\text{S-S})$ with C-S conformation propounded by Sugeta *et al.*⁹² rationalizes the observed $\nu(\text{S-S})$ vibrations of dialkyl disulphides, and was purportedly confirmed by normal coordinate calculations, the available structural information on these compounds from other sources is insufficient to test its validity. However, vibrational studies by Van Wart and Scheraga³¹ on a broad range of cystine-related disulphides, several of whose structures are known, have shown the correlation to be incorrect at least for primary disulphides. Of particular relevance in this regard is the intense $\nu(\text{S-S})$ vibration near 510 cm^{-1} in the Raman spectrum (Table 4) of dithiodiglycolic acid (compd. 27) which is to date the only primary disulphide established to have the T conformation for both C-S bonds. The relationship of Sugeta *et al.*⁹² erroneously predicts a $\nu(\text{C,C})$ vibration near 540 cm^{-1} for this compound.

Of the crystalline disulphides examined by Van Wart and Scheraga,³¹ those categorized as class II (characterized by a close correspondence between the solid-state and solution Raman spectra) were felt to have vibrations that can be correlated with the structures determined from X-ray

diffraction studies because the frequencies are implied to be governed minimally by crystal effects. Table 4 is a compilation of data for some class II disulphides with differing C-S conformations; yet, the dominant $\nu(\text{S-S})$ band occurs close to 510 cm^{-1} in each instance. Hence, the authors asserted "... it is clear that simple rotation about the C-S bond does not cause $\nu(\text{S-S})$ to vary in a uniform manner, as would have been expected if vibrational coupling between $\delta(\text{CCS})$ and $\nu(\text{S-S})$ motions affected $\nu(\text{S-S})$ ". Sugeta's^{92b} normal coordinate analysis of EtSSMe and Et_2S_2 had suggested this coupling to produce a smooth dependence of $\nu(\text{S-S})$ on CC-SS dihedral angle. Van Wart and Scheraga³¹ therefore concluded that these calculations provide no reliable information on the $\nu(\text{S-S})$ vibrations of primary disulphides. However, their claim that Sugeta^{92b} explicitly introduced mixing of $\nu(\text{S-S})$ and $\delta(\text{CCS})$ modes as a means of varying $\nu(\text{S-S})$ in his calculations is not substantiated by the published report. Nonetheless, the overlay technique* adopted by Sugeta^{92b} may well necessitate some such coupling in order to account for the diversity in $\nu(\text{S-S})$. Thus the results for EtSSMe and Et_2S_2 show the differences in $\nu(\text{S-S})$ between rotamers to be consistent with variations in its coupling with $\delta(\text{CCS})$, but do not prove this coupling to cause the differences. Van Wart and Scheraga³¹ have also pointed out that such coupling, if significant, should give rise to some change in $\nu(\text{S-S})$ with increased chain length in straight-chain dialkyl disulphides as a reflection of enhanced mixing of CCS and CCC deformation modes. In fact,

* In this approach, computations on several related molecules are performed simultaneously.

Table 4. Vibrational and Structural Data for Class II Primary Organodisulphides.^{31,120,122-124}

Disulphide ^a	Raman Vibrations (cm ⁻¹)		Dihedral Angles		CCSSCC Configuration
	Solid	Solution ^b	CS-SC	CC-SS	
(23) dibenzyl disulphide	407w 469s 505vs 569w	403w 468m 490m 512m 563w	92°	72° 73°	GGG
(25) bis [2-(N,N'-dimethylamino) ethyl] disulphide	403w 416w 450m 466w 503vs 532m	405m 445m 469m 506s ~528sh	82°	55° 67°	GGG
(26) cyclo-L-cystine	437w 448m 505s 516m	431w 454w 507s ~513sh	-91°	63° 67°	G'GG'
(27) dithiodiglycolic acid	419w 431w 481w 508vs 549w 569m 581m	429m 506s ~517sh 542w 576m	-86°	-167°	TGT
(28) N,N'-diglycyl-L-cystine·2H ₂ O	513m	509w	79°	97°	GGG

^a Structures for compounds 23,25,26 and 27 are shown in Section VI.A.1.

^b Solvents are 1N HCl (compds. 25,27 and 28), benzene (compd. 23) and dimethyl sulphoxide (compd. 26).

they found $\nu(\text{S-S})$ to be nearly invariant for Me_2S_2 through $(n\text{-pentyl})_2\text{S}_2$ (Table 2). Another argument advanced by these authors against the correlation of Sugeta *et al.*⁹² is the absence of a $\nu(\text{C,H})$ vibration in the solution Raman spectrum of Bz_2S_2 despite the expected tendency of the bulky phenyl groups to occupy the site *trans* to sulphur across the C-S bond.

The insensitivity of $\nu(\text{S-S})$ to C-S conformation for the disulphides of Table 4 was noted by Van Wart and Scheraga³¹ to be in accord with their earlier conclusion^{94b} that the 508 cm^{-1} $\nu(\text{S-S})$ band of both EtSSMe and Et_2S_2 is due to at least two rotamers. A minimum of three rotamers had been deduced to co-exist for each liquid in light of the complexity of the low-temperature Raman spectra in the $400\text{-}150\text{ cm}^{-1}$ region.* Both Sugeta *et al.*⁹² and Scott and El-Sabban^{89e} had assumed the presence of only two rotamers for each disulphide. The results of an electron diffraction investigation of EtSSMe by Yokozeki and Bauer^{76c} have done little to clarify the issue, although confirming the co-existence of no fewer than two rotamers in the gas phase. One of these, in a minimum proportion of 36%, was determined to be the TG rotamer, and a TG population in the range 36-45% requires the other species to be the GG and/or G'G rotamers between which the data could not differentiate. However, if the TG proportion is in excess of 50%, then the other rotamers could not be specified uniquely inasmuch as numerous combinations involving G, G', S, S' and C conformations for the

* Van Wart *et al.* detected several bands in this study that had not been reported previously.

ethyl C-S bond (Fig. 10) all conform to the observations.

Having rejected the correlation of Sugeta and co-workers⁹² as it applies to primary disulphides, Van Wart and Scheraga³¹ put forward a new interpretation for the $\nu(\text{S-S})$ vibrations. They attributed the prominent band near 510 cm^{-1} in the Raman spectra of the liquids and solutions to rotamers involving CC-SS dihedral angles of approximately 180° and/or 90° corresponding, respectively, to the T C-S conformation and to a conformation intermediate between G and S referred to as the B conformation. Evidence for the latter, as opposed to the G conformation, was extracted from the published solid-state structures of organodisulphides and cystine residues in proteins among which the greatest proportion of dihedral angles are indeed in the $80\text{--}100^\circ$ range for the B conformation. It is interesting, however, that G conformations do occur for the class II disulphides of known solid-state structure* (Table 4) which are thought to have the same structure in solution. The considerable disparity between the solid-state and solution Raman spectra of class I disulphides was noted by Van Wart and Scheraga³¹ to probably relate to the elimination in solution of intermolecular forces operative in the crystals. Considering that molecular distortions due to these forces may well explain the existence of B conformations in the solid-state, it is quite conceivable that these conformations convert to G conformations upon dissolution, in line with the G conformations for class II disulphides. In support of this contention, recent

* The exception is compound 28 whose place in this category is suspect anyway, being based on a single Raman band.

calculations by Allinger *et al.*¹¹⁹ on EtSSMe and Et₂S₂ have indicated a 'soft' potential energy function for rotation about the C-S bonds (*vide infra*), implying that the CC-SS dihedral angles in disulphides are rather easily deformed, e.g., by crystal-packing forces. Consequently, it seems unjustified to treat the B and G conformations as intrinsically different, particularly since the existence of B conformations in solution remains in question. Nevertheless, Van Wart and Scheraga's³¹ fundamental conclusion that the 510 cm⁻¹ ν (S-S) band of primary disulphides is associated with rotamers involving both G (or B) and T C-S conformations, in contradiction of the relationship of Sugeta *et al.*,⁹² appears to be well-founded.

The ν (S-S) feature near 525 cm⁻¹ for liquid primary disulphides and usually observed as a shoulder in the solution state was argued by Van Wart and Scheraga³¹ to arise from some local interaction within the CCSSCC moiety, since C-S torsion *per se* was thought to not affect ν (S-S) (*vide supra*). This interaction was postulated to be a weak attraction, labelled the 1,4 carbon-sulphur interaction, between aliphatic CH-type groups and sulphur atoms separated by three bonds. Such interaction was suggested to stabilize a C-S conformation, called the A conformation, with a rather small CC-SS dihedral angle. The angle was estimated to be about 20-30° on the grounds that 20% of the dihedral angles for cystine residues in proteins fall within 10° of this range. Evidence cited in support of the 1,4 interaction are the short carbon-sulphur contact distances, less than the van der Waals' distance, uncovered in a survey of organosulphur compounds,³⁰ and the dihedral angles of 10-20° for diaryl disulphides. Reasoning that the 1,4 attraction would perturb ν (S-S), the authors attributed the band at ~525 cm⁻¹

to rotamers with an A conformation for one of the C-S bonds. They drew attention to the absence of this band in the solution Raman spectrum of Bz_2S_2 which also lacks CH-type groups in position for 1,4 carbon-sulphur interaction, in apparent corroboration of their arguments.

The existence of the 1,4 carbon-sulphur interaction was originally inferred from CNDO/2 molecular orbital calculations by Van Wart, Shipman and Scheraga^{30, 125} on the potential energy functions for internal rotation about the C-S bonds of model dialkyl disulphides. The CS-SC dihedral angles were fixed at 90° . For EtSSMe, a pronounced minimum in the potential energy curve was obtained at the C C-S conformation (CC-SS dihedral angle near 0°) for the ethyl group, with a lesser minimum at the T conformation (CC-SS dihedral angle very close to 180°). A similar situation was discovered for Et_2S_2 with stable configurations only for C and T C-S conformations. The order of decreasing stabilities for the rotamers was indicated to be $\text{CG} < \text{TG}$ for EtSSMe and $\text{CGC} < \text{CGT} < \text{TGT}$ for Et_2S_2 , with a difference of 8.8 kJ mol^{-1} between the species. The stable configurations found for *n*-PrSSMe also involve C and T C-S conformations. Finally, the computations on *i*-PrSSMe and *t*-BuSSMe generated minima in the energy curves only for geometries in which a methyl group of the *i*-propyl or *t*-butyl substituent is positioned *cis* to the distal sulphur across the C-S bond.

Allowing for the tendency of CNDO/2 treatments to overestimate attractive nonbonded interactions, Van Wart *et al.*^{30,125} interpreted their results as indicative of some unspecified attraction — the 1,4 carbon-sulphur interaction — across the C-S bonds. Although hydrogen atoms were believed to

participate in the interaction, S...H-C hydrogen-bonding was ruled out in view of the non-colinearity of this arrangement in the disulphides and because the disposition of the hydrogens in EtSSMe and Et₂S₂ was observed to influence little the shapes of the potential energy curves. The genuine minima in these curves were suggested to occur at CC-SS dihedral angles significantly greater than 0°, since opening the angle gives a more reasonable separation between sulphur and the CH-type moiety three bonds removed. Small increases in the C-S bond length and CCS bond angle were shown to permit contact distances in line with those found in cystine-like disulphides at dihedral angles substantially less than for the G conformations in these reference compounds. The moderately stable A C-S conformation alleged to result from the 1,4 interaction was later surmised by Van Wart and Scheraga^{31,94d} to normally have a CC-SS dihedral angle of 20-30° in light of known protein structures. These authors rationalized the absence of a CNDO/2 minimum at the B(or G) conformation, expected on the basis of their vibrational studies, as due to the exaggerated stability of the C conformation in the calculations.

As regards unstrained secondary and tertiary disulphides, Van Wart and Scheraga³¹ assumed their higher $\nu(\text{S-S})$ wavenumbers compared to those of primary disulphides to be a consequence of the additional substituents at the β carbons. An increase of roughly 15 cm⁻¹ for each replacement of a hydrogen situated *trans* to the distal sulphur across the C-S bond by an alkyl group was proposed to explain the observed $\nu(\text{S-S})$ vibrations. This relationship poses difficulties, however, owing to the essentially identical

$\nu(\text{S-S})$ for the GGG and TGT configurations of the CCSSCC fragment in primary disulphides (*vide supra*). It therefore predicts a shift of about 30 cm^{-1} in $\nu(\text{S-S})$ upon substitution of the *trans* hydrogens in the GGG geometry, but no change for substitution of *gauche* hydrogens in the TGT geometry to obtain the same rotamer. Nonetheless, as employed by Van Wart and Scheraga,³¹ their modified form of the correlation of Sugeta *et al.*⁹² is equivalent to the original version in associating rotamers having one or two *trans* carbons with $\nu(\text{S-S})$ bands near 525 cm^{-1} [$\nu(\text{C,H})$] and 540 cm^{-1} [$\nu(\text{C,C})$], respectively. Neither group has discussed the implications concerning the isomerism of secondary disulphides in the liquid state or in solution.

Supporting evidence for the correlation outlined above arises in the Raman spectra of cyclic organodisulphides. Van Wart and Scheraga³¹ have demonstrated that once adjusted by subtraction of 12 cm^{-1} for a $\nu(\text{C,H})$ vibration and 24 cm^{-1} for a $\nu(\text{C,C})$ vibration, the $\nu(\text{S-S})$ wavenumbers for these strained disulphides depend directly on the CS-SC dihedral angle. Thus the 'corrected' $\nu(\text{S-S})$ fall at about 510, 509, 495 and 486 cm^{-1} for angles of approximately 90, 60, 30 and 10° , respectively, giving a linear relationship apart from a flattening-out of the plot near 510 cm^{-1} for angles above 65° . Provided the $\nu(\text{S-S})$ vibration is fairly localized, such a trend is not surprising in view of the parallel linear dependence of S-S bond length on dihedral angle with the bond weakening as the angle closes.^{31,53} Destabilization of the S-S bond with closing of the dihedral angle has consistently been predicted by molecular orbital calculations,^{56,58,62-75} and a CNDO/2 investigation of Me_2S_2 by Van Wart *et al.*⁶⁶ has shown a concomitant

lengthening of the bond and gradual displacement of $\nu(\text{S-S})$ to lower wavenumbers in the case of a pure stretching vibration. By way of contrast, the normal coordinate analysis of Me_2S_2 by Sugeta^{92b} indicated a virtually pure $\nu(\text{S-S})$ mode invariant in wavenumber with S-S torsion when the S-S bond length and force constant are both held constant. This implies that the observed variations in S-S bond length and $\nu(\text{S-S})$ among strained disulphides are indeed interrelated. Van Wart and Scheraga³¹ concluded that the downward shift in $\nu(\text{S-S})$ with closing the CS-SC dihedral angle is at least partly due to weakening of the bond. A $\nu(\text{S-S})$ wavenumber less than 505 cm^{-1} was deduced to signify strain in the S-S bond for which the dihedral angle can be estimated from their experimental curve. Initial disagreement about the linear dependence of $\nu(\text{S-S})$ for disulphides on the CS-SC dihedral angle has now been resolved in light of the effects of substitution at the β carbons on the $\nu(\text{S-S})$ wavenumber.^{93,94}

The most contentious aspect of Van Wart and Scheraga's³¹ interpretation of the vibrational spectra of organodisulphides is the supposed existence of the A C-S conformation for unstrained primary disulphides in the liquid state and in solution. In this regard, the curious shapes of the potential energy curves for rotation about the C-S bonds of simple dialkyl disulphides, viz, the minima in the region for the C conformation, found by Van Wart *et al.*^{30,125} in their CNDO/2 calculations have prompted Allinger and collaborators¹¹⁹ to re-investigate the molecules EtSSMe and Et_2S_2 using primarily semi-empirical molecular mechanics.¹²⁶ The force field employed was that developed for sulphur compounds by Allinger *et al.*^{49,127} in previous studies of thiols, sulphides, cyclic disulphides and sulphur allotropes.

There obtained from the calculations¹¹⁹ a normal dependence of rotational potential energy on dihedral angle with minima at the T, G and G' conformations for the C-S bonds and maxima at the C, S and S' conformations (Fig. 10). As detailed in Table 5, the GG and TG rotamers of EtSSMe were computed to be nearly isoenergetic at approximately 2.8 kJ mol^{-1} lower energy than the G'G rotamer. A barrier height of about 4 kJ mol^{-1} was found between these stable geometries. In a similar trend for Et_2S_2 , the GGG, GGT and TGT rotamers were calculated to differ by less than 0.2 kJ mol^{-1} and to lie roughly 2.5 kJ mol^{-1} lower in energy than the GGG' rotamer, while the G'GG' rotamer was determined to be destabilized to the extent of 9.4 kJ mol^{-1} relative to the most stable geometry. The CGC configuration emerged as a high energy transition state between rotamers. As acknowledged by Allinger *et al.*,¹¹⁹ the absence of a minimum at the A conformation for either molecule does not deny its existence, since no special methyl-sulphur attraction was provided for in the calculations. In defense of their own proposals, Van Wart and Scheraga^{94d} have pointed out that owing to the 'softness' of the molecular mechanics potential energy functions, even a small stabilization from the 1,4 carbon-sulphur interaction could produce a minimum in the A region.

In quest of any unusual effects related to the 1,4 interaction, Allinger and his associates¹¹⁹ also undertook *ab initio* molecular orbital calculations on various rotamers of EtSSMe using the optimized geometries from molecular mechanics. The computed relative energies (Table 5) are in good agreement with the molecular mechanics results, and no indication of any

Table 5. Relative Energies (kJ mol^{-1}) for Rotamers of EtSSMe from Various Calculations.^{119,128}

Rotamer ^a	Molecular Mechanics	<i>Ab initio</i> sp ^b	CNDO/2		MINDO/3 sp
			sp	spd	
GG	0.00	0.00	2.85	3.81	3.77
TG	0.04	0.25	0.00	0.00	0.00
G'G	2.85	2.43	6.57	3.97	5.02
S'G	3.93	5.77	5.94	6.07	
SG	4.73	5.27	6.07	5.56	
CG	8.87	12.80	5.36	6.40	7.53

^a The conformations refer to the C-S and S-S bonds, respectively.

^b Basis orbital set.

influential 1,4 attraction was forthcoming from these calculations. On the contrary, a weakly antibonding overlap between the sulphur and methyl orbitals across the SSCH_2CH_3 fragment was found for the C C-S conformation. The calculated charge distributions showed intramolecular hydrogen-bonding to be negligible in all the rotamers examined. Furthermore, although attraction between the slightly positive sulphur and the slightly negative methyl carbon would indeed be maximized in the C conformation, any resultant stabilization was noted to be largely offset by repulsion between sulphur and the slightly positive methyl hydrogens which become most positive in this geometry. Van Wart and Scheraga^{94d} have argued that because the *ab initio* treatment employed an inadequate basis set of orbitals and ignored the region for the A conformation where the 1,4 carbon-sulphur interaction is thought to be significant, the outcome decides nothing about this conformation. It should be recalled, however, that the 1,4 interaction was conceived on the basis of CNDO/2 minima in the region for the C conformation,^{30,125} in sharp disagreement with the *ab initio* results¹¹⁹ for this region.

Allinger *et al.*¹¹⁹ performed CNDO/2 computations on EtSSMe as well to probe the role of d orbitals, missing from the *ab initio* study, in the potential energy function. The results for the optimized geometries (Table 5) show the T and G C-S conformations to be considerably favoured over the C conformation whether or not d orbitals are included in the basis set.

On the other hand, rigid rotation* about the C-S bond of the TG rotamer led

* The structural parameters other than dihedral angle are held fixed during rigid rotation.

to relative energies for the CG configuration of -8.71 and $15.9 \text{ kJ mole}^{-1}$ with and without d orbitals, respectively. The former value agrees excellently with the earlier CNDO/2 findings of Van Wart *et al.*³⁰ predicated on rigid rotation with d orbitals included. Consequently, the peculiarly high stability of the C conformation calculated by these latter authors can be traced to the combined effects of d orbital participation and the rigid rotor approximation in their CNDO/2 approach.

A more recent investigation of EtSSMe by Boyd¹²⁸ using the modified-intermediate-neglect-of-differential-overlap (MINDO/3) computational method afforded the relative energies summarized in Table 5. The C C-S conformation for the ethyl group was again determined to be the least stable and no evidence was obtained for attractive 1,4 carbon-sulphur interaction. In fact, the outcome pointed to a net repulsive interaction between sulphur and the methyl group across the SSCH_2CH_3 moiety.

The molecular mechanics and *ab initio* calculations by Allinger *et al.*¹¹⁹ have presented a conventional picture of the variation of potential energy with internal rotation about a single bond. Moreover, the results were observed by the authors to be consistent with experimental evidence on the rotational isomerism for EtSSMe and Et_2S_2 . Thus the rotamer stabilities $\text{GG} \sim \text{TG} > \text{G}'\text{G}$ obtained for EtSSMe are in line with the interpretation of the liquid-state Raman spectrum by Van Wart *et al.*^{94b} in terms of the co-existence of two rotamers of comparable stability together with a third, less stable rotamer. The gas-phase electron diffraction data^{76c} indicate these rotamers to be indeed the TG, GG and GG' species provided the TG population

is 36-45% as is implied by the computed energies*. It is also worth noting that the optimized geometry for the GG rotamer determined by molecular mechanics¹¹⁹ compares very favourably with the electron diffraction structure.^{76c} In the case of Et₂S₂, the stabilities[#] GGG ~ GGT ~ TGT > GGG' ~ TGG' >> G'GG' are in accord with the conclusion of Van Wart *et al.*^{94b} on the basis of Raman data that at least two rotamers of roughly equal stability together with a less stable rotamer are present in the liquid. Furthermore, the relative energies calculated by molecular mechanics for the G'G rotamer of EtSSMe and the GGG' rotamer of Et₂S₂ lie within the range of estimates from vibrational studies (Sect. VI.A). In view of these observations, Allinger and co-workers¹¹⁹ deduced that the spectroscopically detectable higher energy rotamers of the two disulphides involve the G' C-S conformation.

In the opinion of Van Wart and Scheraga,^{94d} the molecular mechanics results for EtSSMe and Et₂S₂ do not explain the appearance of the $\nu(\text{S-S})$ vibration at $\sim 525 \text{ cm}^{-1}$ for these and other primary disulphides, since the G' C-S conformation as well as the T and G (or B) conformations are associated with the band at $\sim 510 \text{ cm}^{-1}$. This view is founded on the prominent $\nu(\text{S-S})$ feature at 506 cm^{-1} in the Raman spectrum³¹ of cyclo-L-cystine (Table 4) which has the G' conformation for both C-S bonds. However, the CHCH₂SSCH₂CH

* The Boltzman distribution at room temperature for the energies of Table 5 is 44% GG, 43% TG and 14% G'G.

Although they did not report an energy for the TGG' rotamer, Allinger *et al.*¹¹⁹ intimated that it was very near that of the GGG' rotamer.

fragment of this molecule is constrained in a bicyclic system with the CH groups locked into a diketopiperazine ring. It is therefore entirely possible that despite its normal CS-SC dihedral angle,¹²³ this moiety is not representative of unstrained primary disulphides, in which case neither are its Raman vibrations. Van Wart and Scheraga³¹ have remarked that subtle changes in the molecular forces within a disulphide are sufficient to shift $\nu(\text{S-S})$ by 15 cm^{-1} or so. Hence, it should be noted that the first ultra-violet absorption maximum for cyclo-L-cystine occurs at 305 nm, compared to values in the vicinity of 250 nm for dialkyl disulphides, due to interaction of the S-S bond with the diketopiperazine chromophore.¹²⁹ Inasmuch as the location of the $\nu(\text{S-S})$ band near 510 cm^{-1} for cyclo-L-cystine may thus be fortuitous, arising as a consequence of the special environment of its $\text{CHCH}_2\text{SSCH}_2\text{CH}$ grouping, this observation provides rather tenuous grounds on which to dismiss the assignment of the $\nu(\text{S-S})$ at $\sim 525 \text{ cm}^{-1}$ for primary disulphides to rotamers with a G' C-S conformation. No other data hitherto appear to conflict with this assignment. Observe that the absence of this feature for Bz_2S_2 , which Van Wart and Scheraga³¹ attributed to the inability of the molecule to stabilize the A conformation via the 1,4 carbon-sulphur interaction, is consistent with the considerable destabilization of the G' C-S conformation by steric hindrance involving the bulky benzyl substituents, as indicated by a space-filling molecular model (CPK type).

The crux of the molecular mechanics and *ab initio* calculations¹¹⁹ on EtSSMe and Et_2S_2 is that the rotational potential energy functions generated for the C-S bonds readily explain the available experimental data on primary

disulphides with no need to invoke any exceptional nonbonded effects such as the attractive 1,4 carbon-sulphur interaction propounded by Van Wart and Scheraga.^{31,94d} The evidence presented for this interaction is, in fact, all circumstantial and equivocal. Thus the minima found at the C C-S conformation in CNDO/2 studies^{30,125} of dialkyl disulphides appear to relate to deficiencies in the calculations. The 'short' contact distances between sulphur and aliphatic CH-type groups in some organosulphur compounds³⁰ actually occur for G conformations and not for the A conformations suggested to result from the 1,4 interaction. The rather small CC-SS dihedral angles in diaryl disulphides³¹ can be rationalized in terms of conjugation between sulphur $3p_{\pi}$ lone-pair orbitals and the aromatic ring, optimized at an angle of 0° .¹¹⁹ And finally, the dihedral angles of $20-30^{\circ}$ with respect to the C-S bonds of some cystine residues in proteins³¹ are not surprising, despite uncertainties of 20° or more in the calculated values, in light of the low torsional barriers found for EtSSMe and Et₂S₂ by Allinger *et al.*¹¹⁹, implying this structural parameter to be easily distorted by crystal forces. With regard to this last point, the absence of well-defined regions for the CC-SS dihedral angles in solid proteins is underscored by the fact that the absolute values for the 60 cystine residues examined by Van Wart and Scheraga³¹ span the range $10-180^{\circ}$ with at least one angle in each 10° segment. As concluded by Allinger and co-workers,¹¹⁹ the authenticity of the 1,4 carbon-sulphur interaction has not been convincingly demonstrated. By extension, the existence of A conformations stabilized by this interaction for primary disulphides in the liquid state or in solution remains decidedly suspect at this juncture.

Contrary to the claims of Van Wart and Scheraga,^{31, 94d} the weight of evidence to date seems to indicate that the inherently stable conformations with respect to the C-S bonds of primary organodisulphides are the G, T and G' staggered conformations. The order of stabilities for the $\text{CCH}_2\text{SSCH}_2\text{C}$ backbone of the molecules appears to generally be $\text{GGG} \sim \text{GGT} \sim \text{TGT} > \text{GGG}' \sim \text{TGG}' \gg \text{G'GG}'$. On this basis, the bands in the spectra of the liquids and solutions that tend to vanish upon solidification, including the $\nu(\text{S-S})$ feature at $\sim 525 \text{ cm}^{-1}$, are now attributed to the middle pair of configurations with one G' C-S conformation, whereas the remaining bands, including the $\nu(\text{S-S})$ feature at $\sim 510 \text{ cm}^{-1}$, are accredited to the trio of configurations involving only G and T conformations. The G'GG' configuration is too unstable to have a significant presence. The G and T C-S conformations are evidently distinguishable to some extent in the deformation and torsional vibrations,^{94b} but analysis of the low-frequency region where these occur is usually complicated by the broadness of the bands and their natural weakness in some cases, as well as by overlap with substituent vibrations. As a rule, therefore, the spectra offer a clear differentiation only between the comparably stable configurations GGG, GGT and TGT on the one hand, vs. the comparably stable configurations GGG' and TGG' on the other.

The van der Waals' interactions between nonbonded atoms that are generally conceded to play a crucial role in the rotational isomerism about single bonds are explicitly accounted for in molecular mechanics.¹²⁶ So the results for EtSSMe and Et_2S_2 are expected to reflect variations in nonbonded repulsions with internal rotation about the C-S bonds. Comparable

steric effects for Et_2S_3 , if they occur, would explain the close correspondence between the two compounds in both their vibrational spectra and their relative rotamer energies. Consequently, the nonbonded interactions in these molecules have been explored on the basis of calculations* of intramolecular contact distances and with the aid of space-filling molecular models (CPK type).

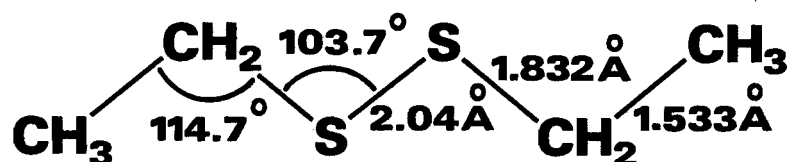
The bond lengths and angles assumed for the calculations (Table 6 and 7) were those found by Jones *et al.*¹³¹ in a neutron diffraction investigation of L-cystine hydrochloride and used by Van Wart *et al.*^{30,125} in their CNDO/2 studies. Comparisons of these parameters with data reported for various cystine-related disulphides^{30,31} show them to be typical of primary disulphides. In light of the available structural data for organopolysulphides,^{28,32-39} these values are also reasonable approximations for Et_2S_3 for which the SSS bond angle was taken from reports on the structures of Me_2S_3 ²⁴ and $(\text{CF}_3)_2\text{S}_3$.^{17a} The dihedral angles about the S-S bonds were fixed at 90° , characteristic of unstrained di- and polysulphides, while the CC-SS dihedral angles were varied among the idealized values for T, G, G' and C conformations (Fig. 10). Contact distances were thus ascertained for a total of ten configurations each for Et_2S_2 , *trans*- Et_2S_3 and *cis*- Et_2S_3 , as summarized in Tables 6 and 7. Only the contacts of the methylene and methyl moieties as a whole were determined, since these adequately elucidate the interactions involving the ethyl substituents. Within the constraints

* Performed using the computer program CART.¹³⁰

Table 6. Nonbonded Contact Distances (\AA) for Et_2S_2 .

Contact ^a	Rotamer ^b			
	TGT	GGG	G'GG'	CGC
$\text{CH}_2 \dots \text{CH}_2$	3.85	3.85	3.85	3.85
$\text{CH}_3 \dots \text{CH}_2$	5.19	4.60	3.55	3.68
$\text{CH}_3 \dots \text{CH}_3$	6.60	5.65	2.68	3.90
$\text{CH}_3 \dots \text{S}$	4.49	3.44	3.44	3.01

^a Molecular structure:

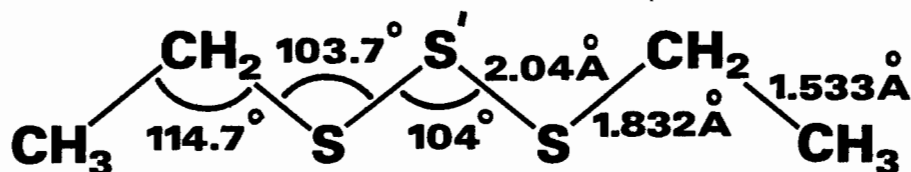


^b The nonbonded separations in the nonsymmetric rotamers are the same as in the corresponding symmetric species, e.g., the $\text{CH}_3 \dots \text{CH}_2$ distances in the TGG rotamer are 5.19\AA for the T half and 4.60\AA for the G half. The exception is the $\text{CH}_3 \dots \text{CH}_3$ separation: 5.70 (TGG), 4.74 (TGG'), 4.70 (TGC), 4.42 (GGG'), 4.85 (GGC), 3.21\AA (G'GC).

Table 7. Nonbonded Contact Distances (\AA) for Et_2S_3 .

Contact ^a	<i>trans</i> -Rotamer ^b				<i>cis</i> -Rotamer ^b			
	TGGT	GGGG	G'GGG'	CGGC	TGG'T	GGG'G	G'GG'G'	CGG'C
$\text{CH}_2 \dots \text{CH}_2$	5.28	5.28	5.28	5.28	3.90	3.90	3.90	3.90
$\text{CH}_3 \dots \text{CH}_2$	6.45	6.20	5.18	5.44	5.18	4.49	2.92	2.01
$\text{CH}_3 \dots \text{CH}_3$	7.52	6.86	5.37	5.82	6.27	4.56	1.59	3.19
$\text{CH}_3 \dots \text{S}'$	4.49	3.44	3.44	3.01	4.49	3.44	3.44	2.01
$\text{CH}_3 \dots \text{S}$	5.31	4.76	3.63	3.81	5.31	4.76	3.63	3.81
$\text{CH}_2 \dots \text{S}$	3.99	3.99	3.99	3.99	3.99	3.99	3.99	3.99

^a Molecular structure:



^b The nonbonded separations in the nonsymmetric rotamers are the same as in the corresponding symmetric species, e.g., the $\text{CH}_3 \dots \text{CH}_2$ distances in the TGGG rotamer are 6.45\AA for the T half and 6.20\AA for the G half. The exception is the $\text{CH}_3 \dots \text{CH}_3$ distance: 7.46 (TGGG), 6.09 (TGGG'), 6.56 (TGGC), 6.86 (GGGG'), 6.26 (GGGC), 5.76 (G'GGC), 5.86 (TGG'G), 3.97 (TGG'G'), 4.51 (TGG'C), 3.61 (GGG'G'), 3.33 (GGG'C), 2.26\AA (G'GG'C).

imposed by rigid rotation about the C-S bonds, none except the contact distances associated with the methyl groups differ between configurations. In molecular mechanics, however, the geometries are allowed to relax in order to minimize the total energy for each configuration considered.

In seeking close nonbonded approaches in Et_2S_2 and Et_2S_3 that may govern stability, the calculated contact distances are compared to the well-known van der Waals' distances due to Pauling¹³² of 4.0 \AA for interactions among methylene and methyl groups, and 3.85 \AA for interaction of either of these groups with a sulphur atom. At separations less than these distances, net repulsion between the moieties in question is assumed to arise from interpenetration of their electron clouds. There is growing evidence, however, that contacts involving sulphur can be considerably closer than previously thought. Furthermore, there are indications¹²⁸ of an orientational dependence of the contact distance related to the spatial characteristics of the lone-pair orbitals. Van Wart *et al.*^{30,125} in their studies of disulphides have suggested a van der Waals' contact distance of 3.40 \AA between sulphur and aliphatic CH-type groups, similar to the value of 3.45 \AA adopted by Nemethy and Scheraga¹³³ for investigations of peptide conformations. On the other hand, it has been argued, notably by Allinger,¹²⁶ that since the van der Waals' distances proposed by Pauling¹³² are based on crystal structures in which the nearest intermolecular approach is controlled partly by attractions involving atoms not at the point of contact, substantially larger values are appropriate for intramolecular interactions. Thus Allinger has opted for a van der Waals' radius of 2.00 \AA for sulphur in his molecular

mechanics calculations,^{49,119,127} vs. the Pauling radius of 1.85 Å.

Despite the uncertainties concerning sulphur, the Pauling contact distances provide adequate guidelines for the present purposes in view of the approximate nature of the computations, especially in the use of rigid geometries and formalized dihedral angles for the rotamers.

As anticipated, the contact distances found for Et₂S₂ (Table 6) explain to a large degree the relative rotamer energies calculated by molecular mechanics¹¹⁹ for this disulphide and also for EtSSMe (*vide supra*). Thus the considerable instability of the G'GG' rotamer of Et₂S₂ is consistent with quite severe CH₃...CH₃ interaction for this geometry, while the lower stability of the GGG' rotamer than that of the GGG rotamer is attributable largely to unfavourable CH₃...CH₂ contact for the G' C-S conformation. Analogous CH₃...CH₃ interaction in the GG' rotamer of EtSSMe similarly accounts for its reduced stability compared to the GG rotamer. The significance of this interaction is demonstrated by the opening of the CCS angle from 110.3° to 112.5° between the optimized geometries for the GG and GG' rotamers.¹¹⁹ The space-filling model of Et₂S₂ shows brushing together of the CH₃ and CH₂ groups for the G' conformation. In presuming this conformation to be precluded by steric hindrance for Et₂S₂ and EtSSMe, however, Scott *et al.*^{89b,e} evidently overstated the importance of alkyl group interactions in these molecules. It is noteworthy that these interactions are generally fairly weak in those Et₂S₂ configurations with a C C-S conformation, indicating the high instability of the CGC rotamer of Et₂S₂ and of the CG rotamer of EtSSMe to be of a different origin, i.e., due to the adverse eclipsing of C-C and C-S bonds. The fact that the C conformation minimizes the

$\text{CH}_3 \dots \text{S}$ separation reveals why the overestimation of nonbonded attraction in CNDO/2 studies^{30,119,125} leads to an apparent potential energy minimum in the C region. The net repulsive nature of this interaction according to molecular mechanics is manifest in the increase in the CCS angle to 116.4° in the optimized geometry for the CG rotamer of EtSSMe.¹¹⁹

The somewhat close $\text{CH}_3 \dots \text{S}$ contact for the G conformation with respect to the C-S bonds of Et_2S_2 would be thought to engender at least a slight preference for the T conformation in which this interaction is negligible. This is particularly so in view of the greater CCS angle for the GG rotamer (110.3°) of EtSSMe than for the TG rotamer (108.9°) in the optimized geometries, suggesting an influence from the $\text{CH}_3 \dots \text{S}$ interaction. Nevertheless, molecular mechanics¹¹⁹ pointed to a marginal preference for the G conformation for both EtSSMe and Et_2S_2 due mainly to destabilizing *vicinal gauche* S...H interactions of which there are one and two in the G and T conformations, respectively (Fig. 10). However, it is now recognized¹³⁴ that the hydrogen atoms may be somewhat oversized in the force field of Allinger *et al.*,^{49, 127} and the reliability of the field may suffer as well from the approximation of spherical electron density at sulphur*. The *ab initio* calculations by Allinger *et al.*¹¹⁹ also showed the G conformation to be slightly favoured for EtSSMe, but the outcome could be biased by the use of the optimized geometries from molecular mechanics in the computations.

* Still, the success of this field for cyclic disulphides and sulphur allotropes implies that the directionality of the sulphur lone-pairs is adequately taken into account in the torsional function for the S-S bonds.

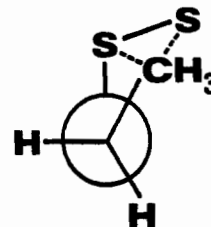
By way of contrast, both CNDO/2^{30,125} and MINDO/3¹²⁸ treatments of EtSSMe have strongly favoured the T conformation, but these results are clearly in disagreement with the evidence from vibrational studies^{31,94b} of two stable rotamers of very similar energy together with a somewhat less stable rotamer. Whether the G or T conformation is the more stable remains unresolved. There can be little doubt, though, regarding the comparable stability for the GG and TG rotamers of EtSSMe and for the GGG, TGG and TGT rotamers of Et₂S₂ predicted by molecular mechanics¹¹⁹ and indicated by vibrational data for these and other cystine-related disulphides.^{31,94b}

The differences in vibrational wavenumbers between rotamers of EtSSMe and Et₂S₂ with a G' C-S conformation compared to those with only G and/or T conformations are attributable to the same nonbonded interactions that account for the relative stabilities (*vide supra*). These interactions might perturb the vibrational force field and/or modify the molecular structures, as is suggested by the optimized geometries for EtSSMe from molecular mechanics.¹¹⁹ Small such effects would explain, for instance, the $\sim 15 \text{ cm}^{-1}$ shift in $\nu(\text{S-S})$. These concepts can be extended to primary disulphides in general in view of their essentially identical $\nu(\text{S-S})$ vibrations. It should be noted that in ignoring nonbonded effects in his normal coordinate calculations, Sugeta^{92b} found no variation in $\nu(\text{S-S})$ amongst the GGG, GGG' and G'GG' rotamers of Et₂S₂, nor between the GG and G'G rotamers of EtSSMe, attesting to the importance of these effects in the observed spectra.

As regards the contact distances calculated for Et₂S₃ (Table 7), discussion of the differences between the *trans* and *cis* rotamers is deferred to Section VI.A.1.ii. It need only be mentioned here that the available

evidence indicates the *trans* rotamer to be decidedly predominant in liquid trisulphides, and hence comparisons at this stage are sought only between *trans*-Et₂S₃ and Et₂S₂. Of note, in particular, is that the CH₃...S contact across the CH₃CH₂SSS fragment of *trans*-Et₂S₃ is negligible for the G and T C-S conformations while significant for the G' conformation, paralleling the situation for the corresponding CH₃...CH₂ contact in Et₂S₂. The space-filling models of the two molecules also reveal such similarities in non-bonded interactions. Attendant destabilization favours the G and T conformations over the G' conformation for both molecules. The shorter-range CH₃...S contact across the CH₃CH₂SS fragment is calculated to be identical for the di- and trisulphide since this moiety is common to both. Consequently, it can be tentatively assumed that the G and T C-S conformations are essentially isoenergetic for *trans*-Et₂S₃, just as they appear to be for Et₂S₂* (*vide supra*). What emerges then are the relative stabilities GGGG ~ GGGT ~ TGGT > GGGG' ~ TGGG' > G'GGG' for the rotamers of *trans*-Et₂S₃, much the same as the order GGG ~ GGT ~ TGT > GGG' ~ TGG' >> G'GG' for Et₂S₂. The two series differ in that the strongly destabilizing CH₃...CH₃ interaction in the G'GG' rotamer of Et₂S₂ is not matched in magnitude by the analogous CH₃...CH₂

* It is interesting that attractive CH₃...S interaction in Et₂S₃ would be expected to stabilize an A-type conformation to a greater extent than for Et₂S₂ because of two such interactions (Figure). Accordingly, the comparable spectral characteristics for the tri- and disulphide seem to require an explanation in terms of repulsive CH₃...S interaction.



interaction in the G'GGG' rotamer of *trans*-Et₂S₃. The proposed order for *trans*-Et₂S₃ is consistent with the evidence from the vibrational spectra of at least a pair of rotamers of similar stability together with a somewhat less stable rotamer (Sect. VI.A). Furthermore, the like patterns of rotamer stabilities for *trans*-Et₂S₃ and Et₂S₂ are in line with the marked resemblances in their vibrational spectra (Sect. VI.A.2) and also with their comparable relative rotamer energies estimated from the temperature-dependence of the spectra (Sect. VI.A). These observations strongly support the present conclusion that the isomerism found for Et₂S₃ arises from internal rotation about the C-S bonds*, as is perforce the case for Et₂S₂. Moreover, Et₂S₃ and Et₂S₂ both display pairs of prominent $\nu(\text{S-S})$ and $\nu(\text{C-S})$ vibrations contrasted with single vibrations for Me₂S₃ and Me₂S₂ for which there can be no C-S isomerism. The vibrational bands that gradually disappear for Et₂S₃ upon cooling are now assigned to the GGGG' and TGGG' *trans*-rotamers while the bands that persist are attributed to the GGGG, GGGT and TGGT *trans*-rotamers. In view of the practically identical $\nu(\text{S-S})$ vibrations for Et₂S₃ and *n*-Pr₂S₃ (Sect. VI.A.2), these assignments appear to apply generally to the CCH₂SSSCH₂C spine of primary organotrisulphides. Changes observed in the Raman spectrum of Et₂S₃ upon solidification of the glass (Sect. VI.A) indicate slight differences between G and T C-S conformations. For the most part, however, the spectra clearly distinguish only between the GGGG, GGGT and TGGT group of configurations vs. the GGGG' and TGGG' group. The shifts

* This isomerism was suggested by Freeman⁸³ to occur in the SSS nucleus of the molecule.

in vibrational wavenumbers between these two groups can be rationalized in terms of the effects of nonbonded interaction in the G' C-S conformation, as discussed above for primary disulphides.

The role of intramolecular nonbonded interactions in the rotational isomerism of secondary di- and trisulphides has been assessed on the basis of space-filling molecular models of *i*-Pr₂S₂ and *i*-Pr₂S₃ with reference to the contact distances calculated for their ethyl analogues (Tables 6 and 7). Again, only the *trans*-trisulphide is considered at this stage. The T and G' staggered conformations for the C-S bonds of *i*-Pr₂S₂ and *trans-i*-Pr₂S₃ (Fig. 11) entail significant nonbonded interaction across the CH₃CHSSCH and CH₃CHSSS fragments, respectively. This creates at least a slight preference for the G conformation in which such interaction is negligible. The T and G' conformations themselves can be theorized to be approximately isoenergetic on the grounds that they differ only by one *vicinal gauche* interaction (S...CH₃ vs. S...H), as do the G and T C-S conformations of Et₂S₂ and EtSSMe (Fig. 10) which are of nearly the same energy (*vide supra*). Unfortunately, the molecular mechanics or electron diffraction studies of *i*-Pr₂S₂ or *i*-PrSSMe that would test this idea have not yet been reported. However, molecular mechanics has indicated quite similar energy gaps between the G and T rotamers of *i*-PrSMe (1.0 kJ mol⁻¹) and EtSMe (1.2 kJ mol⁻¹), with the higher-energy species in each case being the one that minimizes *gauche* CH₃...CH₃ contact.^{127a} These results imply similar nonbonded effects for ethyl and *i*-propyl groups on sulphur. On the premise that the T and G' C-S conformations are indeed of roughly equal energy for *i*-Pr₂S₂ and *i*-Pr₂S₃,

the order of stabilities for the rotamers of the *trans*-trisulphide becomes $GGGG > GGGT \sim GGGG' > TGGT \sim TGGG' \sim G'GGG'$, while the order for the disulphide is $GGG > GGT \sim GGG' \gg TGT \sim TGG' \sim G'GG'$. The last three rotamers of $i\text{-Pr}_2\text{S}_2$ are strongly destabilized by $\text{CH}_3 \dots \text{CH}_3$ steric hindrance. Since the other divisions within both series are due to weakly destabilizing interactions ($\text{CH}_3 \dots \text{S}$ for *trans*- $i\text{-Pr}_2\text{S}_3$ and $\text{CH}_3 \dots \text{CH}$ for $i\text{-Pr}_2\text{S}_2$), the first two groups of rotamers for each compound are expected to co-exist to a significant degree in the liquid. The vibrational spectra confirm the presence of at least two rotamers for each compound at room temperature, and the present study of the temperature-dependence of the Raman spectrum of $i\text{-Pr}_2\text{S}_3$ (Sect. VI.A) points to a single preferred rotamer consistent with the proposed order of stabilities.* Weak evidence for a pair of less stable rotamers for $i\text{-Pr}_2\text{S}_3$ occurs in the spectrum of the metastable phase (Sect. VI.A). The considerably smaller energy difference between the rotamers of $i\text{-Pr}_2\text{S}_3$ than between the Et_2S_3 rotamers (Sect. VI.A), implies that nonbonded interactions are less influential in the former trisulphide. On the other hand, the close resemblance between the spectra of $i\text{-Pr}_2\text{S}_3$ and $i\text{-Pr}_2\text{S}_2$, notably in the $\nu(\text{S-S})$ and $\nu(\text{C-S})$ vibrations, suggests comparable relative stabilities for the first two groups of rotamers for the two compounds. The foregoing discussion leads to assignments of the vibrational bands of $i\text{-Pr}_2\text{S}_3$ that tend to vanish upon cooling to the $GGGT$ and $GGGG'$ *trans*-rotamers, and the bands that persist for the

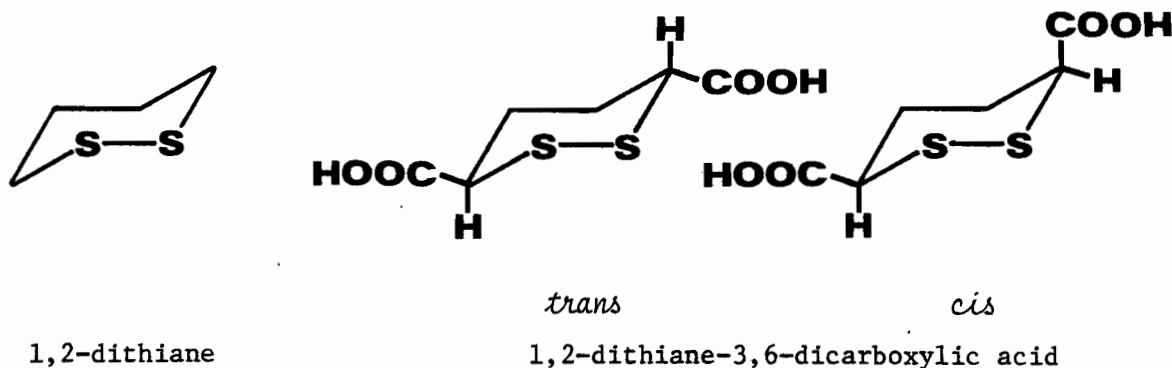
* The temperature-dependence of the vibrational spectra of $i\text{-Pr}_2\text{S}_2$ or other secondary disulphides has not been described thus far in the literature.

solid to the more stable GGGG *trans*-rotamer. By analogy, the spectra of $\text{i-Pr}_2\text{S}_2$ can be assigned in terms of bands (including the $\nu(\text{S-S})$ feature at 527 cm^{-1}) for the GGT and GGG' rotamers on the one hand, and bands (including the $\nu(\text{S-S})$ feature at 543 cm^{-1}) for the preferred GGG rotamer on the other. These assignments can be generalized for the CCHSSCHC skeleton of secondary organodisulphides considering their very similar $\nu(\text{S-S})$ patterns.

The differences between the rotamers of both $\text{i-Pr}_2\text{S}_2$ and *trans*- $\text{i-Pr}_2\text{S}_3$ in the vibrational spectra can be rationalized to arise from nonbonded interaction ($\text{CH}_3\cdots\text{CH}$ and $\text{CH}_3\cdots\text{S}$, respectively) in those configurations with a T or G' C-S conformation, just as similar differences between the rotamers of both Et_2S_2 and *trans*- Et_2S_3 can be explained on the basis of nonbonded interaction ($\text{CH}_3\cdots\text{CH}_2$ and $\text{CH}_3\cdots\text{S}$, respectively) in geometries with a G' C-S conformation. What is not apparent, though, is why such interactions shift $\nu(\text{C-S})$ to lower wavenumbers in the *i*-propyl compounds, but to higher wavenumbers in the ethyl compounds. The answer might be afforded by individual normal coordinate calculations on the molecules, provided enough isotopic data could be collected to define the vibrational force field uniquely in each case. Of particular concern is to establish if the inclusion of force constants for nonbonded interactions is necessary and/or sufficient to account for the observed spectra.

According to correlation for the $\nu(\text{S-S})$ vibrations of secondary disulphides propounded by Van Wart and Scheraga³¹ and by Sugeta and his associates,⁹² the band position depends simply on the occupancy of the sites

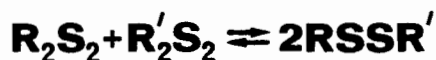
trans to the distal sulphur across the C-S bonds (*vide supra*). On this basis, the band at 543 cm^{-1} for $i\text{-Pr}_2\text{S}_2$ is due to rotamers with carbons in both *trans* sites [$\nu(\text{C,C})$ vibration], while the band at 527 cm^{-1} belongs to rotamers with a *trans* carbon and a *trans* hydrogen [$\nu(\text{C,H})$ vibration]. The present assignments are in agreement insofar as the former band is accredited to the GGG rotamer (two *trans* carbons) and the latter is attributed to the GGT rotamer (a *trans* carbon and a *trans* hydrogen). In dispute, on the other hand, is the assignment of the $\nu(\text{S-S})$ band at 527 cm^{-1} also to the GGG' rotamer (two *trans* carbons). The earlier correlation is suspect, however, owing to its failure for primary disulphides (*vide supra*). Still, the $\nu(\text{S-S})$ vibrations of cyclic organodisulphides appear to support this correlation (*vide supra*) and therefore warrant a re-examination. Van Wart and Scheraga³¹ showed that adjustments of 24 cm^{-1} for a $\nu(\text{C,C})$ vibration and 12 cm^{-1} for a $\nu(\text{C,H})$ vibration were necessary in order for $\nu(\text{S-S})$ to exhibit the theoretically predicted linear dependence on CS-SC dihedral angle. For instance, when applied to *trans*- and *cis*-1,2-dithiane-3,6-dicarboxylic acid in solution, these corrections displace $\nu(\text{S-S})$ from 532 to 508 cm^{-1} and from 518 to 506 cm^{-1} , respectively.³¹ The adjusted wavenumbers



are close to the 509 cm^{-1} value for the parent 1,2-dithiane which is characteristic of a dihedral angle near 60° .³¹ On the other hand, the pattern of uncorrected $\nu(\text{S-S})$ wavenumbers for the three disulphides parallels that for Me_2S_2 (508 cm^{-1}) and the two $i\text{-Pr}_2\text{S}_2$ rotamers (543 and 527 cm^{-1}), with the shift between the pair of acid forms matching closely that between the $i\text{-Pr}_2\text{S}_2$ rotamers (14 cm^{-1} vs. 16 cm^{-1}). A space-filling model of 1,2-dithiane in its preferred chair conformation⁴⁹ reveals that substitution for hydrogen in an equatorial site (*trans* to the distal sulphur) at the β carbon introduces no new nonbonded interactions, whereas substitution into an axial site (*gauche* to the distal sulphur) occasions weak interaction with the *vicinal* methylene group of the ring. Thus, the lower-energy $\nu(\text{S-S})$ band for both the acid and $i\text{-Pr}_2\text{S}_2$ corresponds to the geometry involving nonbonded interaction that is absent in the structure responsible for the higher-energy band. Accordingly, the extent of nonbonded interaction within a linear or cyclic secondary disulphide configuration can be argued to determine $\nu(\text{S-S})$. The attractiveness of this kind of explanation for the variation in $\nu(\text{S-S})$ between different structures lies largely in its applicability to primary disulphides as well.

At this juncture, it is appropriate to point out that the strong $\text{CH}_3\cdots\text{CH}_3$ interaction that appears to preclude some rotamers of Et_2S_2 and $i\text{-Pr}_2\text{S}_2$ is an intrinsic feature of $t\text{-Bu}_2\text{S}_2$ which, nevertheless, exists as a stable entity. However, a space-filling model of the molecule demonstrates rapid attenuation of this contact with opening of the CS-SC dihedral angle. Indeed, both dipole moment¹³⁵ and photoelectron⁵⁵ data indicate a

larger dihedral angle for $t\text{-Bu}_2\text{S}_2$ than for primary and secondary disulphides. Particularly revealing are the dihedral angle-dependent splittings between the first two ionization peaks in the photoelectron spectra: 0.21-0.30 eV for R_2S_2 ($\text{R}=\text{H}, \text{Me}, \text{Et}, n\text{-Pr}, n\text{-Bu}, i\text{-Pr}$) with angles near 90° , 0.95 eV for 1,2-dithiane with an approximately 60° angle, 1.80 eV for 6,8-dithioteic acid with its 35° angle, and 0.60-0.65 eV for $t\text{-Bu}_2\text{S}_2$. These observations have led to dihedral angle estimates of 97.5° ^{55c} and about 110° ^{55a} for $t\text{-Bu}_2\text{S}_2$.^{*} The former value agrees with an estimate from dipole moment measurements,^{55c} while the latter is in line with the 115° angle found for crystalline D-penicillamine disulphide⁴² (compd. 15). Observe that the smallness and constancy of the photoelectron splittings cited above for the R_2S_2 species point to the absence of significant distortion from 90° in the CS-SC dihedral angles, supporting the idea that the predominant rotamers for these disulphides involve minimal interaction between the alkyl substituents. A CART calculation¹³⁰ on the G'GG' rotamer of Et_2S_2 as a rough model of $t\text{-Bu}_2\text{S}_2$ shows that opening the CS-SC dihedral angle from 90 to 110° greatly ameliorates the $\text{CH}_3\cdots\text{CH}_3$ repulsion by increasing the contact distance from 2.7 to 3.4 \AA , although appreciable interaction persists. It is hence worth noting that for the disproportionation equilibria where R



is a primary alkyl substituent, a nearly statistical distribution of molecules

* Although the data do not distinguish between positive and negative deviations from 90° , the former is obvious from steric considerations.

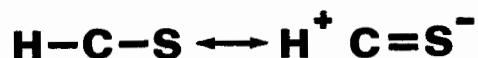
(equilibrium constant $K \sim 4$) obtains when R' is a primary or secondary alkyl group, whereas the unsymmetric disulphide is highly favoured ($K \gg 24$) if R' is a *t*-butyl group.¹³⁶ This disparity has been attributed to hindered rotation about the C-S bonds in *t*-Bu₂S₂ due to interference between the *t*-butyl substituents.¹³⁶

In the case of the *trans* rotamer of *t*-Bu₂S₃, there is presumably some increase from 90° in the CS-SS dihedral angles to ease CH₃...S repulsion across the CH₃CSSS fragment. Similar interactions in *trans*-Et₂S₃ and *trans*-*i*-Pr₂S₃ have been argued above to be mainly responsible for the stability differences between rotamers of these molecules. The smaller dipole moment found for *t*-Bu₂S₃ than for Me₂S₃ and Et₂S₃ may reflect distortion in the former molecule.¹³⁵ An X-ray diffraction investigation of the related compound *trans*-(CCl₃)₂S₃^{23c,d} has indicated dihedral angles of 94±2° with considerable asymmetry in the SCl₃ tetrahedra. The latter, however, was explained in terms of interaction between the central sulphur and chlorine atoms.

Another interesting aspect of the $\nu(\text{S-S})$ vibrations of dialkyl disulphides, and similarly of dialkyl trisulphides, is the shift to higher wave-numbers in going from primary to secondary to tertiary species (Table 2). Although the reasons for this trend remain unclear, the shifts are plainly not a consequence of increasing mass at the carbon atoms since the reverse trend is predicted on this basis. Nor are the high $\nu(\text{S-S})$ values for the tertiary disulphides due to dihedral angle distortion since concomitant destabilization of the S-S bond should, if anything, lower $\nu(\text{S-S})$ relative to primary and secondary disulphides. Differences in the electron-donating

ability of substituents ($t\text{-Bu} > i\text{-Pr} > \text{Et} > \text{Me} > \text{H}$)¹³⁷ also do not seem to be a dominant factor for $\nu(\text{S-S})$ in view of the very similar wavenumbers for H_2S_2 , Me_2S_2 and the major rotamers of EtSSMe and Et_2S_2 , and because increasing the electron density at sulphur should actually displace $\nu(\text{S-S})$ downwards owing to weakening of the S-S bond. This destabilization of the bond is expected on the grounds that the transfer of electron density onto the sulphur atoms worsens the interaction between the lone-pairs. Boyd⁵⁶ has noted that both lone-pair molecular orbitals for the S-S bond of H_2S_2 and of Me_2S_2 have a node between the atoms and that drainage of electron density from these nodes strengthens the bond. Conversely, increased donation of electron density into the nodal regions, as occurs across the series Me_2S_2 , Et_2S_2 , $i\text{-Pr}_2\text{S}_2$ and $t\text{-Bu}_2\text{S}_2$, destabilizes the bond which should lower $\nu(\text{S-S})$. Inductive effects do influence the photoelectron spectra of disulphides, however, as evidenced by the linear dependence of the first ionization energy (energy to expel an electron from the highest occupied orbital) for unstrained disulphides (CS-SC dihedral angle near 90°) on the sum of the Taft inductive constants for the substituents.¹³⁷ Simple molecular orbital calculations¹³⁷ have shown the pattern to be consistent with an increase in the energy of the highest occupied orbital for more electron-donating substituents. Then again, the greater stabilization of the R_2S_2^+ cation by more electron-releasing groups also explains the trend.⁵⁶ The first ultraviolet absorption band for the dialkyl disulphides, and likewise for dialkyl diselenides, is progressively blue shifted (to higher energy) as the substituents become more electron-releasing.^{138,139} Yet, Bergson¹³⁹ has argued that increased electron-donation to sulphur (or selenium) should produce the

opposite trend due to diminution of the effective nuclear charge with an attendant closing of the energy gap between the ground and excited electronic states. He therefore offered an explanation in terms of a hyperconjugative delocalization of electron density from C-H σ bonds into d orbitals on S (or Se) expressed by the resonance below. This was



suggested to stabilize the excited state more than the ground state and thereby reduce the excitation energy. Because C-C σ bonds are not prone to hyperconjugation, this effect should lessen from primary to secondary to tertiary disulphides (or diselenides) causing the excitation energy to decrease in the reverse order, consistent with the observed spectra.* Noting that hyperconjugation in dialkyl diselenides engenders double-bond character in the C-Se bonds, and thus strengthen them, Bergson¹³⁹ also attributed shifts in $\nu(\text{C-Se})$ to this effect. Analogous reasoning rationalizes the $\nu(\text{C-Se})$ and $\nu(\text{C-S})$ Vibrations (cm^{-1})

R	R_2Se_2 ^{139a}	R_2S_2 ⁹²	R_2S_3 (this work)
Me	570	691	696
Et	536	642,668	644,670
<i>i</i> -Pr	517	596,625	595,626
<i>t</i> -Bu	507	570	573

* Boyd⁵⁶ has recently concluded that the first uv band of *t*-Bu₂S₂ has been misassigned due to its weak intensity and is in reality red shifted relative to Me₂S₂ owing to distortion in the CS-SC dihedral angle. This argument does not apply to *t*-Bu₂Se₂, however, since it does not appear to be distorted appreciably.^{135a}

variations in $\nu(\text{C-S})$ for dialkyl di- and trisulphides.* Since the hyperconjugative resonance depicted above transfers electron density onto sulphur, the S-S bond can be argued to weaken somewhat from tertiary to secondary to primary di- and trisulphides (*vide supra*), i.e., in the same order as the increase in hyperconjugation. It is worth noting that this transfer is specifically into d orbitals and thus may destabilize the S-S bond also by interfering with any coordinate 3p-3d π bonding (Chapter III). The decrease in $\nu(\text{S-S})$ from tertiary to secondary to primary di- and trisulphides is therefore in line with enhanced hyperconjugation in the opposite direction. Left unanswered, however, is how this effect could shift $\nu(\text{S-S})$ considerably between Me_2S_2 and Et_2S_2 , or between Me_2S_3 and Et_2S_3 , while $\nu(\text{S-S})$ remains the same for the former and the principle rotamer of the latter. In addition, it should be pointed out that inductive or hyperconjugative effects would be expected to perturb the S-S bond to only a small extent. Consequently, it is not surprising that S-S dissociation energies evaluated from thermochemical data¹⁴⁰ reveal no systematic variation among dialkyl disulphides, and in fact suggest the energy to be invariant.

An indirect influence of hyperconjugation may arise because of its tendency to displace $\nu(\text{S-S})$ and $\nu(\text{C-S})$ towards each other, i.e., to narrow the energy separation between them. This would enhance the possibility of coupling of the two vibrations that could further draw them together. Coupling of $\nu(\text{S-S})$ with other vibrational modes may also be at the heart of the $\nu(\text{S-S})$

* Although depending on both C-S and C-C conformations, the $\nu(\text{C-S})$ vibrations of dialkyl disulphides clearly shift to lower wavenumbers from primary to secondary to tertiary species.⁹²

variation. The normal coordinate calculations by Sugeta^{92b} have indeed demonstrated that mixing of S-S and C-S stretching modes with *t*-butyl modes can account for the differences in $\nu(\text{S-S})$ and $\nu(\text{C-S})$ among Me_2S_2 , *t*-BuSSMe and *t*-Bu₂S₂, but such coupling is likely an inherent consequence of his use of a single force field for all three disulphides.* On the other hand, differences in vibrational coupling between primary, secondary and tertiary di- and trisulphides related simply to branching at the β carbons may be the dominant factor governing the spectra. In any event, only subtle differences between various di- or trisulphides, e.g., in hyperconjugation or vibrational coupling, would explain the small variations observed in the $\nu(\text{S-S})$ and other vibrations of the molecules.

* Recall that the similar coupling afforded by the computations on EtSSMe and Et₂S₂ has since been refuted (*vide supra*).

VI.A.1.ii S-S Isomerism

The structural information to date on unstrained organotrisulphides (CS-SS dihedral angles near 90°) shows a preponderance of the *trans* geometry for the CSSSC skeleton (Fig. 9). Thus an electron diffraction investigation of Me_2S_3 has pointed to the *trans* rotamer in the gas phase,²⁴ while similar results for gaseous $(\text{CF}_3)_2\text{S}_3$ have been found to be consistent with an assumed *trans* structure.^{17a} The present vibrational study of Me_2S_3 and $\text{Me}_2\text{S}_3-d_6$ indicates the *trans* rotamers to predominate in the liquid state also (*vide infra*). The trisulphides $(\text{I-CH}_2\text{CH}_2)_2\text{S}_3$,^{23a,b} $(\text{CCl}_3)_2\text{S}_3$,^{23c,d} compound 8³⁵ and compound 9³⁶ have all been established by X-ray diffraction studies to be *trans* in the crystalline state. On the other hand, $\text{S}_3(\text{CN})_2$ ⁵¹ and compound 21⁵² are *cis* in the solid state. However, the SSS nucleus of both molecules appears to be involved in intermolecular interactions that may determine the structure. These latter compounds are significant, though, in revealing the intrinsic differences between the *cis* and *trans* arrangements to be not so great as to preclude the former.

The preference for the *trans* rotamer is evidently due to both energy and entropy effects. In the first place, this configuration is favoured 2 to 1 over the *cis* geometry by virtue of its greater entropy from mixing of *dl* pairs ($\Delta S = R \ln 2 = 5.77 \text{ JK}^{-1} \text{ mol}^{-1}$), irrespective of any energy difference between the two. Furthermore, the *trans* geometry is substantially lower in energy according to molecular mechanics calculations on Me_2S_3 ($\Delta E = 3.8 \text{ kJ mol}^{-1}$) and H_2S_3 ($\Delta E = 1.3 \text{ kJ mol}^{-1}$) by Snyder and Harpp.^{141*} The greater

* Incidentally, these calculations yielded rotational potential energy minima only at the *trans* and *cis* rotamers, attesting to the importance of the 90° dihedral angle for the S-S bonds.

energy for the *cis* rotamers was indicated to arise from interaction between the polar S-C or S-H bonds and also from angle-bending and torsional strain in the case of Me_2S_3 . Slightly destabilizing contact between the methyl groups in *cis*- Me_2S_3 is implied by a space-filling molecular model and is predicted on the basis of the $\text{CH}_2\cdots\text{CH}_2$ distance (marginally less than the van der Waals' distance) calculated in this work for *cis*- Et_2S_3 (Table 7). These latter calculations have further revealed the $\text{CH}_3\cdots\text{CH}_2$ interaction across the $\text{CH}_3\text{CH}_2\text{SSSCH}_2$ moiety to be considerable for the G' C-S conformation, so that only the GGG'G, GGG'T and TGG'T *cis*-rotamers, if any, would be expected for Et_2S_3 . Similar effects for G' and T C-S conformations in the case of *i*- Pr_2S_3 would seem to destabilize substantially all except the GGG'G *cis*-rotamer. For *t*- Bu_2S_3 , on the other hand, no *cis* structure is free of severe $\text{CH}_3\cdots\text{CH}_3$ interference in addition to unfavourable $\text{CH}_3\cdots\text{CH}_2$ contact (as in G'GG'G' Et_2S_3) unless the CS-SS dihedral angles are opened significantly, thereby creating highly destabilizing torsional strain in the S-S bonds. Consequently, only the *trans* rotamer is expected to exist for *t*- Bu_2S_3 . Snyder and Harpp¹⁴¹ have noted that the greater stability of the *trans* compared to the *cis* rotamer of Me_2S_3 and H_2S_3 found by molecular mechanics is mirrored by the outcome of CNDO/B calculations on the two molecules ($\Delta E = 0.4 \text{ kJ mol}^{-1}$) and by MINDO/3 calculations for H_2S_3 ($\Delta E = 5.0 \text{ kJ mol}^{-1}$), although details were not given.

The smallest barrier height between the *trans* and *cis* rotamers of Me_2S_3 and H_2S_3 computed by Snyder and Harpp¹⁴¹ is only 31.0 and 29.7 kJ mol^{-1} , respectively, for interconversion through the transition state shown below.



Accordingly, the authors concluded that the two rotamers equilibrate rapidly over this barrier. This is in disagreement with the earlier suggestion by Wieser *et al.*⁸² that *trans*-H₂S₃ alone exists in CS₂ or CCl₄ solution at room temperature based on the greater intramolecular S...H hydrogen-bonding accommodated by this geometry. Such nonbonded interaction was inferred from the anomalous ¹H nmr resonance for H₂S₃ compared to its homologues.¹⁴² However, the vibrational force field derived by Wieser *et al.*⁸² for the *trans* rotamer was noted to predict no significant differences between rotamers. In addition, Snyder and Harpp¹⁴¹ have calculated nearly identical S-S stretching and SSS bending force constants for *trans*- and *cis*-H₂S₃, further predicting the vibrational spectra of the two rotamers to differ minimally. Still, their co-existence in the fluid phases now seems highly probable in light of the recent evidence from molecular mechanics.¹⁴¹ Indeed, the molecular mechanics energy differences in conjunction with the aforementioned entropy differences between the rotamers lead to *trans* ⇌ *cis* equilibrium constants of 0.30 and 0.11 for H₂S₃ and Me₂S₃, respectively, commensurate with *cis* proportions of approximately 23% and 10%, respectively.

The present assignment of the Me₂S₃ vibrational spectra to the *trans* rotamer is based on the positions of the symmetric and antisymmetric δ(CSS) vibrations. The former should be polarized in the Raman spectrum while the

latter should be depolarized for both the *trans* and *cis* rotamers (Sect. VI.A.2.i). According to the normal coordinate calculations (Sect. VI.A.2.i.a), these vibrations occur at nearly the same wavenumbers for the two geometries, *but* the antisymmetric mode is the higher energy band in the *trans* case, while the symmetric mode is at higher energy in the *cis* case. In the actual Raman spectrum of liquid Me_2S_3 (Fig. 1b), two substantially polarized bands (one for the $\delta(\text{SSS})$ vibration) appear near 200 cm^{-1} together with an overlapping pair of essentially depolarized bands centered at 275 cm^{-1} . This situation is clearly consistent only with the *trans* rotamer, and comparable Raman data for $\text{Me}_2\text{S}_3\text{-}d_6$ (Fig. 2b) likewise indicate the *trans* rotamer in the liquid state. In view of these observations, it is worth noting that the higher wavenumber component of the overlapping pair of $\delta(\text{HSS})$ vibrations near 860 cm^{-1} for H_2S_3 is the polarized mode,⁸² since this circumstance implies, by analogy with Me_2S_3 , a predominance of the *trans* rotamer. Wieser *et al.*⁸² did not report whether their force field predicts an interchange of the symmetric and antisymmetric $\delta(\text{HSS})$ vibrations between the *trans* and *cis* rotamers.

The vibrational spectra of Me_2S_3 and $\text{Me}_2\text{S}_3\text{-}d_6$ afford only circumstantial evidence for the co-existence in the liquids of some *cis* rotamer together with the *trans* rotamer. For instance, the depolarization ratio for the Raman feature in the vicinity of 270 cm^{-1} for the two molecules is estimated from the change in band area upon rotating the analyzer in the beam of scattered radiation (Sect. V.B) to be 0.65 and 0.68, respectively, vs. a theoretical ratio of 0.75 for a totally depolarized vibration. This discrepancy may arise from an underlying symmetric $\delta(\text{CSS})$ vibration for the

cis rotamer. However, neither of the overlapping bands centered at 275 cm^{-1} for Me_2S_3 is attributable to the *cis* rotamer because the two vibrations appear to have identical depolarizing characteristics (Fig. 1b). Furthermore, their relative intensities seem to be insensitive to temperature and both persist in the solid state (Figs. 1c and 1d). A vibrational feature for both Me_2S_3 and $\text{Me}_2\text{S}_3\text{-}d_6$ that may well be due to the *cis* rotamer, however, is the indistinct low-energy shoulder on the $\nu(\text{S-S})$ infrared absorption (see Fig. 1a). Since the main infrared band is the antisymmetric $\nu(\text{S-S})$ vibration of the *trans* rotamer which occurs at lower energy than its symmetric $\nu(\text{S-S})$ vibration evident in the Raman spectrum (Figs. 1b and 2b), this shoulder is reasonably positioned for the antisymmetric mode of the *cis* rotamer. The corresponding symmetric mode is not observed directly in the Raman spectrum, but may be partly responsible, along with the antisymmetric $\nu(\text{S-S})$ vibration of the *trans* rotamer and a ^{34}S satellite (Sect. VI. A.2), for the asymmetry on the low-energy side of the $\nu(\text{S-S})$ feature. Attempts to resolve this vibration by band-fitting procedures were abandoned on the grounds that an unequivocal distinction between three or four bands in the envelope was highly unlikely. As anticipated, the liquid-state spectra of *t*- Bu_2S_3 provide no evidence of the *cis* rotamer, while any spectral effects related to the *cis* rotamer of Et_2S_3 or *i*- Pr_2S_3 are obscured by the isomerism about the C-S bonds in the liquids.

A *cis*-to-*trans* conformational rearrangement in Me_2S_3 explains the irreversible transformation from Solid I to Solid II observed in the Raman spectrum (Sect. VI.A). The inherently more stable geometry found in Solid II

can be assumed to be the *trans* rotamer (*vide supra*), while initial crystallization in the *cis* geometry to give Solid I can be rationalized to arise from some advantage in the crystal-packing of this form. Softening of the lattice with increasing temperature permits a conversion to the preferred *trans* structure which then persists independent of temperature. The detection in the vibrational spectra of two solid-state variations for 2-propanethiol,¹¹⁶ ethylenediamine,¹⁴³ 1,4-dichloro-2-butyne¹⁴⁴ and 1,4-diiodobutane¹⁴⁵ has previously been interpreted in terms of conformational differences. In the present case, the existence of *cis*-Me₂S₃ in the solid state is very plausible in view of the known *cis* structures for S₃(CN)₂⁵¹ and compound 21⁵² as solids. Furthermore, the only substantial dissimilarities in the spectra of Solids I and II above 100 cm⁻¹ are in the regions for the CSS and SSS deformation modes (Figs. 1c and 1d), in line with the predictions from normal coordinate analysis of the *trans* and *cis* rotamers (Sect. VI.A.2.i.a). Should both solids involve only the more stable, *trans* rotamer, it seems very unlikely that differences in molecular structure or intermolecular interaction could cause the observed shifts in the lower deformation modes without significantly affecting the higher mode. On the other hand, if this latter vibration is the symmetric $\delta(\text{CSS})$ feature of the *cis* rotamer in Solid I and the antisymmetric $\delta(\text{CSS})$ feature of the *trans* rotamer in Solid II, then the near coincidence is not surprising in light of the normal coordinate calculations. Finally, it is worth recalling that the metastable states obtained during the glass-to-solid phase changes (Sect. VI.A) exhibit bands for both solid-state modifications. This implies the existence of different molecular configurations in Solid I and

II since there seems no reason to expect one rotamer to adopt at once two different crystal-lattice arrangements of different energy. The present spectrum of Solid I appears to be the first observation of a dialkyl trisulphide in the pure *cis* configuration.

The room-temperature ^1H nmr spectra of organotrisulphides^{8,106,146} show no evidence of *cis-trans* isomerism.* For example, Bz_2S_3 in CS_2 solution yields a singlet CH_2 resonance with the same half-width as the corresponding resonance for Bz_2S_2 ,¹⁰⁶ consistent with a single rotamer or rapid equilibration between rotamers. However, Snyder and Harpp¹⁴¹ have reported exchange broadening in the ^1H nmr spectra of both Bz_2S_3 and $t\text{-Bu}_2\text{S}_3$ beginning at -100°C to -105°C , although details were not furnished. This effect for the former may relate to *trans-cis* isomerism, but could also originate in isomerism about the C-C bond joining the methylene group and the ring, as it suggested by the present Raman data (Sect. VI.B). On the other hand, the observation for $t\text{-Bu}_2\text{S}_3$ remains a mystery since the *cis* rotamer is highly disfavoured by $\text{CH}_3\cdots\text{CH}_3$ steric hindrance (*vide supra*). Conformational effects in the nmr spectra of cyclic organotrisulphides^{15b,148} are due, of course, to changes in the configuration of the ring as a whole.

Also of interest with respect to *cis-trans* isomerism are the dipole moments (in benzene solution) determined for Me_2S_3 (1.66D, 30°C),^{20b}

* It is worth mentioning that nmr studies¹⁴⁷ of Et_2S_2 , $i\text{-Pr}_2\text{S}_2$ and Bz_2S_2 down to -95°C have revealed no effects from C-S isomerism, as would be expected considering the small rotational barriers calculated for EtSSMe and Et_2S_2 by molecular mechanics.¹¹⁹

Et₂S₃ (1.64D, 30°C),^{20a} *t*-Bu₂S₃ (1.18D, 25°C)^{135a} and (*n*-hexadecyl)₂S₃ (1.63D, 30°C).^{20c} Kushner *et al.*^{20b} have suggested that Me₂S₃ exists as a *trans-cis* mixture on the grounds that the observed dipole moment is between the theoretical values for the *cis* rotamer (greater than the 2.01D moment calculated for free rotation) and the *trans* rotamer (approximately 0). On the basis of similar arguments, Woodrow *et al.*^{20c} concluded that these rotamers also co-exist for (*n*-hexadecyl)₂S₃. The rather small dipole moment for *t*-Bu₂S₃ was intimated by Cumper *et al.*^{135a} to be due to dihedral angle distortion, as for *t*-Bu₂S₂.¹³⁵ However, although much greater than the dipole moment of ~0 suggested above for pure *trans* rotamer, the reduced value for *t*-Bu₂S₃ compared to Me₂S₃ supports the idea of a *trans-cis* mixture for the latter inasmuch as steric hindrance seems to preclude *cis-t*-Bu₂S₃ (*vide supra*). The larger value for Me₂S₃ may therefore indicate the presence of some *cis* rotamer. The similar dipole moments for Me₂S₃, Et₂S₃ and (*n*-hexadecyl)₂S₃ are consistent with the discovery of comparable dipole moments among *n*-alkyl disulphides.^{20b,135a}

Evidence pertaining to S-S isomerism in organotetrasulphides is very limited in the literature. However, Woodrow *et al.*^{20c} have suggested the co-existence of *trans-trans*, *trans-cis* and *cis-cis* rotamers (Fig. 9) for (*n*-hexadecyl)₂S₄ in benzene solution at 30°C on the basis of its dipole moment of 2.16D compared to values of 2.01D, 2.01D and 2.93D, respectively, calculated for the individual geometries. A mixture of about 14% *cis-cis* rotamer and about 86% of the other two was noted to rationalize the experimental dipole moment. In qualitative agreement with this distribution, a space-filling molecular model (CPK type) of Me₂S₄ indicates significant

destabilizing $\text{CH}_3 \dots \text{CH}_3$ contact only in the *cis-cis* rotamer, although weak $\text{CH}_3 \dots \text{S}$ interaction across the CH_3SSS moiety may disfavour somewhat the *trans-cis* rotamer as well. All three rotamers are chiral and hence equally probable statistically, i.e., on entropy grounds. A model of *trans-trans*- Et_2S_4 shows the absence of intramolecular nonbonded interaction when the C-S conformations are G and/or T, while indicating weak interaction across the $\text{CH}_3\text{CH}_2\text{SSS}$ moiety for the G' C-S conformation, as for *trans*- Et_2S_3 (Table 7). For *trans-cis*- Et_2S_4 , the model suggests weak contact across the CH_2SSSS fragment independent of C-S conformation. The G' C-S conformation in the *trans* half of the molecule gives rise to additional $\text{CH}_3 \dots \text{S}$ interaction as in the *trans-trans* rotamer while the G' conformation in the *cis* half engenders substantial interaction across the $\text{CH}_3\text{CH}_2\text{SSSS}$ grouping, similar to $\text{CH}_3 \dots \text{CH}_2$ interaction in *trans*- Et_2S_3 rotamers with a G' C-S conformation. Considerable $\text{CH}_2 \dots \text{CH}_2$ interaction occurs in all *cis-cis* rotamers of Et_2S_4 , while the G' C-S conformation involves very strong interaction between the ethyl substituents. These observations point to the co-existence of several *trans-trans* and *trans-cis* rotamers, especially those with G and T C-S conformations, in liquid Et_2S_4 at room temperature, with little *cis-cis* rotamer expected in the mixture. Although the observed vibrational spectra of Et_2S_4 are relatively simple in appearance (Fig. 7), they do indicate rotational isomerism about both the C-S and S-S bonds (Sect. VI.A.2.ii).

VI.A.2 Vibrational Assignments

The fundamental vibrations of the dialkyl trisulphides examined in this study divide to a large degree into two categories of localized modes: (1) vibrations of the alkyl substituents and (2) vibrations of the CSSSC skeleton. Assignments for the former are made in terms of the conventional alkyl group vibrations in the literature, as outlined in Fig. 12, and are based on available assignments for dialkyl disulphides and for related alkanethiols and chloroalkanes*, especially when supported by normal coordinate calculations. The skeletal modes are the C-S and S-S stretching vibrations [$\nu(\text{C-S})$ and $\nu(\text{S-S})$], the CSS and SSS deformation vibrations [$\delta(\text{CSS})$ and $\delta(\text{SSS})$] and the torsional vibrations about the C-S and S-S bonds [τ_{CS} and T_{SS}][‡]; these separate into the classes 6a + 5b for the *trans* rotamer (C_2 local symmetry) or 6a' + 5a'' for the *cis* rotamer (C_s local symmetry). The a and a' vibrations are symmetric (in-phase) concerted vibrations of the two halves of the CSSSC moiety, whereas the b and a'' vibrations are their antisymmetric (out-of-phase) counterparts. All the vibrations should be both infrared and Raman active with the a and a' modes being polarized in the Raman spectra, while the b and a'' modes should be depolarized. In accordance with the conclusions of Section VI.A.1.ii, the assignments for the observed skeletal fundamentals are for the most part proposed on the basis of the *trans* rotamer in light of the results of vibrational calculations on H_2S_n (n=3,4)⁸²

* Analogous RS and RCl (R=alkyl group) moieties normally yield very comparable vibrational spectra.¹⁴⁹

‡ Including τ_{CS} in this category is a matter of convenience, since it could also be considered an alkyl group vibration.

Figure 12. Alkyl Group Vibrations for R_2S_3 ($R = \text{Me, Et, } n\text{-Pr, } i\text{-Pr, } t\text{-Bu}$)^a.

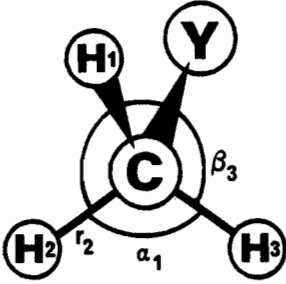
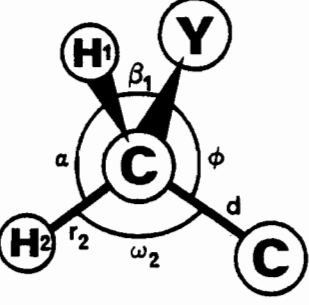
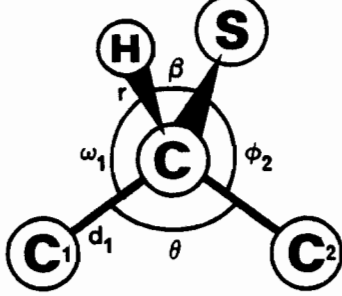
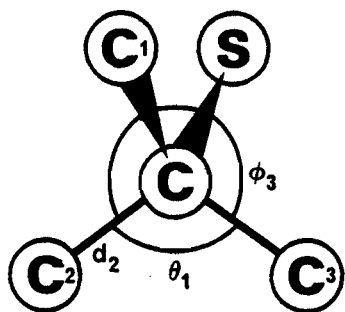
 <p>Y = S, C</p>	<p>CH₃ asym. str.: $2r_1 - r_2 - r_3$ $r_2 - r_3$ CH₃ sym. str.: $r_1 + r_2 + r_3$ CH₃ asym. def.: $2\alpha_1 - \alpha_2 - \alpha_3$ $\alpha_2 - \alpha_3$ CH₃ sym. def.: $\alpha_1 + \alpha_2 + \alpha_3 - \beta_1 - \beta_2 - \beta_3$ CH₃ rock.: $2\beta_1 - \beta_2 - \beta_3$ $\beta_2 - \beta_3$</p>
 <p>Y = S, C</p>	<p>CH₂ asym. str.: $r_1 - r_2$ CH₂ sym. str.: $r_1 + r_2$ CH₂ sciss.: $4\alpha - \omega_1 - \omega_2 - \beta_1 - \beta_2$ CH₂ wagg.: $\omega_1 + \omega_2 - \beta_1 - \beta_2$ CH₂ twist.: $\omega_1 - \omega_2 - \beta_1 + \beta_2$ CH₂ rock.: $\omega_1 - \omega_2 + \beta_1 - \beta_2$ C-C str.: d CCY def.: ϕ</p>
	<p>CH str.: r CH wagg.: $2\beta - \omega_1 - \omega_2$ $\omega_1 - \omega_2$ CC₂ asym. str.: $d_1 - d_2$ CC₂ sym. str.: $d_1 + d_2$ CCS asym. def.: $\phi_1 - \phi_2$ CCS sym. def.: $\theta - \beta - \omega_1 - \omega_2 + \phi_1 + \phi_2$ CCC def.: $2\theta - \phi_1 - \phi_2$</p>

Figure 12. (continued)



CC_3 asym. str.:	$2d_1 - d_2 - d_3$
	$d_2 - d_3$
CC_3 sym. str.:	$d_1 + d_2 + d_3$
CC_3 asym. def.:	$2\theta_1 - \theta_2 - \theta_3$
	$\theta_2 - \theta_3$
CC_3 sym. def.:	$\theta_1 + \theta_2 + \theta_3 - \phi_1 - \phi_2 - \phi_3$
CC_3 rock.:	$2\phi_1 - \phi_2 - \phi_3$
	$\phi_2 - \phi_3$

^a Abbreviations: str., stretching; def., deformation; rock., rocking; sciss., scissoring; wagg., wagging; twist., twisting; sym., symmetric; asym., antisymmetric.

and Me_2S_3 (this work, Sect. VI.A.2.i.a) and with reference to assignments to date for the CSSC backbone of dialkyl disulphides.^{31,83,88-94,150} Effects of C-S isomerism on the alkyl group and skeletal vibrations of Et_2S_3 , $n\text{-Pr}_2\text{S}_3$ and $i\text{-Pr}_2\text{S}_3$ are discussed for the compounds individually in the following sections. Non-fundamental vibrations detected for the trisulphides are attributed to overtone, combination or difference levels where reasonable. Difference bands have negligible intensity in the spectra at 15K, however, owing to the extremely low populations of the excited vibrational states.

The general weakness of the coupling between skeletal and alkyl group vibrations in both dialkyl di- and trisulphides is suggested by the nearly identical spectra for homologous pairs in the regions for the latter modes, despite the different sulphur chain length. Similarly, the alkyl group vibrations of the di- and trisulphides are much like those of the corresponding alkanethiols and chloroalkanes, further attesting to minimal mixing of these modes with the skeletal modes in the former species. That the methyl group and skeletal vibrations in Me_2S_3 and $\text{Me}_2\text{S}_3\text{-}d_6$ are highly localized is also evidenced by the occurrence of only a slight shift in $\nu(\text{S-S})$ between the molecules together with a small shift in $\nu(\text{C-S})$ consistent with the greater mass of the CD_3 substituent.* Apparently, the stretching vibrations involve very little motion within the CH_3 and CD_3 moieties.

The normal coordinate analysis of these molecules indicates a considerable

* Treating the S-CH_3 and S-CD_3 units as isolated diatomics, the Teller-Redlich product rule¹⁵¹ predicts a $\nu(\text{S-CD}_3)/\nu(\text{S-CH}_3)$ ratio of 0.941 in good agreement with the experimental ratio of 0.937.

partitioning into skeletal vibrations on the one hand and methyl vibrations on the other.

It is worth mentioning here that assignments in the literature for dialkyl sulphides^{117, 152-154} are of limited help in studies of di- and trisulphides because of the much more complex nature of the spectra for the monosulphides. For instance, the CH_3 rocking modes of Me_2S appear as four distinct features at 1030, 972, 950 and 906 cm^{-1*} vs. a pair of nearly coincident bands close to 950 cm^{-1} for both Me_2S_2 and Me_2S_3 . Such differences are even more pronounced if the alkyl groups enter into rotational isomerism. Thus, Et_2S yields very complicated patterns of multiple ethyl group vibrations pointing to the co-existence of three rotamers in the liquid state,^{117b, 153a} whereas the ethyl group vibrations of Et_2S_2 and Et_2S_3 exhibit little evidence of rotational isomerism (Sect. VI.A.2.ii). The marked simplification in the alkyl group vibrations on going from a monosulphide to the analogous di- and polysulphides is attributable to reduced mechanical interaction of the substituents at the substantially increased separations between them. The two groups then vibrate essentially independent of each other so that the spectrum becomes a simple superposition of their individual patterns reflecting their local geometries only. As a consequence, the vibrations of the matched substituents in a symmetric di- or polysulphide tend to be accidentally degenerate when the two substituents are in the same conformation, giving the semblance of a single group in the spectrum.

* Although several differing assignments have been suggested, these are the ones best reproduced by force field calculations.¹⁵²

Indications of different alkyl group conformations for a symmetric di- or polysulphide can be interpreted as showing the co-existence of at least two rotamers on the premise that the most stable rotamer has the same, lowest-energy conformation for both alkyl substituents. Incidentally, the spectrum of an unsymmetric disulphide is practically an overlay of the spectra for the related symmetric disulphides,^{83,92} e.g., the EtSSMe spectrum is a summation of the Et₂S₂ and Me₂S₂ spectra.^{92, 94b} This demonstrates the alkyl groups to be non-interacting and further implies that their vibrations do not couple significantly with those of the CSSC core.

As a final general comment on the dialkyl trisulphides, the feeble Raman bands found at 5-10 cm⁻¹ to low energy of the prominent ν(S-S) and ν(C-S) vibrations in the spectra at 15K are tentatively ascribed to satellite vibrations involving the ³⁴S isotope (natural abundance 4.22%). Similar weak features adjacent to the ν(C-S) bands of Me₂S and Me₂S-d₆ in the solid-state Raman spectra have previously been explained in this manner.^{152e} Support for these assignments comes from application of the Teller-Redlich product rule¹⁵¹ to the C-S and S-S bonds as isolated entities to obtain calculated ratios of 0.992 and 0.985 for ν(C-³⁴S)/ν(C-³²S) and ν(³²S-³⁴S)/ν(³²S-³²S), respectively. Taking 650 and 500 cm⁻¹ as 'typical' ν(C-³²S) and ν(³²S-³²S) vibrations, respectively, isotopic shifts to lower energy of 5 cm⁻¹ and 7.5 cm⁻¹ are predicted. The correspondence between these estimated displacements and those observed in the spectra lends credence to the suggested assignments.

VI.A.2.1 Dimethyl Trisulphide and Dimethyl Trisulphide-d₆

For the reasons outlined in Section VI.A.1.ii, the proposed assignments (Tables 8 and 9) for the vibrational spectra of Me_2S_3 and $\text{Me}_2\text{S}_3\text{-d}_6$ as liquids (Figs. 1a,b and 2a,b) and for Solid II Me_2S_3 (Fig. 1d) are referred to the *trans* rotamer, while the Raman spectrum of Solid I Me_2S_3 (Fig. 1c) is assigned in terms of the *cis* rotamer.* These assignments follow largely from ones in the literature for Me_2S_2 ,^{89a,90,92} the data for which bear a remarkable resemblance to those for the trisulphide, with confirmation from the present normal coordinate calculations (Sect. VI.A.2.1.a). In the case of $\text{Me}_2\text{S}_3\text{-d}_6$, reference has also been made to studies showing the effects of deuteration on the spectra of Me_2S .¹⁵²

Under the overall C_2 symmetry for *trans*- Me_2S_3 (or *trans*- $\text{Me}_2\text{S}_3\text{-d}_6$), the in-phase and out-of-phase coupled motions of the two methyl groups (Fig. 12) account for 9a + 9b vibrations, respectively, of the 27 fundamental vibrations for the molecule. Because of accidental degeneracy between corresponding *a* and *b* modes, however, the actual spectra of the liquid are consistent with a single CH_3 (or CD_3) moiety. To a good approximation, the vibrations conform to C_{3v} local symmetry with symmetric a_1 modes and antisymmetric degenerate *e* modes. The weak splitting of the latter into *a'* and *a''* components for C_s local symmetry is probably due to departure from genuine tetrahedral geometry, but may relate to the non-colinearity between the S-S and C-S bonds

* The origins of Solids I and II were discussed in Section VI.A.

Table 8. Vibrational Wavenumbers (cm^{-1}) and Assignments for Me_2S_3^a .

Infrared ^b	Raman ^b			Assignment ^c
	Liquid	Solid I	Solid II	
2990 m	2990 sh			} CH_3 asym. str.
2983 sh	2984 m			
2912 s	2912 s p			CH_3 sym. str.
2838 w	2841 vw p			$2 \times 1426 = 2852$
2812 w	2813 w p	d	d	$2 \times 1414 = 2828$
2717 vw				$1304 + 1426 = 2730$
2587 vw				$2 \times 1304 = 2608$
d	d			
			1441 vvw	
		1429 sh	1433 vw	$484 + 956 = 1440$
1426 s	1427 w	1424 w	1425 m	} CH_3 asym. def.
	} dp	1421 vw	1421 m	
		1410 sh		
1414 s	1414 w	1406 m	1411 m	
	1383 vw	1388 vw	1381 vw	$2 \times 696 = 1392$
1304 s	1305 w p	1307 vw	1313 vw	} CH_3 sym. def.
		1298 w	1303 w	
1116 vw				$1304 - 184 = 1120$
1105 vw				
~1025 vw,br				$1304 - 281 = 1023$
		964 sh	969 vvw	$274 + 695 = 969$
		960 w	961 w	$2 \times 480 = 960$
952 sh	953 w p	956 w	956 w	} CH_3 rock.
949 s		949 vw	953 w	
			946 vvw	
			939 vvw	
753 ww,br				$281 + 478 = 759$

Table 8. (continued)

Infrared ^b		Raman ^b		Assignment ^c
Liquid	Liquid	Solid I	Solid II	
	696 s p	701 s	695 s	sym. $\nu(\text{C-S})$
694 w		699 sh		asym. $\nu(\text{C-S})$
		692 vw	689 w	^{34}S satellite
	486 vs p	488 vs	484 vs	sym. $\nu(\text{S-S})$
		485 sh		^{34}S satellite
478 s	479 ^e	480 s	480 m	asym. $\nu(\text{S-S})$
472 sh				$\nu(\text{S-S})$ <i>cis</i> rotamer ^e
		475 sh	475 w	} ^{34}S satellites
		472 sh		
d	281 m	} dp?	288 m	} Fermi resonance: 170 + 170 = 277 and asym. $\delta(\text{CSS})$
	270 sh		279 sh	
			274 s	
		285 m		} Fermi resonance: 101 + 181 = 282 and sym. $\delta(\text{CSS})$
		274 s		
	210 m p		219 a	sym. $\delta(\text{CSS})$
		198 m		asym. $\delta(\text{CSS})$
	184 s p	189 m	170 s	} $\delta(\text{SSS})$
		181 m		
		149 w	~140 sh	} sym. and asym. τ_{CS}
		133 w	133 s	
		128 w	127 m	
		101 m	107 m	} sym. and asym. T_{SS}
		83 m	94 m	
		77 m	76 m	
		69 s	63 s	
		58 m		
		52 m		lattice vibrations
		47 s		
		49 w		
		44 w		
		34 w		
		15 w		

Table 8. (continued)

-
- ^a The spectra of the liquid and Solid II are assigned on the basis of the *trans* rotamer; Solid I is assigned as the *cis* rotamer.
- ^b Abbreviations: s, strong; m, medium; w, weak; v, very; sh, shoulder; br, broad; p, polarized; dp, depolarized. See footnote c, Fig. 13 for other abbreviations.
- ^c See Fig. 12 for the methyl group vibrations.
- ^d Region not recorded.
- ^e See text.

Table 9. Vibrational Wavenumbers (cm^{-1}) and Assignments for Liquid Me_2S_3 - d_6^a .

Infrared ^b	Raman ^b	Assignments ^c
2247 m	2248 m dp	} CD_3 asym. str.
2238 sh	2237 m dp	
	2153 vw p	
2121 s	2121 s p	CD_3 sym. str.
2077 w	2079 w p	2 x 1043 = 2086
2056 w	2057 w p	2 x 1031 = 2062
1982 w	1981 w p	2 x 1001 = 2002
d	d	
1043 s	1044 w dp	} CD_3 asym. str.
1031 s	1033 w dp	
1000 m	1001 m p	CD_3 sym. str.
947 vw, br	945 w, br p	2 x 475 = 950
882 w, br		
745 m	749 m p	} CD_3 rock.
723 w	~725 w, br	
	652 s p	sym. $\nu(\text{C-S})$
649 w		asym. $\nu(\text{C-S})$
	500 w	disulphide
~488 sh		745 - 257 = 488
	482 vs p	sym. $\nu(\text{S-S})$
475 s	476 ^e	asym. $\nu(\text{S-S})$
471 sh		$\nu(\text{S-S})$ <i>cis</i> rotamer ^e
	442 w	tetrasulphide
	257 s, br dp?	asym. $\delta(\text{CSS})$
d	209 s p	sym. $\delta(\text{CSS})$
	171 s p	$\delta(\text{SSS})$

^a Assignments are based on the *trans* rotamer.

^b For abbreviations see footnote b, Table 8.

^c See footnote c, Table 8.

^d Region not recorded.

^e See text.

in the SSCH_3 (or SSCD_3) fragment as well. Even so, the depolarization data for the methyl groups require an explanation on the basis of polarized a_1 vibrations and depolarized e vibrations for C_{3v} local symmetry. Under C_s symmetry, the a' components from the e modes should be polarized contrary to observation*, while all the vibrations are predicted to be somewhat polarized for C_2 symmetry owing to a contribution from an a mode in each case. In his detailed study of Me_2S_2 , Frankiss^{90b} invoked the overall C_2 symmetry of that molecule to rationalize the discrepancies found between the CH_3 deformations in the infrared (1430, 1415 and 1303 cm^{-1}) and Raman (1426, 1419 and 1311 cm^{-1}) spectra of the liquid. No such shifts have been detected in the present work for any of the methyl group vibrations of liquid Me_2S_3 or $\text{Me}_2\text{S}_3-d_6$, however. The multiplicity in these vibrations for Me_2S_3 in its solid states is attributable to intermolecular vibrational coupling in the crystal lattice (Davydov or correlation splitting).¹⁵⁵

The potential energy distributions from the normal coordinate analysis of Me_2S_3 and $\text{Me}_2\text{S}_3-d_6$ (Tables 10 and 11) show the standard descriptions for methyl group vibrations (Fig. 12) to be very satisfactory for these molecules, despite significant mixing of deformation and rocking modes. The proposed assignments for the CD_3 rocking vibrations at 747 and 723 cm^{-1} warrant comment since the alternative assignments at 749 cm^{-1} (Raman) and 745 cm^{-1} (infrared) are more consistent with the small separation between the CH_3

* The polarized character for the CH_3 and CD_3 rocking vibrations is in line with C_s symmetry provided the a' component is assumed to dominate in the Raman spectrum.

Table 10. Fundamental Vibrations and Potential Energy Distributions for *trans*-Me₂S₃.

No.	Vibrations (cm ⁻¹) ^a		Potential energy distribution ^b
	Obsd.	Calcd.	
1	2990	3001	} 101% CH ₃ asym. str.
2	2984	3000	
3	2912	2929	101% CH ₃ sym. str.
4	1426	1430	} 82% CH ₃ asym. def. + 12% CH ₃ rock.
5	1414	1430	
6	1304	1306	106% CH ₃ sym. def. + 4% sym. ν (C-S)
7	953	954	88% CH ₃ rock. + 19% CH ₃ asym. def.
8	949	949	89% CH ₃ rock. + 19% CH ₃ asym. def.
9	696	694	106% sym. ν (C-S)
10	486	487	104% sym. ν (S-S) ^d
			109% "
			112% "
11	210	218	78% sym. δ (CSS) + 20% δ (SSS)
			76% " + 21% "
			74% " + 22% "
12	184	184	43% δ (SSS) + 25% sym. τ_{cs} + 21% sym. δ (CSS)
			45% " + 25% " + 23% "
			47% " + 26% " + 24% "
13	c	145	72% sym. τ_{cs} + 25% δ (SSS)
			71% " + 28% "
			70% " + 30% "
14	c	78	89% sym. T_{ss} + 11% δ (SSS)
			88% " + 12% "
			88% " + 13% "

Table 10. (continued)

No.	Vibrations (cm^{-1}) ^a		Potential energy distribution ^b
	Obsd.	Calcd.	
15	2990	3001	} 101% CH ₃ asym. str.
16	2984	3000	
17	2912	2929	101% CH ₃ sym. str.
18	1426	1430	} 82% CH ₃ asym. def. + 12% CH ₃ rock.
19	1414	1430	
20	1304	1306	106% CH ₃ sym. def.
21	953	954	88% CH ₃ rock. + 19% CH ₃ asym. def.
22	949	949	89% CH ₃ rock. + 19% CH ₃ asym. def.
23	694	694	106% asym. $\nu(\text{C-S})$
24	478	478	102% asym. $\nu(\text{S-S})$
25	275.5	273	92% asym. $\delta(\text{CSS})$ + 8% asym. T_{ss}
26	c	159	98% asym. τ_{cs}
27	c	104	90% asym. T_{ss} + 8% asym. $\delta(\text{CSS})$

^a Vibrations 1-14 are of *a* symmetry, and 15-27 are of *b* symmetry. Average error on the calculated wavenumbers is 0.49%.

^b Distributions are in terms of symmetry coordinate force constants (Appendix) and therefore show the percentage contributions to the potential energy from the symmetry coordinates specified in Fig. 13. Only contributions of 10% or greater are reported except to allow comparisons between the normal and deuterated species. Values in excess of 100% are due to negative contributions from interaction force constants.

^c Not detected.

^d The three distributions refer to the force fields from calculations 1-3, respectively, in Table 13.

Table 11. Fundamental Vibrations and Potential Energy Distributions for *trans*-Me₂S₃-d₆.

No.	Vibrations (cm ⁻¹) ^a		Potential energy distribution ^b
	Obsd.	Calcd.	
1	2247	2224	} 101% CD ₃ asym. str.
2	2237	2223	
3	2121	2096	101% CD ₃ sym. str.
4	1043	1023	} 86% CD ₃ asym. def. + 8% CD ₃ rock.
5	1031	1022	
6	1000	1003	104% CD ₃ sym. def. + 16% sym. ν(C-S)
7	747	737	89% CD ₃ rock. + 13% CD ₃ asym. def.
8	723	726	92% CD ₃ rock. + 14% CD ₃ asym. def.
9	652	652	93% sym. ν(C-S)
10	482	483	101% sym. ν(S-S) ^d
			106% "
			109% "
11	209	203	59% sym. δ(CSS) + 37% δ(SSS)
			57% " + 39% "
			54% " + 42% "
12	171	172	43% δ(SSS) + 38% sym. δ(CSS) + 6% sym. τ _{cs}
			46% " + 41% " + 6% "
			48% " + 43% " + 6% "
13	c	106	91% sym. τ _{cs} + 9% δ(SSS)
			90% " + 10% "
			90% " + 11% "
14	c	70	90% sym. T _{ss} + 9% δ(SSS)
			90% " + 10% "
			90% " + 11% "

Table 11. (continued)

Vibrations (cm^{-1}) ^a			Potential energy distribution ^b
No.	Obsd.	Calcd.	
15	2247	2224	} 101% CD_3 asym. str.
16	2237	2223	
17	2121	2096	101% CD_3 sym. str.
18	1043	1023	} 86% CD_3 asym. def. + 8% CD_3 rock.
19	1031	1022	
20	1000	1003	104% CD_3 sym. def. + 16% asym. $\nu(\text{C-S})$
21	747	736	89% CD_3 rock. + 13% CD_3 asym. def.
22	723	725	92% CD_3 rock. + 14% CD_3 asym. def.
23	649	652	93% asym. $\nu(\text{C-S})$
24	475	475	100% asym. $\nu(\text{S-S})$
25	257	258	89% asym. $\delta(\text{CSS})$ + 10% asym. T_{ss}
26	c	117	88% asym. τ_{cs} + 10% asym. T_{ss}
27	c	92	80% asym. T_{ss} + 12% asym. τ_{cs} + 8% asym. $\delta(\text{CSS})$

^{a-d} See footnotes a-d, Table 10. Average error on the calculated wavenumbers is 0.86%.

rocking modes for Me_2S_3 and Me_2S_2 . Furthermore, the CH_3 rocks of Me_2Se_2 and the CD_3 rocks of $\text{Me}_2\text{Se}_2-d_6$ have both been reported as single infrared and Raman bands that are nearly coincident.¹⁵⁶ Nevertheless, the present calculations have pointed to a considerable wavenumber gap between the two CD_3 rocking vibrations of $\text{Me}_2\text{S}_3-d_6$ regardless of which input was used. Thus, the 749 and 745 cm^{-1} band pair led to calculated values of 743 and 729 cm^{-1} (cf. Table 11), while also giving a poorer fit for the CH_3 rocking vibrations of Me_2S_3 (959 and 952 cm^{-1} , cf. Table 10). Hence, the assignments of Table 9 appear to be the more reasonable within the context of the calculations performed in this work. These calculations also suggest appreciable admixing of $\nu(\text{C-S})$ character into the CH_3 or CD_3 symmetric deformation vibration, especially for $\text{Me}_2\text{S}_3-d_6$, as evidenced by a significant involvement of the interaction force constant between the two modes in the potential energy distribution, as well as by a small $\nu(\text{C-S})$ contribution to the distribution for the deformation vibration. Similar effects have been noted previously for Me_2Se_2 ¹⁵⁶ and MeSeH .¹⁵⁷

The skeletal vibrations of Me_2S_3 and $\text{Me}_2\text{S}_3-d_6$ appear in the region below 700 cm^{-1} . The intense $\nu(\text{S-S})$ and $\nu(\text{C-S})$ vibrations in the Raman spectra of the liquids are identified as the symmetric modes by their highly polarized character, and therefore the infrared absorptions at slightly lower wavenumbers are accredited to the corresponding antisymmetric vibrations (Tables 8 and 9). Frankiss^{90b} has proposed analogous assignments for the $\nu(\text{C-S})$ vibrations of Me_2S_2 . Rotating the analyzer in the beam of scattered radiation to measure depolarization in the Raman spectra (Sect. V.B) exposes a weak feature to low energy of the primary $\nu(\text{S-S})$ band for both Me_2S_3 and

$\text{Me}_2\text{S}_3-d_6$ (Figs. 1b and 2b). Since these new bands are clearly much less polarized than the main Raman bands and also coincide with the antisymmetric $\nu(\text{S-S})$ bands in the infrared spectra, they are assigned to the latter modes as well, in agreement with Freeman's⁸³ interpretation of this feature for Me_2S_3 . It is unlikely that these extra bands are the symmetric $\nu(\text{S-S})$ vibrations for the *cis* rotamers thought to be present in low concentration in the liquids (Sect. VI.A.1.ii), inasmuch as a drastic reduction in intensity for such a vibration should occur upon rotation of the analyzer, as observed for the *trans* rotamer. On the other hand, the shoulders on the low-energy side of the $\nu(\text{S-S})$ infrared absorptions are tentatively ascribed to the *cis* rotamers (Sect. VI.A.1.ii). In the solid state, both the *trans* (Solid II) and *cis* (Solid I) rotamers of Me_2S_3 exhibit distinct symmetric and antisymmetric $\nu(\text{S-S})$ vibrations in the Raman spectra. The calculated potential energy distributions for the $\nu(\text{C-S})$ and $\nu(\text{S-S})$ vibrations of Me_2S_3 (Table 10) and $\text{Me}_2\text{S}_3-d_6$ (Table 11) suggest these fundamentals to be largely unmixed with other modes of the molecules, notwithstanding the abovementioned $\nu(\text{C-S})$ character in the symmetric CH_3 and CD_3 deformation vibrations. Worth noting also are the overtones of the $\nu(\text{C-S})$ and $\nu(\text{S-S})$ vibrations, since these are frequently observed for the trisulphides. The former overtone for Me_2S_3 is seen to shift in position along with $\nu(\text{C-S})$ itself.

The $\delta(\text{SSS})$ and symmetric $\delta(\text{CSS})$ vibrations for the *trans* rotamers of Me_2S_3 and $\text{Me}_2\text{S}_3-d_6$ in the liquids account for the considerably polarized, lowest-energy pair of bands in the Raman spectra, while the Raman feature at substantially higher energy in each case is associated with the antisymmetric $\delta(\text{CSS})$ vibration. It was noted in Section VI.A.1.ii that the latter

appears to be slightly polarized due to the underlying symmetric $\delta(\text{CSS})$ mode of the *cis* rotamer. These assignments are in accord with those for the antisymmetric and symmetric $\delta(\text{CSS})$ vibrations of Me_2S_2 at 274 and 240 cm^{-1} , respectively,^{90b} the former band being essentially coincident with that for Me_2S_3 . Then again, the higher energy for the symmetric $\delta(\text{CSS})$ vibration of Me_2S_2 compared to Me_2S_3 suggests this mode to be substantially coupled with the $\delta(\text{SSS})$ mode in the trisulphide; the calculated potential energy distributions for Me_2S_3 (Table 10) and $\text{Me}_2\text{S}_3\text{-}d_6$ (Table 11) bear this out. Thus, the bands at 210 and 209 cm^{-1} are primarily symmetric $\delta(\text{CSS})$ in nature with a significant contribution from the $\delta(\text{SSS})$ mode, while the bands at 184 and 174 cm^{-1} are more highly mixed with a somewhat greater contribution from the $\delta(\text{SSS})$ mode. Similar coupling of bending modes across carbon-sulphur chains has been found in normal coordinate analyses of $\text{CH}_3(\text{SCH}_2)_n\text{SCH}_3$ ($n = 1-3$)^{153b} and the polymers $(\text{CH}_2\text{SS})_n$ and $(\text{CH}_2\text{CH}_2\text{SS})_n$.¹⁵⁸

The assignments for the skeletal deformation vibrations of Solids I and II Me_2S_3 are quite different owing to the reversal in relative positions for the symmetric and antisymmetric $\delta(\text{CSS})$ vibrations of the *trans* and *cis* rotamers predicted by the present normal coordinate calculations (Table 12). In the case of Solid I, the bands at 189 and 181 cm^{-1} merge into a single broad feature in poorly resolved spectra, indicating the splitting to be a crystal effect. The shoulder at 279 cm^{-1} for Solid II may also be a crystal effect. A rationale for the medium intensity band at about 286 cm^{-1} for both Solid I and Solid II is one of Fermi resonance of the $\delta(\text{SSS}) + \text{T}_{\text{ss}}$ combination level with the nearby $\delta(\text{CSS})$ vibration. Such resonance for Solid I requires the symmetric T_{ss} mode (a' symmetry) to be in combination with

Table 12. Skeletal Vibrations of Me_2S_3 and $\text{Me}_2\text{S}_3\text{-d}_6$

Vibrations (cm^{-1}) ^a		Me_2S_3				$\text{Me}_2\text{S}_3\text{-d}_6$			
		<i>trans</i> rotamer			<i>cis</i> rotamer		<i>trans</i> rotamer		<i>cis</i> rotamer
		Obsd.		Calcd.	Obsd.		Obsd.		Calcd.
		Liquid	Solid II		Solid I		Liquid	Calcd.	Calcd.
9	sym. $\nu(\text{C-S})$	696	695	694	701	694	652	652	652
10	sym. $\nu(\text{S-S})$	486	484	487	488	487	482	482	482
11	sym. $\delta(\text{CSS})$	210	219	218	279.5 ^c	267	209	203	251
12	$\delta(\text{SSS})$	184	170	184	185 ^c	194	171	172	187
13	sym. τ_{cs}	b	127	145	130.5 ^c	147	b	106	106
14	sym. T_{ss}	b	94	78	101	84	b	70	76
23	asym. $\nu(\text{C-S})$	694	695	694	699	693	649	652	651
24	asym. $\nu(\text{S-S})$	478	480	478	480	478	475	475	475
25	asym. $\delta(\text{CSS})$	275.5 ^c	281 ^c	273	198	218	257	258	198
26	asym. τ_{cs}	b	133	159	149	160	b	117	118
27	asym. T_{ss}	b	107	104	83	93	b	92	82

^a Vibrations 9-14 are *a* and *a'* modes for the *trans* and *cis* rotamers, respectively; 23-27 are *b* and *a''* modes, respectively. See footnote c, Fig. 13 for abbreviations.

^b Not detected.

^c Average value for two bands (see Table 8).

$\delta(\text{SSS})$ (a' symmetry) to give an A' mode capable of interacting with the symmetric $\delta(\text{CSS})$ mode (a' symmetry), whereas for Solid II, it is the anti-symmetric T_{ss} mode (b symmetry) that is needed to yield a B combination with $\delta(\text{SSS})$ (a symmetry) to interact with the antisymmetric $\delta(\text{CSS})$ vibration (b symmetry). Although the calculations do not indicate an interchange of the symmetric and antisymmetric T_{ss} vibration between the *trans* and *cis* rotamers (Table 12), assignments on the basis of these results can only be tentative since no allowance has been made for intermolecular forces in the crystals. Accordingly, the above assessments of the bands near 286 cm^{-1} for Solids I and II remain quite plausible.

The final skeletal vibrations, internal rotations about the C-S and S-S bonds, are observed only in the spectra of Solids I and II Me_2S_3 . These τ_{cs} and T_{ss} vibrations are assigned with reference to calculated bands for *trans*- and *cis*- Me_2S_3 and $-\text{Me}_2\text{S}_3-d_6$ (Table 12) and in light of the T_{ss} mode at 115 cm^{-1} and the τ_{cs} mode at 134 cm^{-1} (estimated from combination bands) for Me_2S_2 .^{90b} As pointed out above, specific assignments to symmetric and anti-symmetric vibrations would be very tenuous on the basis of the calculations alone. Bands observed below 80 cm^{-1} in the spectra of the solids are attributed to lattice modes.

VI.A.2.i.a Normal Coordinate Calculations

Normal coordinate analysis of Me_2S_3 and $\text{Me}_2\text{S}_3-d_6$ was undertaken as an aid to the vibrational assignments and to explore differences between the spectra of the *trans* and *cis* rotamers. The calculations were performed

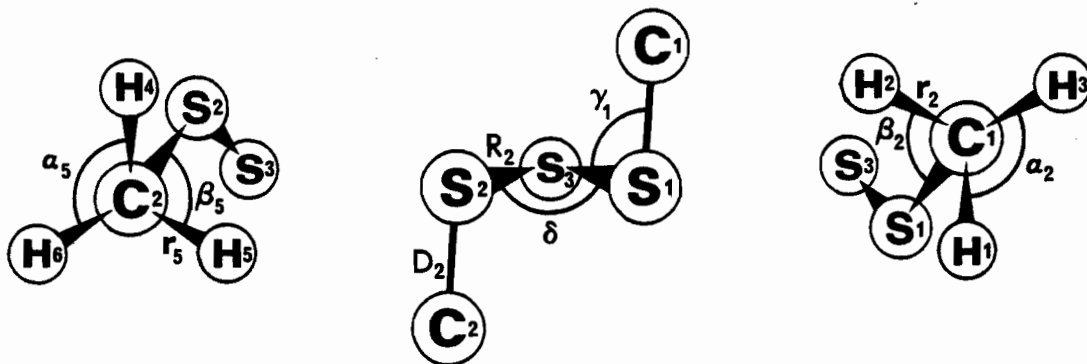
according to the familiar Wilson GF matrix approach,¹⁵⁹⁻¹⁶³ using the set of computer programs ZMAT, WMAT and OVEREND originally written by Overend *et al.*¹⁶⁴ but adapted to the IBM 360/75 computer at McGill University.

A synopsis of the theoretical foundation for this method and some practical aspects of its application together with a brief discussion of the programs is given in the Appendix.

The internal coordinates and associated symmetry coordinates for *trans*- and *cis*-Me₂S₃ and -Me₂S₃-d₆ are defined in Fig. 13. The structure of the CSSSC backbone of the molecules was taken from the electron diffraction investigation of Me₂S₃ by Donahue and Shoemaker^{23b,24} except that the C-S bonding distance was revised from 1.78 to 1.80 Å to bring it within the normal range (Chapter III). Tetrahedral geometry was assumed for the methyl groups which were further assumed to be in staggered configurations. Thus, the structural parameters used in the computations were C-S bond length; 1.80 Å, S-S bond length, 2.04 Å; C-H bond length, 1.09 Å; CSS and SSS bond angles, 104°; HCH and SCH bond angles, 109.47°; CS-SS dihedral angles, 93°; HC-SS dihedral angles ±60 and 180°. The vibrational wavenumbers employed in the calculations were those measured in the infrared and Raman spectra of the liquids (Tables 8 and 9). A Urey-Bradley potential energy function^{159-163, 165} (Appendix) was adopted as a basis for the analysis in light of its earlier use in vibrational studies of dialkyl sulphides^{152f,153,154} and disulphides.^{92b,158} Refinements of the force constants for the trisulphides were carried out for the *trans* rotamer predominant in the liquid state (Sect. VI.A.1.ii), after which the results were extended to the *cis* rotamer. Owing to the nature of the problem, the collections of force constants related to the methyl moieties

Figure 13. Internal and Symmetry Coordinates for *trans*- and *cis*-Me₂S₃.

Internal Coordinates^a



Symmetry Coordinates^b

CH ₃ asym. str. ^c	$S_1, S_{15} = 12^{-\frac{1}{2}} \left[(2r_1 - r_2 - r_3) \pm (2r_4 - r_5 - r_6) \right]$
	$S_2, S_{16} = 1/2 \left[(r_2 - r_3) \pm (r_5 - r_6) \right]$
CH ₃ sym. str.	$S_3, S_{17} = 6^{-\frac{1}{2}} \left[(r_1 + r_2 + r_3) \pm (r_4 + r_5 + r_6) \right]$
CH ₃ asym. def.	$S_4, S_{18} = 12^{-\frac{1}{2}} \left[(2\alpha_1 - \alpha_2 - \alpha_3) \pm (2\alpha_4 - \alpha_5 - \alpha_6) \right]$
	$S_5, S_{19} = 1/2 \left[(\alpha_2 - \alpha_3) \pm (\alpha_5 - \alpha_6) \right]$
CH ₃ sym. def.	$S_6, S_{20} = 12^{-\frac{1}{2}} \left[(\alpha_1 + \alpha_2 + \alpha_3 - \beta_1 - \beta_2 - \beta_3) \pm \right.$ $\left. (\alpha_4 + \alpha_5 + \alpha_6 - \beta_4 - \beta_5 - \beta_6) \right]$
CH ₃ rock.	$S_7, S_{21} = 12^{-\frac{1}{2}} \left[(2\beta_1 - \beta_2 - \beta_3) \pm (2\beta_4 - \beta_5 - \beta_6) \right]$
	$S_8, S_{22} = 1/2 \left[(\beta_2 - \beta_3) \pm (\beta_5 - \beta_6) \right]$
C-S str. [$\nu(\text{C-S})$]	$S_9, S_{23} = 2^{-\frac{1}{2}} \left[D_1 \pm D_2 \right]$

Figure 13. (continued)

Symmetry Coordinates ^b	
S-S str. [$\nu(\text{S-S})$]	$S_{10}, S_{24} = 2^{-\frac{1}{2}} \begin{bmatrix} R_1 \pm R_2 \\ \gamma_1 \pm \gamma_2 \end{bmatrix}$
CSS def. [$\delta(\text{CSS})$]	$S_{11}, S_{25} = 2^{-\frac{1}{2}} \begin{bmatrix} R_1 \pm R_2 \\ \gamma_1 \pm \gamma_2 \end{bmatrix}$
SSS def. [$\delta(\text{SSS})$]	$S_{12} = \delta$
C-S tor. [τ_{cs}]	$S_{13}, S_{26} = 2^{-\frac{1}{2}} \begin{bmatrix} \tau_1 \pm \tau_2 \\ T_1 \pm T_2 \end{bmatrix}$
S-S tor. [T_{ss}]	$S_{14}, S_{27} = 2^{-\frac{1}{2}} \begin{bmatrix} \tau_1 \pm \tau_2 \\ T_1 \pm T_2 \end{bmatrix}$
Redundancy	$S_{28}, S_{29} = 12^{-\frac{1}{2}} \begin{bmatrix} (\alpha_1 + \alpha_2 + \alpha_3 + \beta_1 + \beta_2 + \beta_3) \pm \\ (\alpha_4 + \alpha_5 + \alpha_6 + \beta_4 + \beta_5 + \beta_6) \end{bmatrix}$

^a Only one of each kind of bond length or bond angle displacement is indicated. The r , α and β coordinates with the same subscripts transform identically under the local C_{3v} symmetry of the CH_3 moieties. Torsional coordinates (not shown) are τ_1 and τ_2 for internal rotation about the $\text{C}_1\text{-S}_1$ and $\text{C}_2\text{-S}_2$ bonds, and T_1 and T_2 for internal rotation about the $\text{S}_1\text{-S}_3$ and $\text{S}_2\text{-S}_3$ bonds.

^b The first coordinate corresponds to the positive option and the second coordinate to the negative option. These are the a and b species (*trans* rotamer, C_2 symmetry), or the a' and a'' species (*cis* rotamer, C_s symmetry), respectively, except for reverse assignment for the torsional symmetry coordinates of the *cis* rotamer.

^c Abbreviations: str., stretching; def., deformation; rock., rocking; tor., torsion; sym., symmetric; asym., antisymmetric.

and to the CSSSC skeleton could be treated separately.

Two Urey-Bradley force fields (U.B.F.F.'s) were tested for the methyl groups: (1) that reported for dialkyl disulphides by Sugeta,^{92b} and (2) that developed for dialkyl sulphides by Shiro and his associates.^{152f, 153} These differ primarily in the H(SCH) and F(SCH) force constants* (Table 13). Refinement of either field led to the methyl group field given in Table 13 which is quite similar to Sugeta's field. As in both trial U.B.F.F.'s, the force constant F(HCH) was fixed at $0.200 \text{ mdyne } \text{\AA}^{-1}$, necessitating the introduction of a stretch-stretch interaction force constant for the C-H bonds $[p(\text{C-H})]$ in order to satisfactorily reproduce the CH_3 stretching vibrations. Without $p(\text{C-H})$, these vibrations could not be fit even allowing F(HCH) to vary in the calculations. Once a $p(\text{C-H})$ value was established (Table 13), however, refinement of the rest of the CH_3 force constants resulted in $F(\text{HCH}) = 0.196 \text{ mdyne } \text{\AA}^{-1}$ with minimal changes in the other force constants as well, indicating the fixed value used for this force constant to be a reasonable constraint on the force field. Apart from the $p(\text{C-H})$ modification, the simple U.B.F.F. proved quite adequate for the methyl groups of Me_2S_3 and $\text{Me}_2\text{S}_3\text{-}d_6$ (Tables 10 and 11). Its failure to account for the lifting of the degeneracy (for genuine C_{3v} symmetry) of the antisymmetric stretching and deformation vibrations is expected as a consequence of the true tetrahedral geometry employed for the methyl groups. In assuming purely

* In transferring bending force constants from these fields for use in OVEREND, the units were adjusted from $\text{mdyne } \text{\AA}^{-1}$ to $\text{mdyne-}\text{\AA}$ by multiplying by the two bond lengths in the angle.

tetrahedral CH_3 groups for Me_2S_2 , Sugeta^{92b} also found no splitting of the antisymmetric modes. On the other hand, because of the complexity in the methyl group vibrations of Me_2S , Shiro *et al.*^{152f} had to modify the basic U.B.F.F. extensively to achieve an acceptable fit for the vibrations. The present calculation of CH_3 and CD_3 vibrations at higher and lower wavenumbers, respectively, than those observed for Me_2S_3 and $\text{Me}_2\text{S}_3\text{-d}_6$, is believed to relate to the input of wavenumbers uncorrected for anharmonicity.

The starting point in deriving a U.B.F.F. for the skeletal vibrations of Me_2S_3 and $\text{Me}_2\text{S}_3\text{-d}_6$ was the field of Sugeta^{92b} for dialkyl disulphides which is very similar to the field obtained by Hayashi *et al.*¹⁵⁸ for $(\text{CH}_2\text{SS})_n$ and $(\text{CH}_2\text{CH}_2\text{SS})_n$. The additional force constants $\text{H}(\text{SSS})$ and $\text{F}(\text{SSS})$ for the trisulphides were initially set equal to $\text{H}(\text{CSS})$ and $\text{F}(\text{CSS})$, and a *vicinal* non-bonded interaction constant $\text{C}(\text{CSSS})$ was included. Torsional force constants for the C-S and S-S bonds were transferred as fixed values from Sugeta's field. Early on in the calculations it became apparent that the vibrational data used do not uniquely define a force field for the molecules, and so the focus shifted to seeking a field in line with the ones of Sugeta and Hayashi *et al.* for disulphides. Accordingly, $\text{F}(\text{CSS})$ was fixed at $0.250 \text{ mdyne } \text{\AA}^{-1}$, as in these fields. This restriction and the introduction of a stretch-stretch interaction constant for the S-S bonds $[\text{p}(\text{S-S})]$, led to the force fields summarized in Table 13 for which the corresponding internal coordinate force constants (Appendix) are reported in Table 14.

What emerges from the computations is a very high correlation (interdependence) among the force constants $\text{K}(\text{S-S})$, $\text{H}(\text{SSS})$, $\text{F}(\text{SSS})$ and $\text{p}(\text{S-S})$. Refinement of the field in the absence of $\text{p}(\text{S-S})$ (calc.4) resulted in a large

Table 13. Modified Urey-Bradley Force Fields for Me_2S_3 and $\text{Me}_2\text{-S}_3\text{-d}_6$.

Methyl Group Force Constants ^a (Dispersions)				
K (C-H)				4.467 (0.032)
K (C-S)				1.920 (0.169)
H (HCH)				0.411 (0.007)
H (SCH)				0.412 (0.079)
F (HCH)				0.200 ^b
F (SCH)				0.382 (0.071)
κ (CH_3)				0.122 (0.046)
p (C-H)				-0.092 (0.012)

CSSSC Group Force Constants ^a (Dispersions)				
	Calc. 1	Calc. 2	Calc. 3	Calc. 4
K (C-S)	1.920 (0.049)	1.920 (0.049)	1.919 (0.049)	1.917 (0.049)
K (S-S)	2.106 (0.053)	2.094 (0.055)	2.078 (0.057)	1.924 (0.060)
H (CSS)	0.431 (0.064)	0.434 (0.066)	0.436 (0.068)	0.457 (0.082)
H (SSS)	0.364 (0.900)	0.107 (0.550)	-0.081 (0.422)	-0.835 (0.201)
F (CSS)	0.250 ^b	0.250 ^b	0.250 ^b	0.250 ^b
F (SSS)	0.127 (0.441)	0.271 (0.293)	0.387 (0.238)	1.001 (0.144)
C (CSSS)	0.033 (0.037)	0.031 (0.039)	0.030 (0.040)	0.016 (0.049)
p (S-S)	0.250 ^b	0.225 ^b	0.200 ^b	0.0 ^b
Y (C-S)	0.045 ^b	0.045 ^b	0.045 ^b	0.045 ^b
Y (S-S)	0.150 ^b	0.150 ^b	0.150 ^b	0.150 ^b

^a K, bond-stretching ($\text{mdyne } \text{\AA}^{-1}$); H, angle-bending ($\text{mdyne } \text{\AA}^{-1}$); F, *geminal* nonbonded repulsion ($\text{mdyne } \text{\AA}^{-1}$); C, *vicinal* nonbonded repulsion ($\text{mdyne } \text{\AA}^{-1}$); κ , internal tension ($\text{mdyne } \text{\AA}^{-1}$); Y, internal rotation ($\text{mdyne } \text{\AA}^{-1}$); p, stretch-stretch interaction (modifications to basic field) ($\text{mdyne } \text{\AA}^{-1}$). The equivalent S.I. units are Nm^{-1} with numerical values 100 times those reported here, i.e., 1 Nm^{-1} (Newtons per meter) = $100 \text{ mdynes } \text{\AA}^{-1}$ (millidynes per Angstrom).

^b Fixed force constants.

Table 14. Internal Coordinate Force Fields for the
CSSSC Skeleton of Me_2S_3 and $\text{Me}_2\text{S}_3\text{-d}_6^a$.

No.	Force constant ^b	Calc. 1	Calc. 2	Calc. 3	Calc. 4
1	C-S str.	2.98	2.98	2.98	2.97
2	S-S str.	2.37	2.44	2.49	2.68
3	CSS bd.	0.88	0.88	0.88	0.88
4	SSS bd.	0.71	0.71	0.73	1.06
5	S-S, S-S str.-str.	0.37	0.44	0.49	0.68
6	C-S, S-S str.-str.	0.18	0.18	0.18	0.17
7	S-S, SSS str.-bd.	0.16	0.29	0.39	0.91
8	S-S, CSS str.-bd.	0.24	0.24	0.24	0.23
9	C-S, CSS str.-bd.	0.21	0.21	0.21	0.20
10	CSS, SSS bd.-bd.	0.04	0.03	0.03	0.02

^a Generated by the U.B.F.F. in Table 13.

^b Units: stretching (str.) and stretch-stretch interaction, $\text{mdyne } \text{\AA}^{-1}$; bending (bd.) and bend-bend interaction, $\text{mdyne-}\text{\AA} \text{ rad}^{-1}$; stretch-bend interaction, mdyne rad^{-1} . Internal coordinates in force constants 5 and 6 have an atom in common and in 7-10 have a bond in common. Other force constants generated by the U.B.F.F. are numerically less than 0.025.

F(SSS) and a negative H(SSS), an intuitively unsatisfying solution.

The reason for this outcome is suggested by a simple calculation with all the interaction force constants set equal to zero, in which case the symmetric and antisymmetric $\nu(\text{S-S})$ vibrations of Me_2S_3 are predicted to lie at 461 and 499 cm^{-1} , respectively (455 and 493 cm^{-1} for $\text{Me}_2\text{S}_3-d_6$). It appears, therefore, that within the context of the present calculations, a substantial stretch-stretch interaction force constant (constant 5, Table 14) is required to reproduce the observed $\nu(\text{S-S})$ vibrations. This is achieved in calc. 4 through the generation of a large F(SSS) force constant, necessitating a negative H(SSS) force constant in order to fit the skeletal deformation vibrations, i.e., to offset the large stretch-bend interaction force constant (constant 7, Table 14) that arises. The incorporation of an explicit stretch-stretch force constant $[p(\text{S-S})]$ as a modification to the U.B.F.F. greatly mitigates this problem, permitting a vibrational fit with much more reasonable force constants (Tables 13 and 14). As is apparent from the results of calc. 1-3, the value chosen for $p(\text{S-S})$ dramatically influences the Urey-Bradley force constants, while affecting the physically more meaningful internal coordinate force constants (Appendix) to a lesser extent. The uncertainty in the values of H(SSS) and F(SSS) in the U.B.F.F. is underscored by their large dispersions. A fixed value of 0.275 or 0.300 $\text{mdyne } \text{\AA}^{-1}$ for $p(\text{S-S})$ caused the calculations to cycle without reaching a solution, whereas larger values brought about divergence (Appendix). Attempts to modify the U.B.F.F. with a stretch-bend force constant instead of $p(\text{S-S})$ resulted in divergence except for a value of -0.050 mdyne rad^{-1} which gave a field very much like that from calc. 4, showing this force constant to be poorly defined

in the problem. Thus, Tables 13 and 14 delineate fairly well the possible force fields for Me_2S_3 and $\text{Me}_2\text{S}_3\text{-}d_6$ under the constraint that $F(\text{CSS}) = 0.250 \text{ mdyne } \text{\AA}^{-1}$. When allowed to refine, this latter force constant tended to go to a very small value with a concomitant increase in $H(\text{CSS})$, adding further to the doubt regarding the actual force field. In addition, it should be noted that the true field is also in doubt because of the approximate geometry and liquid-state vibrational wavenumbers (uncorrected for intermolecular forces) used for the molecules.

All the force fields discussed above calculated the same wavenumbers for the fundamental vibrations of the CSSSC skeleton (Table 12). Moreover, the descriptions of the vibrations from the potential energy distributions (Tables 10 and 11) are practically the same for calc. 1-3 and quite similar descriptions emanated from calc. 4 and even from the aforementioned computations in which $F(\text{CSS})$ was refined. Although the force field is clearly at issue, there can be little doubt concerning the proposed vibrational assignments for Me_2S_3 and $\text{Me}_2\text{S}_3\text{-}d_6$.

VI.A.2.ii Diethyl Trisulphide and Diethyl Tetrasulphide

It was concluded in Section VI.A.1.i that the species co-existing in significant proportions in liquid Et_2S_3 are the pair of *trans* rotamers GGGG' and TGGG' of similar stability together with the trio of somewhat lower-energy *trans* rotamers GGGG, GGGT and TGGT also of comparable stability. All except the GGGG and TGGT rotamers of C_2 symmetry are asymmetric (C_1 symmetry). The overt differences between the two groups of rotamers in the vibrational spectra of the liquid were attributed to intramolecular nonbonded

interaction for the G' C-S conformation. The absence of such interaction for either the G or T C-S conformation results in essentially identical spectra for the species within each group. In the assignments (Table 15) proposed for the vibrational spectra of Et_2S_3 (Fig. 3), bands specifically associated with the GGGG' and TGGG' rotamers are indicated as G', while those belonging specifically to the GGGG, GGGT and TGGT rotamers are designated G and T. The use of these latter symbols in the case of the metastable phase in-between the glassy and solid states (Sect. VI.A) is meant to draw attention to the presence of at least two of the three rotamers, although precise assignments are not feasible. Which one of the species GGGG or TGGT prevails in the solid is similarly in question (Sect. VI.A.1.i), but the former is tentatively assumed in light of the marginal preference for the G over the T C-S conformation in EtSSMe and Et_2S_2 according to molecular mechanics.¹¹⁹ The spectra of liquid Et_2S_3 provide no direct evidence for any of the *cis* rotamers GGG'G, GGG'T or TGG'T that might be present in low concentrations (Sect. VI.A.1.ii). Assignments for all the spectra are made with reference to available assignments for Et_2S_2 ,^{89b,c,f,92,94b} EtSH ^{116,166} and EtCl ,¹⁶⁷ as well as from comparisons with Me_2S_3 .

The CH_3 and CH_2 vibrations of the ethyl groups (Fig. 12) in liquid Et_2S_3 are for the most part consistent with a single moiety of C_s local symmetry, with polarized symmetric modes (α' symmetry) and depolarized antisymmetric modes (α'' symmetry). However, the depolarization data should be viewed with caution since the SSCH_2CH_3 fragment has C_s symmetry only for the T C-S conformation, the G and G' conformations giving no local symmetry for this moiety. Detailed assignments for the ethyl group vibrations are not

Table 15. Vibrational Wavenumbers (cm^{-1}) and Assignments for Et_2S_3 .^a

Infrared ^b		Raman ^b		Assignment ^c
Liquid	Liquid	Metastable Phase	Solid	
2971 s,br	2966 m,br dp			CH_3 asym. str.
2927 s	2926 s p			CH_3 sym. str.
2908 sh	2909 s p	d	d	CH_2 asym. str.
2868 s	2870 m p?			CH_2 sym. str.
2818 m	2819 w p			2 x 1418 = 2836
2726 vw	2727 w p			2 x 1372 = 2744
d	d			
1453 sh	1455 sh dp	1459 w	1453 w	CH_3 asym. def.
		1454 w	1450 w	
1446 s	1448 m dp	1447 m	1446 m	
1438 sh	1439 sh dp			
		1442 sh	1441 vw	479 + 968 = 1447
			1436 vw	479 + 963 = 1442
			1419 w	CH_2 sciss.
1417 m	1419 m dp		1414 w	
			1408 m	
			1398 sh,br	153+1252=1405; 646+760=1406
1372 s	1375 vw p?	1375 vw	1374 vw	CH_3 sym. def.
		1370 vw	1368 vw	
		~1288 vvw	1287 vvw	2 x 646 = 1292
1279 m				2 x 641 = 1282
		1259 sh	1258 sh	219 + 1035 = 1254
1252 vs	1254 w p	1253 m	1252 w	CH_2 wagg.
		1240 w,br	1241 w	CH_2 twist.
	1239 w dp		1237 w	
		1234 sh	1232 w	

G'

Table 15. (continued)

Infrared ^b		Raman ^b		Assignment ^c	
Liquid	Liquid	Metastable Phase	Solid		
		~1124 vvw	1122 vvw	479+646=1125; 362+760=1122	
1049 m	1051 m p	1058 w	1058 m	CH ₃ rock.	T
		1054 sh			
1027 w	1030 w dp	1034 w	1035 m		
		1026 sh	1025 vw	265+760=1025; 376+646=1022	
		970 sh			T
967 m	968 w,br dp	965 w,br	968 w	C-C str.	
			963 w		
		954 sh	956 sh		
	~954 sh	951 w	952 w	2 x 479 = 958	
		946 w		2 x 475 = 950	
			943 vvw		
		938 sh	937 vvw		
779 w	~780 vvw				G'
758 m	760 w p	760 w	760 w	CH ₂ rock.	T
		757 sh			
			753 vvw	2 x 376 = 752	
668 vw	670 m p				G'
641 w	644 s p	649 sh		sym. and asym. v(C-S)	T
		647 s	646 s		
			639 vw	³⁴ S satellite	G
498 sh	499 s p			sym. and asym. v(S-S)	G'
	485 vs p	486 vs	488 vs	sym. v(S-S)	G,T
		479 s	479 s	asym. v(S-S)	G
480 s	479 ^e	475 s			
			474 sh	³⁴ S satellites	T
			471 sh		

Table 15. (continued)

Infrared ^b	Raman ^b			Assignment ^c	
Liquid	Liquid	Metastable Phase	Solid		
d	362 w, br dp	439 vvw	440 vw	tetrasulphide	
		375 w	376 w	} sym. CCS def.	G
		372 sh			T
		361 m	362 m	} asym. CCS def.	G
		356 sh			T
	328 m p			CCS def.	G'
	~265 w, br	291 sh		} asym. $\delta(\text{CSS})$	T
		283 s	283 s		G
		269 w	265 vw	CH ₃ torsion	
	202 s, br p?	~233 sh			T
		221 s	219 s	} sym. $\delta(\text{CSS})$	G
	160 sh p				G'
	149 s p	152 s	153 s	} $\delta(\text{SSS})$	G
		148 sh			T
			129 vw	} sym. and asym. τ_{CS} and T_{SS}	
		103 w	106 w		
		92 sh	94 m		
		87 m	88 m		
		73 sh	75 m		
		67 m	68 m		
		57 m	59 m	lattice	
			49 sh	vibrations	
		47 m	47 m		
		38 sh	41 vw		
		34 sh	30 m		
		28 w	20 m		

Table 15. (continued)

- ^a All assignments are based on the *trans* rotamer.
- ^b For abbreviations see footnote b, Table 8.
- ^c See Fig. 12 for the ethyl group vibrations and Fig. 13 for the skeletal vibrations. Explanations for the symbols G, T and G' are given in the text.
- ^d Region not recorded.
- ^e See text.

attempted here. The apparent effects of C-S isomerism in the liquid-state spectra are (1) the shoulder on the main CH_3 antisymmetric deformation vibration, (2) the second CH_2 rocking vibration and (3) the second CCS deformation vibration, all of which are missing in the metastable phase. In the latter state, this isomerism is evident in shoulders on the CH_3 rocking, C-C stretching, CH_2 rocking and CCS deformation vibrations that disappear upon complete solidification. Multiplicity in the ethyl group vibrations for both the metastable and solid states is attributable to crystal effects, except in the case of the CCS deformation vibrations which seem to require an explanation in terms of coupling between the ethyl substituents. The symmetric mode is assigned at higher energy in agreement with Sugeta's^{92b} normal coordinate calculations on Et_2S_2 . The assignments for the CH_2 wagging and twisting modes at 1253 and 1239 cm^{-1} , respectively, warrant comment considering the lack of consensus with respect to these vibrations for Et_2S_2 . Sugeta^{92b} assigned the former at 1278 cm^{-1} and the latter at 1254 cm^{-1} , while Scott *et al.*^{89b} assigned them at 1258 and 1309 cm^{-1} , respectively, and Allum *et al.*^{89f} suggested the two vibrations to be nearly coincident at 1251 cm^{-1} . In the present study, the 1279 cm^{-1} band for both Et_2S_2 and Et_2S_3 is concluded to be the $\nu(\text{C-S})$ overtone found generally for the trisulphides. Such overtones have been reported as well for the $\nu(\text{C-S})$ and $\nu(\text{C-Cl})$ vibrations of EtSH ¹¹⁶ and EtCl ,^{167a} respectively. As regards the 1239 cm^{-1} band of Et_2S_3 , observed also for Et_2S_2 , the only reasonable assignment other than as a fundamental would be to the combination band $479 + 760 = 1239 \text{ cm}^{-1}$, which seems unlikely in view of the splitting of this band, but not the 479 and 760 cm^{-1} bands, in the Raman spectrum of the solid.

In the skeletal vibrations of Et_2S_3 , the most obvious evidence of C-S isomerism is the occurrence of two $\nu(\text{C-S})$ and $\nu(\text{S-S})$ vibrations of which the higher-energy one in each case vanishes from the Raman spectrum upon solidification, indicating them to be due to the GGGG' and TGGG' rotamers. Also attributable to these species is the shoulder at 160 cm^{-1} that is suggested here to be a symmetric $\delta(\text{CSS})$ vibration. Other changes between the spectra of the liquid and metastable states (Sect. VI.A) in the region for the deformation vibrations are too dramatic to determine what features due to these rotamers have disappeared. On the other hand, the disappearance between the metastable and solid states of shoulders on the deformation and $\nu(\text{C-S})$ vibrations and of a distinct $\nu(\text{S-S})$ vibration allow these Raman features to be identified as T bands (*vide supra*). The proposed assignments for the skeletal vibrations of Et_2S_3 are quite similar to those for Me_2S_3 , particularly for the spectra of the solids, on which they are based primarily. It is worth noting that as in the case of Me_2S_3 , the antisymmetric $\nu(\text{S-S})$ vibration for liquid Et_2S_3 can be detected in the Raman spectrum by rotating the analyzer in the beam of scattered radiation.

The assignments (Table 16) for the vibrational spectra of Et_2S_4 as a liquid (Fig. 7) are made by analogy with the spectra of Et_2S_3 and with reference to the normal coordinate analysis of H_2S_4 by Wieser *et al.*⁸² As discussed in Sect. VI.A.1.ii, a number of *trans-trans* and *trans-cis* rotamers are expected to co-exist for the tetrasulphide on the basis of intramolecular nonbonded interactions. Furthermore, the isomerism about the C-S bond within a *trans* fragment can be deduced to be very similar to that for *trans*- Et_2S_3 , and thus it is not surprising to find comparable evidence of

Table 16. Vibrational Wavenumbers (cm^{-1}) and Assignments for Liquid Et_2S_4 .

Infrared ^a	Raman ^a	Assignment ^b	
2977 s		} CH_3 asym. str.	
2966 s			
2927 s		CH_3 sym. str.	
2909 sh		CH_2 asym. str.	
2867 m	c	CH_2 sym. str.	
2819 w		$2 \times 1416 = 2832$	
2727 vw		$2 \times 1372 = 2744$	
c			
1450 sh	1453 sh	} CH_3 asym. def.	
1445 s	1448 w		
1437 sh	1437 sh		G'
1416 m	1417 w	CH_2 sciss.	
1372 m	1375 vw	CH_3 sym. def.	
1274 m		$2 \times 640 = 1280$	
1252 s	1252 w	CH_2 wagg.	
1237 sh	1239 vw	CH_2 twist.	
1048 m	1051 w	} CH_3 rock.	
1028 w	1030 vw		
966 m	967 vw	C-C str.	
	~930 br, vw		
	868 br, w	$2 \times 438 = 876$	
778 w		} CH_2 rock.	G'
758 m	758 vw		
665 vw	666 m p	} sym. and asym. $\nu(\text{C-S})$	G'
640 w	640 s p		
~508 sh	~506 sh	sym. and asym. $\nu(\text{S-S})$	} end G' S-S bonds
497 m		asym. $\nu(\text{S-S})$	
	487 s p	sym. $\nu(\text{S-S})$	

Table 16. (continued)

Infrared ^a	Raman ^a	Assignment ^b
481 m		$\nu(\text{S-S})$ <i>trans-cis</i> rotamers ^d
	~454 sh	$\nu(\text{S-S})$ } central G'
439 vw, br	438 vs p	$\nu(\text{S-S})$ } S-S bond
c	363 br dp?	} sym. and asym. CCS def. G'
	329 m p	
	~270 vbr dp?	} sym. and asym. $\delta(\text{CSS})$
	220 m, br p	
	~145 s, br p	} sym. and asym. $\delta(\text{SSS})$
	155 s, br p	

^a For abbreviations see footnote b, Table 8.

^b See footnote c, Table 15.

^c Region not recorded.

^d See text.

rotational isomerism in the spectra of the two compounds. Features that can therefore be attributed to Et_2S_4 rotamers with a G' C-S conformation in the *trans* fragment are the low-energy shoulder on the CH_3 antisymmetric deformation vibration and the CH_2 rocking, CCS deformation and $\nu(\text{C-S})$ vibrations assigned as G' bands for Et_2S_3 (*vide supra*). These same rotamers are concluded to account for the shoulders on the high-energy side of the main $\nu(\text{S-S})$ bands in both the Raman and infrared spectra.* The assignments for the $\nu(\text{S-S})$ vibrations of the end and central S-S bonds of Et_2S_4 are in keeping with the assignments for H_2S_4 .⁸² In the case of Bz_2S_4 , all three $\nu(\text{S-S})$ bands are observed in both the infrared and Raman spectra of the solid (Sect. VI.B). The above assessment for the $\nu(\text{S-S})$ vibrations of Et_2S_4 leaves the infrared absorption at 481 cm^{-1} as a direct indication of isomerism about the S-S bonds. This feature is probably associated with *trans-cis* rotamers since the predominant species are presumably the *trans-trans* rotamers (Sect. VI.A.1.ii). The appearance of a low-energy shoulder on the primary $\nu(\text{S-S})$ absorption of Me_2S_3 was earlier suggested to similarly arise from S-S isomerism (Sect. VI.A.1.ii). Consistent with the idea of several rotamers co-existing in liquid Et_2S_4 is the broadness of the Raman bands for the CSS and SSS deformation vibrations.

* The shoulder at 454 cm^{-1} in the Raman spectrum may be Et_2S_5 impurity, however, since disproportionation of Et_2S_4 under laser irradiation is shown by the growth of a $\nu(\text{S-S})$ band at this position (Sect. VI.A).

VI.A.2.iii Di-n-propyl Trisulphide

The assignments (Table 17) for the vibrational spectra of liquid $n\text{-Pr}_2\text{S}_3$ (Fig. 4) are proposed in light of literature assignments for $n\text{-Pr}_2\text{S}_2$,^{89f} $n\text{-PrSH}$ ¹⁶⁸ and $n\text{-PrCl}$ ^{167c,169} and on the basis of the present assignments for Et_2S_3 (Table 15). Although rotational isomerism about both the C-C and C-S bonds of $n\text{-Pr}_2\text{S}_3$ renders the spectra considerably more complex than those for liquid Et_2S_3 (Fig. 3), the close correspondence between these two primary trisulphides in the $\nu(\text{S-S})$ vibrations implies that their C-S isomerism is very comparable (Sect. VI.A.1.i). The $\nu(\text{C-S})$ vibrations are also quite similar except that $n\text{-Pr}_2\text{S}_3$ exhibits two pairs of bands because of C-C isomerism which is responsible as well for the multiplicity in the n -propyl group vibrations (Fig. 12). The stable C-C conformations for $n\text{-PrSH}$ and $n\text{-PrCl}$ have been deduced from vibrational studies^{167c,168,169} to be T and G with the former being of lower energy, but no consistent pattern of assignments emerges from these studies. Moreover, normal coordinate analyses of these molecules have indicated both appreciable overlap of bands for the two configurations and significant mixing of vibrational modes. Accordingly, and since the temperature dependence of the $n\text{-Pr}_2\text{S}_3$ spectra was not investigated, only approximate assignments without distinction between bands for T and G C-C conformations are suggested here for the n -propyl vibrations. In the case of the $\nu(\text{C-S})$ vibrations, it is the former of the band pairs at 733 and 706 cm^{-1} and at 657 and 633 cm^{-1} that seems to be associated with the apparently more stable T C-C conformation, insofar as it is the 655 cm^{-1} $\nu(\text{C-S})$ band for liquid $n\text{-PrSH}$ that disappears upon solidification while the 705 cm^{-1} band persists.¹⁶⁸ Such assignments are also in agreement with the

Table 17. Vibrational Wavenumbers (cm^{-1}) and Assignments for Liquid $n\text{-Pr}_2\text{S}_3$.

Infrared ^b	Raman ^b	Assignments ^c	
2963 s,br	2965 s,br dp	CH ₃ asym. str.	
2930 s	2930 vs p	CH ₃ sym. str.	
	~2920 sh	}	CH ₂ asym. str.
2901 sh	2901 vs p		
2873 s	2872 vs p	}	CH ₂ sym. str.
~2860 sh	~2855 sh		
	2809 w p?		2 x 1413 = 2826
2730 w	2733 w p		2 x 1377 = 2754
2656 w	~2654 vw,br		1290 + 1377 = 2667
d	d		
1459 sh		}	CH ₃ asym. def.
1454 s	1455 s dp		
1443 sh	1444 s dp	}	CH ₂ sciss.
1430 m	1434 m dp		
1412 m	1413 s dp	}	CH ₃ sym. def.
1376 s	1378 w p?		
1336 m		}	CH ₂ wagg.
1331 sh	1334 w p		
1294 sh		}	CH ₂ twist.
1287 s	1290 m p		
1281 sh		}	CH ₂ twist.
1229 s	1232 m p		
1202 w	1205 w dp?	}	C-C str.
1192 sh	~1195 sh		
1087 m	1090 m p	}	CH ₃ rock.
1076 w	1077 w dp?		
1049 m	1048 sh,br	}	CH ₃ rock.
1032 w	1030 s p		

Table 17. (continued)

Infrared ^b	Raman ^b	Assignments ^c	
	955 w,br	2 x 481 = 962	
894 m	895 sh	C-C str.	
886 m	890 m p		
843 sh,br	846 w dp?	CH ₂ rock.	
827 w	830 w p		
788 sh	789 sh		
780 m	784 m p		
739 sh	742 sh		
730 m	733 m p		G'
703 w	706 s p	sym. and asym. ν (C-S)	G,T
656 vw	657 m p		G'
632 w	633 s p		G,T
495 sh	498 sh	sym. and asym. ν (S-S)	G'
	486 vs, p	sym. ν (S-S)	G,T
481 m	480 ^e	asym. ν (S-S)	
438 w	440 s p	CCC def.	
	414 m p?		
	379 s p	CCS sym. and asym. def.	
	349 w p		
	322 w,br dp?		
d	295 m,br p?	δ (CSS)	
	~255 sh	δ (SSS)	
	243 s,br	torsion	
	~140 vs,vvbr		

^a Assignments are based on the *trans* rotamer. Symbols refer to the C-S conformations.

^b For abbreviations see footnote b, Table 8.

^c See Fig. 12 for the *n*-propyl group vibrations and Fig. 13 for the skeletal vibrations.

^d Region not recorded.

^e See discussion for Me₂S₃ (Sect. VI.A.2.i.) and Et₂S₃ (Sect. VI.A.2.ii.).

correlation for $\nu(\text{C-S})$ of dialkyl disulphides propounded by Sugeta *et al.*⁹² The secondary splitting of the $\nu(\text{C-S})$ vibrations of $n\text{-Pr}_2\text{S}_3$ is believed to show (as for Et_2S_3) differences between rotamers with a G' C-S conformation in the CCSSCC fragment and rotamers with only G and/or T conformations. In the region for deformation and torsional vibrations, the bands are for the most part very poorly resolved in the Raman spectrum at room temperature, as might be anticipated for the co-existence of quite a number of rotamers in the liquid owing to internal rotation about both the C-C and C-S bonds.

VI.A.2.iv Di-*i*-propyl Trisulphide

The species co-existing in significant amounts in liquid $i\text{-Pr}_2\text{S}_3$ were concluded in Section VI.A.1.i to be the pair of *trans* rotamers GGGT and GGGG' of comparable stability together with the more stable *trans* rotamer GGGG. The latter structure has C_2 symmetry while the other two are asymmetric (C_1 symmetry). Apparently, intramolecular nonbonded interactions for the T and G' C-S conformations absent for the G conformation cause some of the fundamental vibrations to be shifted between the two groups of rotamers. In the proposed assignments (Table 18) for the spectra of $i\text{-Pr}_2\text{S}_3$ (Fig. 5), bands attributable specifically to the GGGT and GGGG' rotamers are marked T, G', whereas bands unique to the GGGG rotamer are indicated as G. Any GGG'G *cis* rotamer that might be present in the liquid (Sect. VI.A.1.ii) is not detected in the spectra. Assignments for $i\text{-Pr}_2\text{S}_3$ are based on those available for $i\text{-PrSH}$ ¹¹⁶ and $i\text{-PrCl}$,¹⁷⁰ and on the present assignments for the other dialkyl trisulphides.

Table 18. Vibrational Wavenumbers (cm^{-1}) and Assignments for $i\text{-Pr}_2\text{S}_3$.^a

Infrared ^b		Raman ^b		Assignment ^c
Liquid	Liquid	Metastable Phase	Solid	
2971 sh	~2975 sh dp			} CH_3 asym. str.
2960 s	2961 s dp			
2925 s	2924 s p			} CH_3 sym. str.
2912 sh	2908 s p?			
2889 sh	~2890 sh	d	d	2 x 1447 = 2894
2865 s	2862 s p			CH str.
2807 vw				1480 + 1364 = 2824
2751 vw	2754 w p			2 x 1381 = 2762
2721 vw	2717 w p			2 x 1364 = 2728
d	d			
~1470 sh	~1473 sh	~1475 sh	~1475 br	1057 + 423 = 1480
		~1463 sh	1466 sh	1157+315=1472; 1109+364=1473
1460 s	1459 sh dp		1462 w	} CH_3 asym. def.
		1455 sh	1455 w	
		1448 w	1450 w	
1448 s	1446 m dp	1445 w	1446 w	
1441 sh		1442 sh	1440 w	
			1436 sh	
1380 s	1382 vw dp?	1380 vw		} CH_3 sym. def.
1364 s	1365 vw dp?	1364 vw	1369 vvw	
			1364 ww	
1312 w	1313 w p?	1312 w	1311 w	} CH wagg.
			1308 sh	
	1295 vw dp	1293 vw		
1245 s	1245 w p	1245 sh, br		
			1237 sh	} CH wagg.
1231 s	1232 m p	1232 w	1234 sh	
			1231 m	

T, G'

T, G'

T, G'

Table 18. (continued)

Infrared ^b	Raman ^b			Assignment ^c
	Liquid	Metastable Phase	Solid	
1152 s	1155 w dp	1156 w	1157 w	CH ₃ rock. + CC ₂ sym. str.
1105 w	1108 w dp	1109 w	1109 w	CC ₂ asym. str.
1047 s	1051 m p	1054 w	1057 m	CH ₃ rock.
		1049 sh	1052 vw	927+131=1058; 632+423=1055
~1040 sh	1044 sh	1041 sh		CH ₃ rock. T,G'
	987 vw p?	988 vw, br	983 w	2 x 497 = 994
			973 vvw	
947 vw	950 w dp	949 vw	954 w	CH ₃ rock.
			952 sh	
927 w	928 vw dp?	928 vw	931 vw	
			927 vw	
883 vw	885 w p	886 vw		CC ₂ sym. str. + CH ₃ rock. T,G'
872 w	875 m p	877 w	878 m	
			870 vvw	505 + 367 = 872
758 vvw				1245 - 488 = 757
627 w	626 s p	629 s	635 s	sym. v(C-S)
			632 sh	asym. v(C-S)
			628 sh	³⁴ S satellite
595 vw	595 m p	597 m		sym. and asym. v(C-S) T,G'
	506 vs p	507 vs	505 vs	sym. v(S-S) G
			503 sh	³⁴ S satellite
		502 sh		sym. v(S-S) T,G'
497 m	496 ^e	497 sh	492 m	asym. v(S-S)
			488 sh	³⁴ S satellite
488 sh	488 m p	486 m		sym. and asym. v(S-S) T,G'

Table 18. (continued)

Infrared ^b	Raman ^b			Assignment ^c
	Liquid	Metastable Phase	Solid	
458 w	456 w p	457 w		CCC def. T, G'
418 vw	418 s p	420 m, br	423 s	
			419 sh	2 x 212 = 224
		359 w	367 w	CCS sym. and asym. def.
	353 m dp?		364 w	
		352 m	352 m	
d	312 s p	315 m	315 s	
			276 w	CH ₃ torsion
			268 w	
			259 vw	
			234 vw	131 + 113 = 244
			218 sh	2 x 113 = 226; 131 + 89 = 220
	~204 sh dp?	211 s	212 s	asym. δ (CSS) G
	195 s p	198 s		
	135 vs p	~142 sh		sym. δ (CSS) T, G'
		135 s	136 sh	
			131 s	δ (SSS) G
			113 m	sym. and asym. τ_{cs} and T_{ss}
			107 sh	
			89 m	
			77 m, br	
		63 m	67 w	
			63 sh	lattice vibrations
			49 s	
			39 m, br	
			35 sh	

Table 18. (continued)

^a All assignments are based on the *trans* rotamer.

^b For abbreviations see footnote b, Table 8.

^c See Fig. 12 for the *i*-propyl group vibrations and Fig. 13 for the skeletal vibrations. Explanations for the symbols T,G' and G are given in the text.

^d Region not recorded.

^e See footnote e, Table 17.

As for the ethyl group vibrations of Et_2S_3 , the *i*-propyl group vibrations (Fig. 12) of $i\text{-Pr}_2\text{S}_3$ appear to be consistent with a single moiety of C_3 local symmetry, except that conformational effects are quite evident in the spectra. Thus, two CH wagging vibrations, a CC_2 symmetric stretching vibration and a CCC deformation vibration all vanish with progressive solidification of the liquid, indicating them to be T,G' features. A CH_3 symmetric deformation vibration and a CH_3 rocking vibration are assigned likewise since they also seem to disappear for the solid. Splitting of the Raman bands for the GGGG rotamer in the solid can be explained in terms of crystal effects. Among the skeletal modes of $i\text{-Pr}_2\text{S}_3$, a $\nu(\text{C-S})$ vibration, a $\nu(\text{S-S})$ vibration, a symmetric $\delta(\text{CSS})$ vibration and an antisymmetric $\delta(\text{CSS})$ vibration are all identified as T,G' bands by their disappearance upon complete solidification. In addition, the observation of four distinct $\nu(\text{S-S})$ vibrations for the metastable state (Sect. VI.A) implies differentiation between the GGGT and GGGG' rotamers in the spectra. The assignments suggested for the skeletal deformation vibrations are quite similar to those for $t\text{-Bu}_2\text{S}_3$ (Sect. VI.A.2.v).

VI.A.2.v Di-*t*-butyl Trisulphide

The assignments (Table 19) for the spectra of $t\text{-Bu}_2\text{S}_3$ (Fig. 6) are referred to the *trans* rotamer which is felt to be the only stable structure for the molecule (Sect. VI.A.1.ii). These assignments are proposed on the basis of those in the literature for $t\text{-Bu}_2\text{S}_2$,^{89d,f,92,150} $t\text{-BuSH}$ ¹⁵⁰ and $t\text{-BuCl}$ ¹⁷¹, as well as from comparisons with the other dialkyl trisulphides. The CH_3

Table 19. Vibrational Wavenumbers (cm^{-1}) and Assignments
for $t\text{-Bu}_2\text{S}_3$.^a

Infrared ^b	Raman ^b		Assignments ^c
	Liquid	Solid	
2973 sh	~2975 sh		CH ₃ asym. str.
2961 s	2962 s dp		
2940 s	2939 m dp?		
2923 s	2920 s p		CH ₃ sym. str.
2897 s	2896 s p		
2861 s	2860 m p?		
2816 vw		d	1363 + 1456 = 2819
2802 vw			1363 + 1445 = 2808
2772 vw	2774 w p		2 x 1389 = 2778
2724 vw			1363 + 1389 = 2745
d	d		
1470 s		1469 vvw	CH ₃ asym. def.
1458 sh	1456 m dp	1457 m	
1453 s		1455 sh	
	1449 sh	1447 sh	
~1440 sh,br	1445 m dp	1438 m	
		1434 sh	
1389 m	1392 vw p?	1390 w	CH ₃ sym. def.
1363 vs	1364 vw p?	1366 vw	
		1362 vw	
1215 m	1217 w dp	1220 m	CC ₃ asym. str.
		1213 sh	414+805=1219; 287+931=1218
		1194 vvw	398+801=1199; 267+931=1198
		1182 vw	
1164 vs,br	1167 m p	1167 s	CH ₃ rock.
1135 s	1138 vw p?	1138 w,br	2 x 574=1148
		1031 vw	CH ₃ rock.
1018 m	1020 w dp	1024 w	
		1018 vw	

Table 19. (continued)

Infrared ^b Liquid	Raman ^b		Assignments ^c
	Liquid	Solid	
	992 vw, br p?	993 w	2 x 499 = 998
931 w	932 s dp	937 w 930 m	} CH ₃ rock.
		808 m	
801 w	802 m p	805 m 801 m	} CC ₃ sym. str.
574 m	573 vs p	574 vs ~567 sh	sym. and asym. ν (C-S) ³⁴ S satellite
	511 vs p	513 vs 510 sh	sym. ν (S-S) ³⁴ S satellite
499 m	498 sh	497 m 492 sh	asym. ν (S-S) ³⁴ S satellite
	418 w p	423 w 414 w	} CC ₃ asym. def.
	401 w dp	403 w 398 w	
	363 m p	366 s 361 sh	} CC ₃ sym. def.
d	318 vw dp	320 w	} CC ₃ rock.
	304 sh	309 m	
	296 m p	299 m	
	~280 sh, vbr	285 w 270 sh	} CH ₃ torsion
		264 vw	
		209 w	
		195 vw	
	188 s p	186 vs	asym. δ (CSS)

Table 19. (continued)

Infrared ^b	Raman ^b		Assignments ^c
Liquid	Liquid	Solid	
	132 vs p	137 s	sym. δ (CSS)
		131 vs	δ (SSS)
		96 w	
		86 s	
		76 sh	τ_{cs}
		67 s	T_{ss} and
		53 s	lattice vibrations
		40 s	

^a Assignments are for the *trans* rotamer.

^b For abbreviations see footnote b, Table 8.

^c See Fig. 12 for the *t*-butyl group vibrations and Fig. 13 for the skeletal vibrations.

^d Region not recorded.

and CC_3 vibrations of the *t*-butyl substituents (Fig. 12) for liquid $t\text{-Bu}_2\text{S}_3$ conform largely to C_{3v} local symmetry with splitting of the CH_3 modes due to coupling of the three moieties. However, as for the CH_3 vibrations of Me_2S_3 (Sect. VI.A.2.i), the CC_3 antisymmetric deformation and rocking vibrations (degenerate e modes for genuine C_{3v} symmetry) separate into a' and a'' modes for C_s local symmetry. Additional multiplicity in the rocking vibrations, particularly for the solid, implies coupling between the two *t*-butyl groups which may also be the reason for the further splitting of the deformation modes in the solid. Other splittings of the *t*-butyl group vibrations upon solidification are attributable to crystal effects. The suggested assignments for the bands at 1165 and 1135 cm^{-1} to a CH_3 rocking vibration and the $\nu(\text{C-S})$ overtone, respectively, are in accord with the interpretation of Green *et al.*^{89d} for the corresponding bands of liquid $t\text{-Bu}_2\text{S}_2$. On the other hand, Sugeta^{92b} assigned these bands for $t\text{-Bu}_2\text{S}_2$ as CC_3 antisymmetric stretching and CH_3 rocking vibrations, respectively. It is worth noting that Green *et al.*^{89d} found the symmetric $\nu(\text{C-S})$ vibration for $t\text{-Bu}_2\text{S}_2$ at 576 cm^{-1} in the Raman spectrum and the antisymmetric vibration at 566 cm^{-1} in the infrared spectrum, while these modes are coincident at 574 cm^{-1} for $t\text{-Bu}_2\text{S}_3$. The situation for the disulphide may reflect weak interaction between the *t*-butyl groups (Sect. VI.A.1.ii). The symmetric and antisymmetric $\nu(\text{S-S})$ vibrations of $t\text{-Bu}_2\text{S}_3$ are more distinguishable in the Raman and infrared spectra of the liquid than for the other trisulphides, the latter vibration appearing as a shoulder on the main $\nu(\text{S-S})$ feature in the Raman spectrum. Similar to the findings for $i\text{-Pr}_2\text{S}_3$ (Sect. VI.A.2.iv), the two symmetric skeletal deformation vibrations for $t\text{-Bu}_2\text{S}_3$ are resolved in the Raman spectrum only in the solid state.

VI.B Dibenzyl Derivatives

The infrared and laser-Raman spectra recorded for Bz_2S_n ($n = 1-4$) in the solid state are reproduced in Figs. 14-17, while the corresponding vibrational wavenumbers and proposed assignments are compiled in Table 20. Structural elucidation of Bz_2S_2 by X-ray diffraction^{31,120} has shown the GGG configuration for the CCH_2SSCH_2C core of the molecule (CS-SC dihedral angle = 92° , CC-SS dihedral angles = 72 and 73°) with the phenyl rings orientated mutually perpendicular (angle between the planes = 91°). In essence, therefore, the molecule has a two-fold axis of rotation and C_2 overall symmetry.* The CH_2SSSCH_2 backbone of crystalline Bz_2S_3 can be assumed to be *trans* with C_2 local symmetry in light of the available structural information on organotrisulphides (Sect. VI.A.1.i). Similarly, Bz_2S_4 is most probably in the *trans-trans* geometry also with C_2 local symmetry in the solid state.

As for the dialkyl polysulphides (Sect. VI.A.2), the vibrations of the dibenzyl derivatives examined in this work separate largely into substituent modes and skeletal modes. This situation is demonstrated by the very similar spectra for the four compounds except where the stretching and deformation vibrations of the CS_nC ($n = 1-4$) skeleton are expected. Early studies of the infrared spectra ($950-400\text{ cm}^{-1}$) of Bz_2S_n ($n = 3-8$) by Minoura and Moriyoshi⁶ have also revealed a strong resemblance between

* The crystal space group of Bz_2S_2 now appears to be $C2/c$ and not Cc as originally suggested.¹⁷²

Table 20. Vibrational Wavenumbers (cm^{-1}) and Assignments for Crystalline Bz_2S_n ($n = 1-4$)

Bz_2S		Bz_2S_2		Bz_2S_3		Bz_2S_4		Assignments ^b
Infrared ^a	Raman	Infrared	Raman	Infrared	Raman	Infrared	Raman	
			3074 m				3061 m	20b (b_2)
	3059 s		3071 m		3063 m		3058 m	
	3054 s		3054 s		3052 s		3049 s	20a (a_1)
	3042 m		3045 m		3038 m		3036 m	$\nu(\text{CH})$ 2 (a_1)
	3032 m							13 (a_1)
c		c	3031 m	c	3029 m	c	3028 m	
	3027 m							
	3005 w		3007 w		3004 w		3004 w	7b (b_2)
	2980 w		2979 w, br		2982 w		2980 w	2 x 1496 = 2992
							2960 m	CH_2 asym. str.
	2955 m		2969 m		2955 m		2955 sh	
	2920 s		2911 s		2918 s		2914 s	CH_2 sym. str.
	c		c		c		c	
1601 m	1602 s	1601 m	1602 s	1603 m	1604 s	1601 w	1603 s	$\nu(\text{CC})$ 8a (a_1)
1583 m	1585 m	1583 w	1585 w	1584 w	1584 m	1584 w	1584 m	
				1538 w, br		1544 w, br		8b (b_2)
1493 s	1496 vw	1496 s	1497 vw	1496 s	1498 vw	1494 s	1495 w	$\nu(\text{CC})$ 19a (a_1)
1453 s	1455 vw	1453 s	1454 vw	1452 s	1455 vw	1453 s	1454 vw	
							1425 w	
1413 s	1416 m	1410 m	1411 w	1413 s	1415 w	1415 s	1415 w	CH_2 sciss.
		1337 vw	1338 vw	1333 vw	1335 w	1335 w		$\nu(\text{CC})$ 14 (b_2)
1323 vw	1326 vw		1325 vw	1320 vw	1321 vw	1323 w	1325 vw	

Table 20. (continued)

Bz_2S		Bz_2S_2		Bz_2S_3		Bz_2S_4		Assignments ^b
Infrared ^a	Raman	Infrared	Raman	Infrared	Raman	Infrared	Raman	
	1294 vw	1292 vw	1296 vw	1293 vw	1294 vw	1291 vw	1295 vw	$\beta(CH)$ 3 (b_2)
	1253 s				1252 vw	1260 vw	1254 vw	CH_2 wagg.
1233 m	1235 w		1234 s	1233 m	1233 s	1237 m	1238 s	CH_2 twist.
		1225 m	1227 sh		1227 m	1231 m	1233 s	
							1229 sh	
						1202 sh		
1197 w	1202 s	1199 m	1201 m	1198 m	1199 w	1198 m	1201 m	X sens. 7a (a_1)
1182 w	1189 w,br		1191 vw	1183 w	1184 vw		1186 vw	$\beta(CH)$ 9a (a_1)
		1182 w	1181 vw			1178 w	1181 sh	
	1169 w							
	1165 sh		1162 w	1159 m	1161 m	1158 w	1160 w	$\beta(CH)$ 9b (b_2)
1161 w	1158 w		1155 vw	1152 vw	1153 vw	1156 sh	1155 w	
1138 w	1142 vw	1139 vw	1143 vw		1142 vw	1144 vw	1145 vw	
				1135 m				
					1128 vvw		1136 vw	
				1106 w,br				
1070 m		1071 m	1072 vw	1068 m		1071 m	1072 vw	$\beta(CH)$ 15 (b_2)
	1036 sh		1039 sh		1042 vw		1034 sh	$\beta(CH)$ 18a (a_1)
1029 m	1030 m	1030 m	1032 m	1032 m	1034 w	1030 m	1031 m	
1002 w	1003 vs	1000 vw	1001 vs	1001 w	1002 vs	1000 m	1001 vs	ring 1 (a_1)
992 w	992 w		991 vw		991 vw	987 w	989 vw	$\gamma(CH)$ 5 (b_1)
			983 vw		988 vw			

Table 20. (continued)

Bz_2S		Bz_2S_2		Bz_2S_3		Bz_2S_4		Assignments ^b
Infrared ^a	Raman	Infrared	Raman	Infrared	Raman	Infrared	Raman	
	974 vw					969 vw		} $\gamma(CH)$ 17a (a_2)
968 vv		971 w		963 vw	946 vw		971 vv	
	969 vw					966 vw		
					939 vv			} $\gamma(CH)$ 17b (b_1)
921 sh	929 vw				927 vw		922 vw	
913 m		912 w	917 vw	908 m	910 vw	914 m	916 vw	
897 sh							877 vw	} $\gamma(CH)$ 10b (b_1)
						873 vw	868 vw	
		864 m	862 w					
				858 m	864 vw	858 w		
		860 sh	858 sh					
850 vv	851 vw	849 vw			851 vw		848 vw	} $\gamma(CH)$ 10a (a_2)
842 vv						844 vw	843 vw	
822 vw	823 w		821 vw				820 vw	
	808 sh		812 w			816 vw	814 w	} $\gamma(CH)$ 10a (a_2)
803 vw	805 m	804 w	807 sh	805 w	806 w	806 w	806 w	
	778 m		773 sh					
		766 s	768 m			770 sh	771 w	} X sens. 12 (a_1) CH ₂ rock.
770 s	767 m			765 s	766 w			
		759 s				765 s	767 m	
	714 m							} $\nu(C-S)$
	708 w							

Table 20. (continued)

Bz_2S		Bz_2S_2		Bz_2S_3		Bz_2S_4		Assignments ^b
Infrared ^a	Raman	Infrared	Raman	Infrared	Raman	Infrared	Raman	
703 s			704 m					} $\phi(CC)$ 4 (b_1)
	696 m							
696 s		697 s		694 s	696 vvw	697 s	701 vw	
673 m	674 s	660 s	661 vs	661 s	662 s	659 s	660 vs	$\nu(C-S)$
622 vw	621 m	620 w	619 m	621 w	619 m	620 vw	619 m	$\alpha(CCC)$ 6b (b_2)
		572 m						} X sens. 16b (b_2)
567 m	567 w	567 m	570 vw	566 s	564 vw	565 m	564 vw	
		506 w	505 s					$\nu(S-S)$
			502 sh					^{34}S satellite
						494 m	494 s	asym. $\nu(S-S)$ } end
						485 w	485 s	sym. $\nu(S-S)$ } S-S
				485 w	484 vs			sym. $\nu(S-S)$
				474 m	475 m			asym. $\nu(S-S)$
				468 sh	468 s	471 m	471 s	} X sens. 6a (a_1)
471 m	468 m	469 m	468 m	463 m	464 sh	467 sh	468 sh	
						436 vw	435 vs	$\nu(S-S)$ central bond
							431 sh	^{34}S satellite
	411 vvw		409 vw		407 vvw		411 vvw	$\phi(CC)$ 16a (a_2)
c	349 w	c		c		c	354 vw	} CCS def.
	335 vw		343 m		356 vw		347 w	

Table 20. (continued)

Bz_2S		Bz_2S_2		Bz_2S_3		Bz_2S_4		Assignments ^b
Infrared ^a	Raman	Infrared	Raman	Infrared	Raman	Infrared	Raman	
	308 m		308 m		307 vw		310 m	X sens. 18b (b_1)
	286 vw		289 vw		293 m		289 w	
			216 m		263 s		261 m	sym. and asym. δ (CSS)
			186 s		220 w		231 w	
							220 vw	
	185 s							δ (CSC)
					164 s		197 m	δ (SSS)
							158 vs	
c		c	156 m	c		c		τ_{cs}
			142 s		145 s		132 vs	
	117 vs		113 sh		112 s		121 vs	X sens. 11 (b_1)
	102 vs		103 s					
			97 s		96 s		92 vs	
					81 vs		76 vs	
	68 vs		62 vs				67 vs	T_{ss} and lattice vibrations
	52 vs		56 vs		55 vs			
			47 vs				45 vs	
	39 vs		34 s				36 vs	
							30 vs	

Table 20. (continued)

^a For abbreviations see footnote b, Table 8.

^b See Fig. 12 for the CH₂ group vibrations and Fig. 13 for the skeletal vibrations. The phenyl group vibrations are $\nu(\text{CH})$, in-plane C-H stretching; $\nu(\text{CC})$, in-plane C-C stretching; $\beta(\text{CH})$, in-plane CCH bending; $\gamma(\text{CH})$, out-of-plane CCH bending; ring (see ref.174) $\phi(\text{CC})$, out-of-plane C-C torsion; $\alpha(\text{CCC})$, in-plane CCC bending; X sens., substituent-sensitive vibrations.

^c Region not recorded.

homologues. The virtually identical $\nu(\text{C-S})$ vibrations for Bz_2S_n ($n = 2-4$) suggest that all three molecules have G C-S conformations in the solid state as found for Bz_2S_2 ,^{31,120} although G and T conformations would be predicted to afford very comparable $\nu(\text{C-S})$ wavenumbers (Sect. VI.A.1.i). The close correspondence in the benzyl group vibrations of Bz_2S_n ($n = 1-4$) implies the absence of significant interaction between the π electrons of the phenyl rings and the lone-pair $3p_\pi$ electrons on sulphur. Blokhim *et al.*¹⁷³ have arrived at the same conclusion on the basis of the very similar X-ray fluorescence spectra for the four species. On the other hand, the progressive shift to low field for the CH_2 resonance in the ^1H nmr spectra of Bz_2S_n ($n = 1-7$)⁸ indicates some electronic variation across the series. This does not appear to appreciably affect the vibrational spectra, however.

The benzyl group vibrations of Bz_2S_n ($n = 1-4$) divide further into vibrations of the methylene moiety and the phenyl ring. The former are assigned on the basis of the present assignments for Et_2S_3 (Table 15) and, except for the CH_2 rocking mode, these vibrations do not overlap with the phenyl group vibrations. Somewhat surprisingly, the CH_2 vibrations of Bz_2S are not more complex than those of the other derivatives, even though coupling of the *geminal* CH_2 moieties would be anticipated as in the case of dialkyl sulphides.^{117,152-154} It is also worth noting that the CCS deformation vibrations for solid Bz_2S_n ($n = 2,3$) are simpler than those for liquid Et_2S_n ($n = 2,3$) owing to the absence of rotational isomerism in the solid state.

The phenyl groups of Bz_2S_n ($n = 1-4$) can be treated as monosubstituted benzene derivatives for purposes of analyzing the spectra. Thus the

Whiffen mode descriptions¹⁷⁴ and the Wilson nomenclature¹⁷⁵ advanced by Green¹⁷⁶ in vibrational studies of monosubstituted benzenes have been adopted for the present assignments (see footnote b, Table 20). Assuming C_{2v} local symmetry for the phenyl moiety (X axis perpendicular to the plane of the ring) the vibrations belong to the classes $11a_1 + 10b_2 + 3a_2 + 6b_1$ where the first two representations correspond to in-plane vibrations and the others are out-of-plane vibrations. These modes should all be Raman active while all but the a_2 modes should be infrared active. Nonetheless, since the local symmetry of the benzyl substituent as a whole is more closely C_s with a' in-plane modes and a'' out-of-plane modes, the a_2 vibrations are weakly observed in the infrared spectra. The majority of the phenyl group vibrations are quite invariant in wavenumber among monosubstituted benzenes, whereas the six substituent-sensitive (X sens.) vibrations ($3a_1 + b_2 + 2b_1$) involving substantial motion of the substituents undergo significant displacements from one compound to another. Of course, these latter modes are minimally shifted among the species Bz_2S_n ($n = 1-4$) for which they also parallel rather closely the X sens. modes of ethyl benzene.^{176b} By and large, the assignments (Table 20) for the phenyl group vibrations follow directly from Green's assessments for monosubstituted benzenes, although there is some question concerning the $\gamma(CH)$ vibrations 10a (a_2 symmetry) and 10b (b_1 symmetry). In contrast to Green's assignments, the latter mode is attributed at higher wavenumber in the present work on the grounds that the a_2 mode should absorb only weakly in the infrared. However, exact assignments for the $\gamma(CH)$ vibrations are made difficult by the fact that the $1000-800\text{ cm}^{-1}$ region where they are expected is replete with both

infrared and Raman features, many of which are presumably non-fundamentals. Multiple assignments for these and other phenyl group vibrations are meant to indicate alternative assignments. In some cases, band splitting may arise from crystal effects.

It should be pointed out that the common vibrational description for monosubstituted benzenes¹⁷⁶ as used in Table 20 for Bz_2S_n ($n = 1-4$), are very approximate in nature and can, in fact, be misleading in some instances. For example, detailed normal coordinate analyses of toluene and several deuterated analogues by La Lau and Snyder¹⁷⁷ have indicated extensive vibrational coupling for these molecules. In particular, the in-plane $\nu(CC)$ and $\beta(CH)$ modes were determined to be highly mixed over the range $1605-1080\text{ cm}^{-1}$ for the normal species. Less pronounced coupling was found between out-of-plane $\phi(CC)$ and $\dot{\gamma}(CH)$ modes. The important observation with respect to Bz_2S_n ($n = 1-4$) is that the phenyl group vibrations are apparently analogous to those for monosubstituted benzenes. The actual modes are likely to be complex internal distortions of the phenyl groups as a whole.

The assignments (Table 20) for the skeletal vibrations of Bz_2S_n ($n = 1-4$) are proposed on the basis of the present assignments for dialkyl polysulphides (Sect. VI.A.2) and literature assignments for Bz_2S_2 ^{31,89f} and related di- and monosulphides. Dramatic differences in these vibrations for the four species reflect the variation in sulphur chain length, extension of the chain being accompanied by a considerable increase in the complexity of the spectra (Figs. 14-17). However, the symmetric and anti-symmetric $\nu(C-S)$ vibrations are coincident for Bz_2S_n ($n = 2-4$), as for

dialkyl di- and polysulphides, while Bz_2S yields two separate $\nu(\text{C-S})$ bands (the higher-energy of which is split into two components), as for dialkyl sulphides. Since the latter molecule has no $\nu(\text{S-S})$ vibrations, its 510-430 cm^{-1} region shows only the phenyl mode 6a. For the other dibenzyl derivatives, this mode is observed together with the $\nu(\text{S-S})$ vibrations which are in line with those for primary di- and polysulphides. As in the case of R_2S_3 ($\text{R} = \text{Me}, \text{Et}, i\text{-Pr}, t\text{-Bu}$) in the solid state (Sect. VI.A.2), the anti-symmetric $\nu(\text{S-S})$ vibration of solid Bz_2S_3 appears as a distinct Raman feature to low energy of the intense band due to the symmetric $\nu(\text{S-S})$ vibration. On the other hand, the former band for liquid R_2S_3 is clearly discerned only upon rotating the analyzer in the beam of scattered radiation (Sect. V.B) or in the infrared spectra. Similarly, the symmetric and anti-symmetric $\nu(\text{S-S})$ vibrations for the end S-S bonds of Bz_2S_4 are well resolved in its solid-state Raman and infrared spectra, unlike the situation for liquid Et_2S_4 (Sect. VI.A.2.ii) or for H_2S_4 in solution.⁸² Apart from the very weak band at 220 cm^{-1} for Bz_2S_4 , the number of Raman bands detected for each of the species Bz_2S_n ($n = 1-4$) in the 265-160 cm^{-1} region is consistent with the theoretical number of skeletal deformation vibrations to which the bands are therefore attributed. Only tentative assignments are suggested for vibrations found below this region.

The Raman spectra (750-400 cm^{-1}) of Bz_2S_n ($n = 1-3$) in the liquid state at 60°C* are shown in Fig. 18. The spectra in CCl_4 and benzene solution at ambient temperature are essentially identical except for poorer signal-to-noise ratios and a somewhat greater relative intensity for the

* Once melted (mp 71°C), Bz_2S_2 persisted in the glassy state upon cooling in the capillary tube.

feature at 702 cm^{-1} for Bz_2S_2 and Bz_2S_3 . Similar data for Bz_2S_2 as a liquid and in benzene solution (below 600 cm^{-1}) were reported by Allum *et al.*^{89f} and Van Wart and Scheraga,³¹ respectively. A comparison of the present spectra with those of the solids (Table 21) indicates little change upon going into the fluid phases apart from the appearance of the seemingly variable-intensity feature at 702 cm^{-1} for Bz_2S_2 and Bz_2S_3 . In the case of Bz_2S , the solid-state bands at 714 and 708 cm^{-1} merge into a single feature at about 712 cm^{-1} with no additional bands becoming apparent. The observations on Bz_2S_2 and Bz_2S_3 provide evidence of rotational isomerism in the fluid phases, the 702 cm^{-1} band presumably being a $\nu(\text{C-S})$ vibration for one or more rotamers not present in the solids. The absence at the same time of a new $\nu(\text{S-S})$ band to high energy of the main $\nu(\text{S-S})$ vibration, as found for primary dialkyl di- and trisulphides in the liquid state (Sect. VI.A.1), leads to the conclusion that the new species do not involve the G' C-S conformation, in agreement with the considerable destabilization of this geometry by steric interaction according to space-filling molecular models (CPK type). On the other hand, the additional $\nu(\text{C-S})$ vibration may distinguish between G and T C-S conformations for the dibenzyl derivatives, although such is not the case for the dialkyl compounds. However, in view of the dependence of $\nu(\text{C-S})$ on C-C conformation for dialkyl disulphides (and evidently also for $n\text{-Pr}_2\text{S}_3$ (Sect. VI.A.2.iii)), a perhaps more likely origin for the extra $\nu(\text{C-S})$ feature is from isomerism with respect to the methylene-ring C-C bond. The molecular models of Bz_2S_2 and Bz_2S_3 do point to hindered rotation about the C-C bond for the G C-S conformation. It is worth mentioning that conformational effects found in the low-temperature

Table 21. Raman Spectra (750-400 cm^{-1}) for Bz_2S_n ($n = 1-3$) in Various States.

Bz_2S			Bz_2S_2			Bz_2S_3			Assignment ^b
Liquid	Solution ^a	Solid	Liquid	Solution ^a	Solid	Liquid	Solution ^a	Solid	
		714 m							} $\nu(\text{C-S})$
~710 sh	713 w	708 w	702 m	700 m		703 w	702 m		
701 w	700 w	696 m	689 s	688 s	704 m	692 m	691 m	696 vvw	$\phi(\text{CC})$ 4 (b_1)
680 s	679 s	674 s	658 s	658 s	661 s	661 m	662 m	662 s	$\nu(\text{C-S})$
620 m	620 m	621 m	621 m	620 m	619 m	620 w	620 m	619 m	$\alpha(\text{CCC})$ 6b (b_2)
~565 w,br		567 w	564 w	565 w	570 vw	~565 vw,br	~560 vw,br	564 vw	X sens. 16b (b_2)
					505 s			484 vs	} $\nu(\text{S-S})$
			513 s	512 s		490 s	489 s	475 m	
	c				502 sh			475 m	} X sens. 6a (a_1)
468 w		468 m	470 m	470 m	468 m	468 s	468 s	468 s	
								464 sh	
		411 vvw	406 vw	~404 w,br	409 vw		~405 vw,br	407 vvw	$\phi(\text{CC})$ 16a (a_2)

^a Solvents are CCl_4 (above 600 cm^{-1}) and benzene (below 600 cm^{-1}).

^b See footnote b, Table 20.

^c Region not recorded.

^1H nmr spectra of Bz_2S_3 by Snyder and Harpp¹⁴¹ and of BzSSR (R = various substituents) by Fraser *et al.*¹⁷⁸ have been attributed to retarded rotation about the S-S bonds. The latter authors deduced that the AB quartet for the CH_2 resonance obtained upon cooling was not due to hindered rotation about the C-S bonds on the grounds that this would require the highly unlikely existence of exclusively G C-S conformations in solution, since no singlet for the T conformation was detected. Neither group has considered the possible effects of C-C isomerism, however.

Figures 14-17. Infrared and Laser-Raman Spectra of Crystalline Dibenzyl Derivatives.

Figure 14. Bz_2S

Figure 15. Bz_2S_2

Figure 16. Bz_2S_3

Figure 17. Bz_2S_4

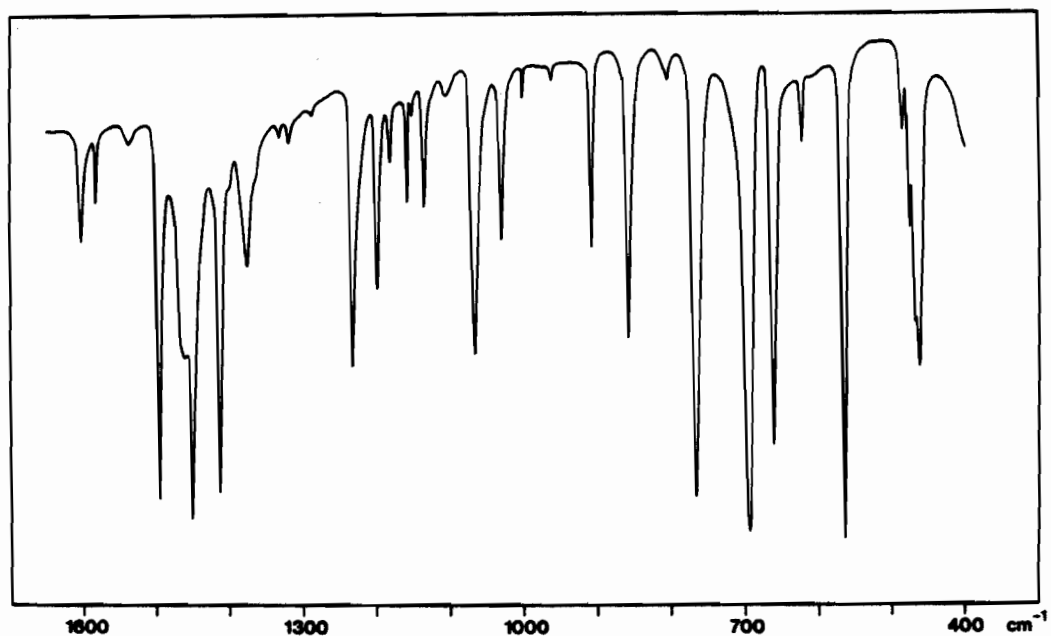


Figure 16a. Infrared Spectrum of Crystalline Bz_2S_3 .

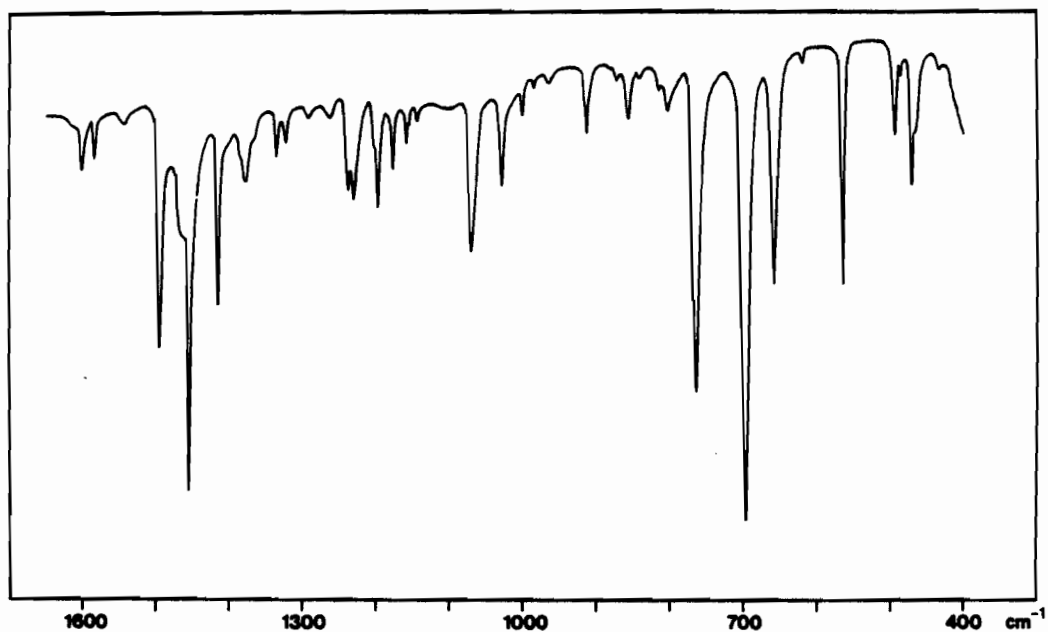


Figure 17a. Infrared Spectrum of Crystalline Bz_2S_4 .

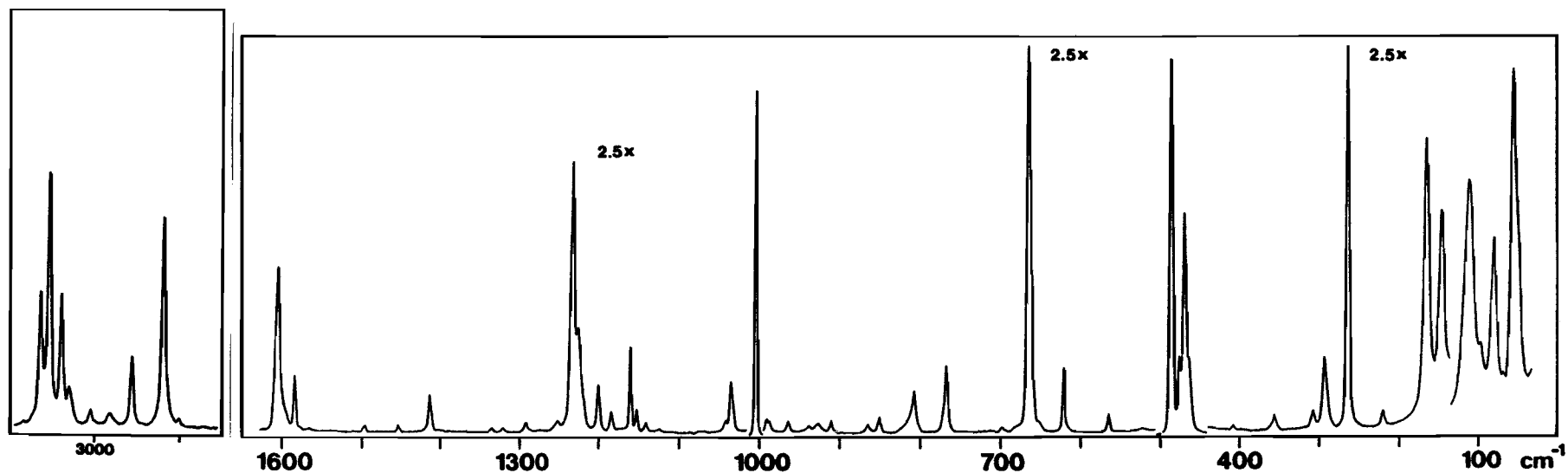


Figure 16b. Laser-Raman Spectrum of Crystalline Bz_2S_3 .

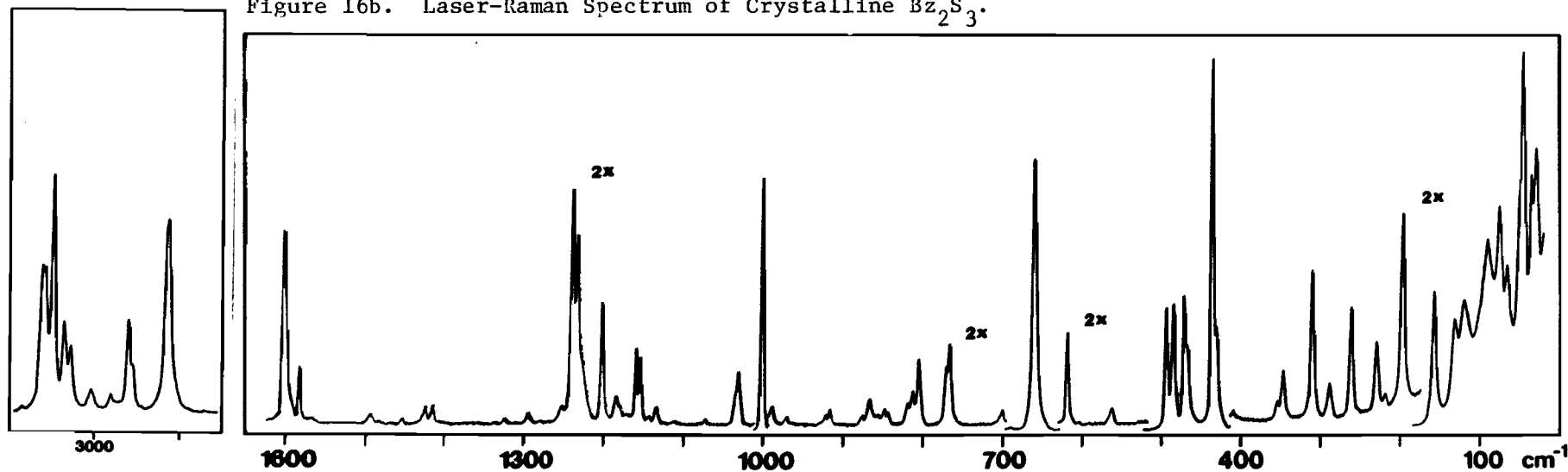
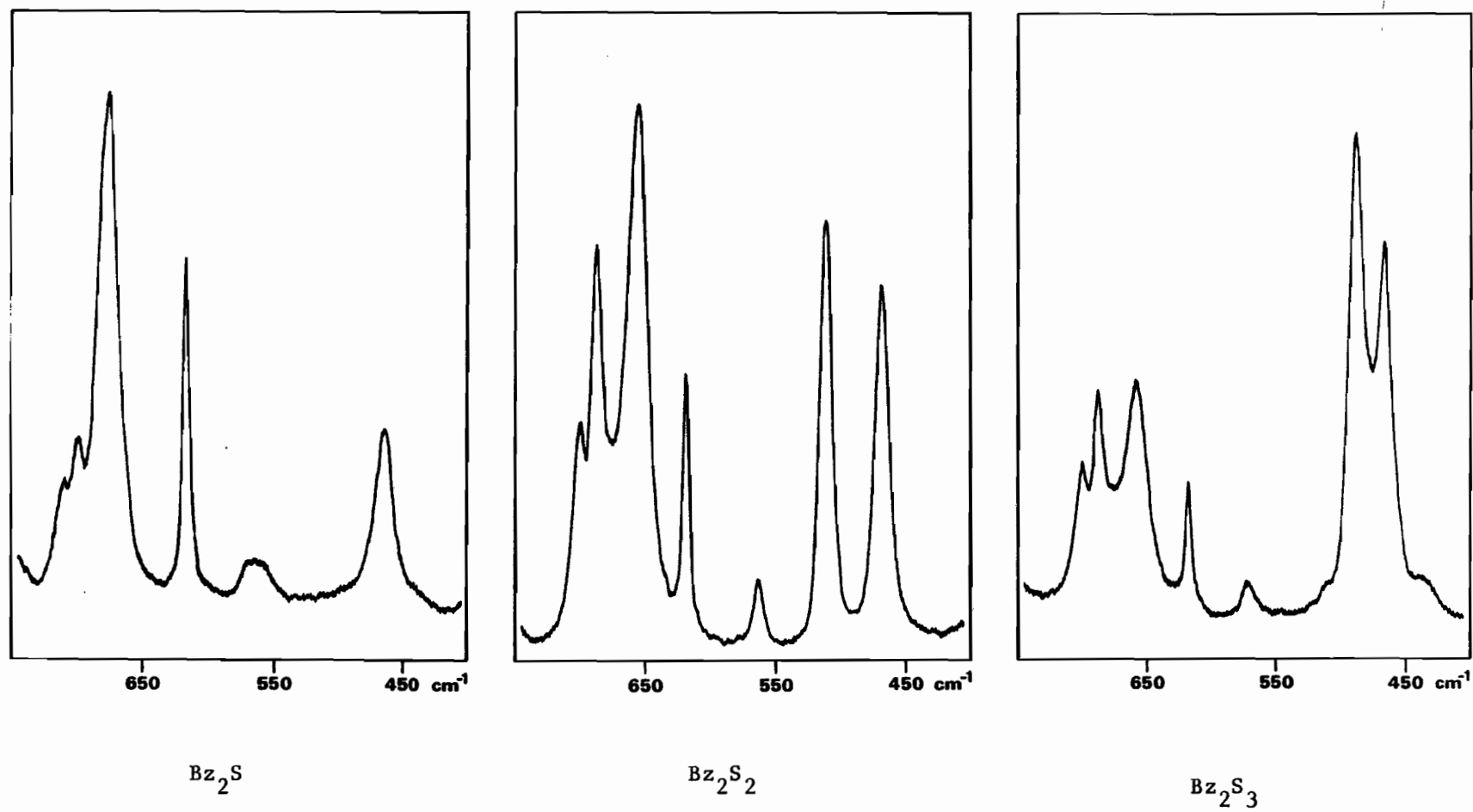


Figure 17b. Laser-Raman Spectrum of Crystalline Bz_2S_4 .

Figure 18. Laser-Raman Spectra of Dibenzyl Derivatives in the Liquid State.



VI.C Diphenyl Di- and Trisulphides

The infrared and laser-Raman spectra for crystalline $(4\text{-R-Ph})_2\text{S}_3$ (R = Br, Me, OMe, *t*-Bu) and $(4\text{-R-Ph})_2\text{S}_2$ (R = Br, Me, OMe) are presented in Figs. 19-25. Tables 22-25 give the corresponding vibrational wave-numbers and proposed assignments. Structure determinations of numerous aromatic disulphides (sp^2 carbon bonded to sulphur) by X-ray diffraction^{30,179} have revealed the G CSSC configuration with dihedral angles generally within 20° of 90° , although an angle as small as 50° has been reported.¹⁸⁰ The CC-SS dihedral angles usually fall near $10\text{-}20^\circ$ (A conformation)* or less frequently in the vicinity of 90° (B conformation)*. Van Wart *et al.*³⁰ have drawn attention to the longer C-S bond in the former cases as a rule, whereas delocalization of $3p_\pi$ sulphur electron density onto the aromatic ring should, it was argued, shorten the bond due to the resultant double-bond character. They therefore concluded that such conjugation, albeit maximized for low values of the CC-SS dihedral angle, is not the reason for the A conformation. On the other hand, Allinger *et al.*¹¹⁹ have noted that the larger CSS bond angles associated with the A conformations imply greater steric repulsion in these structures which may cause an extension of the C-S bond in spite of its increased bond order. An interesting relationship pointed out by Shefter¹⁸¹ is that the S-S bond length is substantially greater for the B than for the A conformation. This suggests that the latter geometry does involve significant delocalization of

* These terms are borrowed from Van Wart and Scheraga.³¹

$3p_{\pi}$ electron density away from sulphur, thereby stabilizing the bond (Chapter III). Recently, Higashi *et al.*¹⁷⁹ have deduced that such delocalization favours the A conformation for aromatic disulphides except when a strongly electron-donating group occurs in the β position (adjacent to the sulphur-bonded carbon) or in the *ortho* position of the ring, in which case the B conformation is preferred to avoid transfer of electron density into the $3p_{\pi}$ sulphur orbitals.* In some instances, however, the A conformation appears to be precluded for steric reasons, and groups more distant from the C-S bond were concluded to affect the S-S bond minimally. The absence of significant influence on the S-S bond of diphenyl disulphides from *para* substituents is indicated by the present vibrational data for $(4-R-Ph)_2S_2$ ($R = Br, Me, OMe$) insofar as the $\nu(S-S)$ vibration is essentially invariant (*vide infra*) despite the greater electron-releasing ability of the Me and OMe substituents (Hammett σ_{para} parameters:¹⁸² Me, -0.13; MeO, -0.11; Br, + 0.27). Accordingly, all three disulphides can be assumed to have A C-S conformations as found for $(4-NO_2-Ph)_2S_2$ ¹⁸³ and for Ph_2S_2 ¹⁸⁴ itself. By the same token, A C-S conformations can be assumed for the trisulphides $(4-R-Ph)_2S_3$ ($R = Br, Me, OMe, t-Bu$) for which the CSSSC skeleton is most likely in the *trans* configuration (Sect. VI.A.1.ii).

As far as possible, the vibrational assignments (Tables 22-25) for the *para*-substituted diphenyl di- and trisulphides are proposed in terms of localized vibrations of the substituents, the phenyl rings and the CS_nC

* Higashi *et al.*¹⁷⁹ designated these A and B structures equatorial and axial, respectively, after Shefter.¹⁸¹

($n = 2, 3$) chains. The majority of the vibrations are associated with the phenyl rings and are assigned primarily with reference to the extensive studies of unsymmetrically 1,4-disubstituted benzenes by Green and co-workers¹⁸⁵ whose nomenclature and mode descriptions are adopted. On the basis of C_{2v} local symmetry (X axis perpendicular to the plane), the in-plane modes are $11a_1 + 10b_2$ while the out-of-plane modes are $3a_2 + 6b_1$, as for the phenyl group vibrations of Bz_2S_n ($n = 1-4$) (Sect. VI.B) for which essentially the same approximate descriptions apply. However, nine of the modes ($5a_1 + 2b_2 + 2b_1$), compared to six for the dibenzyl derivatives, are now substituent-sensitive (X sens.), i.e., are considerably dependent on the identity of the substituents. Some of these are nearly invariant among the diphenyl derivatives because of the sulphur substituent common to them all. Again, as in the case of Bz_2S_n ($n = 1-4$), the a_2 modes of the diphenyl derivatives are forbidden in the infrared spectra for strict C_{2v} symmetry, but are observed with significant intensity owing to the lowering of the symmetry by the substituents. As acknowledged by Green,^{185a} his descriptions for the vibrations of disubstituted benzenes should be viewed as crude approximations, and normal coordinate analyses of 1,4-X-Ph-F (X = Cl, Br),¹⁸⁶ 1,4-X-Ph-NO₂ (X = F, Cl, Br, I)¹⁸⁷ and 1,4-X-Ph-NH₂ (X = F, Cl, Br, I)¹⁸⁷ have indeed indicated complex vibrational modes for these molecules. Consequently, the present assignments for diphenyl di- and trisulphides should be taken only to show a close correspondence with the vibrations of related 1,4-disubstituted benzenes. In addition, multiple assignments for some of the phenyl modes are meant to point out regions for the vibrations where

specific assignments to fundamentals and non-fundamentals are untenable. However, band-splitting in some instances is probably due to crystal effects. Assignments for the skeletal vibrations take into account the proposed assignments for the other compounds investigated in this work (Sect. VI.A.2 and VI.B) and also assignments for Ph_2S_2 by Green.^{176b} Most of these vibrations appear to be coupled to some degree with the phenyl modes.

VI.C.1 Di-4-Bromophenyl Di- and Trisulphide

The phenyl group vibrational assignments (Table 22) for $(4\text{-Br-Ph})_2\text{S}_n$ ($n = 2,3$), particularly for the X sens. modes, are based on those due to Green *et al.*^{183a,b} for 1,4-Br-Ph-Y ($Y = \text{Cl}, \text{SH}, \text{SMe}$). Apart from the X sens. vibrations and $\phi(\text{CC})$ 16b (*vide infra*), only the Kekulé mode¹⁸⁸ requires comment. In keeping with the assignments for the other diphenyl derivatives, this vibration is assigned at about 1265 cm^{-1} compared to assignments at about 1220 cm^{-1} for the reference compounds. The assignments for the X sens. vibrations near 1080, 1070 and 725 cm^{-1} follow directly from the reference compounds. The first of these bands occurs for all of the di- and trisulphides, and can be deduced to be significantly $\nu(\text{C-S})$ in nature in view of the substantial degree of $\nu(\text{C-Cl})$ character in the corresponding vibration for 1,4-disubstituted benzenes with a Cl substituent according to partial normal coordinate analyses.¹⁸⁹ These same calculations point to considerable $\nu(\text{C-Br})$ character in the X sens. vibration at about 260 cm^{-1} for $(4\text{-Br-Ph})_2\text{S}_n$ ($n = 2,3$). The appearance of this mode at the same position for the di- and trisulphide as well as for the reference compounds implies minimal coupling with the skeletal vibrations. This can also be said of the out-of-plane

Table 22. Vibrational Wavenumbers (cm^{-1}) and Assignments for Crystalline $(4\text{-Br-Ph})_2\text{S}_n$ ($n = 2, 3$).

$(4\text{-Br-Ph})_2\text{S}_2$		$(4\text{-Br-Ph})_2\text{S}_3$		Assignments ^b
Infrared ^a	Raman	Infrared	Raman	
	3075 w		3070 w	$\nu(\text{CH})$ 20b (b_2)
			3052 m	$\nu(\text{CH})$ 2 (a_1)
d	3059 s	d	3048 m	$\nu(\text{CH})$ 20a (a_1)
	3052 m		3042 m	$\nu(\text{CH})$ 7b (b_2)
	c		c	
	1581 w			
1567 w	1569 sh	1570 w	1573 m	$\nu(\text{CC})$ 8a (a_1)
1558 w	1564 s	1560 w	1561 m	$\nu(\text{CC})$ 8b (b_2)
1545 sh	1548 w			
1467 s	1471 w	1472 s	1472 w	$\nu(\text{CC})$ 19a (a_1)
	1455 br, vw		1455 vvw	
d		d		
	1444 br, vw		1443 vw	
			1398 br, vw	$\nu(\text{CC})$ 19b (b_2)
1384 m	1388 w	1387 m	1383 br, vw	
d		d		
	1298 w			
	1293 vvw		1294 w	$\beta(\text{CH})$ 3 (b_2)
1264 vvw	1266 vw	1262 w	1264 w	Kekulé 14 (b_2)
1225 vvw			1216 vvw	
	1179 m			
		1175 w	1177 m	$\beta(\text{CH})$ 9a (a_1)
	1174 m			
1111 w	1111 vw	1110 w	1111 vw	$\beta(\text{CH})$ 15 (b_2)
1090 w		1094 w		
		1084 m	1084 m	X sen. (a_1)
1080 m	1083 s	1076 s	1075 sh	

Table 22. (continued)

(4-Br-Ph) ₂ S ₂		(4-Br-Ph) ₂ S ₃		Assignments ^b
Infrared ^a	Raman	Infrared	Raman	
1068 m	1067 vs 1055 w 1041 vw	1069 vs 1051 sh 1021 vw 1010 vs	1068 s 1052 w	X sens. (a ₁)
1007 s	1010 w 981 vw 958 vw	1006 s	1009 br,vw	{ β(CH) 18a (a ₁)
954 vw	948 vw	957 w 955 sh 948 vw	956 br,vw	
942 vw		943 w	944 w	{ γ(CH) 17a (a ₂)
826 m	828 vvw 814 w	911 br,w		
811 vs	808 vvw	827 m	825 br,vw 816 w	{ γ(CH) 10a (a ₂)
723 m	725 s	813 vs 810 vs 727 m	810 w	
693 w	696 w	722 m	728 m	{ X sens. (a ₁)
606 br,w	628 m 621 sh	700 w	701 vw	
	538 vs 533 sh	691 vw 628 vw	692 vw 625 m 619 vvw	{ φ(CC) 4 (b ₁)
496 m	497 s			
				α(CCC) 6b (b ₂)
				v(S-S)
				³⁴ S satellite
		508 m	509 s	X sens. (a ₁)

Table 22. (continued)

(4-Br-Ph) ₂ S ₂		(4-Br-Ph) ₂ S ₃		Assignments ^b
Infrared ^a	Raman	Infrared	Raman	
			495 sh	
477 m	473 m	497 s	492 m	} $\phi(\text{CC})$ 16b (b_1)
		487 w	486 m	
		468 w	467 m	
		455 m	455 s	sym. $\nu(\text{S-S})$
419 w				
	402 w		405 w	} $\phi(\text{CC})$ 16a (a_2)
			398 w	
	364 m		347 m	} $\delta(\text{CSS}) + \text{X sens. } (b_2)$
	330 m		332 m	
	309 m		321 m	
	295 m		298 m	X sens. (b_1)
c		c	263 m	} X sens. (a_1)
	258 s		258 m	
			224 m	
	223 m		214 m	} $\delta(\text{CSS}) + \delta(\text{SSS})$ + X sens. (b_2)
			181 m	
	177 m		162 s	
	149 s		136 sh	} torsion and lattice vibrations
	120 vs		123 m	
	103 s		108 s	X sens. (b_1)
	97 s			
	89 s			
	72 m		66 s	} torsion and lattice vibrations
	65 m		57 sh	
	49 vs		52 vs	
	40 vs		41 vs	
	25 vs		29 vs	
	21 vs			

Table 22 (continued)

^a For abbreviations, see footnote b, Table 8.

^b See footnote b, Table 20 for the phenyl group vibrations and Fig. 13 for the skeletal vibrations. The Kekulé mode is the 'ring-breathing' vibration of benzene.¹⁸⁸

^c Region not recorded.

^d Region obscured by Nujol absorptions.

X sens. modes at about 295 and 105 cm^{-1} . However, such does not seem to be the case for the remaining three X sens. vibrations, which are all in-plane modes and thus quite capable of coupling with the skeletal modes. Green *et al.*^{185b} have invoked coupling of the CSC deformation vibration of 1,4-Br-Ph-SMe with two of the X sens. vibrations in order to explain the bands at 363, 324 and 158 cm^{-1} compared to the X sens. modes at 318 and 182 cm^{-1} for 1,4-Br-Ph-SH and at 333 and 194 cm^{-1} for 1,4-Br-Ph-Cl. Similar coupling between $\delta(\text{CSS})$ and $\delta(\text{SSS})$ skeletal deformation modes and these two X sens. b_2 modes is assumed to occur in $(4\text{-Br-Ph})_2\text{S}_n$ ($n = 2,3$). The final X sens. vibration is nearly invariant at about 490 cm^{-1} for the above disubstituted benzenes and is readily assigned at 497 cm^{-1} for $(4\text{-Br-Ph})_2\text{S}_2$. This leaves the band at 475 cm^{-1} as $\phi(\text{CC})$ 16b, very near its location for the disubstituted benzenes. By way of contrast, this region for $(4\text{-Br-Ph})_2\text{S}_3$ is rather complex. The grouping of three features at about 490 cm^{-1} is suggested to encompass $\phi(\text{CC})$ 16b, while the band at 509 cm^{-1} is assigned as the X sens. vibration which is felt to be coupled to some extent with the symmetric $\nu(\text{S-S})$ skeletal vibration. Such coupling explains both the upward shift in the X sens. mode relative to its position for the disulphide and the downward shift in $\nu(\text{S-S})$ compared to the other trisulphides. Moreover, this assessment allows the band at 467 cm^{-1} to be assigned to the antisymmetric $\nu(\text{S-S})$ vibration (unmixed because it is of different symmetry) in agreement with its assignment for the other trisulphides. The $\nu(\text{S-S})$ vibration of the disulphide occurs at 538 cm^{-1} as for the other disulphides and close to its position for Ph_2S_2 (523 cm^{-1}) and $(4\text{-Me-Ph})_2\text{S}_2$ (519 cm^{-1}) as liquids.^{89f}

VI.C.2 Di-4-Methylphenyl Di-and Trisulphide

The assignments (Table 23) for the methyl group vibrations (Fig. 12) of $(4\text{-Me-Ph})_2\text{S}_n$ ($n = 2,3$) are made with reference to Green's^{185a} assignments for 1,4-Me-Ph-X ($X = \text{F, Cl, Br, I}$) and La Lau and Snyder's¹⁷⁷ normal coordinate analyses of various methyl-substituted benzenes and their deuterated analogues. These calculations show the vibrations to be quite separate from the phenyl group vibrations. For the most part, the assignments for the latter follow straightforwardly from those for 1,4-Me-Ph-X ($X = \text{Cl, SH}$)¹⁸⁵ and are very similar for the di- and trisulphide except for the pair of b_2 X sens. modes that are coupled with the skeletal deformation vibrations. However, as for $(4\text{-Br-Ph})_2\text{S}_n$ ($n = 2,3$), the $\phi(\text{CC})$ mode 16b is at significantly higher wavenumber for the trisulphide. Although not an X sens. vibration, this mode does shift considerably among 1,4-disubstituted benzenes. In the low-energy region of the Raman spectra, $(4\text{-Me-Ph})_2\text{S}_2$ and $(4\text{-Me-Ph})_2\text{S}_3$ are very different because of the different sulphur chain lengths and coupling between the skeletal deformation and the b_2 X sens. phenyl modes. There are no clear assignments for the b_1 X sens. modes (assigned at 304 and 132 cm^{-1} for 1,4-Me-Ph-Cl),^{185a} although the bands at about 320 and 115 cm^{-1} for both the di- and trisulphide are reasonable candidates. The $\nu(\text{S-S})$ vibrations occur at 543 cm^{-1} for the disulphide, compared to a value of 519 cm^{-1} reported^{89f} for the liquid, and at 473 and 463 cm^{-1} for the trisulphide. The appearance of the antisymmetric vibration at lower wavenumber for $(4\text{-Me-Ph})_2\text{S}_3$ is consistent with dialkyl trisulphides (Sect. VI.A.2) and Bz_2S_3 (Sect. VI.B).

Table 23. Vibrational Wavenumbers (cm^{-1}) and Assignments
for Crystalline $(4\text{-Me-Ph})_2\text{S}_n$ ($n = 2, 3$).

$(4\text{-Me-Ph})_2\text{S}_2$		$(4\text{-Me-Ph})_2\text{S}_3$		Assignments ^b
Infrared ^a	Raman	Infrared	Raman	
	3056 sh			$\nu(\text{CH})$ 20a (a_1)
	3051 s		3058 m	$\nu(\text{CH})$ 2 (a_1)
	3035 sh			} $\nu(\text{CH})$ 20b (b_2)
	3031 m		3035 m	
d	3022 w	d	3020 w	$\nu(\text{CH})$ 7b (b_2)
	2972 w		2971 br,w	CH_3 asym. str.
	2935 sh			
	2915 br,m		2916 br,s	CH_3 sym. str.
	2865 br,w		2863 br,w	2 x 1453 = 2906
	c		c	
1595 m	1597 vs	1593 m	1593 vs	$\nu(\text{CC})$ 8a (a_1)
1569 w	1573 br,w	1564 w	1564 w	$\nu(\text{CC})$ 8b (b_2)
			1551 vw	
1490 s	1491 m	1488 s	1489 m	$\nu(\text{CC})$ 19a (a_1)
d	~1450 br,w	d	1453 vw	CH_3 asym. def.
			1412 w	
	1398 vw			} $\nu(\text{CC})$ 19b (b_2)
1398 m	1396 vw	1397 m		
			1384 m	} CH_3 sym. def.
d	1376 s	d	1378 sh	
1305 m	1307 m	1301 s	1302 m	$\beta(\text{CH})$ 3 (b_2)
1274 vw	1277 m	1275 w	1278 w	Kekulé 14 (b_2)
			1261 br,w	
	1243 br,w	1243 vw		
1232 vw				
1211 m	1213 s	1210 m	1213 m	X sens. (a_1)

Table 23. (continued)

(4-Me-Ph) ₂ S ₂		(4-Me-Ph) ₂ S ₃		Assignments ^b
Infrared ^a	Raman	Infrared	Raman	
1183 m	1184 m	1178 s	1180 m	β(CH) 9a (a ₁)
			1135 vvw	
1118 s	1119 w	1117 w	1117 vvw	{ β(CH) 15 (b ₂)
1098 w		1104 m	1105 vw	
1078 m	1075 vs	1086 vw	1085 vs	X sens. (a ₁)
	1056 w		1065 w	
1042 br,m	1044 br,vvw	1041 br,w		CH ₃ rock.
1016 s	1017 vw	1016 m	1017 w	β(CH) 18a (a ₁)
		967 w	970 vvw	CH ₃ rock.
960 w		947 w	950 br,vw	γ(CH) 17a (a ₂)
937 w	938 vw		926 w	γ(CH) 5 (b ₁)
841 w		844 m		{ γ(CH) 10a (a ₂)
836 w	835 vw	839 sh		
	812 m		821 w	{ γ(CH) 11 (b ₁)
802 vs		809 vs	811 w	
	796 vs	798 w	799 s	X sens. (a ₁)
696 vw	697 w	705 w	708 m	φ(CC) 4 (b ₁)
			700 sh	
636 vw	636 s	636 vw	637 s	X sens. (a ₁)
620 w	622 m	630 w	632 s	α(CCC) 6b (b ₂)
542 vw	543 s			ν(SS)
	539 sh			³⁴ S satellite
489 s	486 br,w	505 s	506 s	{ φ(CC) 16b (b ₁)
481 s	480 sh			
			473 vs	sym. ν(S-S)
		464 m	463 s	asym. ν(S-S)
			429 m	

Table 23. (continued)

(4-Me-Ph) ₂ S ₂		(4-Me-Ph) ₂ S ₃		Assignments ^b
Infrared ^a	Raman	Infrared	Raman	
c	412 m	c	411 br,vw	$\phi(\text{CC})$ 16a (a_2)
	402 m		389 m	} X sens. (a_1)
	395 m			
	346 m		371 vw	} X sens. (b_1)
	316 s		325 s	
	305 m		268 m	
	299 m		259 sh	} $\delta(\text{CSS}) + \delta(\text{SSS})$
	218 s		198 s	
	176 m		191 sh	
	168 m			} X sens. (b_1)
	147 s		139 s	
	125 sh			
	114 vs		116 sh	
	101 vs		95 br,s	
	77 vs			
	66 s			
	54 s		60 br,s	torsion and
	45 s		34 s	lattice
	32 vs		26 s	vibrations

^a For abbreviations, see footnote b, Table 8.

^b See Fig. 12 for the methyl group vibrations and footnote b, Table 22, for the other modes.

^c Region not recorded.

^d Region obscured by Nujol.

VI.C.3 Di-4-Methoxyphenyl Di- and Trisulphide

The methoxy group vibrations of $(4\text{-MeO-Ph})_2\text{S}_n$ ($n = 2,3$) are the conventional methyl group vibrations (Fig. 12) together the C-O stretching, COC deformation and C-O torsional vibrations. The present assignments (Table 24) are in agreement with those of Horak *et al.*¹⁹⁰ for 1,4-MeO-Ph-X ($X = \text{F, Cl, Br, I}$), while Owen and Hester¹⁹¹ assigned one of the CH_3 rocking vibrations in the $900\text{-}800\text{ cm}^{-1}$ region and the COC deformation vibration at about 310 cm^{-1} for these disubstituted benzenes. The close similarities between $(4\text{-MeO-Ph})_2\text{S}_n$ ($n = 2,3$) and $(4\text{-Me-Ph})_2\text{S}_n$ ($n = 2,3$) in the $650\text{-}450\text{ cm}^{-1}$ region except for the feature near 520 cm^{-1} for the former species strongly supports the assignment of these extra features to the COC deformation mode. It is also worth noting that the CH_3 symmetric stretching vibration of $(4\text{-MeO-Ph})_2\text{S}_n$ ($n = 2,3$) appears to be in Fermi resonance with the first overtone of the CH_3 symmetric deformation mode as in the disubstituted benzenes.

Assignments (Table 24) for the phenyl group vibrations of the di- and trisulphide are based on those of Green *et al.*^{185d} for *para*-substituted phenols with reference as well to the assignments of Horak *et al.*¹⁹⁰ and Owen and Hester¹⁹¹ for *para*-substituted anisoles. These two groups of molecules yield very similar vibrational spectra apart from the substituent vibrations. Once again, the di- and trisulphide by and large give rise to very comparable phenyl group vibrations. In this instance, however, the $\phi(\text{CC})$ mode 16b seems to be at higher wavenumber for the disulphide, contrary to the situation for $(4\text{-R-Ph})_2\text{S}_n$ ($\text{R} = \text{Br, Me; } n = 2,3$) (Sects. VI.C.1 and VI.C.2). As for these other di- and trisulphides, the marked differences

Table 24. Vibrational Wavenumbers (cm^{-1}) and Assignments for Crystalline $(4\text{-MeO-Ph})_2\text{S}_n$ ($n = 2, 3$)

$(4\text{-MeO-Ph})_2\text{S}_2$		$(4\text{-MeO-Ph})_2\text{S}_3$		Assignments ^b
Infrared ^a	Raman	Infrared	Raman	
	3088 w		3084 w	$\nu(\text{CH})$ 20b (b_2)
	3071 m		3064 s	$\nu(\text{CH})$ 2 (a_1)
	3063 s		3058 m	$\nu(\text{CH})$ 20a (a_1)
			3042 m	} $\nu(\text{CH})$ 7 (b_2)
	3035 w		3037 m	
	3025 sh, br			} CH_3 asym. str.
	3002 m		3007 m	
d	2999 sh	d		
	2980 br, vw			
	2965 w		2973 w	CH_3 asym. str.
	2941 m		2942 m	F.R. ^e : CH_3 sym. str. + 2 x 1442 = 2844
	2924 br, vw		2928 w	
	2904 br, vw		2906 w	2 x 1460 = 2920
			2881 vw	2 x 1448 = 2896
			2866 vw	
	2838 m		2838 m	F.R.: 2 x 1442 = 2884 + CH_3 sym. str.
	^c		^c	
1594 s	1593 vs	1589 s	1587 vs	$\nu(\text{CC})$ 8a (a_1)
1573 m	1574 m	1569 m	1568 m	$\nu(\text{CC})$ 8b (b_2)
			1552 vw	
	1497 w	1495 s	1497 m	$\nu(\text{CC})$ 19a (a_1)
1495 s	1495 sh	1489 sh	1489 w	
	1469 vvw	d	1474 vvw	
	1458 w	1460 s	1460 w	} CH_3 asym. def.
1457 s	1455 sh	1450 m	1448 w	
1440 m	1441 vw	1443 m	1441 vw	CH_3 sym. def.
			1428 vw	

Table 24. (Continued)

(4-MeO-Ph) ₂ S ₂		(4-MeO-Ph) ₂ S ₃		Assignments ^b
Infrared ^a	Raman	Infrared	Raman	
1406 w	1409 br,vw	1408 w	1407 w	v(CC) 19b (b ₂)
d		d		
1302 m	1307 w	1302 m	1304 m	β(CH) 3 (b ₂)
1288 br,s	1294 br,w	1292 s	1292 m	Kekulé 14 (b ₂)
		1278 vw	1280 vw	
	1257 sh		1265 vvw	
1248 br,s	1248 m	1250 br,s	1247 m	X sens. (a ₁)
	1241 sh			
	1183 s	1180 m	1182 m	CH ₃ rock.
1177 s		1174 s	1177 s	β(CH) 9a (a ₁)
1152 vw	~1155 br,vvw	1151 vw	1153 vvw	CH ₃ rock.
			1138 br,vvw	
1120 w	1125 br,vw		1124 vw	
1108 w	1109 vw	1106 m	1109 w	β(CH) 15 (b ₂)
1084 vw	1081 vs	1089 m	1090 vs	X sens. (a ₁)
	1065 vw		1068 w	
		1045 br,sh		
1033 m	1035 w			
		1028s	1027 w	} C-O str.
1026 m	1028 w			
1006 m	1008 w	1007 vw	1008 m	β(CH) 18a (a ₁)
961 vvw	966 br,vw	968 w	968 vw	γ(CH) 17a (a ₂)
934 vvw	935 vvw	936 vw	938 vw	γ(CH) 5 (b ₁)
925 vw	927 vvw		922 br,w	
831 m	833 vw	842 s	840 w	} γ(CH) 10a (a ₂)
	826 vw		834 sh	
823 s	822 vw			
		811 s	813 w	} γ(CH) 11 (b ₁)
815 s	816 vw			

Table 24. (Continued)

$(4\text{-MeO-Ph})_2\text{S}_2$		$(4\text{-MeO-Ph})_2\text{S}_3$		Assignments ^b
Infrared ^a	Raman	Infrared	Raman	
794 m	794 vs	799 m	799 s	X sens. (a_1)
	709 w			
706 vw	702 w	713 w	713 m	} $\phi(\text{CC})$ 4 (b_2)
637 w	638 m			
		639 w	639 s	} X sens. (a_1)
633 sh	635 sh			
621 m	624 m	626 vw	626 m	$\alpha(\text{CCC})$ 6b (b_2)
534 vvw	536 s			$\nu(\text{SS})$
516 vw	518 w	524 m	525 br,w	COC def.
506 m	506 m	499 w	499 s	$\phi(\text{CC})$ 16b (b_1)
488 vw	491 br,w			
			472 vs	sym. $\nu(\text{S-S})$
		460 w	462 s	asym. $\nu(\text{S-S})$
	423 vvw			
	417 vvw		416 w	} $\phi(\text{CC})$ 16a (a_2)
395 vvw	399 w			
	366 m		384 s	X sens. (a_1)
	348 m			
	339 m		340 s	X sens. (b_1)
	326 w		311 w	
c		c		
	287 m		247 m	} $\delta(\text{CSS}) + \delta(\text{SSS})$ + 2 X sens. (b_2)
	248 br,m		227 m	
	213 m		213 m	
	167 m		198 m	
	146 br,sh		186 m	} X sens. (b_1)
	115 br,sh		152 s	
	106 br,vs		120 m	C-O torsion

Table 24. (Continued)

$(4\text{-MeO-Ph})_2\text{S}_2$		$(4\text{-MeO-Ph})_2\text{S}_3$		Assignments ^b
Infrared ^a	Raman	Infrared	Raman	
	90 br,vs		100 s	
	86 br,vs		90 s	
	65 s		70 vs	torsion and
	42 vs		53 s	lattice
	31 vs		42 s	vibrations
	22 vs		32 m	

^a For abbreviations, see footnote b, Table 8.

^b See Fig. 12 for the methyl group vibrations and the text for the other methoxy group vibrations. See footnote b, Table 22, for the other modes.

^c Region not recorded.

^d Region obscured by Nujol.

^e F.R. = Fermi Resonance.

between $(4\text{-MeO-Ph})_2\text{S}_2$ and $(4\text{-MeO-Ph})_2\text{S}_3$ in the low-energy region of the Raman spectra can be attributed to mixing of the skeletal deformation and the b_2 X sens. phenyl modes in addition to the different sulphur chain lengths. One of the b_1 X sens. modes is tentatively assigned at 340 cm^{-1} . Specific assignments for other vibrations in this region are not attempted. The $\nu(\text{S-S})$ vibration is observed at 536 cm^{-1} for the disulphide, while the symmetric and antisymmetric $\nu(\text{S-S})$ vibrations of the trisulphide are found at 472 and 462 cm^{-1} , respectively. The latter bands are virtually identical to those for $(4\text{-Me-Ph})_2\text{S}_3$ (Sect. VI.C.2).

VI.C.4 Di-*t*-Butylphenyl Trisulphide

Assignments (Table 25) for $(4\text{-}t\text{-Bu-Ph})_2\text{S}_3$ are proposed by analogy with the other trisulphides examined (Sects. VI.C.1., VI.C.2, VI.C.3), especially $(4\text{-Me-Ph})_2\text{S}_3$ for which the X sens. phenyl group vibrations are predictably quite similar. Some of the *t*-butyl group vibrations (Fig. 12) and phenyl group vibrations may well be overlapping and assignments are generally made for the latter modes in such cases. In the low-energy region of the Raman spectra, coupling of skeletal deformation and b_2 X sens. modes is expected as for the other trisulphides. The symmetric and antisymmetric $\nu(\text{S-S})$ vibrations at 473 and 467 cm^{-1} parallel those for $(4\text{-R-Ph})_2\text{S}_3$ ($\text{R} = \text{Me, OMe}$).

Table 25. Vibrational Wavenumbers (cm^{-1}) and Assignments for Crystalline (4-*t*-Bu-Ph) $_2\text{S}_3$.

Infrared ^a	Raman	Assignments ^b
	3063 m	$\nu(\text{CH})$ 20a (a_1)
	3057 m	$\nu(\text{CH})$ 2 (a_1)
	3046 sh	$\nu(\text{CH})$ 20b (b_2)
	3023 w	$\nu(\text{CH})$ 7b (b_2)
d	2967 br,s	} CH_3 asym. str.
	2959 br,s	
	2926 br,m	
	2903 s	} CH_3 sym. str.
	2866 br,m	
	c	
1590 m	1590 vs	$\nu(\text{CC})$ 8a (a_1)
1557 w	1556 vw	$\nu(\text{CC})$ 8b (b_2)
1495 m	1498 vvw	$\nu(\text{CC})$ 19a (a_1)
1486 s	1489 w	} CH_3 asym. def.
d	1463 w	
	1446 m	
1398 s	1402 sh	} $\nu(\text{CC})$ 19b (b_2)
d	1395 br,w	
1363 s	1362 br,vw	CH_3 sym. def.
1305 m	1307 w	$\beta(\text{CH})$ 3 (b_2)
1278 sh	1282 w	Kekulé 14 (b_2)
1269 s	1271 w	CC_3 asym. str.
1203 m	1204 m	X sens. (a_1)
	1198 m	} $\beta(\text{CH})$ 9a (a_1)
1197 sh	1194 m	
1117 s	1116 m	$\beta(\text{CH})$ 15 (b_2)
	1086 vs	X sens. (a_1)

Table 25. (Continued)

Infrared ^a	Raman	Assignments ^b
1081 m	1081 s	} CH ₃ rock.
1023 w	1027 br,vw	
1010 s	1012 w	β(CH) 18a (a ₁)
967 w		} CH ₃ rock.
959 vw		
942 vw		
935 vw	934 w	γ(CH) 17a (a ₂)
925 w	923 w	γ(CH) 5 (b ₁)
	841 w	γ(CH) 10a (a ₂)
831 s		} γ(CH) 11 (b ₁)
824 s	826 w	
820 sh	820 vvw	
737 m	740 s	X sens. (a ₁)
729 m	731 sh	CC ₃ sym. str.
720 m	721 w	φ(CC) 4 (b ₁)
	636 m	} α(CCC) 6b (b ₂)
637 vw	634 sh	
589 w	588 s	X sens. (a ₁)
557 s	559 vw	} CC ₃ asym. def.
547 s		
507 w	506 s	φ(CC) 16b (b ₁)
494 vw	495 s	CC ₃ sym. def.
	473 vs	sym. ν(S-S)
471 m	467 sh	asym. ν(S-S)
450 w	449 m	} CC ₃ rock.
417 w	416 m	

Table 25. (Continued)

Infrared ^a	Raman	Assignments ^b
	404 w	$\phi(\text{CC})$ 16a (a_2)
	361 w	
	348 m	X sens. (a_1)
	290 br,vw	X sens. (b_1)
	265 br,w	
	210 m	$\delta(\text{CSS}) + \delta(\text{SSS})$
	191 m	+ 2 X sens. (b_2)
	169 s	X sens. (b_1)
	148 s	
	104 vs	torsion and
	65 vs	lattice vibrations

^a For abbreviations, see footnote b, Table 8.

^b See Fig. 12 for the *t*-Butyl group vibrations and footnote b, Table 22, for the other modes.

^c Region not recorded.

^d Region obscured by Nujol.

Figures 19-25. Infrared and Laser-Raman Spectra of Crystalline Diphenyl Di- and Trisulphides.

Figure 19. $(4\text{-Br-Ph})_2\text{S}_3$

Figure 20. $(4\text{-Br-Ph})_2\text{S}_2$

Figure 21. $(4\text{-Me-Ph})_2\text{S}_3$

Figure 22. $(4\text{-Me-Ph})_2\text{S}_2$

Figure 23. $(4\text{-MeO-Ph})_2\text{S}_3$

Figure 24. $(4\text{-MeO-Ph})_2\text{S}_2$

Figure 25. $(4\text{-}t\text{-Bu-Ph})_2\text{S}_3$

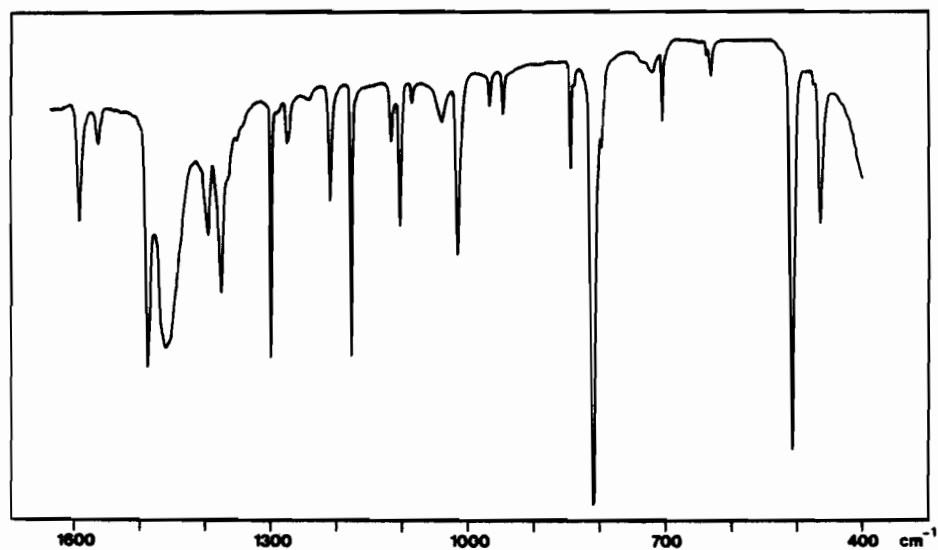


Figure 21a. Infrared Spectrum of Crystalline $(4\text{-Me-Ph})_2\text{S}_3$.

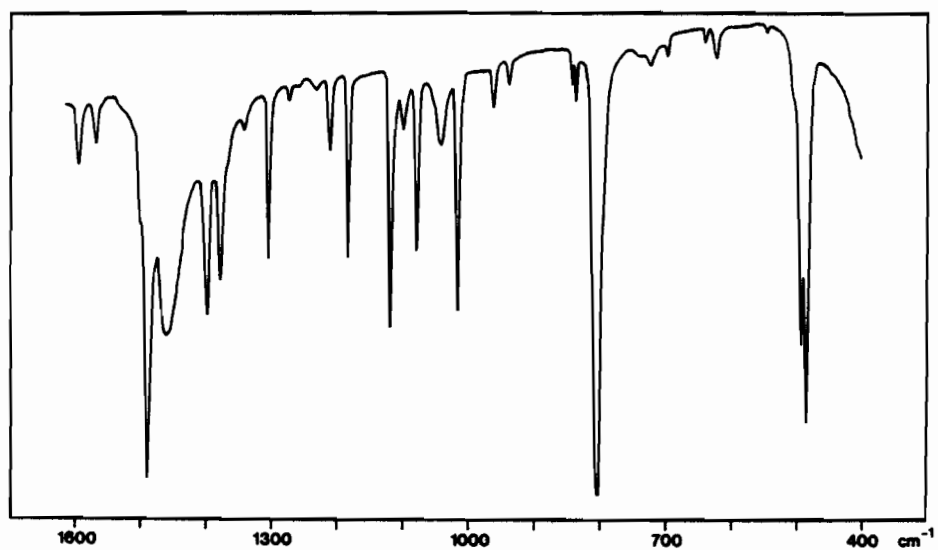


Figure 22a. Infrared Spectrum of Crystalline $(4\text{-Me-Ph})_2\text{S}_2$.

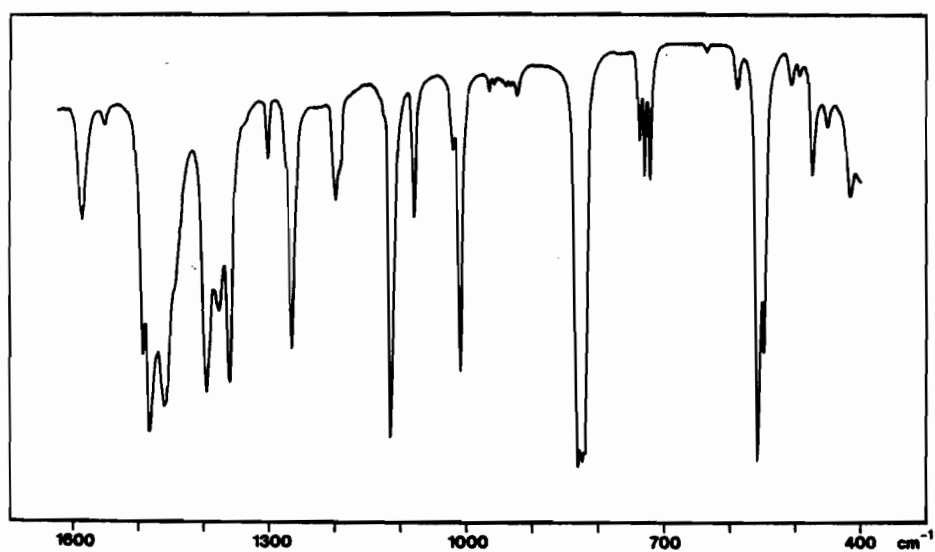


Figure 25a. Infrared Spectrum of Crystalline $(4\text{-}t\text{-Bu-Ph})_2\text{S}_3$.

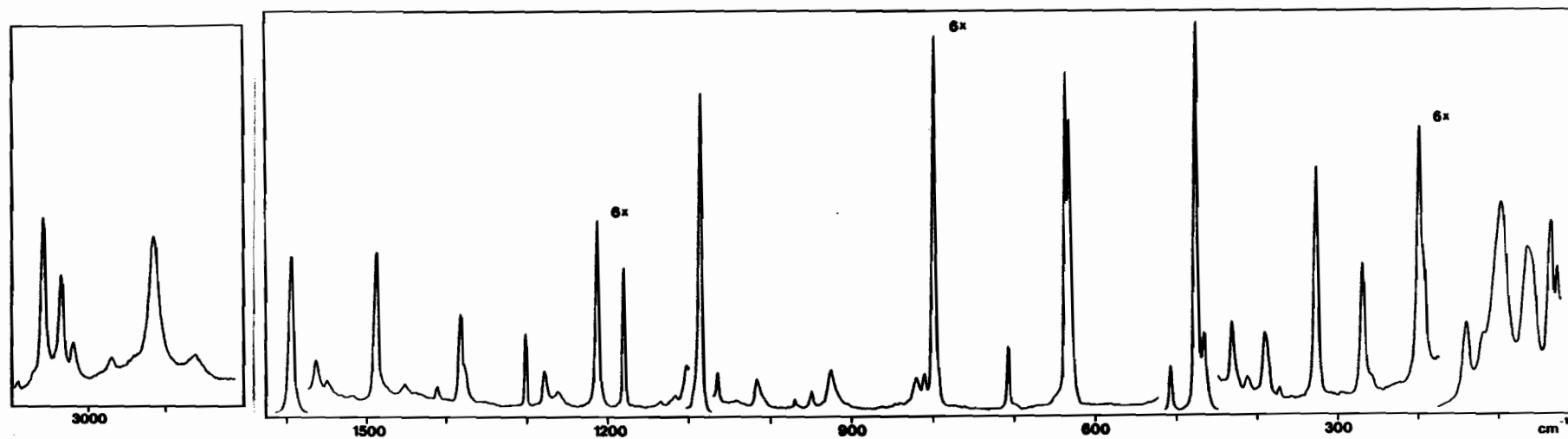


Figure 21b. Laser-Raman Spectrum of Crystalline $(4\text{-Me-Ph})_2\text{S}_3$.

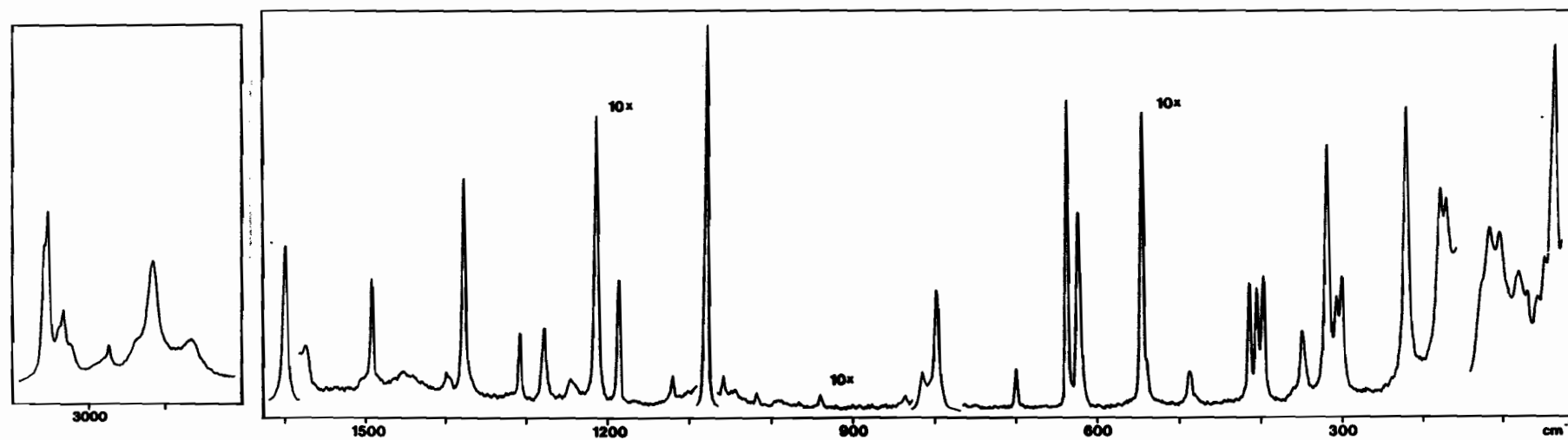


Figure 22b. Laser-Raman Spectrum of Crystalline $(4\text{-Me-Ph})_2\text{S}_2$.

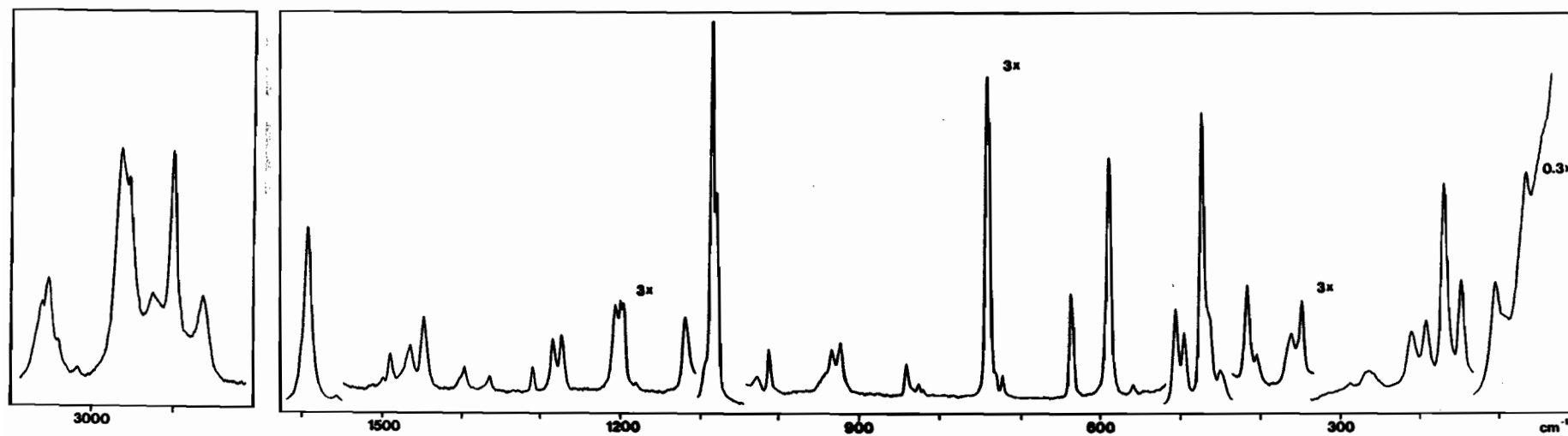


Figure 25b. Laser-Raman Spectrum of Crystalline $(4\text{-}t\text{-Bu-Ph})_2\text{S}_3$.

VII. Summary and Contributions to Knowledge

(1) The infrared and laser-Raman spectra of the dialkyl trisulphides Me_2S_3 , $\text{Me}_2\text{S}_3\text{-}d_6$, Et_2S_3 , $n\text{-Pr}_2\text{S}_3$, $i\text{-Pr}_2\text{S}_3$ and $t\text{-Bu}_2\text{S}_3$, and the dialkyl tetrasulphide Et_2S_4 have been recorded in the accessible regions for fundamental vibrations. Apart from partial accounts of the spectra of Me_2S_3 , Et_2S_3 , $n\text{-Pr}_2\text{S}_3$ and Et_2S_4 , these molecules have not been investigated previously. Complete vibrational assignments have now been proposed for all the aforementioned species. The vibrations divide to a large degree into localized modes for the alkyl substituents and the CS_nC ($n = 3,4$) skeleton with the symmetric $\nu(\text{S-S})$ vibrations appearing as very prominent Raman features in the $520\text{-}430\text{ cm}^{-1}$ region.

(2) Normal coordinate analysis of Me_3S_3 and $\text{Me}_2\text{S}_3\text{-}d_6$ has confirmed that the vibrations separate into methyl group and skeletal vibrations, although the vibrational force field could not be determined uniquely. These calculations have also strongly supported the assignments for the skeletal vibrations of the other trisulphides. Furthermore, they have indicated the *trans* rotamer to predominant in liquid Me_2S_3 , consistent with molecular mechanics calculations. Only circumstantial evidence for the co-existence of some *cis* rotamer in liquid Me_2S_3 was found, while no evidence of *cis* rotamer was detected for the other trisulphides in the liquid state. On the other hand, evidence for some *trans-cis* rotamer of Et_2S_4 together with the apparently more preferred *trans-trans* rotamer was observed in the spectra of the liquid.

(3) Studies of the Raman spectrum of Me_2S_3 at low temperature have revealed the existence of two solid-state variations (Solids I and II) deduced to

correspond to the *cis* and *trans* rotamers, respectively. Solid I is believed to be the first observation of a dialkyl trisulphide in the pure *cis* form.

(4) The temperature-dependence of the Raman spectra of Et_2S_3 and $i\text{-Pr}_2\text{S}_3$ have provided unambiguous evidence for rotational isomerism about the C-S bonds. On the basis of comparisons with organodisulphides, the rotamers co-existing in significant proportions in liquid Et_2S_3 have been concluded to be the pair of *trans* rotamers GGGG' and TGGG' of comparable stability together with the somewhat more favoured group of *trans* rotamers GGGG, GGGT and TGGT also of comparable stability. In the case of $i\text{-Pr}_2\text{S}_3$, the rotamers deduced to be present in appreciable amounts in the liquid are the *trans* rotamers GGGT and GGGG' of similar stability along with the more stable *trans* rotamer GGGG. Measurements of the variation with temperature in the relative intensity of the $\nu(\text{C-S})$ bands for the two groups of rotamers of Et_2S_3 and $i\text{-Pr}_2\text{S}_3$ has led to calculated enthalpy differences of 1.10 ± 0.29 and $0.39 \pm 0.13 \text{ kJ mol}^{-1}$, respectively. The single rotamer in crystalline $i\text{-Pr}_2\text{S}_3$ has been concluded to be the GGGG species, whereas for Et_2S_3 , it could not be ascertained whether the GGGG or TGGT rotamer prevails in the crystalline state. The close resemblances between Et_2S_4 and Et_2S_3 in the spectra of the liquids have been interpreted as indicative of similar isomerism with respect to the C-S bonds of the two molecules. For $n\text{-Pr}_2\text{S}_3$, the spectra exhibit effects from isomerism about both the C-S and the C-C bonds, the former of which has been determined to be analogous to that for Et_2S_3 .

(5) From careful consideration of the available evidence pertaining to

rotational isomerism with respect to the C-S bonds of organodisulphides, the existence of rotamers with an A C-S conformation for dialkyl di- or trisulphides in the liquid state or in solution, as has been proposed previously for disulphides, has been judged to be decidedly unlikely.

(6) The low-temperature Raman spectrum of $t\text{-Bu}_2\text{S}_3$ has pointed to the presence of a lone rotamer in the liquid as well as in the solid state, as predicted on the basis of steric effects.

(7) Differences between rotamers in the vibrational spectra of Et_2S_3 , $i\text{-Pr}_2\text{S}_3$ and $n\text{-Pr}_2\text{S}_3$ related to C-S isomerism have been attributed to weak intramolecular nonbonded interactions in the higher-energy groups of rotamers for each molecule. On the other hand, the general displacements to greater and lower wavenumbers for the $\nu(\text{S-S})$ and $\nu(\text{C-S})$ vibrations, respectively, with increased substitution at the β carbons have been noted to be consistent with the attendant decrease in hyperconjugation involving C-H σ bonds and sulphur d orbitals. Slight modifications in vibrational coupling with substitution at the β carbons have also been pointed out to rationalize the small shifts observed in these vibrations, however.

(8) Complete vibrational assignments have been proposed for the infrared and laser-Raman spectra recorded for the crystalline dibenzyl derivatives Bz_2S_n ($n = 1-4$). The vibrations have been found to separate into localized modes of the phenyl rings, the methylene moieties and the CS_nC ($n = 1-4$) chains. Only the last of these vibrations differ significantly between compounds. Raman spectra ($750-400\text{ cm}^{-1}$) of Bz_2S_n ($n = 1-3$) as liquids and in solution have afforded evidence of rotational isomerism for Bz_2S_2 and Bz_2S_3

in the appearance of a $\nu(\text{C-S})$ band absent for the solids. Internal rotation about the methylene-ring C-C bond has been suggested to account for this additional feature.

(9) Complete vibrational assignments for the infrared and laser-Raman spectra of the crystalline diphenyl derivatives $(4\text{-R-Ph})_2\text{S}_3$ ($\text{R} = \text{Br}, \text{Me}, \text{OMe}, t\text{-Bu}$) and $(4\text{-R-Ph})_2\text{S}_2$ ($\text{R} = \text{Br}, \text{Me}, \text{OMe}$) have been proposed in terms of vibrations of the *para* substituents, the phenyl rings and the CS_nC ($n = 2,3$) skeletons. Except for the $\nu(\text{S-S})$ vibrations, the skeletal vibrations have been concluded to be significantly coupled with some of the phenyl group vibrations.

Appendix

Normal Coordinate Calculations

The standard procedure for normal coordinate analysis of molecular vibrations has become the Wilson **GF** product method for which many detailed discussions can be found, e.g., refs. 159-163. The reader is referred to these sources for a mathematical justification of the approach. This Appendix is intended only to give an overview of the method in terms of the basic concepts and equations involved and to explain the terminology usually employed. The essential aspects of the computer programs due to Overend *et al.*¹⁶⁴ for normal coordinate calculations by this technique are also examined briefly.

The central relationship in the **GF** product method is the comprehensive equation

$$\mathbf{GFL} = \mathbf{LA} \quad (1)$$

which summarizes, in matrix notation, the vibrational problem for a molecule. As outlined below, eq. 1 affords the frequencies for the normal modes of vibration of the molecule and also provides descriptions of these fundamentals in terms of internal coordinates, i.e., changes in the bond lengths, bond angles and dihedral angles from their equilibrium values. The following discussion pertains to a typical non-linear molecular with N atoms for which there are $3N-6$ normal modes.

The symmetric square matrices **G** (kinetic energy matrix) and **F** (force constant matrix) in eq. 1 are of order $3N-6$. In the simple harmonic oscillator approximation for molecular vibrations (satisfactory for small variations in the internal configuration of a molecule), **F** and the inverse of **G** determine the

vibrational potential and kinetic energies, respectively, according to the expressions

$$\text{potential energy: } 2V = \mathbf{R}^t \mathbf{F} \mathbf{R} \quad (2)$$

$$\text{kinetic energy: } 2T = \dot{\mathbf{R}}^t \mathbf{G}^{-1} \dot{\mathbf{R}} \quad (3)$$

where \mathbf{R} is the vector (column matrix) of internal coordinates* and $\dot{\mathbf{R}}$ is the corresponding vector of velocities.[†] The elements of \mathbf{G}^{-1} , the mass factors relating the binary products of the internal coordinate velocities to the kinetic energy, are functions of the atomic masses and structural parameters of the molecule, as are, therefore, the elements of \mathbf{G} itself. The complicated nature of these functions for many pairs of parameters reflects the awkwardness of expressing vibrational kinetic energy using internal coordinates. On the other hand, vibrational potential energy is conveniently written in terms of the internal coordinates and force constants of the molecule (eq. 2). The valence force constants (diagonal elements of \mathbf{F}) measure the inherent stiffness or resistance to distortion in the structural parameters of the molecule due to the distribution of electron density in the bonding. Any such constant may be viewed as the force tending to restore the associated parameter, e.g., a bond or angle, to its equilibrium value in the event of a unit displacement in that parameter, i.e., for a unit internal coordinate. The interaction force constants (off-diagonal elements of \mathbf{F}) take account of how a change in one parameter alters the forces acting on the others because of disruption in the equilibrium electron distribution. Thus,

* The symbol for a matrix followed by a superscript t denotes the transpose of the matrix (rows and columns interchanged).

[†] First derivatives with respect to time.

the constant connecting a pair of parameters may be treated as the force imposed on one of them as a result of a unit displacement in the other, e.g., the force arising in an angle from a unit change in one of its bonds or *vice versa*. Taken collectively, the valence and interaction force constants of the molecule constitute its General Quadratic Valence Force Field. At this juncture, it is worth mentioning that isotopic substitution in a molecule significantly affects G but not F since the bonding is negligibly perturbed by such modifications in the atomic masses.

Of the remaining terms in eq. 1, the eigenvalue matrix Λ is a diagonal matrix of eigenvalues λ that correlate with the harmonic oscillator frequencies ν for the fundamental vibrations of the molecule:

$$\lambda_k = 4\pi^2 \nu_k^2 \quad k = 1, 2, \dots, 3N-6 \quad (4)$$

Finally, the eigenvector matrix L is a square matrix of order $3N-6$ relating the internal coordinate vector R to the normal coordinate vector Q by way of the linear transformation

$$R = LQ \quad (5)$$

By definition, the normal coordinates diagonalize the vibrational potential and kinetic energies:

$$2V = Q^t \Lambda Q \quad (6)$$

$$2T = \dot{Q}^t E \dot{Q} \quad (7)$$

where \dot{Q} is the vector of normal coordinate velocities and E is the identity matrix. Owing to the absence of cross-terms in the expanded energy expressions, the normal coordinates Q_k ($k = 1, 2, \dots, 3N-6$) can be excited independently, and hence they correspond to the independent normal modes of vibration for the molecule. When a single Q_k is activated, eq. 5 simplifies to

$$R = L_k Q_k \quad (8)$$

with the eigenvector L_k , the k^{th} column of L , specifying the internal coordinate amplitudes in the normal coordinate. These amplitudes are the simultaneously achieved maximum deviations in the structural parameters of the molecule from the equilibrium shape during the vibration. Accordingly, the L_k delineate the fundamental vibrations. The complete assemblage of these descriptions for the $3N-6$ normal modes of vibration is the eigenvector matrix L . Additional facets of Λ and L can be seen by substituting eq. 5 into eqs. 2 and 3 and then comparing with eqs. 6 and 7 to arrive at the conditions

$$L^t F L = \Lambda \quad (9)$$

$$L^t G^{-1} L = E \quad \text{or} \quad L L^t = G \quad (10)$$

as constraints on the vibrations beyond that of eq. 1.

Assuming G and F are both known for a molecule, its Λ and L matrices can be evaluated by first decomposing eq. 1 into separate expressions for each normal mode of vibration and rearranging to give

$$(GF - E\lambda_k) L_k = 0 \quad (11)$$

where 0 is the zero matrix. This relationship for any particular λ_k represents a set of $3N-6$ linear homogeneous equations in the internal coordinate amplitudes that comprise the associated L_k . Non-trivial solutions for these amplitudes require the determinant of their coefficients to be zero-valued:

$$| GF - E\lambda_k | = 0 \quad (12)$$

A total of $3N-6$ roots λ_k (one for every fundamental with recurring values indicating degenerate vibrations) satisfy this equation which therefore yields,

in conjunction with eq. 4, the harmonic frequencies for the normal modes of vibration. Substitution of the λ_k one at a time back into eq. 11 leads to the eigenvectors L_k that can be normalized on the basis of eq. 9 recast for an individual normal coordinate Q_k as

$$L_k^t F L_k = \lambda_k \quad (13)$$

The elements of any normalized L_k for the molecule then characterize the corresponding vibration in terms of the contributions from bond-stretching, angle-bending and torsion to a unit displacement in its Q_k . Consequently, calculation of the complete collection of λ_k and normalized L_k (making up the matrices Λ and L , respectively) in the above manner served to fully elucidate the $3N-6$ fundamental vibrations for the molecule.

Although the eigenvectors L_k adequately describe the vibrations, their interpretation is complicated by the different dimensions for bond-stretching and angle-bending factors. It has therefore become conventional to characterize the vibrations on the basis of their potential energies. To this end, the potential energy distribution for a normal mode has been defined in terms of the percentage contributions to its vibrational potential energy from the force constants of the molecule. In light of eqs. 6 and 13, the potential energy for a unit displacement in the k^{th} normal coordinate Q_k is

$$2V = Q_k^2 \lambda_k = \lambda_k = L_k^t F L_k \quad (14)$$

It follows that the contribution from the valence force constant f_{ii} may be expressed as

$$\text{P.E.D. } (f_{ii})_k = \frac{f_{ii} l_{ik}^2}{\lambda_k} \times 100\% \quad (15)$$

where l_{ik} is the normalized amplitude of the i^{th} internal coordinate in the k^{th} normal mode, λ_k is the associated eigenvalue, and l_{ik} refers to the same structural parameter as does f_{ii} . Since these contributions from the valence force constants predominate over the contributions from interaction force constants, the former set alone generally provide a sufficient description of the fundamental vibration.

A further important aspect of normal coordinate analysis is the role of molecular symmetry in facilitating the calculations. To take advantage of the symmetry properties of a molecule, symmetry coordinates are constructed as linear combinations of the internal coordinates according to the transformation

$$S = UR \quad (16)$$

in which S and R are the vectors of symmetry and internal coordinates, respectively, and U is a square orthogonal matrix. New square matrices G and F in symmetry coordinate space can be generated from their internal coordinate counterparts as

$$G = UGU^t \quad (17)$$

$$F = UFU^t \quad (18)$$

and the equations

$$(GF - E\lambda_k)L_k = 0 \quad (19)$$

$$|GF - E\lambda_k| = 0 \quad (20)$$

analogous to eqs. 11 and 12 can then be developed. In these new expressions, L_k represents the symmetry coordinate eigenvector (equal to UL_k) for the k^{th} normal mode, while the corresponding eigenvalue λ_k is the same as in internal coordinate space because U is orthogonal. However, G and F , unlike

G and F , are both blocked-out along the diagonal according to the symmetry classes of the molecule. Because the GF product is blocked-out in the same fashion, it follows that eqs. 19 and 20 factor into separate expressions for each symmetry class. These can be solved independently to find the λ_k and subsequently the L_k by symmetry classes. The latter describe the normal modes of vibration in terms of the symmetry coordinate amplitudes. Alternatively, the normal modes can be characterized by their potential energy distributions with respect to the diagonal elements (symmetry coordinate force constants) of F on the basis of the analogue of eq. 15:

$$\text{P.E.D.}(F_{ii})_k = \frac{F_{ii} L_{ik}^2}{\lambda_k} \times 100\% \quad (21)$$

In any event, the introduction of symmetry coordinates into the calculations greatly simplifies them by breaking up the multiplication of square matrices of order $3N-6$, central to calculations using internal coordinates, into a series of multiplications with smaller matrices.

In actually applying the GF product method to a molecule of interest, the eigenvalues λ_k are determined directly from the vibrational wavenumbers measured in the infrared and Raman spectra, while the kinetic energy matrix G is calculated from the molecular structure and atomic masses.

It is hence the force constant matrix F that must be initially found in order to establish the nature of the fundamental vibrations. The usual approach is to assume a force field for the molecule in light of previous results for related molecules and then to adjust the trial force constants as necessary to satisfy eq. 12. For this purpose, it is convenient to rearrange F into a vector f of unique force constants, i.e., equivalent force constants

appear only once. This allows the force constant corrections to be expressed as a vector Δf which can be evaluated, in the general case, from the least-squares relationship

$$J^t P J \Delta f = J^t P \Delta \lambda \quad (22)$$

where $\Delta \lambda$ is the vector of the differences between the observed and calculated eigenvalues ($\lambda^{\text{obs.}} - \lambda^{\text{calcd.}}$) and P is a diagonal matrix of weighting factors (usually the reciprocals of the vibrational frequencies squared ($1/v_k^2$)) that bias the low-energy vibrations more heavily in the calculations. The Jacobian matrix J is an array of the partial derivatives $\delta \lambda / \delta f$ specifying the dependence of the eigenvalues on the force constants, which happen to be functions solely of the eigenvectors L_k . Accordingly, the determination of the eigenvalues and eigenvectors corresponding to the assumed force field as discussed above leads to the associated matrices $\Delta \lambda$ and J , and therefore to Δf . The latter is composed of refinements to the initial force constants that improve the fit between the calculated and observed eigenvalues. Step-wise repetition of the process starting each cycle with the most recently revised set of force constants frequently yields convergence after only a few iterations. This condition is achieved when the weighted sum $\sum P_k (\lambda^{\text{obs.}} - \lambda^{\text{calcd.}})^2$ has been minimized within the constraints of the calculations and is indicated by a minimal change in Δf and $\Delta \lambda$ between successive iterations. The acceptability of the final force field is judged by its ability to reproduce the known eigenvalues.

The reliability of each force constant in the refined field depends both on the quality of the fit between the calculated and experimental eigenvalues and on the magnitude of the Jacobian elements related to that constant. Thus,

a variance-covariance matrix M can be derived as

$$M = \sigma^2 J^t P J \quad (23)$$

in which σ^2 is the variance for the least-squares fit of the eigenvalues:

$$\sigma^2 = \frac{1}{(m-n)} \sum_k P_k (\lambda_k^{\text{obs.}} - \lambda_k^{\text{calcd.}})^2 \quad (24)$$

In this latter expression, P_k is the weighting factor for λ_k and $(m-n)$ is the degrees of freedom equal to the difference between the number of eigenvalues and the number of force constants under refinement. Since the diagonal elements of M specify the variance for the force constants, the square roots are the standard deviations (usually termed dispersions) which indicate the level of confidence associated with the calculated constant. The off-diagonal elements of M show the covariance or extent of interdependence between pairs of force constants, a large value showing that the two constants govern the vibrations similarly. However, comparisons between pairs of force constants are more readily made on the basis of the much larger correlation coefficients generated by scaling the covariances with the reciprocals of the corresponding variances ($p(f_i, f_j) = M_{ij}/M_{ii}^{1/2} M_{jj}^{1/2}$).

In view of the laboriousness of the calculations outlined above, the only practical approach for all but very simple molecules is to use computer techniques. Unfortunately, however, attempts to refine a force field by computer methods often results in divergence, i.e., in an increase in $\Delta\lambda$ between successive iterations. Although a poor choice of trial force constants is sometimes the reason, the difficulty is usually one of poorly defined roles for some of the interaction force constants. Two extreme situations are common: (1) the force constants in question have only small Jacobian elements and thus have little influence on the least-squares fit, or (2) these constants

have substantial values for several of their Jacobian elements and hence govern quite a few of the fundamental vibrations. The latter circumstance implies high correlation among groups of force constants whose separate values are hard to pinpoint. To bring about convergence in the refinement of the force field, at least some of the problematic constants must be held fixed in magnitude throughout the computations or be allowed to vary with only a limited number of other constants. Judicious constraints of this type ordinarily affect the direction of the calculations relatively little because the vibrational potential energy is determined primarily by the valence force constants. Good approximations are still obtained for the eigenvectors and potential energy distributions for the normal modes of vibration.

It should be noted that the number of force constants simultaneously refined in any normal coordinate calculation may not exceed the number of eigenvalues or else neither eq. 12 nor 22 can be solved. Moreover, the degrees of freedom should be large for a statistically meaningful least-squares treatment. To minimize the number of force constants in a problem, only the essential terms of the General Quadratic Valence Force Field (G.Q.V.F.F.) for the molecule are usually included and values for some force constants are frequently transferred from related molecules. In addition, the degrees of freedom can be increased through the incorporation of data for isotopically substituted molecules which serves to extend the number of eigenvalues associated with the force field. The usefulness of these substitutions is restricted, however, by the interdependence of vibrational frequencies for isotopic molecules as expressed by the Teller-Redlich product rule.¹⁵¹

A popular method of limiting the number of independent force constants for a molecule is through the use of the Urey-Bradley Force Field (U.B.F.F.)¹⁶⁵ consisting of valence-type force constants together with nonbonded repulsions between atoms. These repulsion force constants embody the interaction force constants (between pairs of internal coordinates) of the G.Q.V.F.F. and also account partly for the valence force constants therein. For instance, the *geminal* nonbonded repulsion in a bent triatomic moiety partitions into stretch-stretch and stretch-bend interaction force constants and contributions to the stretching and bending valence force constants of the G.Q.V.F.F.. The values of these latter constants are found by adding the above contributions to the corresponding Urey-Bradley valence force constants. In effect, then, the U.B.F.F. is an internally constrained G.Q.V.F.F. with explicit interdependence among groups of force constants. Refinement of the U.B.F.F. follows the same line as for the G.Q.V.F.F. except that the appropriate least-squares relationship (eq. 22) becomes

$$(\mathbf{JZ})^t \mathbf{P} (\mathbf{JZ}) \Delta \Phi = (\mathbf{JZ})^t \mathbf{P} \Delta \lambda \quad (25)$$

In this expression, $\Delta \Phi$ is the vector of corrections to the Urey-Bradley force constants in the vector Φ and \mathbf{Z} is the transformation matrix from Urey-Bradley to internal coordinate space ($f = \mathbf{Z}\Phi$). The advantage of the U.B.F.F. over the G.Q.V.F.F. lies in the significant reduction in the number of force constants to be evaluated. However, satisfactory application of the U.B.F.F. often requires the introduction of some internal coordinate interaction force constants to modify the intrinsic interrelationships among the force constants, thereby detracting from the simplicity of the basic field. Nevertheless, the modified U.B.F.F. has enjoyed considerable success in vibrational

calculations, particularly for molecules with tetrahedral fragments.

In force field refinements by the approach outlined above using the series of computer programs ZMAT, WMAT and OVEREND,¹⁶⁴ an additional mathematical technique is employed to expedite the calculations. Thus the program WMAT evaluates the kinetic energy matrix G for each isotopic molecule from the atom masses and molecular structure and subsequently generates W matrices for input to OVEREND. This second step involves establishing a new coordinate system for the molecule wherein the modified G is equal to the identity matrix ($W^{-1}G(W^{-1})^t = \bar{G} = E$). Owing to the incorporation of the U matrix into the redefinition of the coordinates, transforming the force constant matrix F in OVEREND ($W^tFW = \bar{F}$) leads to a revised form of eq. 20 in which GF is replaced by \bar{F} :

$$|\bar{F} - E\lambda_k| = 0 \quad (26)$$

The two equations have the same eigenvalues λ_k and both factor by symmetry classes, but solutions for λ_k are more easily determined from eq. 26 because \bar{F} , unlike GF , is symmetric.

Besides the W matrices for the isotopic molecules, the necessary input to OVEREND is (1) the trial force constants entered as the vector f (Φ for the U.B.F.F.), (2) the Z matrix calculated in ZMAT from the molecular structure*, (3) the vibrational wavenumbers for the normal modes of each isotopic molecule to be internally converted to the eigenvalues, and (4) a listing of the force constants to be refined. The calculations proceed by first evaluating \bar{F} and solving eq. 26 to obtain the eigenvalues corresponding to the test force field. The eigenvectors C_k in the coordinate system specified

* Even if Urey-Bradley force constants are excluded, Z is needed to convert f to F .

by W are then determined on the basis of the following analogue of eq. 19

$$(\bar{F} - E \lambda_k) C_k = 0 \quad (27)$$

from which the internal coordinate eigenvectors are found ($L_k = WC_k$). At this point, the Jacobian matrix J is constructed and force constant corrections are generated using the least-squares eq. 22 (eq. 25 for the U.B.F.F.). These refinements of the force field continue until convergence or divergence, the latter of which necessitates the imposing of constraints as discussed earlier. Assuming convergence, calculation of the variance-covariance matrix M results in the dispersions for the refined force constants and the correlation coefficients between pairs of these constants. Finally, the potential energy distributions for the normal modes of vibration are determined. The OVEREND output related to the refinement of the force field includes the eventual force constants of both f and F with dispersions and correlation coefficients for the refined constants, details concerning the adjustments in each iteration, and the Jacobian matrix (J or JZ depending on the type of force field) for each isotopic molecule. The output associated with the fundamental vibrations for each isotopic molecule includes a comparison of the observed and calculated wavenumbers and characterizations of the vibrations in terms of their eigenvectors and potential energy distributions.

REFERENCES

- (1) B. Meyer, *Chem. Rev.*, 76, 367, (1976); *Adv. Inorg. Rad. Chem.*, 18, 287 (1976).
- (2) (a) A.S. Cooper, W.L. Bond and S.C. Abrahams, *Acta Crystallogr.*, 14, 1008 (1961); (b) A. Caron and J. Donahue, *ibid.*, 18, 562 (1965).
- (3) J. Donahue, A. Caron and E. Goldfish, *J. Am. Chem. Soc.*, 83, 3748 (1961).
- (4) (a) R. Steudel and H.-J. Mausle, *Angew. Chem. Int. Ed. Engl.*, 16, 112 (1977); (b) M. Schmidt and H.D. Block, *ibid.*, 6, 955, (1967); (c) R. Steudel and H.-J. Mausle, *ibid.*, 18, 152 (1979).
- (5) (a) M. Schmidt, B. Block, H.D. Block, H. Kopf and E. Wilhelm, *ibid.*, 7, 632 (1968); (b) R. Steudel and H.-J. Mausle, *ibid.*, 17, 56 (1978); (c) M. Schmidt and E. Wilhelm, *ibid.*, 5, 964 (1966); (d) *Idem.*, *J. Chem. Soc., Chem. Comm.*, 111 (1970); (e) M. Schmidt, E. Wilhelm, T. Daebaerdemacher, E. Heller and A. Kutoglu, *Z. Anorg. Allg. Chem.*, 405, 153 (1974).
- (6) Y. Minoura and T. Moriyoshi, *Trans. Faraday Soc.*, 59, 1019, 1504 (1963).
- (7) T. Nakabayashi, J. Tsurugi and T. Yabuta, *J. Org. Chem.*, 29, 1236 (1964).
- (8) D. Grant and J.R. Van Wazer, *J. Am. Chem. Soc.*, 86, 3012 (1964).
- (9) (a) M.H. Brodnitz, C.L. Pollack and P.P. Vallon, *J. Agr. Food Chem.*, 17, 760 (1969); (b) M. Bolens, P.J. De Valois, H.J. Wobben and A. Van der Gen, *ibid.*, 17, 984 (1969); (c) D.M. Oaks, H. Hartman and K.P. Dimick, *Anal. Chem.*, 36, 1560 (1964); (d) L. Schreyen, P. Dimick, F. Van Wassenhove and N. Schamp, *J. Agr. Food Chem.*, 24, 336, 1147 (1976); (e) S. Dembele and P. Dubois, *Ann. Technol. Agr.*, 22, 121 (1973); (f) H. Nishimura, K. Fujcurara, J. Mizuntani and Y. Obata, *J. Agr. Food Chem.*, 19, 992 (1971); (g) H. Kameoka and A. Miyake, *Nippon Noegi Kagaku Kaishi*, 48, 385 (1974) [*C.A.*, 81: 152425c (1974)]; (h) W.G. Galetto and A.A. Bednarezyk, *J. Food Sci.*, 40, 1165 (1975).
- (10) J.P. Marion, F. Müggler-Chawan, R. Viani, J. Bricourt, D. Raymond and R.H. Egli, *Helv. Chim. Acta*, 50, 1509 (1967).
- (11) G. Casnati, R. Ricca and M. Paran, *Chim. Ind. Milano*, 49, 57 (1967).
- (12) R.E. Moore, *J. Chem. Soc., Chem. Comm.*, 1168 (1971).
- (13) S.J. Wratten and D.J. Faulker, *J. Org. Chem.*, 41, 2465 (1976).
- (14) K. Morita and S. Kobayashi, *Tetrahedron Lett.*, 573 (1966); *Chem. Pharm. Bull.*, 15, 988 (1967).

- (15) (a) R. Hodges and J.S. Shannon, *Aust. J. Chem.*, 19, 1059 (1966);
(b) D. Brewer, R. Rahman, S. Safe and A. Taylor, *J. Chem. Soc. Chem. Comm.*, 1571 (1968); (c) R. Rahman, S. Safe and A. Taylor, *J. Chem. Soc. (C)*, 1665 (1969); (d) E. Francis, R. Rahman, S. Safe and A. Taylor, *J. Chem. Soc., Perkin Trans. 2*, 470 (1972).
- (16) J.S. Jorczak, "Introduction to Rubber Technology", M. Morton, ed., Reinhold Book Corporation, New York, 1968, p. 363.
- (17) (a) H.J.M. Bowen, *Trans. Faraday Soc.*, 50, 452 (1954); (b) C.C. Price and S. Oae, "Sulphur Bonding", Ronald Press Co., New York, 1962, p.41.
- (18) (a) H.P. Koch, *J. Chem. Soc.*, 394 (1949); (b) Y. Minoura, *J. Chem. Soc. Japan, Pure Chem. Sect.*, 73, 131, 244 (1952); (c) R.N. Hazeldine and J.M. Kidd, *J. Chem. Soc.*, 3219 (1953); (d) L. Schotte, *Arkiv Kemi*, 9, 361 (1956); (e) J. Tsurugi and T. Nakabayashi, *J. Org. Chem.*, 24, 807 (1959); 26, 2483 (1961).
- (19) (a) F. Féher and H.J. Berthold, *Chem. Ber.*, 88, 1634 (1955); (b) F. Féher, G. Krause and K. Vogelbruch, *ibid.*, 90, 1570 (1957).
- (20) (a) H.E. Westlake, H.L. Laquer and C.P. Smyth, *J. Am. Chem. Soc.*, 72, 436 (1950); (b) L.M. Kushner, G. Gorin and C.P. Smyth, *ibid.*, 477 (1950); (c) C.C. Woodrow, M. Carmack and J.G. Miller, *J. Chem. Phys.*, 19, 951 (1951).
- (21) Y. Minoura, *J. Chem. Soc. Japan, Pure Chem. Sect.*, 75, 869 (1954).
- (22) A. Faura and A. Ilicerto, *Ann. Chim. (Rome)*, 43, 509 (1953).
- (23) (a) I.M. Dawson and J.M. Robertson, *J. Chem. Soc.*, 1256 (1948); (b) J. Donahue, *J. Am. Chem. Soc.*, 72, 2701 (1950); (c) H.J. Berthold, *Z. Anorg. Allg. Chem.*, 352, 237 (1963); (d) F. Féher and K.H. Linke, *ibid.*, 327, 151 (1964).
- (24) J. Donahue and V. Shoemaker, *J. Chem. Phys.*, 16, 92 (1948).
- (25) (a) R. Steudel, R. Reinhardt and F. Schuster, *Angew. Chem. Int. Ed. Engl.*, 16, 715 (1977); (b) Y. Watanabe, *Acta Crystallogr.*, B30, 1396 (1974); (c) R. Steudel, R. Reinhardt and F. Schuster, *Angew. Chem. Int. Ed. Engl.*, 17, 57 (1978); (d) A. Kutoglu and E. Heller, *ibid.*, 5, 965 (1966); (e) T. Debaerdemaeker and A. Kutoglu, *Cryst. Struct. Comm.*, 3, 611 (1974).
- (26) (a) H.G. Schnering and N.K. Goh, *Naturwiss.*, 61, 272 (1974); (b) S. Yamaoka, J.T. Lemley, J.M. Jenks and H. Steinfink, *Inorg. Chem.*, 14, 129 (1975); (c) S.C. Abrahams and J.L. Bernstein, *Acta Crystallogr.*, B25, 2365 (1969); (d) R. Tegman, *ibid.*, B29, 1473 (1973);

- (26) (e) B. Leclerc and T.S. Kabre, *ibid.*, B31, 1675 (1975); (f) P. Woodward, *J. Chem. Soc., Dalton Trans.*, 1314 (1976); (g) S.C. Abrahams and E. Gibson, *Acta Crystallogr.*, 6, 206 (1953); (h) A. Hordvik and E. Sletten, *Acta Chem. Scand.*, 22, 3029 (1968).
- (27) (a) D. Barnard, T.H. Houseman, M. Porter and B.K. Tidd, *J. Chem. Soc., Chem. Comm.*, 371 (1969); (b) S. Safe and A. Taylor, *J. Chem. Soc. (C)*, 432 (1970).
- (28) P.H. Lauer, "Sulphur in Organic and Inorganic Chemistry", Vol. 3, A. Senning, ed., M. Dekker, New York, 1972, p. 91.
- (29) R. Rahman, S. Safe and A. Taylor, *Quart. Rev.*, 24, 208 (1970).
- (30) H.E. Van Wart, L.L. Shipman and H.A. Scheraga, *J. Phys. Chem.*, 79, 1436 (1975).
- (31) H.E. Van Wart and H.A. Scheraga, *ibid.*, 80, 1812, 1823 (1976).
- (32) M. Nishikawa, K. Kamiya, S. Kobayashi, K. Morita and Y. Tomiie, *Chem. Pharm. Bull.*, 15, 756 (1967).
- (33) F. Féher and J. Lex., *Z. Anorg. Allg. Chem.*, 423, 103 (1976).
- (34) (a) B.J.R. Davis and I. Bernal, *Proc. Natl. Acad. Sci. U.S.A.*, 70, 279 (1973); (b) M. Przybylska and E.M. Gopalakrishna, *Acta Crystallogr.*, 30B, 597 (1974); (c) F.R. Ahmed and M. Przykylska, *ibid.*, 33B, 168 (1977).
- (35) S. Husbye, *Acta Chem. Scand.*, 27, 756 (1973).
- (36) (a) L.F. Power and R.D.G. Jones, *Acta Crystallogr.*, B27, 181 (1971); (b) L.F. Power, K.E. Turner, F.H. Moore and R.D.G. Jones, *J. Cryst. Struct.*, 5, 125 (1975).
- (37) J.S. Ricci and I. Bernal, *J. Chem. Soc. (B)*, 1928 (1971).
- (38) F. Féher, A. Klaeren and K.H. Linke, *Acta Crystallogr.*, B28, 534 (1972).
- (39) F. Lemmer, F. Féher, A. Gieren, S. Hechtfisher and W. Hoppe, *Angew. Chem. Int. Ed. Engl.*, 9, 313 (1970).
- (40) (a) L.F. Power, R.D.G. Jones, J. Pletcher and M. Sax, *J. Chem. Soc., Perkin Trans. 2*, 1817 (1975); (b) R.D.G. Jones and L.F. Power, *Acta Crystallogr.*, B32, 1801 (1976).
- (41) (a) C. Szantay, M.P. Kotick, E. Shefter and T.J. Bordos, *J. Am. Chem. Soc.*, 89, 713 (1967); (b) E. Shefter, M.P. Kostick and T.J. Bardos,

- (41) *J. Pharm. Sci.*, 56, 1297 (1967).
- (42) J.D. Lee and M.W.R. Bryant, *Acta Crystallogr.*, B27, 2325 (1971).
- (43) R.E. Rosenfield, Jr., and R. Parthasarathy, *ibid.*, B31, 462 (1975).
- (44) (a) O. Foss and O. Tjomsland, *Acta Chem. Scand.*, 12, 1810 (1958);
(b) R.M. Stroud and H.C. Carlisle, *Acta Crystallogr.*, B28, 304 (1972).
- (45) (a) O. Foss, K. Johnson and T. Reistad, *Acta Chem. Scand.*, 18, 2345 (1964); (b) T. Debaerdemaeker, *Cryst. Struct. Comm.* 4, 565 (1975).
- (46) (a) J. Fridrichson and A. McL. Mathieson, *Acta Crystallogr.*, 18, 1043 (1965); (b) J. Fridrichson and A. McL. Mathieson, *ibid.*, 23, 439 (1967); (c) D.B. Cosulick, N.R. Nelson and J.H. Van der Hende, *J. Am. Chem. Soc.*, 90, 6519 (1968); (d) H.P. Weber, *Acta Crystallogr.*, B28, 2945 (1972); (e) K.H. Michel, M.O. Chaney, N.D. Jones, M.M. Hochm and R. Nagarajan, *J. Antibiot.* 27, 57 (1974).
- (47) J. Toussaint and L. Dideberg, *Bull. Soc. R. Sci. Liege*, 36, 666 (1967).
- (48) G.H. Wahl, Jr., J. Bordner, D.N. Harpp and J.G. Gleason, *J. Chem. Soc., Chem. Comm.*, 985 (1972).
- (49) N.L. Allinger, M.J. Hickey and J. Kao, *J. Am. Chem. Soc.*, 98, 2741 (1976).
- (50) A.R. Gregory and M. Przybylska, *J. Am. Chem. Soc.*, 100, 943 (1978).
- (51) (a) Féher and K.H. Linke, *Z. Anorg. Allg. Chem.*, 327, 151 (1964);
(b) J.W. Bats, *Acta Crystallogr.*, B33, 2264 (1977).
- (52) N.J. Brondmo, S. Esperas and S. Husbye, *Acta Chem. Scand.*, A29, 93 (1975).
- (53) A. Hordvik, *ibid.*, 20, 1885 (1966).
- (54) J.L. Kice, "Sulphur in Organic and Inorganic Chemistry", Vol. 1, A Senning, ed., M. Dekker, New York, 1972, p. 153.
- (55) (a) H. Bock and G. Wagner, *Angew. Chem. Int. Ed. Engl.*, 11, 150 (1972);
(b) G. Wagner and H. Bock, *Chem. Ber.*, 107, 68 (1974); (c) A.D. Baker, M. Brisk and M. Gellender, *J. Electron Spectrosc. Relat. Phenom.*, 3, 227 (1974); (d) R.C. Colton and J.W. Rabalais, *ibid.*, 3, 345 (1974);
(e) M.F. Guimon, C. Guimon and G. Pfister-Guillouzo, *Tetrahedron Lett.*, 441 (1975).
- (56) D.B. Boyd, *J. Am. Chem. Soc.*, 94, 8799 (1972); *Theor. Chim. Acta*, 30,

- (56) 137 (1973); *J. Phys. Chem.*, 78, 1554 (1974).
- (57) L. Pauling, *Proc. Natl. Acad. Sci. U.S.A.*, 35, 495 (1949); "The Nature of the Chemical Bond", Cornell University Press, Ithaca, N.Y., 1960, p. 134.
- (58) G. Bergson, *Arkiv Kemi*, 12, 233 (1957); 16, 315 (1961); 18, 409 (1962).
- (59) R.W. Woody, *Tetrahedron*, 24, 1273 (1973).
- (60) L.J. Saethre, *Acta Chem. Scand.*, A29, 558 (1975).
- (61) (a) G. Winnewisser, M. Winnewisser and W. Gordy, *J. Chem. Phys.*, 49, 3465 (1968); (b) M. Winnewisser and J. Hause, *Z. Naturforsch.*, 23A, 56 (1968).
- (62) S.D. Thompson, D.G. Carroll, F. Watson, M. O'Donnell and S.P. McGlynn, *J. Chem. Phys.*, 45, 1367 (1966).
- (63) J. Linderberg and J. Michl, *J. Am. Chem. Soc.*, 92, 2619 (1970).
- (64) H. Yamabe, H. Kato and T. Yonezawa, *Bull. Chem. Soc. Jpn.*, 44, 22, 604 (1971).
- (65) J. Webb, R.W. Strickland and F.S. Richardson, *J. Am. Chem. Soc.*, 95, 4775 (1973).
- (66) H.W. Van Wart, L.L. Shipman and H.A. Scheraga, *J. Phys. Chem.*, 78, 1848 (1974).
- (67) K. Kimura and K. Osafune, *Bull. Chem. Soc. Jpn.*, 48, 2421 (1975).
- (68) J.P. Snyder and L. Carlsen, *J. Am. Chem. Soc.*, 99, 2931 (1977).
- (69) M.E. Schwartz, *J. Chem. Phys.*, 51, 4182 (1969).
- (70) A. Veillard and J. Demuynck, *Chem. Phys. Lett.*, 4, 476 (1970).
- (71) I.H. Hiller, V.R. Sanders and J.F. Wyatt, *Trans. Faraday Soc.*, 66, 2665 (1970).
- (72) D.W. Davies, *Chem. Phys. Lett.*, 28, 520 (1974).
- (73) J.A. Pappas, *Chem. Phys.*, 12, 397 (1976).
- (74) P.H. Blustin, *Theor. Chim. Acta*, 48, 1 (1978).
- (75) L.A. Eslava, J.B. Putnam, Jr., and L. Pederson, *Int. J. Pept. Protein Res.*, 11, 149 (1978).

- (76) (a) D. Sutter, H. Dreizler and H.D. Rudolph, *Z. Naturforsch.*, 20A, 1676 (1965); (b) B. Beagley and K.T. McAloon, *Trans. Faraday Soc.*, 67, 3216 (1971); (c) A. Yokozeki and S.H. Bauer, *J. Phys. Chem.*, 80, 618 (1976).
- (77) T. Gillbro, *Phosphorous and Sulphur*, 4, 133 (1978).
- (78) R. Steudel, *Angew. Chem. Int. Ed. Engl.*, 14, 655 (1975).
- (79) B. Meyer, L. Peter and K. Spitzer, *Inorg. Chem.*, 16, 27 (1977).
- (80) (a) G.B. Bonino and R. Manzoni-Ansidei, *Mem. R. Accad. Sci. Inst. Bologna*, 1, 3 (1933/34); (b) W.G. Pai, *Ind. J. Phys.*, 9, 231 (1935); (c) P. Donzelot and M.C. Chaix, *Compt. Rend.*, 202, 851 (1936); (d) L. Médard and F. Deguillon, *ibid.*, 203, 1518 (1936); (e) R. Vogel-Höegler, *Acta Physica Austriaca*, 1, 311 (1947).
- (81) F. Féher and G. Winkhauss, *Z. Anorg. Allg. Chem.*, 288, 123 (1956).
- (82) H. Wieser, P.J. Krueger, E. Muller and J.B. Hyne, *Can. J. Chem.*, 47, 1633 (1969).
- (83) S.K. Freeman, "Application of Laser Raman Spectroscopy", Wiley-Interscience, New York, N.Y., 1974, Chapter 8.
- (84) J. Tsurgi and T. Nakabayashi, *J. Org. Chem.*, 25, 1744 (1960).
- (85) M.M. Coleman, J.L. Koenig and J.R. Sheldon, *J. Polym. Sci., Phys.*, 12, 1001 (1974).
- (86) C.D. DesJardins and J. Passmore, *J. Fluorine Chem.*, 9, 53 (1977).
- (87) M.E. Peach, *Int. J. Sulphur Chem.*, 8, 27 (1973).
- (88) (a) H.W. Thompson and I.F. Trotter, *J. Chem. Soc.*, 481 (1946); (b) N. Sheppard, *Trans. Faraday Soc.*, 46, 429 (1950).
- (89) (a) D.W. Scott, H.L. Finke, M.E. Gross, G.B. Guthrie and H.M. Huffman, *J. Am. Chem. Soc.*, 72, 2424 (1950); (b) D.W. Scott, H.F. Finke, J.P. McCullough, M.E. Gross, R.E. Pennington and G. Waddington, *ibid.*, 74, 2478 (1952); (c) W.N. Hubbard, D.R. Douslin, J.P. McCullough, D.W. Scott, S.S. Todd, J.F. Messerly, I.A. Hossenlopp, A. George and G. Waddington, *ibid.*, 80, 3547 (1958); (d) J.H.S. Green, D.J. Harrison, W. Kyaston and D.W. Scott, *Spectrochim. Acta*, 25A, 1313 (1969); (e) D.W. Scott and M.Z. El-Sabban, *J. Mol. Spectrosc.*, 31, 362 (1969); (f) K.G. Allum, J.A. Greighton, J.H.S. Green, G.J. Minkoff and L.J.S. Prince, *Spectrochim. Acta*, 24A, 927 (1968).

- (90) (a) M. Hayashi, *Nippon Kagaku Zasshi*, 78, 101 (1957); (b) S.G. Frankiss, *J. Mol. Struct.*, 3, 89 (1969).
- (91) R.C. Lord and N. Yu, *J. Mol. Biol.*, 50, 509 (1970).
- (92) (a) H. Sugeta, A. Go and T. Miyazawa, *Chem. Lett.*, 83 (1972); *Bull. Chem. Soc. Jpn.*, 46, 3407 (1973); (b) H. Sugeta, *Spectrochim. Acta* 31A, 1729 (1975).
- (93) (a) E.J. Bastian and R.B. Martin, *J. Phys. Chem.*, 77, 1129 (1973); (b) R.B. Martin, *ibid.*, 78, 855 (1974).
- (94) (a) H.E. Van Wart, A. Lewis, H.A. Scheraga and F.D. Saeva, *Proc. Natl. Acad. Sci. U.S.A.*, 70, 2619 (1973); (b) H.E. Van Wart, F. Cardinaux and H.A. Scheraga, *J. Phys. Chem.*, 80, 625 (1976); (c) H.E. Van Wart, H.A. Scheraga and R.B. Martin, *J. Phys. Chem.*, 80, 1832 (1976); (d) H.E. Van Wart and H.A. Scheraga, *Proc. Natl. Acad. Sci. U.S.A.*, 74, 13 (1977).
- (95) L.A. Nimon and V.D. Neff, *J. Mol. Spectrosc.*, 26, 175 (1968); (b) D.W. Scott, J.P. McCullough and F.H. Kruse, *ibid.*, 13, 313 (1964); (c) R. Steudel and D.F. Eggers, Jr., *Spectrochim. Acta*, 31A, 879 (1975); (d) R. Steudel, *ibid.*, 31A, 1065 (1975); (e) R. Steudel and H.-J. Maüsle, *Z. Naturforsch.*, 33A, 951 (1978).
- (96) (a) M. Gardner and A. Rogstad, *J. Chem. Soc., Dalton Trans.*, 599 (1973); (b) R. Steudel and F. Shuster, *J. Mol. Struct.*, 44, 143 (1978).
- (97) (a) G.J. Janz, E. Roduner, J.W. Coutts and J.R. Downey, Jr., *Inorg. Chem.*, 15, 1751 (1976); (b) G.J. Janz, J.W. Coutts, J.R. Downey, Jr., and E. Roduner, *ibid.*, 15, 1755 (1976); (c) G.J. Janz, J.R. Downey, Jr., E. Roduner, G.J. Wasilczyk, J.W. Coutts and A. Eluard, *ibid.*, 15, 1759 (1976).
- (98) (a) F.P. Daly and C.W. Brown, *J. Phys. Chem.*, 79, 350 (1975); (b) A.T. Ward, *Mat. Res. Bull.*, 4, 581 (1969).
- (99) F.P. Daly and C.W. Brown, *J. Phys. Chem.*, 77, 1859 (1973).
- (100) T. Chivers and I. Drummond, *Inorg. Chem.*, 11, 2525 (1972).
- (101) D.N. Harpp and T.G. Back, *J. Labelled Compds.*, 11, 95 (1975).
- (102) D.K. Ash, PhD. Thesis, McGill University, 1973.
- (103) D.N. Harpp, K. Steliou and T.H. Chan, *J. Am. Chem. Soc.*, 100, 1222 (1978).

- (104) CRC Handbook of Chemistry and Physics, 60th Ed., CRC Press Inc., Boca Raton, Florida, (1979-80).
- (105) S. Hayashi, M. Furukawa, J. Yamamoto and K. Homamura, *Chem. Pharm. Bull.*, 15, 1310 (1967).
- (106) D.J. Martin and R.H. Pearce, *Anal. Chem.*, 38, 1604 (1966).
- (107) E.L. Colichman and D.L. Love, *J. Am. Chem. Soc.*, 75, 5736 (1953).
- (108) T.J. Wallace, *ibid.*, 86, 2018 (1964).
- (109) E.E. Reid, "Organic Chemistry of Bivalent Sulphur", Vol. III, Chemical Publishing Company, New York, 1960.
- (110) Z.S. Arigan and L.A. Wiles, *J. Chem. Soc.*, 4709 (1962).
- (111) W.A. Bonner, P.J. Werth, Jr., and Max Roth, *J. Org. Chem.*, 97, 1575 (1962).
- (112) R.E. Hester, "Raman Spectroscopy", H.A. Szymanski, ed., Plenum Press, New York, 1967, p.101.
- (113) M.C. Tobin, "Laser Raman Spectroscopy", Wiley-Interscience, New York, 1971.
- (114) T.L. Pickering, K.J. Saunders and A.V. Tobolsky, *J. Am. Chem. Soc.*, 89, 2364 (1967).
- (115) E. Muller and J.B. Hyne, *ibid.*, 91, 1907 (1969).
- (116) D. Smith, and J.P. Devlin, D.W. Scott, *J. Mol. Spectrosc.*, 25, 174 (1968).
- (117) (a) M. Sakakibara, H. Matsuura, I. Harada and T. Shimanouchi, *Bull. Chem. Soc. Jpn.*, 50, 111 (1977); (b) M. Ohta, Y. Ogaura, H. Matsuura, I. Harada and T. Shimanouchi, *ibid.*, 50, 380 (1977); (c) Y. Ogawa, M. Ohta, M. Sakakibara, H. Matsuura, I. Harada and T. Shimanouchi, *ibid.*, 50, 650 (1977); (d) M. Sakakibara, I. Harada, H. Matsuura and T. Shimanouchi, *J. Mol. Struct.*, 49, 29 (1978).
- (118) A. Langseth and H.J. Bernstein, *J. Chem. Phys.*, 8, 410 (1940).
- (119) N.L. Allinger, J. Kao and H-M. Chang and D.B. Boyd, *Tetrahedron*, 32, 2867 (1976).
- (120) J.D. Lee and N.W.R. Bryant, *Acta Crystallogr.*, B25, 2497 (1969).

- (121) D.J. Mitchell, *ibid.*, 998 (1969).
- (122) T. Otterson, L.G. Warner and K. Seff, *ibid.*, B29, 2954 (1973).
- (123) H.C. Mez, *Cryst. Struct. Comm.*, 3, 657 (1974).
- (124) H.L. Yabel, Jr., and E.W. Hughes, *Acta Crystallogr.*, 7, 291 (1954).
- (125) H.E. Van Wart, L.L. Shipman and H.A. Scheraga, *J. Phys. Chem.*, 79, 1428 (1975).
- (126) N.L. Allinger, *Adv. Phys. Org. Chem.*, 13, 1 (1976).
- (127) (a) N.L. Allinger and M.J. Hickey, *J. Am. Chem. Soc.*, 97, 5167 (1975); (b) J. Kao and N.L. Allinger, *Inorg. Chem.*, 16, 35 (1977).
- (128) D.B. Boyd, *J. Phys. Chem.*, 82, 1407 (1978).
- (129) R.W. Strickland and F.S. Richardson, *J. Chem. Soc., Perkin Trans.*, 2, 1818 (1976).
- (130) R.N. Jones, ed., National Research Council of Canada Bull. No. 15 (1976).
- (131) D.D. Jones, I. Bernal, M.N. Fray and T.F. Koetzle, *Acta Crystallogr.*, B30, 1220 (1974).
- (132) L. Pauling, "The Nature of the Chemical Bond", Cornell University Press, Ithaca, N.Y. (1960).
- (133) G. Nemethy and H.A. Scheraga, *Biopolymers*, 3, 155 (1965).
- (134) (a) L.S. Bartell, *J. Am. Chem. Soc.*, 99, 3279 (1977); (b) N.L. Allinger, D. Hindman and H. Hönig, *ibid.*, 3282 (1977).
- (135) (a) M.T. Rogers and T.W. Campbell, *J. Am. Chem. Soc.*, 74, 4742 (1952); (b) C.W.N. Cumper, J.F. Read and A.I. Vogel, *J. Chem. Soc.*, 5323 (1965).
- (136) (a) L. Haraldson, C.J. Slaughter, S. Sunner and E. Varde, *Acta Chem. Scand.*, 14, 1509 (1960); (b) B. Nelander and S. Sunner, *J. Am. Chem. Soc.*, 94, 3576 (1972).
- (137) (a) L.S. Levitt and B. Levitt, *Chem. Ind.*, 3, 132 (1973); (b) L.S. Levitt and C. Parkanyi, *Int. J. Sulphur Chem.*, 329 (1973).
- (138) (a) N.A. Rosenthal and G. Oster, *J. Am. Chem. Soc.*, 83, 4445 (1961); (b) C.W.N. Cumper, J.F. Read and A.I. Vogel, *J. Chem. Soc. (A)*, 239 (1966).

- (139) (a) G. Bergson, *Arkiv Kemi*, 13, 11 (1958); (b) G. Bergson, G. Claesson and L. Schotte, *Acta Chem. Scand.*, 16, 1159 (1962).
- (140) (a) H. Mackle and R.T.B. McClean, *Trans. Faraday Soc.*, 60, 669 (1963); (b) H. Mackle, *Tetrahedron*, 19, 1159 (1963); (c) *ibid.*, 20, 611 (1964).
- (141) J.P. Snyder and D.N. Harpp, *Tetrahedron Lett.*, 197 (1978).
- (142) E. Muller and J.B. Hyne, *Can. J. Chem.*, 46, 3587 (1968).
- (143) (a) H. Brusset, Nguyen Quy Dao and M. Jouan, *Proc. Int. Conf. Raman Spectrosc.*, 3rd, 226 (1972); (b) M. Jouan and Nguyen Quy Dao, *C.R. Acad. Sci.*, 274c, 1987 (1972).
- (144) L. Mannik, P.A. Sipos and M.K. Phibbs, *Can. J. Spectrosc.*, 21, 105 (1976).
- (145) (a) M.K. Phipps, *ibid.*, 22, 137 (1977); (b) M. Sakakibara, H. Matsuura and H. Murata, *J. Mol. Struct.*, 55, 21 (1979).
- (146) B.D. Vineyard, *J. Org. Chem.*, 31, 601 (1966).
- (147) H. Kessler and W. Rundel, *Chem. Ber.*, 101, 3350 (1968).
- (148) (a) B. Milligan and J.M. Swan, *J. Chem. Soc.*, 2901 (1965); (b) S. Kabuss, A. Luttringhaus, H. Friebolin and R. Mecke, *Z. Naturforsch.*, B21, 320 (1966).
- (149) H.J. Boonstra and L.C. Rinzema, *Rec. Trav. Chim.*, 79, 962 (1960).
- (150) R. Gaufres, A. Perez and J.-L. Bribes, *Bull. Soc. Chim. Fr.*, 2898 (1971).
- (151) G. Herzberg, "Infrared and Raman Spectra of Polyatomic Molecules", Van Nostrand Reinhold Co., New York, 1945.
- (152) (a) J.-P. Perchard, M.-T. Ford and M.-L. Josien, *J. Chim. Phys.*, 645 (1964); (b) H. Gerding and J.W. Ypenburg, *Rec. Trav. Chim.*, 85, 616 (1966); *ibid.*, 90, 885 (1971); (c) J.R. Allkins and P.J. Hendra, *Spectrochim. Acta*, 22, 2075 (1966); (d) J.M. Freeman and T. Henshall, *J. Mol. Struct.*, 1, 31 (1967); *Can. J. Chem.*, 46, 2175 (1968); (e) M. Tranquille, M. Fouassier, M.F. Lautié-Mouneyrac, P. Dizabo and M.T. Forel, *C.R. Acad. Sci.*, 270C, 1085 (1965); (f) Y. Shiro, M. Ohsaku, M. Hayashi and H. Murata, *Bull. Chem. Soc. Jpn.*, 43, 609 (1970); (g) M. Tranquille, P. Labarbe, M. Fouassier and M.T. Forel, *J. Mol. Struct.*, 8, 273 (1971); (h) G. Geiseler and G. Hanschmann, *ibid.*, 293 (1971); 11, 283 (1972); (i) J.W. Ypenburg, *Rec. Trav. Chim.*, 91, 671 (1972); (j) O. Gebhardt and S.J. Cyvin, *J. Mol. Struct.*, 12, 205 (1972);

- (152) (k) P. Labarbe and M.-T. Forel, *J. Chim. Phys.*, 180 (1972);
(l) I.W. Levin, R.A.R. Pearce and R.C. Spiker, Jr., *Spectrochim. Acta*, 31A, 41 (1975).
- (153) (a) M. Ohsaku, Y. Ohsaku, Y. Shiro and M. Murata, *Bull. Chem. Soc. Jpn.*, 45, 113, 954, 956, 3035, 3480 (1972); 46, 1399 (1973); (b) M. Ohsaku, *ibid.*, 47, 965 (1974); 48, 707, 742, 1037 (1975); *J. Sci. Hiroshima Univ. Ser. A*, 38, 51 (1974); *Spectrochim. Acta*, 31A, 1271 (1975); (c) M. Ohsaku, H. Murata and Y. Shiro, *ibid.*, 33A, 467 (1977); *J. Mol. Struct.*, 42, 31 (1977); (d) M. Ohsaku and H. Murata, *Spectrochim. Acta*, 34A, 869 (1978).
- (154) N. Norimasa, H. Sugeta and T. Miyazawa, *Bull. Chem. Soc. Jpn.*, 48, 2417, 3573 (1975).
- (155) G. Turrell, "Infrared and Raman Spectra of Crystals", Academic Press, London, 1972.
- (156) W.H. Green and A.B. Harvey, *J. Chem. Phys.*, 49, 3586 (1968).
- (157) A.B. Harvey and M.K. Wilson, *ibid.*, 45, 678 (1966).
- (158) M. Hayashi, Y. Shiro and H. Murata, *Bull. Chem. Soc. Jpn.*, 39, 1857, 1861 (1966).
- (159) E.B. Wilson, J.C. Decius and P.C. Cross, "Molecular Vibrations", McGraw-Hill Book Co. Inc., New York, 1955.
- (160) P. Gans, "Vibrating Molecules", Chapman and Hall Ltd., London, 1975.
- (161) K. Nakamoto, "Infrared and Raman Spectra of Inorganic and Coordination Compounds," 3rd Ed., John Wiley and Sons, New York, 1978.
- (162) N.B. Colthup, L.H. Daly and S.E. Wiberley, "Introduction to Infrared and Raman Spectroscopy", 2nd Ed., Academic Press, New York, 1975.
- (163) L.H. Jones, "Inorganic Vibrational Spectroscopy", Vol. 1, Marcel Dekker Inc., New York, 1971.
- (164) (a) J. Overend and J.R. Scherer, *J. Chem. Phys.*, 32, 1289 (1960);
(b) C.D. Needham, Ph.D. Thesis, University of Minnesota, 1965.
- (165) H.C. Urey and C.A. Bradley, *Phys. Rev.*, 38, 1969 (1931).
- (166) A.J. Barnes, H.E. Hallam and J.D.R. Howells, *J. Chem. Soc., Faraday Trans. 2*, 737 (1972).
- (167) (a) S. Allen and H.J. Bernstein, *Can. J. Chem.*, 32, 1124 (1954); (b) F.A. Miller and F.E. Kiviat, *Spectrochim. Acta*, 25A, 1363 (1969);

- (167) (c) R.G. Snyder and J.H. Schachtschneider, *J. Mol. Spectrosc.*, 30, 290 (1969); (d) A.B. Dempster and G. Zerbi, *ibid.*, 39, 1 (1971); (e) S. Suzuki and A.B. Dempster, *J. Mol. Struct.*, 32, 339 (1976).
- (168) (a) M. Hayashi, J. Shiro and H. Murata, *Bull. Chem. Soc. Jpn.*, 39, 112 (1966); (b) T. Torgrimsen and P. Klaeboe, *Acta. Chem. Scand.*, 24, 1137 (1970).
- (169) (a) M. Hayashi, K. Ohno and H. Murata, *Bull. Chem. Soc. Jpn.*, 46, 2332 (1973); (b) K. Tanabe and S. Saeki, *J. Mol. Struct.*, 27, 79 (1975); (c) Y. Ogawa, S. Imazeki, H. Yamaguchi, H. Matsuura, I. Harada and T. Shimanouchi, *Bull. Chem. Soc. Jpn.*, 51, 748 (1978).
- (170) (a) C.G. Opaskar and S. Krimm, *Spectrochim. Acta*, 23A, 2261 (1967); (b) W.H. Moore and S. Krimm, *ibid.*, 29A, 2025 (1973); (c) P. Klaboe, *ibid.*, 26A, 87 (1970); (d) T. Sundius, *ibid.*, 32A, 415 (1976); *J. Mol. Spectrosc.*, 64, 45 (1977).
- (171) (a) W. Hüttner and W. Zeil, *Spectrochim. Acta*, 22, 1007 (1966); (b) R.C. Williams and J.W. Taylor, *J. Am. Chem. Soc.*, 95, 1710 (1973); (c) J.C. Evans and G. Y.-S. Lo, *ibid.*, 88, 2118 (1966).
- (171) (a) W. Hüttner and W. Zeil, *Spectrochim. Acta*, 22, 1007 (1966); (b) R.C. Williams and J.W. Taylor, *J. Am. Chem. Soc.*, 95, 1710 (1973); (c) J.C. Evans and G.Y.-S. Lo, *ibid.*, 88, 2118 (1966).
- (172) (a) J.D. Lee and M.W.R. Bryant, *Naturwissenschaften*, 56, 36 (1969); (b) B. Van Dijk and G.J. Visser, *Acta Crystallogr.*, 27B, 846 (1971); (c) H. Einspahr and J. Donahue, *ibid.*, 847 (1971); (d) J.D. Lee, *ibid.*, 847 (1971); (e) R. Srinivasan and B.J. Vijayalakshmi, *ibid.*, 28B, 2615 (1972).
- (173) M.A. Blokhin, A.T. Shuvaev, E.I. Fedorov, V.P. Kurbatov, O.A. Osipov and A.V. Kozinkin, *Izv. Akad. Nauk. SSSR, Ser. Fiz.*, 38, 544 (1974).
- (174) D.H. Whiffen, *J. Chem. Soc.*, 1350 (1956).
- (175) E.B. Wilson, *Phys. Rev.*, 45, 706 (1934).
- (176) (a) J.H.S. Green, W. Kynaston and A.S. Lindsey, *Spectrochim. Acta*, 17, 486 (1961); (b) J.H.S. Green, *J. Chem. Soc.*, 2236 (1961); *Spectrochim. Acta*, 17, 607 (1961); *ibid.*, 18, 39 (1962); *ibid.*, 24A, 1627 (1968).
- (177) C. La Lau and L.G. Snyder, *ibid.*, 27A, 2073 (1971).
- (178) R.R. Fraser, G. Boussard, J.K. Saunders, J.B. Lambert and C.E. Mixan, *J. Am. Chem. Soc.*, 93, 3822 (1971).

- (179) L.S. Higashi, M. Lundeen and K. Seff, *J. Am. Chem. Soc.*, 100, 8101 (1978).
- (180) E. Shefter, M.P. Kotick and T.J. Bardos, *J. Pharm. Sci.*, 56, 1293 (1967).
- (181) E. Shefter, *J. Chem. Soc., B*, 903 (1970).
- (182) P.R. Wells, "Linear Free Energy Relationships", Academic Press, London 1968.
- (183) J.C. Ricci and I. Bernal, *J. Am. Chem. Soc.*, 91, 4078 (1969).
- (184) (a) J.D. Lee and M.W.R. Bryant, *Acta Crystallogr.*, 25B, 2094 (1969); (b) M. Sacerdoti, G. Gilli and P. Domiano, *ibid.*, 31B, 327 (1975).
- (185) (a) J.H.S. Green, *Spectrochim. Acta*, 26A, 1503 (1970); (b) J.H.S. Green, D.J. Harrison, W. Kynaston and D.W. Scott, *ibid.*, 1515 (1970); (c) J.H.S. Green and D.J. Harrison, *ibid.*, 1925 (1970); (d) J.H.S. Green, D.J. Harrison and W. Kynaston, *ibid.*, 27A, 2199 (1971).
- (186) N.D. Patel, V.B. Kartha and N.A. Narasimham, *J. Mol. Spectrosc.*, 48, 185; 202 (1973).
- (187) L. Smetankine and J. Etchepare, *J. Mol. Struct.*, 14, 61 (1972); 19, 799 (1973).
- (188) J.R. Scherer and J.C. Evans, *Spectrochim. Acta*, 19, 1739 (1963).
- (189) N. Le Calvé and P. Labarbe, *ibid.*, 26A, 77 (1970).
- (190) M. Horak, E.R. Lippincott and P.K. Khanna, *ibid.*, 23A, 1111 (1967).
- (191) N.L. Owen and R.E. Hester, *ibid.*, 25A, 343 (1969).